UNCLASSIFIED

AD NUMBER
AD855302
LIMITATION CHANGES
TO: **Approved for public release; distribution is unlimited.**
FROM: **Distribution authorized to U.S. Gov't. agencies and their contractors; Critical Technology; JUN 1968. Other requests shall be referred to Air Force Materials Laboratory, Wright-Patterson AFB, 145433. This document contains export-controlled technical data.**
AUTHORITY
USAFSC ltr, 26 May 1972

THIS PAGE IS UNCLASSIFIED

AFML-TR-68-52

AD855302

DESIGN OF A PRODUCTION HYDROSTATIC EXTRUSION PRESS

G. E. Meyer
F. A. Simonen
J. C. Gerdeen
R. J. Fiorentino
A. M. Sabroff

BATTELLE MEMORIAL INSTITUTE
COLUMBUS LABORATORIES

TECHNICAL REPORT AFML-TR-68-52

June 1968

D D C
JUL 25 1969
A

This document is subject to special export controls and each transmittal to foreign governments or foreign nationals may be made only with prior approval of the Manufacturing Technology Division, MATB, of the Air Force Materials Laboratory, Wright-Patterson Air Force Base, Ohio 45433. Distribution of this report is limited because it contains technology identifiable with items on the strategic embargo list excluded from export or re-export under U.S. export act of 1948 (63 STAT.7) as amended (50 U.S.C. Appn. 2020-2031)

MANUFACTURING TECHNOLOGY DIVISION
AIR FORCE MATERIALS LABORATORY
AIR FORCE SYSTEMS COMMAND
WRIGHT-PATTERSON AIR FORCE BASE, OHIO

26 JUL 1968

NOTICE

When Government drawings, specifications, or other data are used for any purpose other than in connection with a definitely related Government procurement operation, the United States Government thereby incurs no responsibility nor any obligation whatsoever; and the fact that the Government may have formulated, furnished, or in any way supplied the said drawings, specifications, or other data, is not to be regarded by implication or otherwise as in any manner licensing the holder or any other person or corporation, or conveying any rights or permission to manufacture, use, or sell any patented invention that may in any way be related thereto.

ACCESSION for
CFSTI WHITE SECTION ☐
DDC BUFF SECTION ☑
UNANNOUNCED ☐
JUSTIFICATION
BY
DISTRIBUTION/AVAILABILITY CODES
DIST. AVAIL. and/or SPECIAL
2

This document is subject to special export controls and each transmittal to foreign governments or foreign nationals may be made only with prior approval of the Manufacturing Technology Division, MATB, of the Air Force Materials Laboratory, Wright-Patterson Air Force Base, Ohio 45433. Distribution of this report is limited because it contains technology identifiable with items on the strategic embargo list excluded from export or re-export under U.S. export act of 1948 (63 STAT.7) as amended (50 U.S.C. Appn. 2020-2031).

Copies of this report should not be returned unless return is required by security considerations, contractual obligations, or notice on a specific document.

DESIGN OF A PRODUCTION HYDROSTATIC EXTRUSION PRESS

G. E. Meyer
F. A. Simonen
J. C. Gerdeen
R. J. Fiorentino
A. M. Sabroff

This document is subject to special export controls and each transmittal to foreign governments or foreign nationals may be made only with prior approval of the Manufacturing Technology Division, MATB, of the Air Force Materials Laboratory, Wright-Patterson Air Force Base, Ohio 45433. Distribution of this report is limited because it contains technology identifiable with items on the strategic embargo list excluded from export or re-export under U.S. export act of 1948 (63 STAT.7) as amended (50 U.S.C. Appn. 2020-2031).

FOREWORD

This final technical report covers work performed under Contract No. F 33615-67-C-1434 from 1 March 1967 through 31 January 1968. It is published for technical information only and does not necessarily represent the recommendations, conclusions, or approval of the Air Force. The manuscript was released by the authors on 31 January 1968 for publication.

This contract with Battelle Memorial Institute of Columbus, Ohio was initiated under Manufacturing Methods Project 140-7, "Design Development for a Hydrostatic Extrusion Press". It was administered under the technical direction of Mr. Gerald A. Gegel of the Metallurgical Processing Branch (MATB), Manufacturing Technology Division, Air Force Materials Laboratory, Wright-Patterson Air Force Base, Ohio.

This project has been accomplished as a part of the Air Force Manufacturing Methods program, the primary objective of which is to implement, on a timely basis, manufacturing processes, techniques and equipment for the economical production of USAF materials and components. The program encompasses the following technical areas:

Metallurgy - Rolling, Forging, Extrusion, Casting, Composites, Powder

Chemical - Propellant, Casting, Ceramics, Graphite, Nonmetallics

Fabrication - Forming, Material Removal, Joining, Components

Electronics - Solid State, Materials and Special Techniques, Thermionics

Suggestions concerning additional Manufacturing Methods efforts required on this or other subjects will be appreciated.

The program was conducted at Battelle by the Metalworking Division with Mr. G. E. Meyer, Research Metallurgical Engineer, as project engineer and Mr. R. J. Fiorentino, Associate Chief, as program manager. Others contributing to the program were Mr. A. M. Sabroff, Chief, of the Metalworking Division and Mr. F. W. Boulger, Senior Technical Advisor of the Department of Process and Physical Metallurgy. Those contributing to the stress analyses of ultrahigh-pressure containers, stems, and dies were Dr. J. C. Gerdeen, Senior Research Mechanical Engineer, Dr. F. A. Simonen, Research Mechanical Engineer, and Dr. L. E. Hulbert, Chief of the Advanced Solid Mechanics Division.

Under subcontract, Bliss-Barogenics, Inc. of Mount Vernon, New York, contributed to the design and costing of the hydrostatic extrusion press and related equipment. Personnel at Bliss-Barogenics who participated in this program were Mr. F. G. Boggio, Production Manager, Mr. A. Moos, Press Designer, Mr. N. Kramarow, Assistant to the Vice President, and Mr. A. Zeitlin, Vice President.

H. A. Johnson

H. A. Johnson, Chief
Metallurgical Processing Branch
Manufacturing Technology Division

ABSTRACT

The overall objective of this program was to develop a design for a production hydrostatic extrusion press. The press was designed to use two high-pressure extrusion containers. One container would have bore dimensions 12-inch diameter x 120 inches long, capable of withstanding a fluid pressure of 250,000 psi. The other container would have a bore 6-inch diameter x 36 inches long, and would contain fluid at pressures up to 450,000 psi. A single press would be used to accommodate either container or both containers simultaneously to permit fluid-to-fluid extrusion. The designs were carried out in sufficient detail to permit a close estimate to be made of the construction and operating costs of the press. The approach to this design study involved evaluating the available tooling and press concepts before arriving at the concept that was refined in detail.

A literature survey supplemented with visits to high-pressure laboratories, was used to critically evaluate potential hydrostatic extrusion concepts and components that could be applied in this study. A survey was made of material suppliers and forging companies to establish the availability of large high-strength components that would be required to construct the large high-pressure containers designed in this program.

A 17,000-ton hydrostatic extrusion press was designed to pressurize both a 12-inch bore, 250,000 psi, multi-ring container and a 6-inch bore, 450,000 psi, fluid-supported container. The 6-inch bore, 450,000 psi container would be constructed by placing the 6-inch liner within the 12-inch container and using fluid at pressures up to 250,000 psi to support it. A dual ram hydraulic system on the press would be used to compress both the 450,000 psi and 250,000 psi fluids at the same time and in a suitable proportion. A materials handling system was designed for the press which could muzzle load up to about 35 billets per hour. A modification of the hydrostatic extrusion press was made so that, the extrusion press can be used for conventional as well as hydrostatic extrusion. Containers of various designs, stems, and dies were stress analyzed extensively.

An economic comparison was made between hydrostatic extrusion and conventional processing for various materials and for production of tubes and shapes. This analysis indicated that there were important areas in which hydrostatic extrusion techniques could produce close-tolerance products at a lower cost than conventional processing. Aluminum alloys could be extruded at a faster rate using hydrostatic rather than conventional extrusion techniques and this results in lower conversion costs. Other areas that may permit cost reductions are the production of thin-wall, seamless tubes and the re-extrusion of shapes to thin sections.

This document is subject to special export controls and each transmittal to foreign governments or foreign nationals may be made only with prior approval of the Manufacturing Technology Division of the Air Force Materials Laboratory, Wright-Patterson Air Force Base, Ohio 45433. Distribution of this report is limited because it contains technology identifiable with items on the strategic embargo list excluded from export or re-export under U.S. export act of 1948 (63 STAT. 7) as amended (50 U.S.C. Appn. 2020-2031).

TABLE OF CONTENTS

	Page
INTRODUCTION	1
General Background	1
Hydrostatic Extrusion at Battelle	1
Program Objectives	2
SUMMARY	4
SURVEY OF FACILITIES AND LITERATURE	7
Hydrostatic Extrusion Concepts	9
Basic Hydrostatic Extrusion Process	9
Augmented Hydrostatic Extrusion	11
Hot Extrusion Under Hydrostatic Pressure	13
Fluid-to-Fluid Hydrostatic Extrusion	13
Semicontinuous Hydrostatic Extrusion	16
Container Design Concepts	17
Analytical Study of Container Design Concepts at Battelle	17
Controlled-Fluid-Fill Container	21
Fluid-Support Multi-ring Container	23
Composite-Ring Container	23
Ring-Segment Container	23
Wire-Wrapped Multiring Container	25
Bridgman-Birch Container	25
Stem Design Concepts	25
DESIGN OF PRODUCTION HYDROSTATIC EXTRUSION PRESS	29
Preliminary Considerations	29
Hydrostatic Extrusion Press Description	30
Tooling Designs	43
Containers	43
Stems	46
Dies	48
Fluids and Seals	49
Press Description	52
Structure of the Press	52
Platens	52
Cylinders and Rams	52
Slip Cylinders	53
Press Supports	53
Alignment of the Press Elements	53
Container and Container Housing	54
Gate Lock Arrangement	54
Runout Table	54
Billet, Dummy Block, and Die Handling Arrangements	54
Saw	54

TABLE OF CONTENTS
(Continued)

Page

Hydraulic Systems Design. 56
Oil Hydraulic System 56
Water Hydraulic System 58
Electrical Equipment 59
Piping 60
Materials Handling System and Press Operating Sequences 61
Solid Extrusions From the 250,000 Psi Container. 65
Tube Extrusion From the 250,000 Psi Container. 67
Extrusion Drawing From the 250,000 Psi Container 71
Solid Extrusion From the 450,000 Psi Container 72
Tube Extrusion From the 450,000 Psi Container. 72
Fluid-to-Fluid Extrusion 76
Time Cycles for General Press Operations 80

ANALYSIS OF TOOLING. 87

Choice of Materials for Container Design. 87
Material Fatigue Strength Considerations 88
Fatigue Behavior of Thick-Walled Cylinders 92
Manufacturing Considerations 97
The Autofrettage Process. 97
Analysis of Multi-ring Containers 99
Multi-ring Container Designs for 250,000 Psi 99
Autofrettaged Multi-ring Container for 250,000 Psi 110
Fluid-Support Container Design for 450,000 Psi 117
Analysis of Additional Loading Effects in Liner 121
Pressure Discontinuity on Bore 121
Pressure Discontinuity on OD of Liner. 124
Stresses in Region of Notch (Seal) in Liner. 124
Analysis of Other Container Designs 127
Sectored Container With No Liner 127
Stem Analysis 130
Stem Buckling 130
Lateral Support of Stems. 133
Analysis of Composite Stems 134
Stem Misalignment 138
Design of Concentric Stems. 142
Required Length of Inner Stem. 142
Buckling of Inner Stem 144
Hoop Stress in Outer Stem. 145
Differential Poisson Expansion of Stems. 145
Tungsten Carbide as a Stem Material. 146
Die Design. 147
Assumed Die Loadings. 147
Calculated Results for Particular Die Designs 150
Die Design 1 150
Die Design 2 150

TABLE OF CONTENTS
(Continued)

Page

Die Design 3 153
Die Design 4 153
Die Design 5 153
Approximate Die Analysis. 153
Summary. 156
. 159

ECONOMIC ANALYSIS OF HYDROSTATIC EXTRUSION 160

Press and Average Conversion Costs. 162
Economic Analysis Applied to Various Materials. 167
AISI 4340 Steel. 167
Aluminum and Aluminum Alloys 172
Titanium and Titanium Alloys 176
Refractory Metals. 178
Nickel-Base Superalloys. 180
Beryllium. 182
Economic Analysis Applied to the Production of Tubing and Thin-Section Shapes 183
Production of Large-Diameter Thin-Walled Tubing. 183
Hydrostatic Extrusion Costs for Producing 10-Inch OD x 1/2-Inch-Wall Tubes 184
Shear-Forming Costs for Producing 10-Inch OD x 0.1-Inch Wall Tubes 187
Hydrostatic Extrusion Costs for Producing 10-Inch OD x 0.1-Inch Wall Tubes 188
Production of Large Thin Sections of a Moderately Complex Shape. 190
Costs for Hydrostatic Extrusion of Ti-6Al-4V Channels. 191
Costs for Conventional Processing of Ti-6Al-4V Channels. 193
Summary of the Economic Analysis 194

APPENDIX I

ESTIMATED TIMETABLE AND MILESTONE CHART FOR CONSTRUCTION OF A DUAL PURPOSE (HYDROSTATIC/CONVENTIONAL) EXTRUSION PRESS 197

REFERENCES 201

LIST OF TABLES

Table		Page
I	General Specifications of 17,000-Ton Hydrostatic Extrusion Press and a Dual-Purpose Press Capable of Both Hydrostatic and Conventional Extrusion	37
II	Hydraulic Power-Station Specifications for the 17,000-Ton Hydrostatic Extrusion Press With a Direct-Drive Oil Hydraulic System	38
III	Hydraulic Power Station Specifications for the 17,000-Ton Press With a Water Hydraulic System	39
IV	Ductility of Steels	98
V	Dimensions and Required Strengths of Rings for the 5-Ring Container	101
VI	Required Interferences for the 5-Ring Design	101
VII	Required Press Forces for Assembly of the 5-Ring Container	102
VIII	Dimensions and Required Strengths of Rings for the 7-Ring Container	103
IX	Required Interferences for the 7-Ring Design	103
X	Required Press Forces for Assembly of the 7-Ring Container	104
XI	Dimensions and Required Strengths of Rings for the 3-Ring Container With an Autofrettaged Liner	114
XII	Required Interferences for the 3-Ring Design	114
XIII	Required Press Forces for Assembly of the 3-Ring Container	115
XIV	Maximum Operating Stresses in Autofrettaged Multi-Ring Container	116
XV	Minimum Residual Stresses in Autofrettaged Multi-Ring Container	116
XVI	Results of Computer Calculation for First Pressure Cycle of Fluid-Supported Liners	120
XVII	Summary of Calculated Stresses in Leading Edge of Die Design 5 and Modifications A, B, and C for Large Billet/Bore Diameter Ratios	155
XVIII	Summary of the Costs to Construct a Hydrostatic Extrusion Press and a Dual Purpose Press of 17,000-Ton Capacity	163

LIST OF TABLES
(Continued)

Table		Page
XIX	Total Estimated Cost for an Extrusion Plant With a Hydrostatic Extrusion Press or a Dual-Purpose Extrusion Press of 17,000-Ton Capacity.	165
XX	Estimated Operating Costs for Hydrostatic Extrusion and Conventional Extrusion on the 17,000-Ton Dual Purpose Press.	166
XXI	Conditions Used in Economic Comparison of Conventional and Hydrostatic Extrusion of AISI-4340 Steels	168
XXII	Hydrostatic and Conventional Extrusion Costs for 4340 Steel as a Function of Die Life.	171
XXIII	Conditions Used in Economic Comparison of Conventional and Hydrostatic Extrusion of Aluminum Alloys.	173
XXIV	Hydrostatic and Conventional Extrusion Costs for Aluminum and Aluminum Alloys as a Function of Extrusion Exit Speeds	174
XXV	Conditions Used in Economic Comparison of Conventional and Hydrostatic Extrusion of Titanium Alloys.	177
XXVI	Hydrostatic and Conventional Extrusion Costs for Titanium as a Function of Die Life.	179
XXVII	Hydrostatic and Conventional Extrusion Costs for Molybdenum as a Function of Die Life.	181
XXVIII	Selling Price of Commercially Produced 10-Inch OD by 1/2-Inch-Wall Tubes and the Manufacturing Cost of a Similar Tube Produced by Hydrostatic Extrusion Techniques.	186
XXIX	Costs for Converting Various Materials to 10-Inch OD X 0.1-Inch Wall X 60-Inch Long Tubes by Shear-Forming and by Hydrostatic Extrusion.	189
XXX	Processing Costs of Ti-6Al-4V Titanium Alloy Channels Produced by Hydrostatic Extrusion Techniques and Channels Machined From Hot Extrusions	195

LIST OF ILLUSTRATIONS

Figure		Page
1	Basic Hydrostatic Extrusion Process	10
2	Schematic Diagram of an Augmented Hydrostatic Extrusion Design Concept Being Used by Fielding & Platt, Ltd. and United Kingdom Atomic Energy Authority (UKAEA) in England	12
3	Tooling Design Concept for Hot Extrusion Under Hydrostatic Pressure as Developed by Sauve	14
4	Fluid-to-Fluid Hydrostatic Extrusion	15
5	Schematic of High-Pressure-Container Design Concepts	19
6	Container Design Concepts	22
7	Container Designs Being Evaluated by Vickers Ltd (England) and ASEA (Sweden)	24
8	Commercial Bridgman-Birch Apparatus	26
9	Vickers' System for Support of Extrusion Stems of Large Length-to-Diameter Ratio	28
10	17,000-Ton Production Hydrostatic Extrusion Press	31
11	17,000-Ton Production Hydrostatic Extrusion Press Designed in Present Program	33
12	Sections of the 17,000-Ton Hydrostatic Extrusion Press Designed in Present Program	35
13	Fluid-to-Air Extrusion With 250,000 Psi Container	41
14	Fluid-to-Air Extrusion With 450,000 Psi Container	42
15	Design Information on 12-Inch Bore, 250,000 Psi Container	44
16	An Auxiliary Container Extension to Produce Long Extrusions Using Fluid-to-Fluid Techniques	47
17	Fluid-Injection Device and Ram Position During Fluid-Injection Sequence	50
18A	Material-Handling System - Billet and Die-Loading Sequence	62
18B	Material-Handling System - Extrusion, Die, and Butt-Unloading Sequence	63
18C	Material-Handling System - Sawing and Butt-Die Separation Sequence	64

LIST OF ILLUSTRATIONS
(Continued)

Figure		Page
19	Support Tube Assembly for Loading Billet Into a 6-Inch Container	66
20	Operational Sequence for Fluid-to-Air Extrusion of a 12-Inch Billet at 250,000 Psi	68
21	Operational Sequence for Fluid-to-Air Extrusion of a 6-Inch Billet at 450,000 Psi	73
22	Typical Arrangement for Fluid-to-Air or Fluid-to-Fluid Extrusion of Tubes From 450,000 Psi Container	75
23	Operational Sequence for Fluid-to-Fluid Extrusion of a 6-Inch Billet From 450,000 to 250,000 Psi	77
24	Operational Sequence for Fluid-to-Fluid Extrusion of a 6-Inch Billet From 450,000 to 100,000 Psi	81
25	Optimum Hardness for Maximum Fatigue Strength of Several Steels	89
26	Unnotched Rotating-Beam Fatigue Limit for Miscellaneous Heat-Treated Steels at Various Ultimate Tensile Strength Levels	91
27	General Trends in Fatigue Strength of Heat-Treated Steels as a Function of Ultimate Tensile Strength	91
28	Portions of Shear Stress Range Diagrams for En 25 Steel at 10^7 Cycles	94
29	Tensile Ultimate and Yield Strength Versus Temperature For AISI-4340 Steel Heated to 200,000 Psi	106
30	Tensile Ultimate Strength of AISI-H11 Alloy Steel Versus Temperature After Various Exposure Times	107
31	Tensile Ultimate and Yield Strength of 18Ni-9Co-5Mo Maraging 300 Steel Versus Temperature	108
32	Residual Hoop Stress in an Autofrettaged AISI 4340 Cylinder With Strain Hardening Effects	111
33	Residual Stresses in Autofrettaged AISI-H11 Steel Liners	113
34	Assumed Pressure Cycles on a Fluid Supported Liner	119
35	Liner and Assumed Discontinuous Pressure Loading on the Bore	122
36	Calculated Stresses for a Liner With a Discontinuous Pressure Applied to the Bore	123

LIST OF ILLUSTRATIONS
(Continued)

Figure		Page
37	Hoop and Axial Stresses in a Liner With Discontinuous Pressure Applied to the Outside Surface	123
38	Loading and Geometry of the Notched Liner	125
39	Detail of Assumed Notch Geometry	125
40	Calculated Contours of Maximum Shear Stress in Notched Liner	126
41	Multi-Ring and Sectored Container Design Concepts Analyzed	128
42	Stem Buckling Pressures Based on Euler and Tangent-Modulus Theories	132
43	Reduction in Load Capacity of Composite Stem Versus Solid Stem of Core Material	135
44	Reduction in Buckling Load of Composite Stem Versus Solid Stem of Core Material	135
45	Increase in Load Capacity of Composite Stem Versus Solid Stem of Core Material	136
46	Increase in Buckling Load of Composite Stem Versus Solid Stem of Sleeve Material	136
47	Composite Design for the 12-Inch-Diameter Stem	137
48	Axial Stress Rise on Stem Surface Due to Pressure Drop at Seal Position	139
49	Assumed Conditions of Stem and Container Misalignment	140
50	Bending Stress in 12-Inch Stem Due to Misalignment as a Function of Axial Stem Stress	140
51	Assumed Loading and Calculated Maximum-Shear-Stress Contours for Analysis of a Stem Seal	141
52	Concentric Stem Configuration Shown With Outer Stem Fully Extended and Inner Stem Fully Retracted	143
53	Concentric Stem Configuration, Shown With Inner Stem in Fully Extended Position	143
54	Die Design 1 - Basic Design Considered in Stress Analysis	148
55	Assumed Loading of Die Design 1 - During Hydrostatic Extrusion	148

LIST OF ILLUSTRATIONS
(Continued)

Figure		Page
56	Elastic Deformation of Die Design 1 During Hydrostatic Extrusion With and Without Fluid Support	151
57	Elastic Deformation of Various Die Configurations During Hydrostatic Extrusion With Fluid Support	152
58	Die Design 5, With Modifications A, B, and C	154
59	Elastic Deformation of Die Design 5 During Hydrostatic Extrusion With Fluid Support	154
60	Maximum Calculated Hoop Stress in Ring Die Compared to Billet Yield Strength as a Function of Percent Reduction in Area and Wall Thickness	158
61	Maximum Calculated Hoop Stress in Ring Die Compared to Fluid Pressure as a Function of Percent Reduction in Area and Wall Thickness	158

BLANK PAGE

DESIGN OF A PRODUCTION HYDROSTATIC EXTRUSION PRESS

by

G. E. Meyer, F. A. Simonen, J. C. Gerdeen,
R. J. Fiorentino, and A. M. Sabroff

INTRODUCTION

General Background

Hydrostatic extrusion is a method of extruding a billet through a die by the action of a pressurized fluid rather than by direct contact with a ram as used in conventional extrusion. The pressurized fluid completely surrounds the billet except at the die orifice. The liquid between the billet and the extrusion container essentially eliminates the billet-container friction and reduces the billet-die friction, which results in extrusion pressures that can be significantly less than corresponding values obtained in conventional extrusion. The pressurized fluid also permits the extrusion of very long billets independent of length-to-diameter (L/D) ratios and permits extrusion of irregularly shaped billets. The hydrostatic extrusion process was first attempted and described by Bridgman[1]*. The process has been developed further by various investigators in the USSR[2,3,4], UK[5,6,7], and USA[8,9,10].

Hydrostatic Extrusion at Battelle

Work on hydrostatic extrusion at Battelle was initiated in June, 1961, under Air Force Contract No. AF 33(600)-43328 and was continued on Air Force Contract No. AF 33(615)-1390 to ascertain the manufacturing capabilities of the process. The work on these contracts resulted in the construction of hydrostatic-extrusion tooling that has a chamber 2-3/8 inches in diameter by 20 inches long and is capable of operating at 250,000 psi at room temperature and at about 225,000 psi at 500 F. Some of the pertinent achievements on these programs were:

(1) Extrusion of high-strength materials such as AISI 4340 steel, Ti-6Al-4V titanium alloy, and 7075 aluminum alloys into rounds, shapes, and tubing at production speeds

(2) Establishment of the technology required for 500 F hydrostatic extrusion

(3) Optimization of critical process variables to produce quality extrusions at minimum pressures

---

* Numbers in parenthesis refer to references.

(4) Computer analysis of several high-pressure-container design concepts based on a fatigue-failure criterion

(5) Refinement of an extrusion-drawing technique suitable for production of wire and shapes

(6) Establishment of die-design concepts that permitted the cold extrusion of beryllium at a 4:1 extrusion ratio without cracking and without the need for fluid counterpressure.

As a result of these and other programs in the USA and throughout the world, there is a very strong interest in the use of the process for production purposes. However, before this can be done, there are many basic questions concerning tooling and the production aspects of the process which must be answered. Some of these are:

(1) What are the maximum pressure and temperature capabilities of the critical tooling components such as the container, stem, and die?

(2) What is the maximum billet diameter and length that can be accommodated?

(3) How many extrusions per hour can be made?

(4) What would the total press cost?

(5) How do the economics of the hydrostatic-extrusion process compare to other processes?

The logical approach to find answers to these and other pertinent questions was to conduct a design study of a hydrostatic production press. This is the final technical report on such a design study.

Program Objectives

The purpose of this program was to develop a design for a production ultrahigh-pressure hydrostatic extrusion press. The design was carried out in sufficient detail to permit a close estimate of the construction and operating costs of the press. This press was designed to use ultrahigh-pressure extrusion containers with the following design goals:

Container A

Bore size:	12-inch diameter x 120 inches long
Operating pressure:	250,000 psi
Operating temperature:	1000 F maximum
Fatigue life:	10^7 cycles

Container B

Bore size:	6-inch diameter x 36 inches long
Operating pressure:	450,000 psi
Operating temperature:	1000 F maximum
Fatigue life:	10^7 cycles

Consideration was given to designing a single press that will accommodate either container independently or both containers simultaneously to permit fluid-to-fluid extrusion.

The program was divided into three interrelated phases:

a) Phase I - Survey of Literature and High-Pressure Facilities

The objective of this phase was to determine and evaluate all the design concepts which have been or are being considered for the design of a hydrostatic extrusion press. This survey was implemented by visits to laboratories and industrial organizations active in high-pressure research and by a detailed review of pertinent literature.

b) Phase II - Investigation and Analysis of Design Parameters

In this phase, the critical tooling components were analyzed and the actual hydrostatic extrusion press and related components were designed.

c) Phase III - Investigation of Process Economics

The objective of this phase was to determine the probable process economics of the hydrostatic-extrusion operation based on the press designed in Phase II.

Bliss-Barogenics, Inc., of Mt. Vernon, New York, participated in Phases II and III as a subcontractor on this program.

SUMMARY

The objective of this program was to develop a design for a production hydrostatic extrusion press. The press was designed to use two high-pressure extrusion containers. One container would have a bore dimension 12-inch diameter x 120 inches long, capable of withstanding a fluid pressure of 250,000 psi. The other container would have a bore 6-inch diameter x 36 inches long and would contain fluid at pressures up to 450,000 psi. A single press would be used to accommodate either container or both containers simultaneously to permit fluid-to-fluid extrusion. The designs were carried out in sufficient detail to permit a close estimate to be made of the construction and operating costs of the press.

The results of the program are summarized briefly below:

(1) A design for a 17,000-ton production hydrostatic extrusion press was established and the costs of construction, operation, and billet conversion were estimated.

(2) Two high-pressure hydrostatic extrusion containers were designed. These containers are described as follows:

(a) 12-inch ID x 82.7-inch OD x 120 inches long (multi-ring design) with a pressure capability of 250,000 psi.

(b) 6-inch ID x 11-1/2-inch OD x 36 inches long (fluid-support design) with a pressure capability of 450,000 psi when placed in the 12-inch ID container and supported with 250,000 psi fluid pressure.

(3) The hydrostatic extrusion press would be capable of:

(a) fluid-to-air extrusion from either 450,000 psi or 250,000 psi.

(b) fluid-to-fluid extrusions from pressures up to 450,000 psi.

(c) combined extrusion and drawing operations (HYDRAW).

(4) Dual-ram press hydraulics systems would be used to independently pressurize the support fluid and the "working" fluid for the 450,000 psi container. The dual-ram system would also be used to control mandrels during tube extrusion and, in addition, could be used to supplement or augment the fluid pressure on the billet.

(5) Stress distributions resulting from seals located on the bore surface and on the stem were calculated. Both locations were shown technically feasible. The seal location on the bore was generally preferred and was used whenever possible.

(6) A materials handling system was devised which could handle up to 35 billets per hour (each 11-inch OD x 96-inches long) for the 12-inch ID container, or up to 47 billets per hour (each 5-inch OD x 24-inches long) for the 6-inch ID container.

(7) Detailed analysis of containers indicated that autofrettage techniques offer the possibility of producing high-efficiency containers which would have a wall ratio of 4 rather than the typical ratio of about 7 for standard multi-ring designs (wall ratio is defined as OD/ID). Limited experimental evidence obtained elsewhere, however, suggests that autofrettaging may lower fatigue life.

(8) Die wall stresses were analyzed and found to be quite high at the initial contact point of the billet. These stresses become critical for relatively small-angle dies since, as the billet diameter approaches the container diameter, the die wall at the initial contact point becomes quite thin. Under these conditions, the stresses are reduced to acceptable levels when die angles 60 degrees or more are used.

(9) The 17,000-ton production press designed for hydrostatic extrusion operations was estimated to cost $5,149,000 only. Installed in a plant with suitable support equipment, the cost was estimated to be $15,586,000.

(10) The 17,000-ton hydrostatic extrusion press was also designed for making conventional hot extrusions as well. Conversion from one process to the other is relatively simple, indicating that a press for hydrostatic extrusion need not be extremely specialized.

(11) A dual-purpose press capable of both hydrostatic and conventional extrusions was estimated to cost $7,062,000. The total cost for the press installed in a plant with suitable support equipment was estimated at $20,101,000.

(12) Conversion costs were determined for hydrostatic extrusion and conventional extrusion and were applied to particular materials and shapes.

(13) Large-diameter, thin-wall seamless tubes could be made much cheaper by hydrostatic extrusion than by conventional processing techniques. For example, hydrostatic extrusion was found to be potentially capable of producing a tube for about 85 percent less than the cost of shear-forming, which is currently the cheapest technique used to make large-diameter, thin-wall seamless tubes.

(14) Hydrostatic re-extrusion of hot-extruded titanium alloy shapes was found to be potentially less expensive (up to about 60 percent) than machining the final shape from a hot-extrusion.

(15) Aluminum alloys could be extruded faster with hydrostatic extrusion techniques than with conventional techniques and could result in lower conversion costs for those materials.

SURVEY OF FACILITIES AND LITERATURE

A survey was made of basic hydrostatic extrusion techniques and high-pressure tooling design concepts that could be applied in the design of a production hydrostatic extrusion press. Laboratories and high-pressure facilities were visited in Europe and the United States. The survey also included material suppliers and forging companies to determine the availability of high-strength materials for high-pressure tooling in the sizes required. The facilities visited and the types of information obtained are given below:

Facility	Personnel	Information Obtained
Vickers, Ltd. (England)	Dr. John Crawley	(1) Design concepts of prototype production hydrostatic-extrusion facility with 4.5-inch bore container for operation at 450,000 psi
ASEA (Sweden)	Mr. Anders Sandin Dr. Hans Lundstrom	(1) Design of 450,000 psi container with 3-1/8-inch bore (2) Latest hydrostatic-extrusion technology developments at ASEA
Fielding & Platt, Ltd. (England)	Mr. R. H. Green	(1) Design of production units of hydrostatic-extrusion tooling for operation at 110,000 psi
Centre d'Etude Nucleaires de Saclay (France)	Mr. Charles Sauve	(1) Results of hot extrusion under hydrostatic pressure (2) Evaluation of press designs for production operations
United Kingdom Atomic Energy Commission (England)	Mr. D. Green	(1) Design details of production hydrostatic extrusion press being fabricated by Fielding & Platt, Ltd. (2) Latest hydrostatic-extrusion technology developments at UKAEA

Facility	Personnel	Information Obtained
National Engineering Laboratory (Scotland)	Dr. H. Ll. D. Pugh	(1) Latest hydrostatic-extrusion technology developments at NEL (2) Evaluation of container-design concepts (3) Concepts for production tooling
University of Bristol (England)	Dr. J. Parry	(1) Fatigue characteristics of high-strength steels as related to use in high-pressure containers
University of Belfast (Ireland)	Prof. B. Crossland	(1) Fatigue characteristics of high-strength steels (2) Properties of materials under high pressure
British Non-Ferrous Metals Research Association (England)	Mr. John Crowther	(1) Ideas for utilization of the process
Commissariat A. L'Energie Atomique High Pressure Laboratory (France)	Dr. D. Francois Mme. Carpentier M. Schauffelberger	(1) Container design for high pressures (2) Effects of hydrostatic pressure on ductility
University of Birmingham (England)	Dr. P. B. Mellor Dr. A. N. Bramley	(1) Preliminary hydrostatic extrusion studies (2) Papers on container design by Imperial College
Watervliet Arsenal Watervliet, New York	Dr. B. Austin Mr. C. Nolan	(1) Container designs (2) Materials of construction (3) Hydrostatic extrusion techniques
Manlabs/Physmet Inc. Cambridge, Mass.	Mr. J. Harvey Dr. A. Kulin	(1) Container designs (2) Materials of construction (3) Stem support techniques
Harwood Engineering Walpole, Mass.	Mr. Keeler Mr. D. Newhall	(1) High-pressure pumps (2) Hydrostatic extrusion tooling design
Ladish Forging Co. Cudahy, Wisconsin	Mr. F. Kole[illegible]i Mr. T. Lilly Mr. W. Heckel	(1) Availability of large, high-strength components (2) Material properties

Facility	Personnel	Information Obtained
Midvale Heppenstall Co. Philadelphia, Penn.	Mr. H. Jackson Mr. M. Acker Mr. J. Weiger Mr. W. McClure	(1) Availability of large, high-strength components (2) Material properties
Allegheny Ludlum Steel Corp.	Mr. A. Booth Mr. W. Peterson	(1) Availability of large, high-strength components
Vasco Steel Company	Mr. R. Henry Mr. A. Bayer	(1) Availability of large, high-strength components
Latrobe Steel Company	Mr. B. [illegible]son Mr. J. Visconti	(1) Availability of large, high-strength components
Lukens Steel Company	Mr. J. King	(1) Availability of large, high-strength components
Kennametal, Inc.	Mr. G. P. McCleary	(1) WC components
General Electric Co. Carboloy Division	Mr. N. V. Monacelli	(1) WC components
Coors Porcelain Company	Mr. W. Wood	(1) Al_2O_3 components

Based on this survey, the following general analysis of basic concepts was made. Particular process details (seals, fluids, etc.) uncovered during the survey will be discussed, where appropriate, in the sections dealing with the design of the press.

Hydrostatic Extrusion Concepts

There are a number of approaches to the method of extrusion under hydrostatic pressure. Several of these are described in the following sections.

Basic Hydrostatic Extrusion Process

The basic hydrostatic extrusion concept is illustrated in Figure 1. This concept is analogous to conventional extrusion except that the force of the ram is transmitted entirely by the fluid. In the vertical position, gravity forces hold the billet in place and it is easy to load the chamber with fluid. Large extrusion presses, however, are generally built to extrude in a horizontal direction. In scaling-up the hydrostatic extrusion process, consideration must be given to the special problems of billet and fluid handling that are encountered in horizontal extrusion.

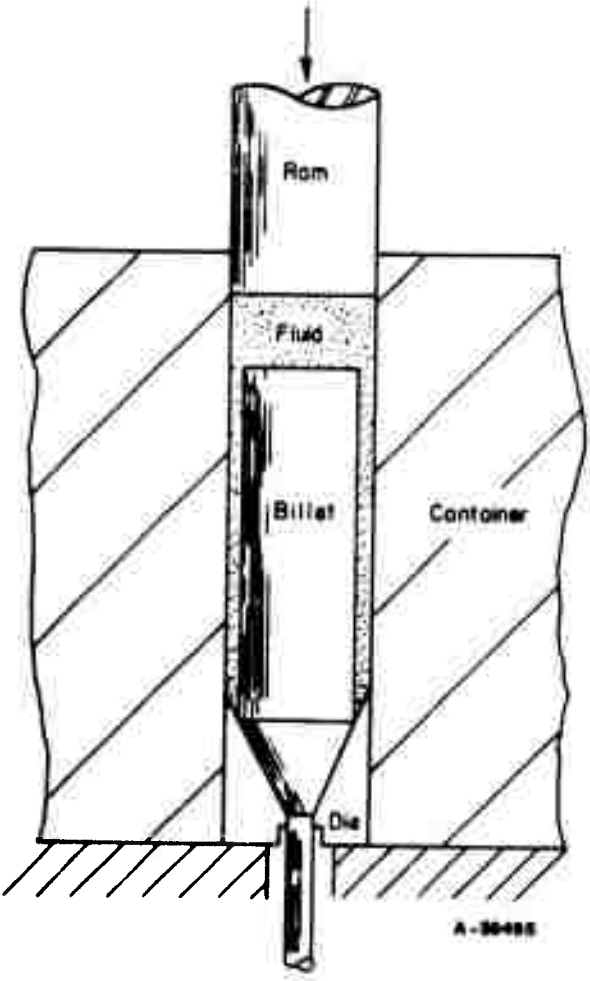

FIGURE 1. BASIC HYDROSTATIC EXTRUSION PROCESS

The tooling is commonly placed between platens of a press to generate the fluid pressure.

Augmented Hydrostatic Extrusion

A 1600-ton, horizontal, hydrostatic extrusion press has been built by Fielding and Platt, Ltd., Gloucester, England. In this design a portion of the extrusion force is transmitted directly to the end of the billet by the ram. For this reason, this technique has been named augmented hydrostatic extrusion. Figure 2 illustrates the basic design. As Ram 1 compresses the fluid in Container 1, the fluid pressure in Container 2 reaches an equal value. The difference between the force in Container 1 and the back pressure exerted by the fluid in Container 2 is applied directly on the end of the billet.

The relationships between the tooling geometry, fluid pressure, and the force applied to the end of the billet can be expressed:

$$P_b = P_f \left(\frac{A_1 - A_2}{A_3} + 1 \right) ,$$

where

P_b = pressure on the end of the billet

P_f = fluid pressure

A_1 = Area of Container 1 of bore diameter, d_1

A_2 = Area of Container 2 or bore diameter, d_2

A_3 = Area of the billet of diameter, d_3.

In a typical case where d_1 = 5 inches, d_2 = 4-3/4 inches, and d_3 = 4-5/8 inches, the augmented pressure, P_b, amounts to 11 percent more than the fluid pressure, P_f. Of course, the amount of pressure augmentation would increase as the billet diameter decreased and/or as $(A_1 - A_2)$ increased. However, the practical limit to P_b which can be applied above P_f is approximately equal to the compressive yield strength of the billet material. Beyond this limit the billet would upset plastically within the pressurized fluid.

An advantage of such a design is that the fluid pressure required for a given extrusion ratio is lower than that required by pure hydrostatic extrusion. This reduces the container-design problems. The intermediate ram also keeps the billet tight against the die to seal the extrusion chamber. The ram remains in contact with the billet throughout the extrusion operation, which is said to control the motion of the billet and prevent both stick-slip and rapid ejection of the billet.

Legend

Component	Cross-Sectional Area
Ram 1	A_1
Ram 2	A_2
Billet	A_3

where $A_1 > A_2 > A_3$

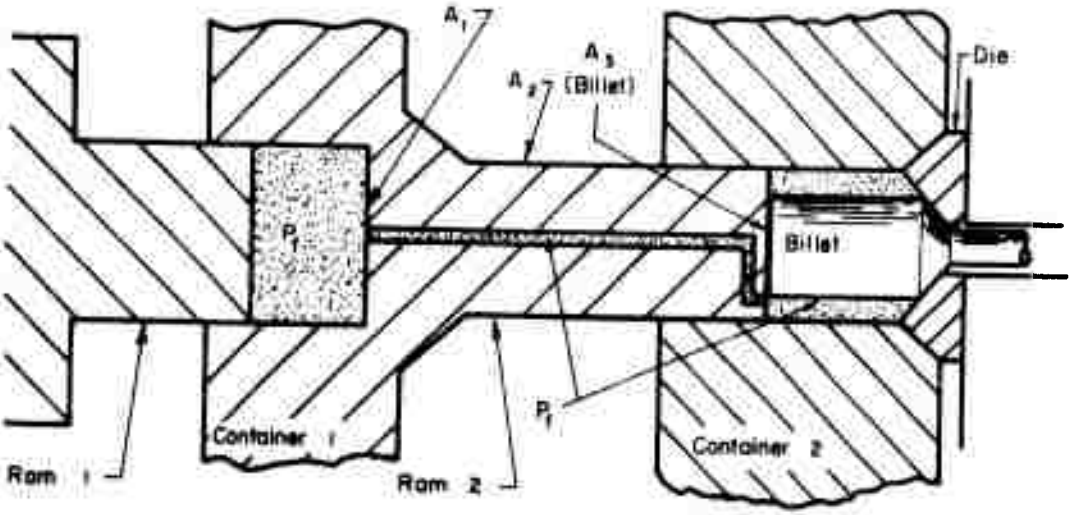

A-56496

FIGURE 2. SCHEMATIC DIAGRAM OF AN AUGMENTED HYDROSTATIC EXTRUSION DESIGN CONCEPT BEING USED BY FIELDING & PLATT, LTD. AND UNITED KINGDOM ATOMIC ENERGY AUTHORITY (UKAEA) IN ENGLAND

One major disadvantage of the design is that the pressure capability of the system is limited to that of Ram 2, which may require multi-ring, shrunk-fit construction in order to withstand pressures much above 180,000 psi. In effect, Ram 2 would be a third container. This appears to be an expensive penalty to pay for the advantages offered by the augmentation feature, especially at higher pressures.

Hot Extrusion Under Hydrostatic Pressure

Sauve at Services des Sciences, Saclay, France, has designed hydrostatic extrusion tooling as shown in Figure 3. Sauve's approach could be considered hot extrusion with lubrication under hydrostatic pressure. This technique was developed to insure pressurized lubrication during extrusion. The pressure medium, which is essentially graphite plus oil with additives, is solid at room temperature but liquifies immediately on contact with the heated billet and container. Mild steel, stainless steels, and tool steels have been extruded at billet temperatures of 1830 F, 2100 F, and 2190 F, respectively, with ram speeds as low as 18.8 inches/min without lubrication problems. A high-pressure relief valve located in Container 2 would permit the ram to remain in contact with the billet. The design details of the relief valve are not known.

One potential disadvantage of this approach, compared to hydrostatic extrusion at room or warm temperatures, is that the die (and mandrel) life would not be expected to be much better than that obtained in conventional hot extrusion.

Fluid-to-Fluid Hydrostatic Extrusion

Various designs have been proposed and constructed that permit an extrusion to be made from one high-pressure chamber into another chamber at a lower pressure. With these techniques, a metal can be processed entirely under compressive load, thus making it theoretically possible to extrude brittle materials without fracture. This concept, shown in Figure 4, has been used effectively by Pugh[5], Bobrowsky[10], Beresnev[2], and others. The technique, however, has several potential disadvantages which may limit its usefulness as a production process:

(1) The second container is costly

(2) The length of extrusion is limited to the length of the second container

(3) Comparatively, excessive time is lost in detaching the second chamber, removing the extrusion, and again locking the second chamber against the first to achieve a seal

(4) A very high pressure relief valve, or equivalent, is needed for the second container so as to keep the back pressure constant as the extrusion exits into the pressurized fluid

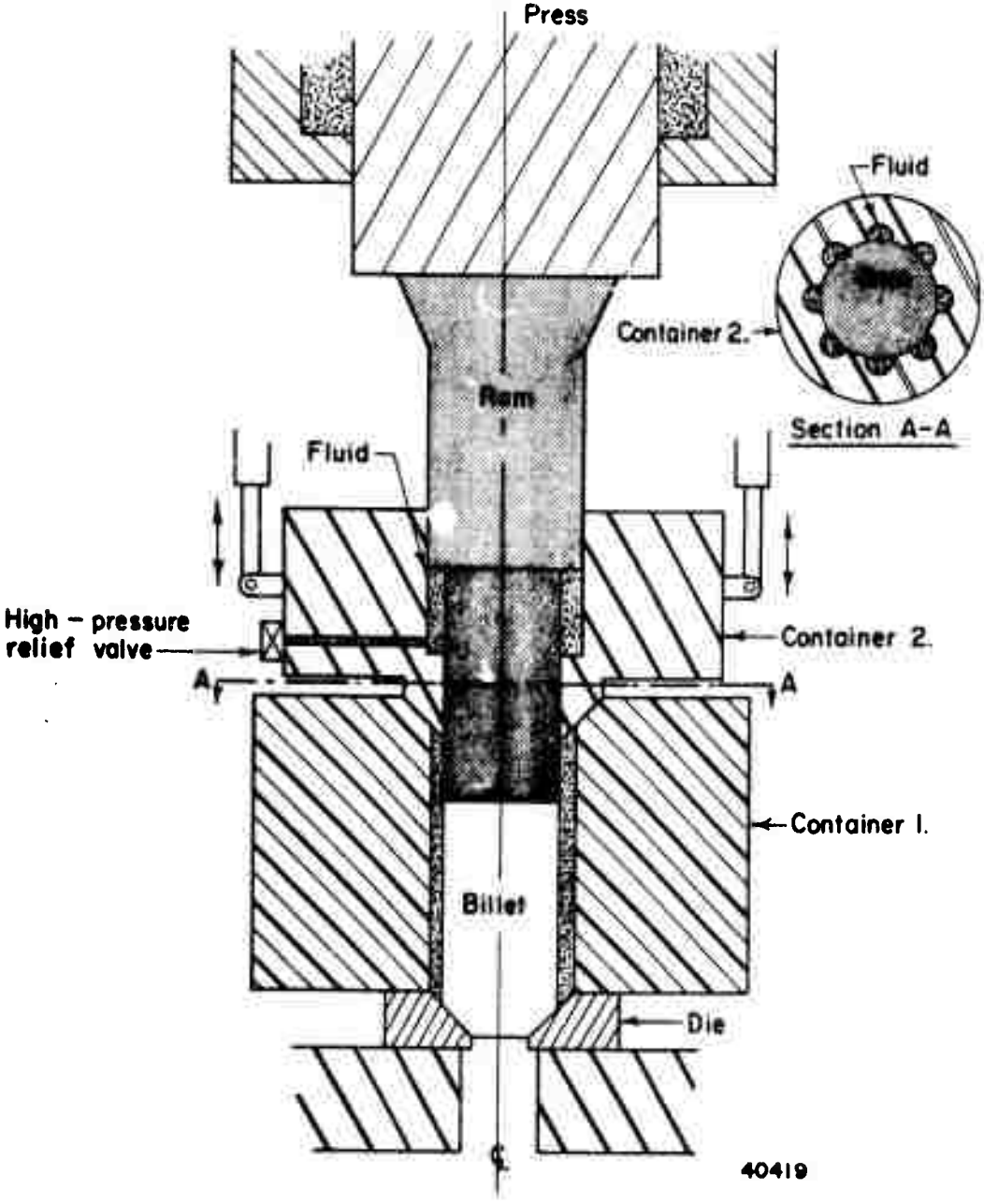

FIGURE 3. TOOLING DESIGN CONCEPT FOR HOT EXTRUSION UNDER HYDROSTATIC PRESSURE AS DEVELOPED BY SAUVE

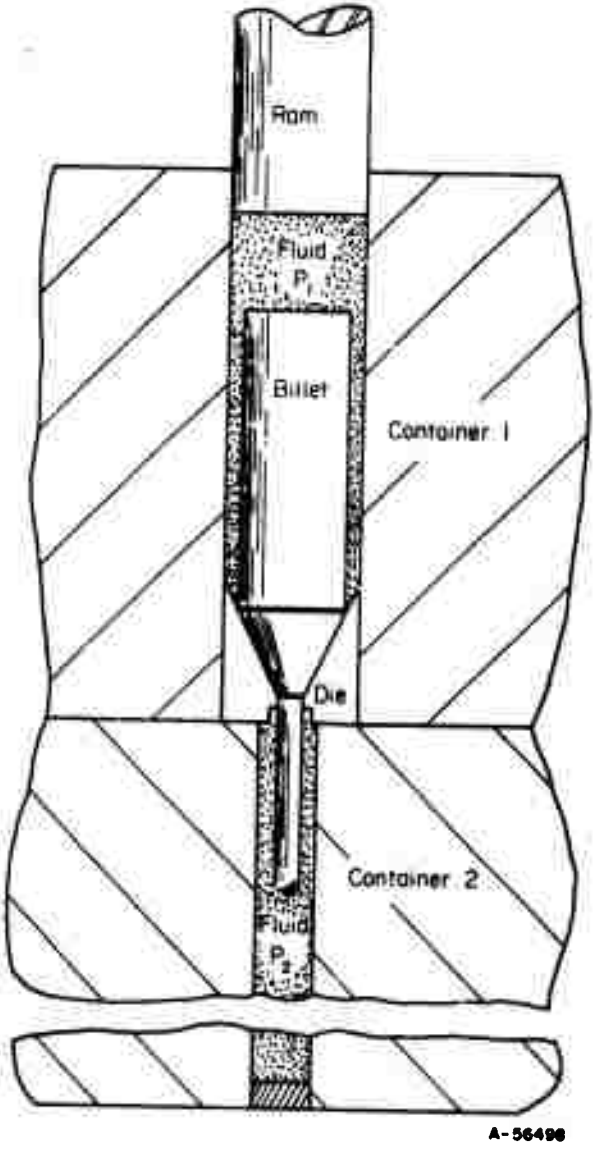

FIGURE 4. FLUID-TO-FLUID HYDROSTATIC EXTRUSION

Fluid pressure P_1 must be greater than fluid pressure P_2. Container 2 must be at least as long as the extrusion.

(5) The extrusion pressure must always be at a level greater than the normal "fluid-to-air" extrusion pressure by the amount of fluid back pressure that is applied.

It appears that these problems can be eliminated entirely by the use of special die-design concepts developed recently at Battelle[11]. Battelle has shown that with proper die design such brittle materials as beryllium can be hydrostatically cold extruded into the atmosphere (fluid-to-air) at a ratio of 4:1 without cracking. However, for some special materials and product shapes, it may still be desirable to use the principle of fluid-to-fluid extrusion. Therefore, consideration was given to incorporating this concept into the design of the production hydrostatic extrusion press evolved in this program.

Semicontinuous Hydrostatic Extrusion

In semicontinuous hydrostatic extrusion, the billet material is fed through a high-pressure seal when the container is at a relatively low pressure. Usually, enough material is fed into the chamber to form several coils if the incoming stock is of such diameter that it can be coiled. Then the fluid pressure is raised until the material extrudes. When the stock in the container becomes straight, there is no driving force to cause further extrusion and extrusion stops. The fluid pressure is lowered, more stock is fed into the container, and the process is repeated. This technique has been applied to relatively soft wire by Lengyel and Alexander[12]. Recently, Slater and Green[13] described a modification of the process by which it was possible to semicontinuously extrude copper and mild steel bar stock without bending the incoming stock. In this case, the force to extrude the bar stock is achieved by a gripping device which is moved forward and backward intermittently by fluid pressure. This process has been applied at relatively low fluid pressures, estimated to be in the range of 180,000 psi. While the concept of semicontinuous hydrostatic extrusion seems attractive at first glance, especially from a production viewpoint, there appear to be a number of potential disadvantages:

(1) Because of the gripping device, the process may be limited to handling round billet stock only, and handling of shapes of even moderate complexity may not be possible.

(2) Thus, the semicontinuous process would be limited in general to making of rounds and simple shapes, which perhaps could be made more economically by hot or cold rolling.

(3) Intermittent restarting of the extrusion will require overcoming very high breakthrough pressures each time, particularly for materials difficult to lubricate.

It seems, therefore, that the process may be one of fairly limited application, and that the gripping device and its controls are special tooling not common to that required for hydrostatic extrusion. For these reasons, the semicontinuous method was not considered in the design of the production hydrostatic extrusion press for the current study.

Container Design Concepts

Limitations are imposed on the construction of large-bore, ultrahigh-pressure containers by both material strength and manufacturing technology. The engineering materials generally used are high-alloy tool steels and carbides. Single-component or monoblock containers are limited in pressure capability to a maximum of about 200,000 psi. To exceed this level, it is necessary to design a multicomponent container with the intent of producing a high compresive hoop prestress in the liner. Through this approach, it is possible for a given liner material to support a much higher internal pressure without failure than would be possible in a monoblock system. The method of achieving the compressive hoop prestress includes shrink-fitting several concentric rings, supporting by fluid pressure or wire-wrapping the liner under high tension. The bore of the liner may also be strengthened by autofrettage. The liner is subjected to the full bore pressure and is the mostly highly stressed component in a container.

To design a container system that can withstand a target pressure of 450,000 psi, it is necessary that the compressive hoop prestress applied to the liner be in this same order. Because of its high compressive strength, tungsten carbide liners have been used at pressures up to about 500,000 psi. However, the cost of very large liners of tungsten carbide is very high. Therefore, for large-bore systems, it is desirable from an economic standpoint to make the liners out of very-high strength steel.

To achieve the high compressive prestresses required on the liner bore, the OD of the container may very well be on the order of 8 times the liner ID. Thus, for liner bores of 12 inches, the container OD may be in the order of 8 feet. The problems of manufacture are increased considerably as the container length increases. Also, the outer components can get so massive that this could present serious problems in heat treatment, machining, and, perhaps, transportation.

In view of these potential problems, it seemed worthwhile to determine and compare various container design concepts on the basis of probable pressure capability, size efficiency (OD/ID ratio), ease of manufacture, and ease of operation.

Analytical Study of Container Design Concepts at Battelle

The purpose of this study (conducted under Contract No. AF 33(615)-1390) was to determine the maximum pressure capability of several container design concepts for potential use in hydrostatic extrusion and forming processes. Containment of bore fluid pressures up to 450,000 psi at room temperature and above were considered.

In the initial phase of the study, four container design concepts were examined and analyzed in detail[14]. These concepts were:

(1) Multi-ring
(2) Ring-segment
(3) Ring-fluid-segment
(4) Pin-segment.

Figure 5 illustrates each container design studied.

In the multi-ring container shown in Figure 5a, successive rings have to be shrink-fitted to induce compressive stresses in the bore. This was one of the first design improvements which permitted exceeding the capacity of a simple, one-piece thick-wall cylinder. The design concept was analyzed extensively by Manning[15, 16, 17] and has been used widely in high-pressure applications. Machining the component rings to close tolerances and assembling the rings with interference fits are operations that become progressively more difficult as the diameter, length, and number of rings increase.

The ring-segment container with only one outer ring was patented by Poulter in 1951.[18] This concept, modified by the addition of a second outer ring, is shown in Figure 5b. The additional ring, which is assembled with an interference fit, improves the overall efficiency of the design and permits the containment of higher pressures. The intent of this design is to use the segments to redistribute the high unit pressure at the bore over a larger surface area at the outer rings. The segments, therefore, act as deintensifiers. Obviously, the segment components cannot withstand any hoop stresses which must be withstood by the outer rings. The inner cylinder is always subject to the full bore pressure, which limits the design strength to the strength of the inner liner.

A ring-fluid-segment container, as illustrated in Figure 5c, makes use of fluid pressure to develop the necessary compressive prestresses in the bore. The outer part of the container is subjected only to the fluid pressure, which can theoretically be varied with the bore pressures to minimize bore stress over an entire pressure cycle. The origin of using a pressurized fluid as a support medium is not clear. Manning[15] referred to a pump designed by the Clark Brothers Company in which the pressurizing cylinder was surrounded by the fluid at delivery pressure. While Manning mentioned that there were other obvious applications of this technique he did not elucidate further on the subject. Pugh and Ashcroft described a fluid-support container and applied it to hydrostatic extrusion in 1962[5]. Gerdeen suggested a fluid-support multi-ring container in March, 1965, and, independently, Meissner[19] received a patent on a very similar design in December, 1965. Meissner's patent application date was October, 1963.

The first application of fluid support to ring-fluid-segment container design is also not clear. Ballhausen[20] patented an approach of this sort in 1963. Another application of the principle was patented by Gerard and Brayman[21], also in 1963. A similar design with additional features was reported by Fuchs[22] in 1965.

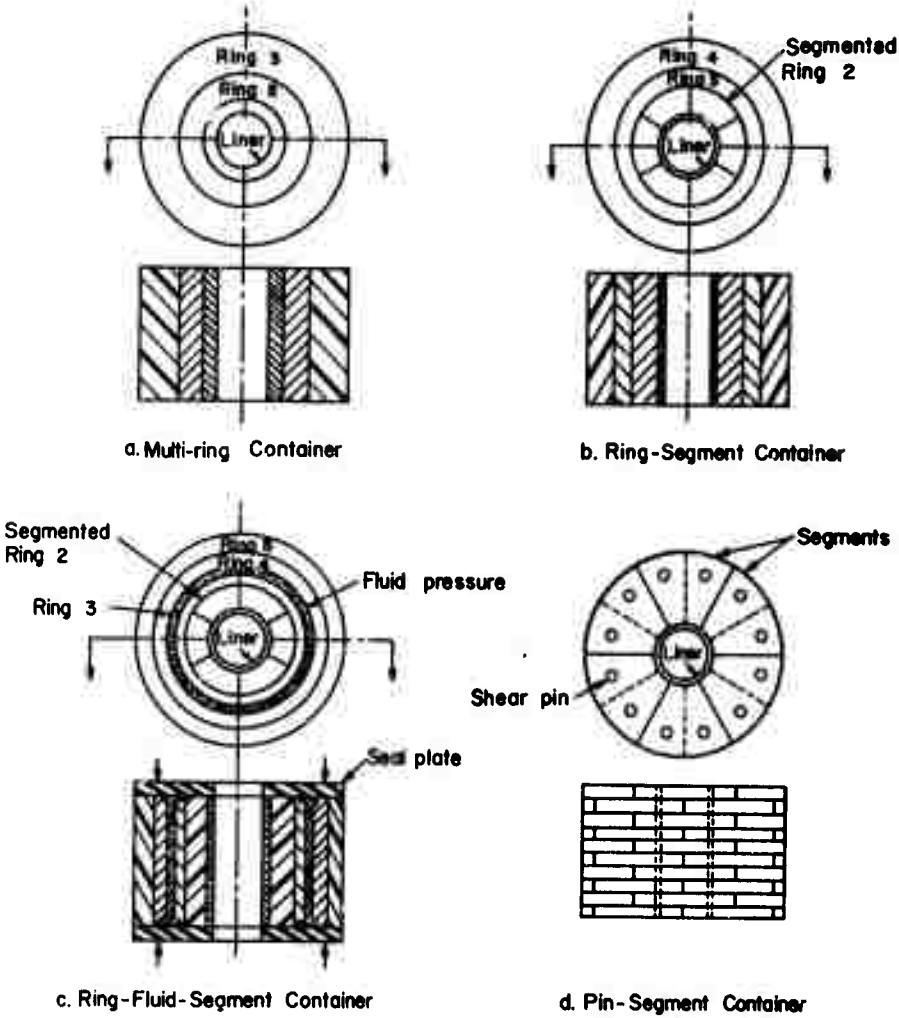

FIGURE 5. SCHEMATIC OF HIGH-PRESSURE-CONTAINER DESIGN CONCEPTS

A pin-segment design, as represented in Figure 5d, was proposed by Zeitlin, Brayman, and Boggio[23]. Like the ring-segment container this pin-segment design uses the segments to reduce the pressure that must be carried by external supports. The pin-segment design uses segmented discs rather than segmented cylinders. External support of the segments is provided by shear pins rather than by an external ring.

During the operation of a hydrostatic extrusion press the container-bore pressure is cycled between a high pressure level and zero pressure for each extrusion. This cyclic operation combined with the high-operating-stress levels make it likely that the container will fail in fatigue.

Thus, a fatigue-failure criterion was developed and applied in this analysis rather than the more commonly used shear-strength analysis. The analysis resulted in the following theoretical pressure limits for a life of 10^4 to 10^5 cycles:

Container Design	Maximum Pressure, psi
Multi-ring	300,000
Ring-segment	300,000
Ring-fluid-segment	1,000,000
Pin-segment	210,000[a]

[a] This assumed no prestress on the liner bore. With prestress, the pressure capability should be closer to that for the multi-ring or ring-segment containers.

These predictions are based on fatigue criterion using materials with ultimate tensile strengths of 300,000 psi for the liner and 200,000 psi for the outer support components, and apply to any operating temperature provided these are the strengths at temperature.

If liners are used with ultimate tensile strengths much greater than 300,000 psi, the theoretical maximum-pressure capability of the various designs may be improved appreciably. To fully utilize these higher strength liners, it must be assumed that they would exhibit the same fatigue behavior as steels with ultimate tensile strengths of 300,000 psi and, further, that ductile outer rings with strength levels greater than 200,000 psi would be available in the sizes required.

The theoretical pressures for each design have little or no practical meaning if the containers are impossible to construct because of their extreme size. Calculations were made for each design to determine the outside diameters that would be required to construct containers with 6-inch and 15-inch bores. The results of the calculations are:

	Outside Diameter, inches	
Container	6-Inch-Bore Design	15-Inch-Bore Design
Multi-ring	51.0	127.5
Ring-segment	60.0	150.0
Ring-fluid-segment	229.5	573.5
Pin-segment	90.4	180.2

Long integral cylinders approaching 50 feet in diameter are currently impossible to machine, heat-treat, or transport. Therefore, to compare the various designs on a more uniform and meaningful basis, an arbitrary, but practical, outside-diameter limit was established at 72 inches. The pressure capability of each design based on this OD limit and on a 10^4 to 10^5 cycles life are:

Container	Bore Diameter, inches	Outside Diameter, inches	Number of Components, N	Maximum Pressure P, psi
Multi-ring	6	51.0	5	300,000
	15	72.0	7	275,000
Ring-segment	6	60.0	6	290,000
	15	72.0	8	265,000
Ring-fluid-segment	6	72.0	10	286,000
	15	72.0	5	118,000
Pin-segment	6	72.0	3	195,000[a]
	15	(b)		

(a) Pressure capability would be greater with prestress on liner.

(b) Impossible to make for a life of 10^4-10^5 cycles unless liner is prestressed.

These values were calculated for particular container geometries and/or support pressures which were described in detail in Reference (12). On the basis of this analysis, it appears that the multi-ring concept may be the most efficient of the four concepts when considered from the standpoint of pressure capability and size.

Controlled-Fluid-Fill Container

Berman[24] proposed a controlled-fluid-fill container shown in Figure 6a. Like the ring-segment-fluid container, this container also uses the fluid-pressure support principle. It is assumed that each ring is made of identically ductile material and that a shear-strength-failure criterion applies. As the pressure in the bore is increased, the pressure in each support chamber is increased by use of independent pumps. The advantage of this design is that when the bore pressure is zero there are no residual stresses on the bore. Furthermore, there are no critical machining or assembling operations required. While these are attractive features, the prospects of supplying and controlling fluid in several annuli at fluctuating pressures make this design appear too complex for a production operation.

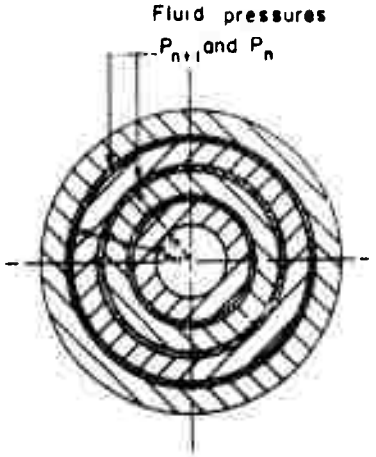

a Controlled Fluid-Fill, Cylindrical-Layered Container

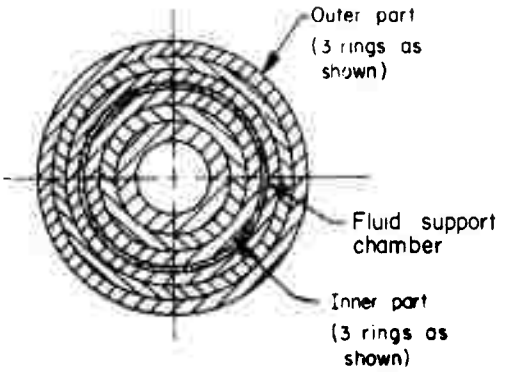

b. Fluid-Support Multi-ring Container

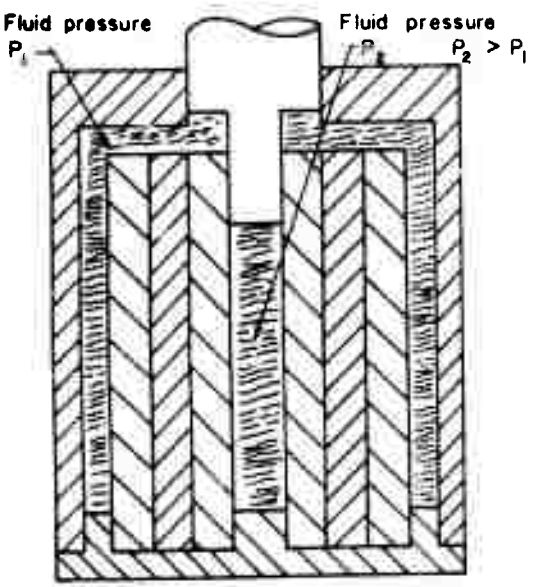

c. Single Ram, Fluid-Support Multi-ring Container

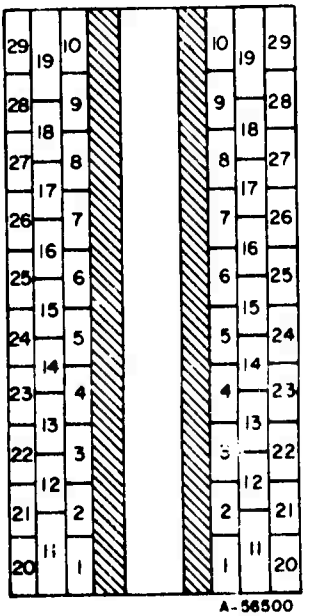

d. Composite Ring Container

FIGURE 6. CONTAINER DESIGN CONCEPTS

Fluid-Support Multi-ring Container

Gerdeen[14] suggested and analyzed a fluid-support multi-ring container. This design is shown in Figure 6b. The use of shrink-fitted rings to provide compressive prestress reduces the size and number of support annuli required by a pure fluid-support design as described in the previous section. Calculations indicated that the internal chamber could withstand 450,000 psi with 250,000 psi fluid pressure in the supporting annuli. Control of the pressure in one annulus is straightforward, especially when compared to the prospects of controlling several fluctuating pressures in several annuli simultaneously, as required in the design above.

Meissner received a patent[19] for the container design shown in Figure 6c. One ram pressurizes both fluid chambers. The fluid pressure differential between chambers is controlled by varying the physical dimensions of each chamber or by using two fluids having different bulk moduli.

Composite-Ring Container

A method of construction which could be used for manufacturing very long high-pressure cylindrical containers was described by Alexander and Lengyel[25] and is shown in Figure 6d. The inner liner would be made of a material with high compressive strength and machined with a 1 to 2-degree taper on the outside diameter. Several layers of high-strength rings would then be pressed into position in a staggered pattern as shown. Advantages of this design are that it is cheaper to produce a large number of small, forged rings than one large cylinder, and that heating or cooling elements possibly could be embedded in the rings. However, the assembly of such a container still could be quite difficult. Moreover, the effect of the joints in the support rings on the pressure capability and fatigue life of the liner must be determined experimentally or analytically before a container of this design could be considered.

Ring-Segment Container

Vickers Ltd. has developed the container tooling shown in Figure 7a[26]. It is designed for use up to 450,000 psi. A feature of this design is that pressure is transmitted from the liner through pie-shaped, relatively thin segments, to full-length longitudinal segments and then to shrink rings. The liner will have a 4.5-inch bore and will be made from tool steel heat treated to a hardness of R_c62-64. The inner segments are made from tungsten carbide, which was selected for this application because of its high compressive strength and elastic modulus. An assumption is made in this design that the liner does not act as a structural member. The design analysis was based on a shear-strength criterion. A sub-scale model of this design is in the process of being evaluated.

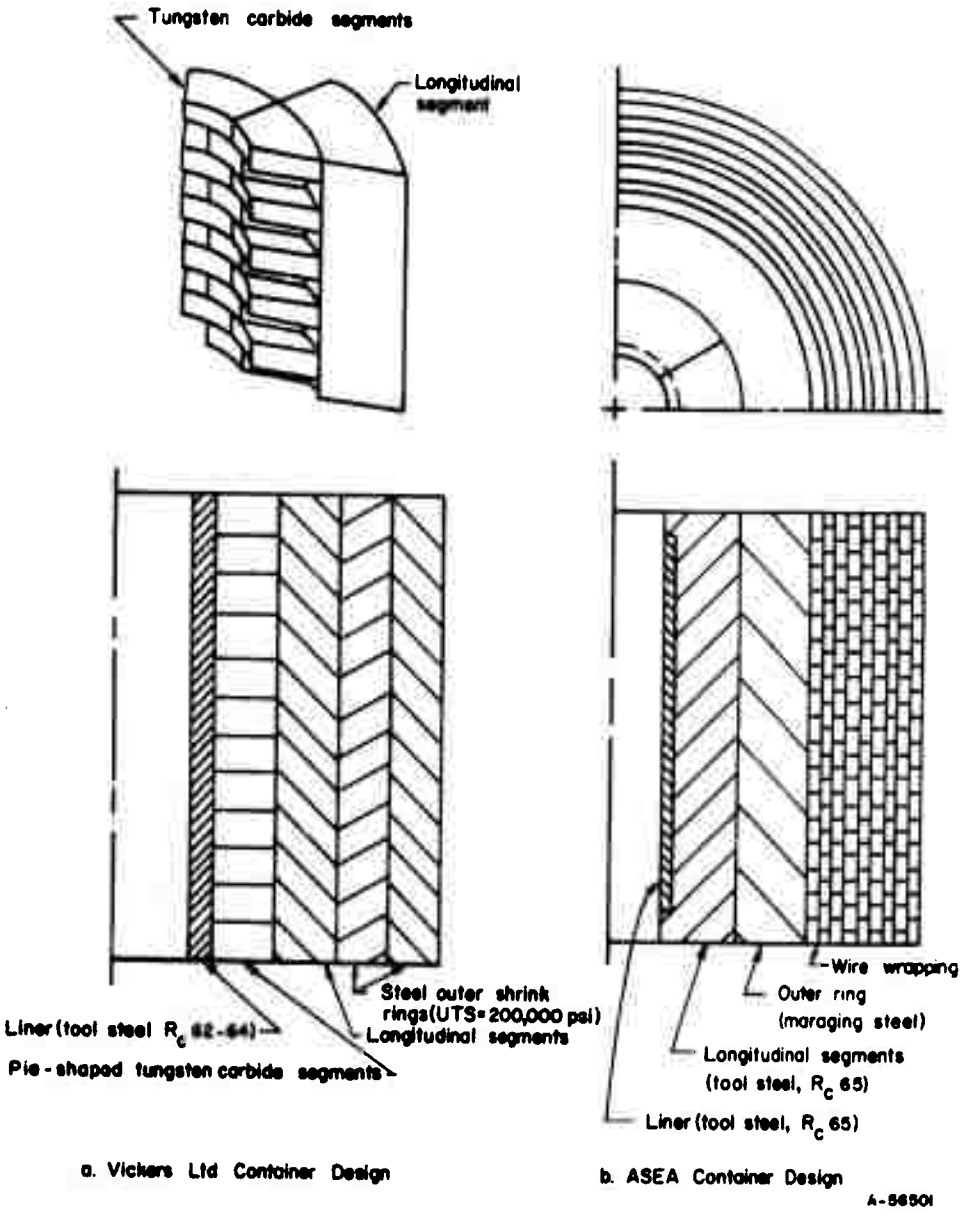

FIGURE 7. CONTAINER DESIGNS BEING EVALUATED BY VICKERS LTD (ENGLAND) AND ASEA (SWEDEN)

Wire-Wrapped Multiring Container

A container as shown in Figure 7b has been designed and built by ASEA, Sweden[27] for use at pressures up to 450,000 psi. The bore is nominally 2.4 inches. The liner and first support ring are constructed from high-speed steel, both heat treated to a hardness of R_c65. The second support ring is made from maraging steel. The entire assembly is wrapped with high-strength wire. Sufficient tension was applied to the wire during the wrapping operation to develop 500,000 psi compressive prestress on the liner bore. ASEA has found that this design is satisfactory for pressures up to about 300,000 psi but liner failures have been experienced at pressures near 450,000 psi.

Bridgman-Birch Container

Figure 8 shows the Bridgman-Birch container design, described by Newhall and Abbot[28], adapted to hydrostatic extrusion up to 450,000 psi fluid pressure, for either fluid-to-air or fluid-to-fluid. As the fluid pressure increases in the bore, the bottom ram forces the tapered liner into the support ring and thereby causes progressive support of the liner. The support ring is made of a single piece of autofrettaged high-quality steel, likely of a maraging variety. This construction apparently results in a good fatigue life since it was claimed that the useful life of the tools is limited by scoring of the liner bore by the stem seals.

It is important to mention that in this particular design the force required to position the tapered liner into the support ring is always greater than the force required to pressurize the liquid. This condition makes it economically impractical to scale up this concept to the sizes required in this study. For example, using this concept, the press in this design study would have a capacity of at least 30,000 tons rather than the 14,000 tons calculated from simple pressure-area relationships.

Stem Design Concepts

One of the advantages of hydrostatic extrusion is that very long billets can be extruded. However, to extrude long billets, stems of unusually high length-to-diameter (L/D) ratios must be used and this could present a stem buckling problem. An analysis of the buckling problem will be presented in a later section.

In the hydrostatic extrusion process the stem does not have to be as long as the billet. This departure from conventional practice is caused by the difference in cross-sectional area between the stem and the billet. The stem can be assumed to have a cross-sectional area A_1 and the billet an area A_2, where $A_1 > A_2$. This is the normal case in hydrostatic extrusion since a fluid has to be present between the billet and the chamber wall. When the stem moves

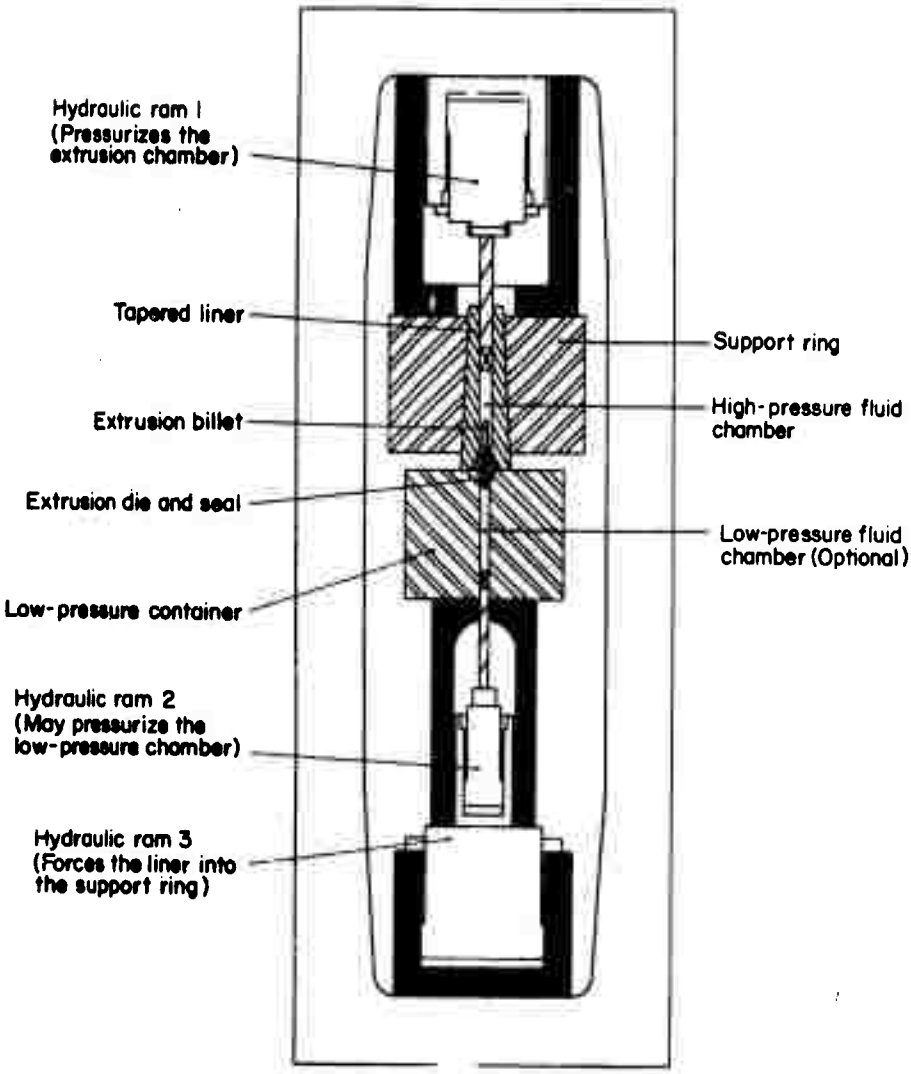

FIGURE 8. COMMERCIAL BRIDGMAN-BIRCH APPARATUS

As shown the equipment could be used for fluid-to-fluid hydrostatic extrusion or fluid-to-air hydrostatic extrusion.

a distance L_1, it displaces a volume of liquid A_1L_1. The billet must move a distance of L_2 to result in an equal displacement. Therefore, extrusion-stem length as a function of billet length is:

$$L_1 = \frac{A_2 L_2}{A_1} \quad .$$

Since A_1 is always greater than A_2, L_1 will always be less than L_2. This analysis neglects small changes in fluid volume due to any pressure fluctuation that might occur during billet extrusion.

Vickers [29] has developed and tested a model of the stem-support system shown in Figure 9. This stem support system has been described in detail by Crawley, Pennell, and Saunders[29]. The tie rods are pretensioned and act to support the main ram, which is free to slide in the conventional manner. The tie rods prevent primary buckling at stress levels considerably above those predicted by Euler buckling theory. A ram 1-1/4-inch in diameter x 60 inches long (L/D = 40) supported by the three rams pretensioned to 11,000 psi was reported to be able to withstand nearly 2.5 times the load which caused an identical unsupported ram to buckle. This appears to be a technically feasible solution to the ram-buckling problem, but the expense of incorporating it into a press design may or may not be excessive, depending on the specific applications of the press.

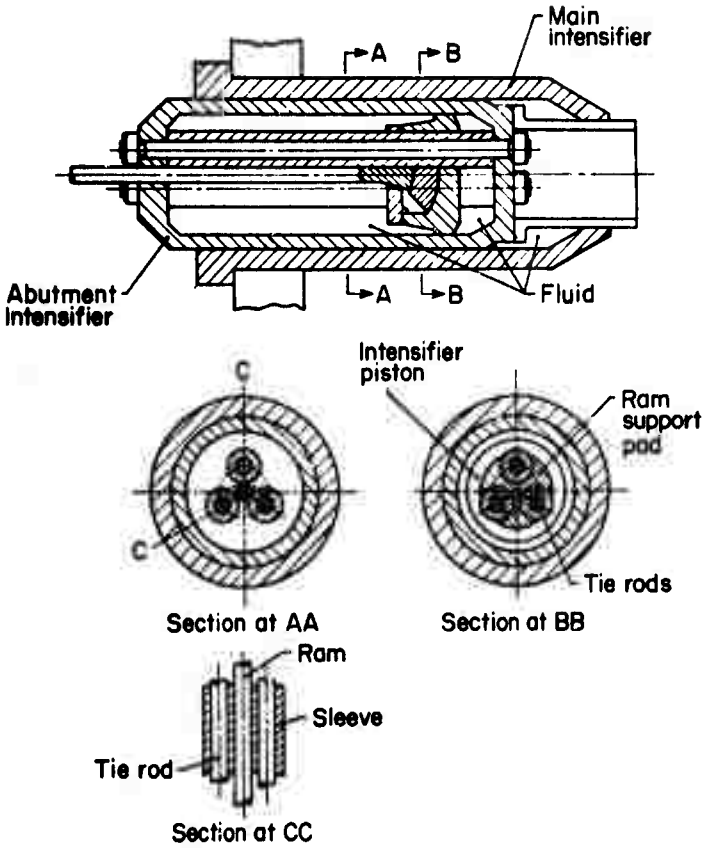

FIGURE 9. VICKERS' SYSTEM FOR SUPPORT OF EXTRUSION STEMS OF LARGE LENGTH-TO-DIAMETER RATIO

DESIGN OF PRODUCTION HYDROSTATIC EXTRUSION PRESS

Preliminary Considerations

In the design of this ultrahigh-pressure hydrostatic extrusion press, there are two basic items that were considered fixed at the beginning of the program:

(1) Hydrostatic extrusion concept
(2) Container sizes and pressure capacity
  (a) 250,000 psi - 12-inch bore x 120 inches long
  (b) 450,000 pso - 6-inch bore x 36 inches long

Once the concepts were decided upon and the basic operational needs defined, the general design of the press took shape. It remained then to design the press hydraulics, materials handling system, and auxiliary tooling to meet the operational requirements of the press.

The relative merits of the various hydrostatic extrusion techniques were compared in order to select a concept for the proposed press. Among the factors which weighed heavily in the selection were flexibility, diverse extrusion-product capability, potential product needs of the Air Force, and equipment cost. After considering the various possibilities, it was decided to use the basic hydrostatic extrusion concept as shown in Figure 1. The UKAEA design with the augmentation feature was considered to be too limited in its application and not very amenable to quick modification for various product needs such as tubing. The CEA method by Sauve for hot extrusion under pressurized lubrication also appeared specialized and did not seem to offer many advantages beyond those of conventional hot extrusion. In addition, it posed the problem of using high-pressure relief valves in the container.

On the basis of a study of container design concepts, multi-ring construction was selected from the standpoint of pressure capability, size efficiency, good prior experience, relative ease of fabrication, and cost. Contacts with steel and forging companies revealed that ring components for the 250,000 psi, 12-inch bore container could be made in the sizes and at the strength levels required. This was not the case for the 450,000 psi, 6-inch bore container. Here, commercially available materials for the outer support rings could not meet the strength requirements. Therefore, it was necessary to consider an alternative design.

The ring-fluid-ring container concept was finally selected for the 450,000 psi operation because it was considered less complex and costly than the other designs thought to be capable of withstanding this pressure. Gerdeen (14) reported that a fluid-support pressure of 250,000 psi would provide adequate support to a single component liner subjected to 450,000 psi fluid pressure. Thus, it was thought that the 6-inch liner could reside inside the 12-inch container and the annulus between them could be pressurized to 250,000 psi to provide the necessary external support to the liner.

A dual, concentric ram concept with two independently controlled hydraulic systems was selected as the method to control the fluid pressure variations required by this concept. (For example, the ability to increase and decrease fluid-support pressure in proportion to the bore pressure promotes better fatigue life). In addition to this function, the dual-ram system offers the added advantages of mandrel manipulation and control during tube extrusion, and pressure augmentation to the 250,000 psi container system.

Hydrostatic Extrusion Press Description

The production hydrostatic extrusion press designed in this program will be described and features of key components discussed in this section. In subsequent sections, details will be presented of the analyses of the containers, stems, dies, and hydraulics.

The proposed hydrostatic extrusion press design is of the horizontal type, rated at 17,000 tons, and is generally similar in design to a conventional extrusion press with a mandrel manipulator. A dual-ram system is used to separate the available tonnage into 6400 tons for the center ram and 10,600 tons for the outer ram. Billets are loaded from the die end of the press, a technique commonly called muzzle loading. The hydrostatic extrusion press is shown in a cut-away pictorial view in Figure 10 and in longitudinal cross-section assembly drawing in Figure 11. Additional design details are shown in various transverse cross sections in Figure 12. The general specifications for the press and power station are summarized on Tables I and II, respectively. Corresponding specifications for a similar press capable of both hydrostatic and conventional extrusion are also shown on Table I for comparison. This dual-purpose press design was developed from the basic hydrostatic extrusion press design and was used in the economic analysis section to determine comparative conversion costs for conventional extrusion. The dual-purpose press concept illustrates that there exists relatively few differences between a hydrostatic extrusion press and a conventional extrusion press, apart from the basic tooling (i.e., the container, stem, and die). A major difference between the two press designs is in the hydraulic system. For the hydrostatic extrusion press, a direct-drive oil hydraulic system is the cheapest method. At very high ram speeds, such as 720 ipm, which are used to conventionally hot extrude steel and titanium, the cost of a direct-drive system becomes prohibitive and a water hydraulic system is less costly. The specifications for a water hydraulic system suitable for both presses are shown on Table III.

Two high-pressure containers would be used on this press for hydrostatic extrusion of solids, tubes, and shapes at fluid pressures of 250,000 psi or 450,000 psi. With proper tooling, the containers can be arranged to make fluid-to-fluid extrusions.

An extrusion-drawing operation is possible by applying a draw force to the exiting extrusion by means of a hydraulic or chain-drive system located in the run-out table area. This process, developed at Battelle and called HYDRAW

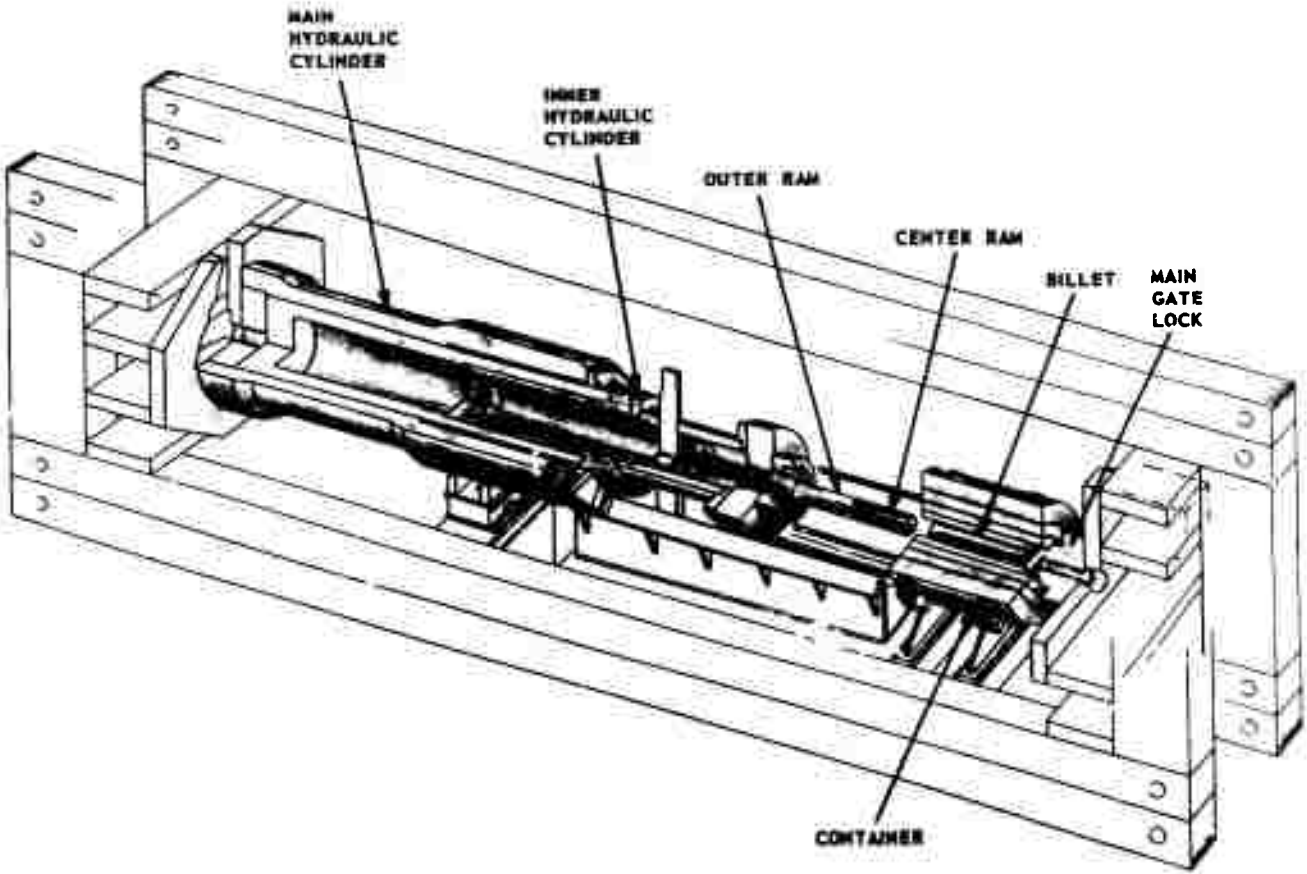

FIGURE 10. 17,000-TON PRODUCTION HYDROSTATIC EXTRUSION PRESS

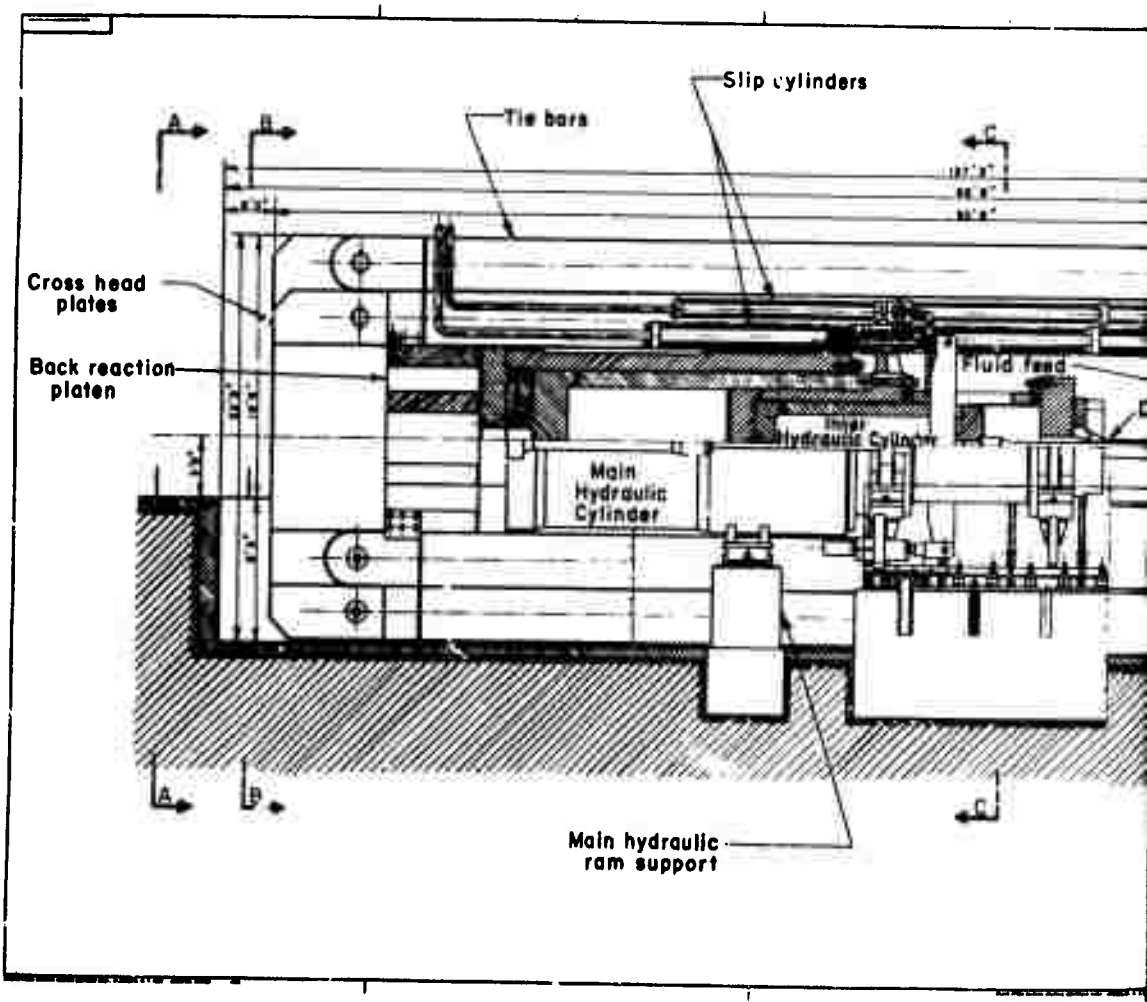

FIGURE 11. 17,000-TON PRODUCTION HYDROSTATIC EXTRUSION PRESS DESIGNED IN PRESENT PROGRAM

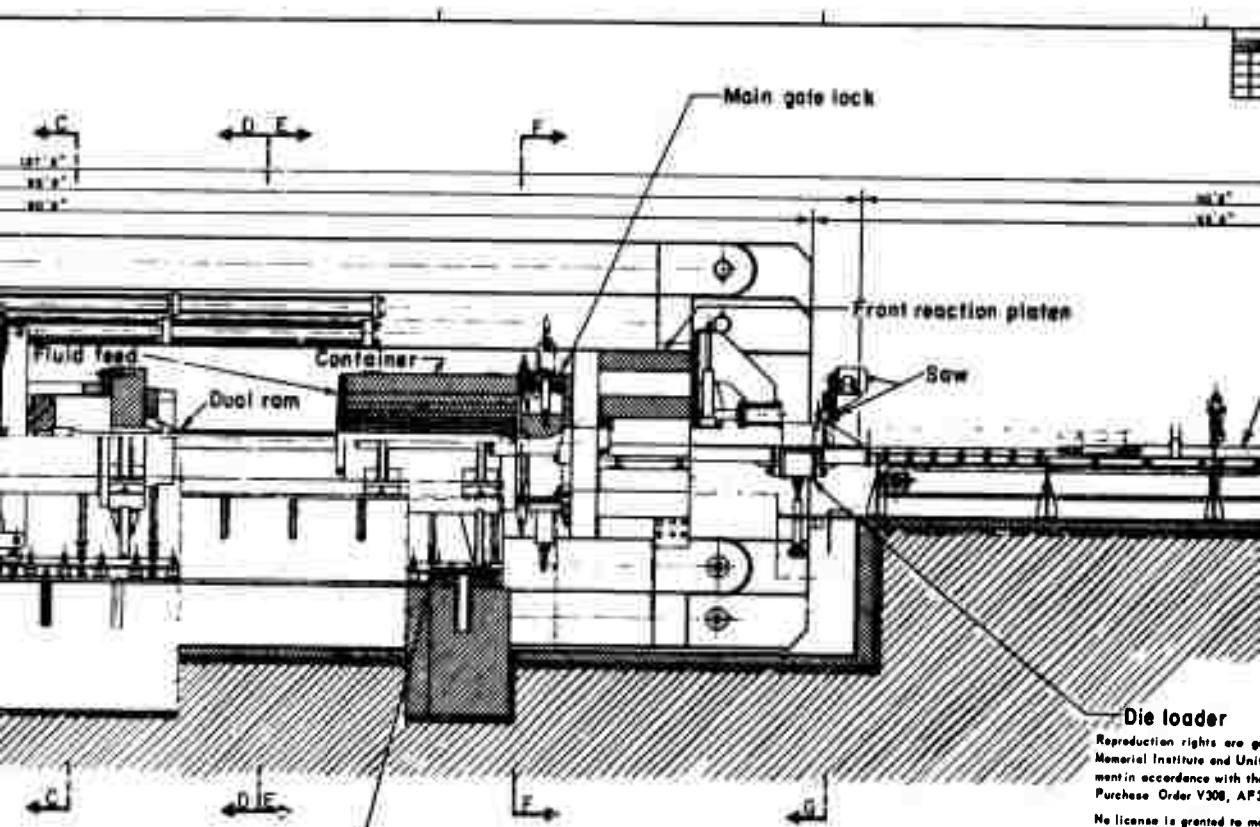

Reproduction rights are g
Memorial Institute and Uni
ment in accordance with th
Purchase Order V308, AF
No license is granted to m
operate equipment items, c
cesses developed by Bl
private expense, in partic
processes covered by
patents.

B

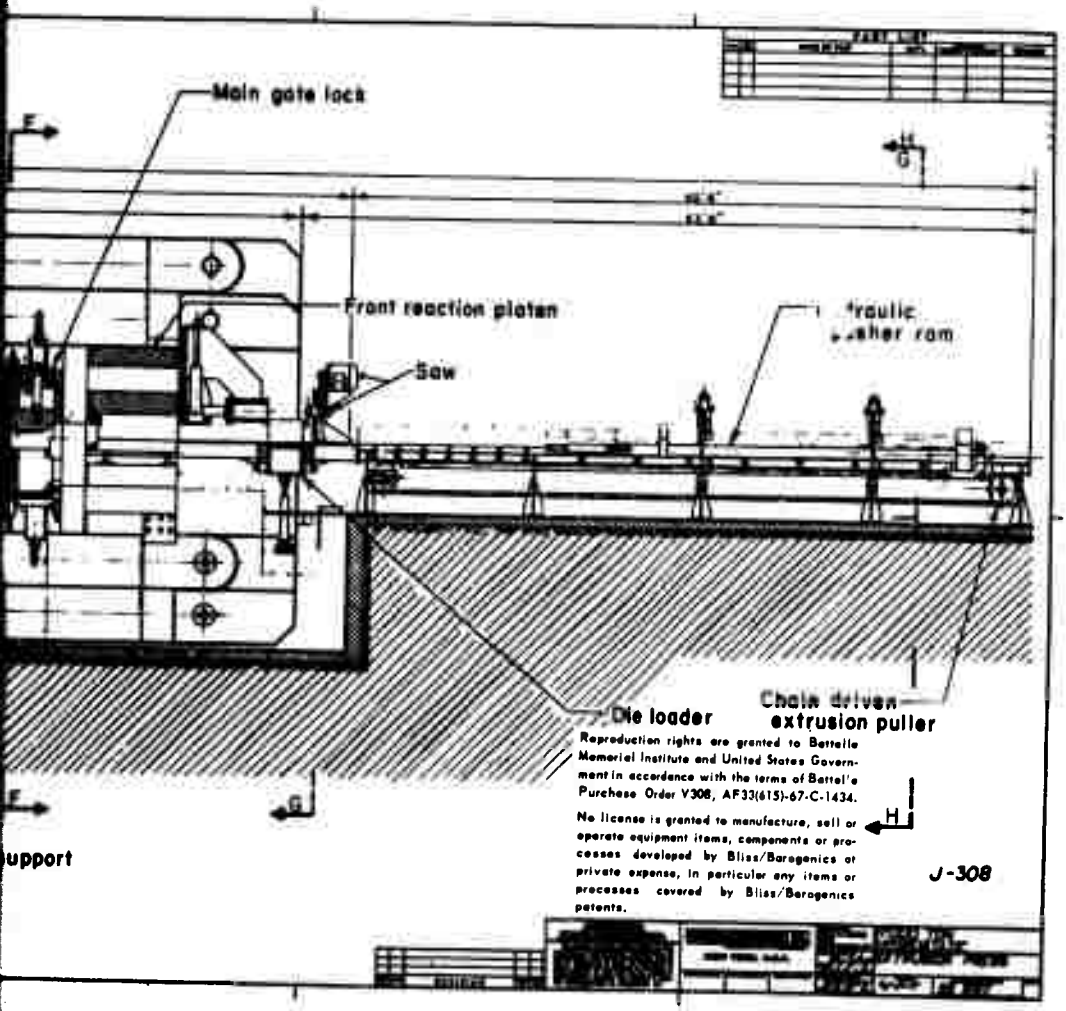

Reproduction rights are granted to Battelle Memorial Institute and United States Government in accordance with the terms of Battel's Purchase Order V308, AF33(615)-67-C-1434.

No license is granted to manufacture, sell or operate equipment items, components or processes developed by Bliss/Baragenics at private expense, in particular any items or processes covered by Bliss/Baragenics patents.

J-308

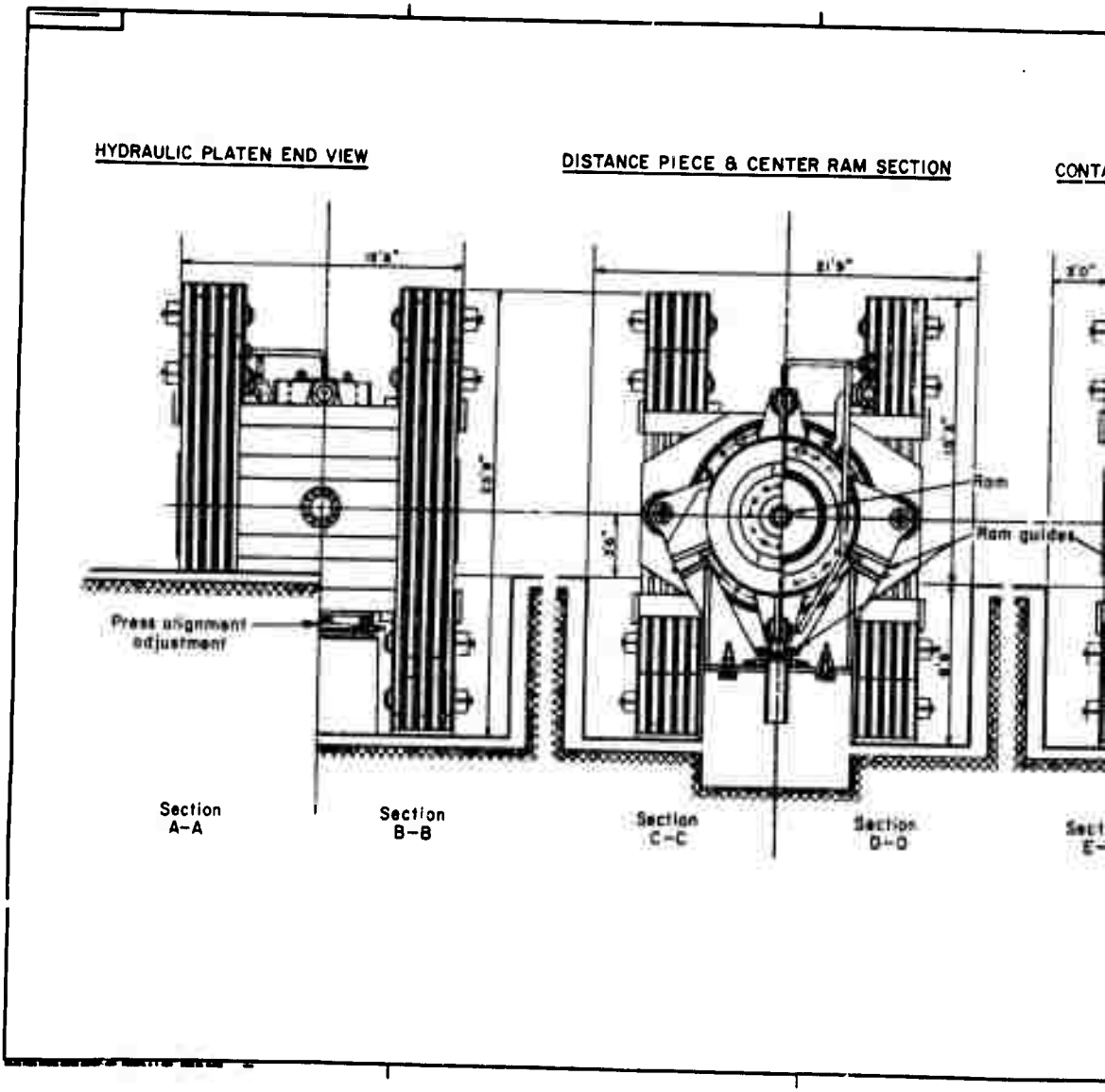

FIGURE 12. SECTIONS OF THE 17,000-TON HYDROSTATIC EXTRUSION PRESS DESIGNED IN PRESENT PROGRAM

PART KEY

CONTAINER & GATE LOCK SECTION

EXTRUSION PLATEN END VIEW

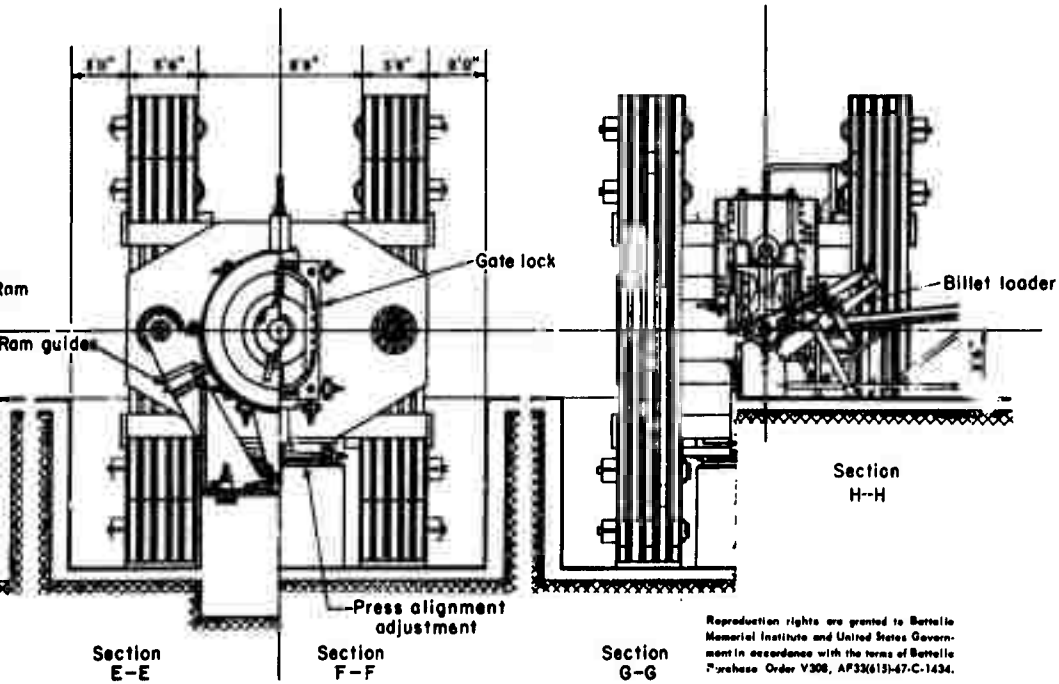

Reproduction rights are granted to Battelle Memorial Institute and United States Government in accordance with the terms of Battelle Purchase Order V308, AF33(615)-67-C-1434.

No license is granted to manufacture, sell or operate equipment items, components or processes developed by Bliss/Berogenics at private expense, in particular any items or processes covered by Bliss/Berogenics patents.

J-308

		11,000 TON HYDROSTATIC EXTRUSION PRESS	
		TITLE SECTIONS	

TABLE I. GENERAL SPECIFICATIONS OF 17,000-TON HYDROSTATIC EXTRUSION PRESS AND A DUAL-PURPOSE PRESS CAPABLE OF BOTH HYDROSTATIC AND CONVENTIONAL EXTRUSION

Specification	Hydrostatic Extrusion Press	Dual-Purpose Extrusion Press
Capacity, tons		
Main cylinder	17,000	17,000
Internal cylinder	6,400	6,400
Main cylinder pullback (total)	100	1,700
Inner cylinder pullback (total)	20	640
Container seal	50	1,700
Container shift (stripping)	75	2,000
Gate lock	50	50
Stroke, inches		
Main cylinder	108	150
Inner cylinder	84	80
Container length	120	72
Ram speed	101 ipm	720 ipm
Press dimensions		
Overall length	90' - 9"	94' - 6"
Overall width	16' - 0"	16' - 0"
Height above floor	15' - 6"	15' - 6"
Height below floor	8' - 3"	8' - 3"
Production capabilities		
Production rates, billets/hr	35	35
Maximum billet sizes		
6-inch diameter liner	5-inch dia x 24 inches	--
12-inch diameter liner	11-inch dia x 96 inches	--
20-inch diameter liner	--	20-inch dia x 65 inches
26-inch diameter liner	--	26-inch dia x 65 inches
32-inch diameter liner	--	32-inch dia x 65 inches
35-inch diameter liner		35-inch dia x 65 inches
Estimated total construction costs	$5,149,000	$7,062,000
Estimated installed cost	$5,989,000	$7,902,000

TABLE II HYDRAULIC POWER-STATION SPECIFICATIONS FOR THE 17,000-TON HYDROSTATIC EXTRUSION PRESS WITH A DIRECT-DRIVE OIL HYDRAULIC SYSTEM

System pressure	5000 psi
Pump manufacturer	Towler
Pump listing	(22) Series "D" (1) Double Type "E"
Total delivery at 5000 psi	22 x 134 = 2948 gpm + + 50 = 3000 gpm
Boost pumps	(4) at 200 hp each
Maximum ram speed	101 ipm
Motor listing	(11) 800 hp/1200 rpm (1) 150 hp/1200 rpm (4) 200 hp/3600 rpm (1) 15 hp/1200 rpm
Total horsepower	9000 hp
Estimated cost	$1,090,600

TABLE III HYDRAULIC POWER STATION SPECIFICATIONS FOR THE 17,000-TON PRESS WITH A WATER HYDRAULIC SYSTEM

Item	Hydrostatic Extrusion Press	Dual-Purpose Extrusion Press
System pressure, psi.	4500	4500
Number of main pumps.	6	8
Total pump delivery, gpm.	6 x 325 = = 1950	8 x 325 = = 2600
Air compressor.	40hp	25hp
Motor list.	(6) 1000 hp/ 1800 rpm	(8) 1000 hp/ 1800 rpm
Accumulator bottle		
Total capacity, cu. ft.	1350	660
Useful volume, gallons.	900	354
Maximum ram speed, ipm	100	720
Maximum stroke, inches	108	150
Estimated costs.	$1,646,800	$1,801,350

offers the advantage of increasing extrusion reduction capability for a given fluid pressure level. The draw stress and fluid pressure are additive on essentially a one-for-one basis. In the present press design, a means for applying a draw force of 300 tons was incorporated.

The basic tooling (container, stem, and die) can attain all the target goals except for hydrostatic extrusion at 1000 F. Conventional heating techniques such as internal heaters and induction heating were considered. Heating results in severe pressure limitations on the containers at temperatures approaching 1000 F. External heaters could be applied to the outside diameter of the container to heat it uniformly to about 500 F, which would limit the pressure capability of the containers to about 225,000 psi. Experimental work has demonstrated that the ability to hydrostatically extrude at 500 F is not essential in most hydrostatic extrusion operations. However, external heaters can easily be added to the container at a later date if desired. Elevated-temperature hydrostatic extrusion would also require development of a high-temperature, high pressure seal that could be easily replaced and have a long service life.

The 250,000 psi extrusion container measures 12-inch ID x 120 inches long. Figure 13 illustrates the use of this container with a typical solid billet. In this tooling configuration, after the billet and the die are pushed into position, the center ram applies a force to seal the billet against the die and then fluid is pumped into the chamber. The outer ram moves forward, pressurizes the fluid and causes the billet to extrude. The center ram may either apply an additional augmentation force of up to 2800 tons on the end of the billet or play no part in the extrusion except to maintain the fluid pressure. The end cap, or billet guide, is press fitted onto the billet before loading to keep the billet horizontal during extrusion. The typical seals shown on Figure 13 will be described and the locations explained in the section dealing with fluids and seals.

This 12-inch container can, of course, take a wide range of billet sizes below 11-inches in diameter. As the diameter of the billet decreases, the amount of fluids increases and a longer stem stroke is required just to pressurize the fluid to a given pressure level. Thus, the maximum billet length decreases as the billet diameter decreases. The minimum billet length approaches 80 inches as the billet diameter approaches zero. This assumes 30 percent compression of the fluid and a die length of only two inches. The billet diameter would be small and the die length could then also be small. As the billet volume is reduced, the amount of working fluid that must be pumped into the container increases, and the cycle time therefore increases for very small diameter billets. The amount of working fluid required for such small billets will be about three times that required for the maximum size billet and the maximum production rate may drop to about 29 billets per hour unless additional pumping capacity is added.

The 450,000 psi liner measures 6-inch ID x 36 inches long and fits within the 12-inch container. Figure 14 shows this tooling in position to extrude a solid billet. The die and billet are loaded in the support tube and all three are pushed into the 12-inch container, until stopped by the 6-inch liner. The interface between the liner and support tube is designed to make the inner bore concentric. The inner support tube forces the billet and die into the 6-inch liner when the end plug is placed in position. After the die and billet are

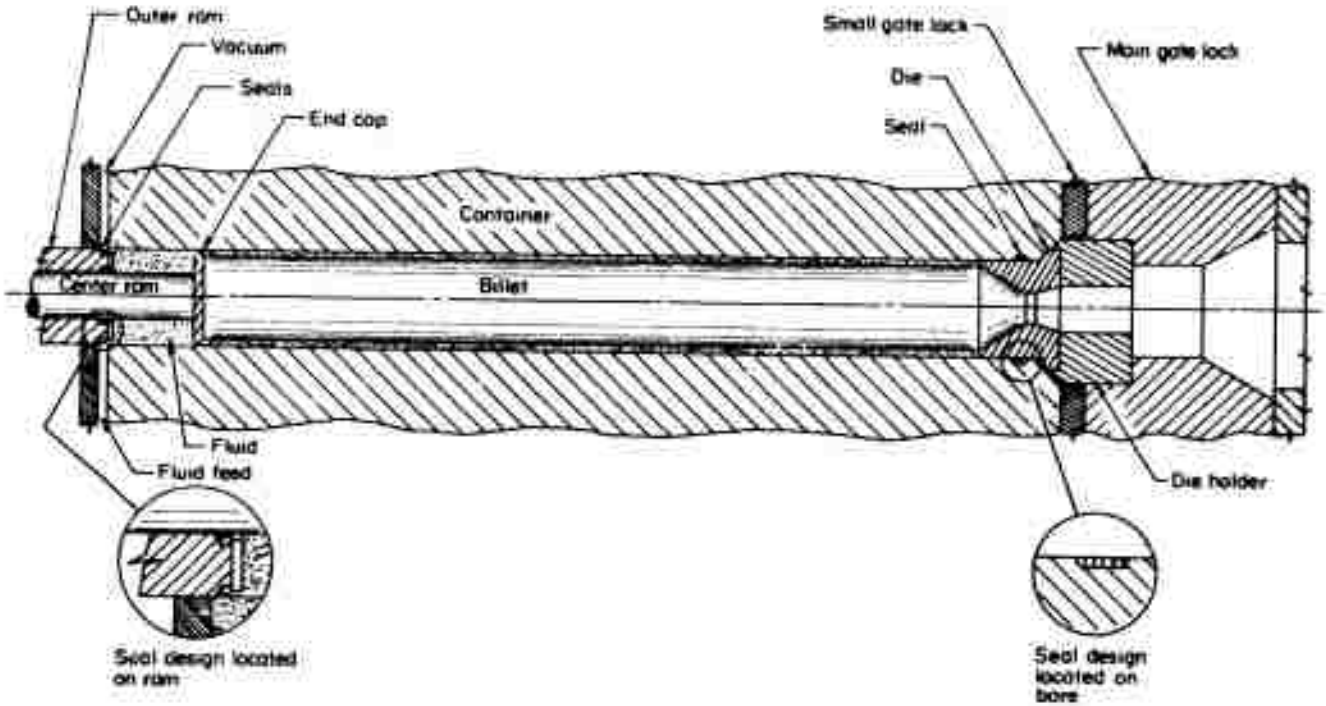

FIGURE 13. FLUID-TO-AIR EXTRUSION WITH 250,000 PSI CONTAINER

Container - 12-inch bore x 120 inches long
Billet - 11-inch diameter x 96 inches long

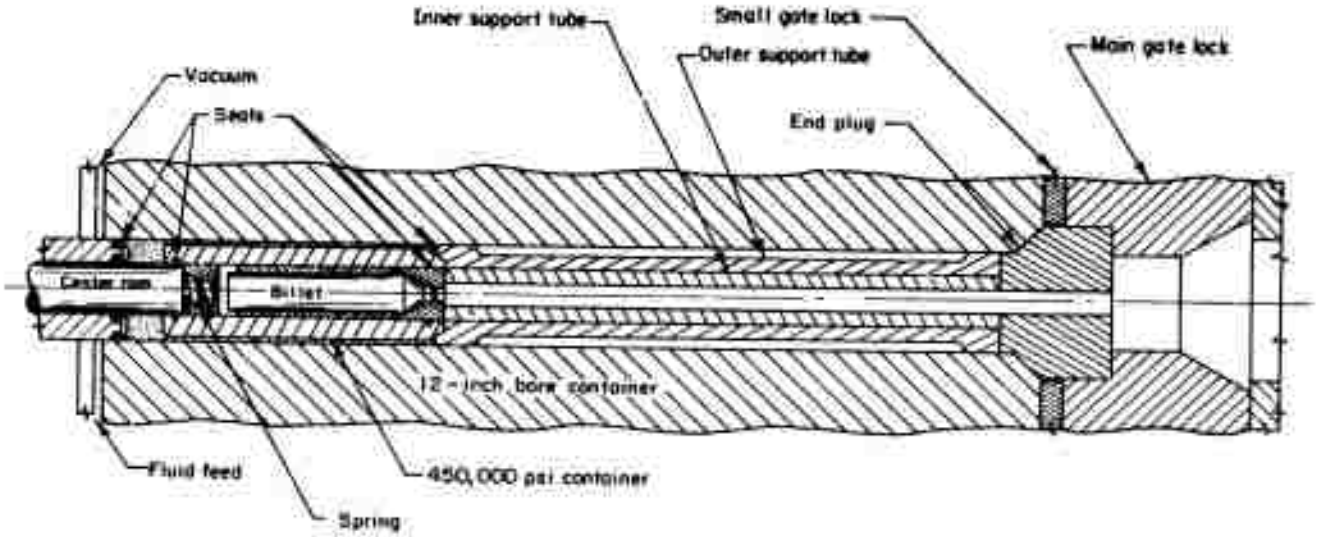

FIGURE 14. FLUID-TO-AIR EXTRUSION WITH 450,000 PSI CONTAINER

Container - 6-inch bore x 36 inches long
Billet - 5-inch diameter x 24 inches long

loaded, a spring attached to the center ram keeps the billet sealed against the die as fluid is pumped into both containers. The outer and center rams move forward in a predetermined proportion to keep the proper relationship between the internal fluid pressure and the outer fluid support pressure, and to cause the billet to extrude.

With a solid end plug and by removing the interior seals on the outer support tube, the tube (with appropriate side holes) would fill with fluid pressurized at the same level as the support fluid. Under these conditions fluid-to-fluid extrusions up to 72-inches long could be made with a pressure difference of 200,000 psi.

A time table and milestone chart for the construction of the dual-purpose press are shown in Appendix I. The estimated time required to build this press is 27 months.

Individual components will be described and detailed process sequences indicated in the following sections.

Tooling Designs

Containers, stems, and dies designed for this press are described. The detailed analysis of these components will be given in a subsequent section.

Containers

The design for the 12-inch bore container capable of withstanding fluid pressures up to 250,000 psi is shown in Figure 13. This design consists of seven concentric rings. Each ring is tapered 1/2 degree so that the rings can be assembled with the calculated interferences by press fitting the rings together. The container has a theoretical pressure capacity of 263,000 psi, and has a predicted life of 10^5-10^6 cycles.

Of the currently available materials, it appears that AISI H-11 steel is most attractive as the 12-inch bore liner material from the standpoint of strength, uniformity of properties in thick sections, and cost. The 12-inch ID liner would be heat-treated to tensile properties of 250,000 psi UTS, and 225,000 psi YS. These properties can be guaranteed by two manufacturers of large forged components. It is assumed that the compressive yield strength of this material is equal to its ultimate tensile strength. In theory, maraging 300 steel would have higher compressive properties as estimated from tensile data and thus would offer a greater margin of safety. For example, tensile properties of 285,000 psi UTS and 260,000 psi YS in thick sections have been reported in sales literature. Manufacturers of large forgings, however, claim that segregation problems (banding, non-uniform grain size) develop in the very large ingots, (e.g., 30-inch diameter which would be required to make this liner. These casting problems can result in a forging with nonuniform properties. Further, maraging steels cost

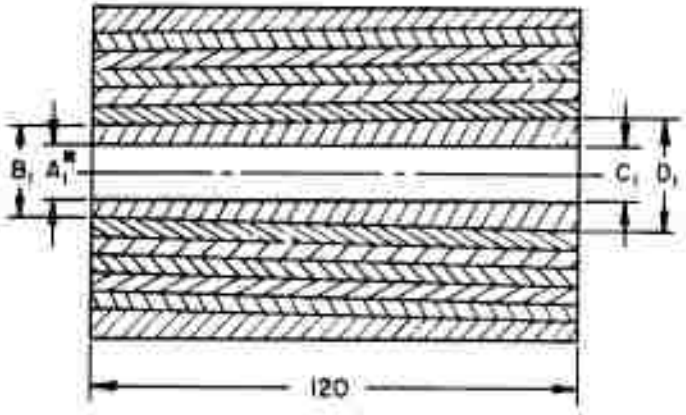

Ring	Ring Dimensions, inches A	B	C	D	Manufactured Interference inch/inch
1	12.0	18.669	12.0	20.770	
					0.00265
2	18.620	26.431	20.715	28.530	
					0.00194
3	26.380	33.451	28.475	35.500	
					0.00213
4	33.380	42.289	35.475	44.389	
					0.00212
5	42.200	53.514	44.295	55.613	
					0.00213
6	53.400	67.559	55.495	67.634	
					-0.0006
7	67.600	82.695	67.695	82.695	

Ring	UTS, psi	TYS, psi	Material	Weight
1	250,000	225,000	H-11	5,540
2	250,000	215,000	H-11	9,540
3	200,000	170,000	4340	11,430
4	200,000	170,000	4340	18,220
5	200,000	170,000	4340	29,260
6	200,000	170,000	4340	49,960
7	175,000	150,000	4340	52,660
				173,610

*Subscript refers to the ring number

FIGURE 6. DESIGN INFORMATION ON 12-INCH BORE, 250,000 PSI CONTAINER

more than twice as much as H-11 steels. However, because technological improvements are continually being made, the relative status of these materials should be evaluated again at the time of container construction.

An alternative five-ring container design was evaluated from the viewpoint of cost. This five-ring container weighed nearly 50,000 pounds more than the seven-ring design. In this particular instance, the material cost saving was in excess of the additional costs for machining and assembling involved in the seven-ring design. The seven-ring design also resulted in rings with thinner walls and the required physical properties could then be obtained with greater certainty.

A limitation on constructing containers of these tapered press-fit designs was found to be length. Assembly forces were calculated to be of the order of 30,000 tons. The maximum daylight available in presses of this rating was found to be about 13 feet. With suitable allowances for the sleeves to protrude before assembly, the maximum container length that would be possible to assemble would be roughly 12 feet.

The 6-inch bore, 450,000 psi container would be constructed by placing the 6-inch liner within the 12-inch bore container and using high pressure fluid to support the liner. This liner would have a wall ratio of about 1.9 with a fluid-support pressure of 250,000 psi to contain an internal fluid pressure of 450,000 psi. This 6-inch liner would be free to move along the bore of the 12-inch container as described in the materials handling section. Wear pads could be attached to the outside surface of the liner to keep the liner concentric in the bore. Moving the 6-inch liner simplifies the materials handling system and permits relatively easy inspection of the seals in the 6-inch liner.

In an alternative 6-inch container design, consideration was given to the use of a 6-inch liner, 105 inches long. This liner would eliminate the need for the support tube assembly (except for fluid-to-fluid extrusion) and would simplify loading of the 6-inch liner, since it could be done much like a 12-inch billet. However, this approach is hampered by the fact that the greater fluid volume needed in this bore would require a large portion of the stem stroke just to compress the fluid to 450,000 psi. The 6-inch stem stroke with the present stem design is limited to about 35 inches. This would mean, at the present time, that while much longer billets could be placed in the 6-inch x 105-inch long liner, the total billet volume extruded from this liner would be appreciably less than that extruded from the 36-inch long liner. Despite the restrictions on billet volume, this long ultrahigh pressure chamber concept may be useful in the re-extrusion of long shapes at high extrusion ratios.

For fluid-to-fluid extrusion, several arrangements were considered:

	Primary System		Back Pressure System	
Method	Pressure, psi	Container Bore, inches	Pressure, psi	Container Bore, inches
A	450,000	6	250,000	12
B	450,000	6	100,000	~ 2
C	250,000	12	100,000	~ 2

Method A is the most compact system since it uses only the 6-inch and 12-inch bore containers already mentioned. The extrusion length is limited to about 72 inches, the available length remaining in the 12-inch bore container. However, it should be possible in the present press design to add auxiliary containers, also of 250,000 psi capability. It is estimated that such containers could have a bore diameter up to about 2 inches and an overall wall ratio of about 7.

In Methods B and C, the back pressure would be provided by a separate hydraulic system, independent of 10,600 and 6400-ton rams. It is visualized that a pump and intensifier system could be used to develop a back pressure up to about 200,000 psi to permit monoblock construction of the auxiliary containers. A scheme for connecting such auxiliary containers to the 250,000 psi, 12-inch bore container is shown in Figure 16. It should be mentioned that the rather small volume outputs of high-pressure pump-intensifier systems means that relatively long times (1 to 10 minutes) may be required just to reach pressure for each extrusion. Thus, the number of extrusions produced per hour would be reduced considerably. For this reason, it is felt that the cost of a fluid-to-fluid operation of this type could only be justified on a 17,000 ton press for very special materials or products which could not be produced by other less expensive means, if at all.

Stems

There are several types of stems that could be used in the proposed press, depending on the operation. For the 250,000 psi, 12-inch bore container, a solid stem (108 inches long) would have an L/D = 9. According to the stress analysis to be discussed later, this stem should not buckle at stresses up to about 300,000 psi. A spring would be used to keep the billet against the die during fluid fill.

An interesting alternative to this design is to have a dual, concentric ram system in which the center ram bears directly on the billet-end while the outer ram pressurizes the fluid. The main potential advantage of this arrangement is to supply an additional force to the billet beyond that exerted by the fluid pressure. If the center ram is 7 inches in diameter, for example, the stem pressure it can exert on a 7-inch diameter billet is about 330,000 psi. This is 80,000 psi or 32 percent greater than the 250,000 psi maximum fluid pressure. As the billet diameter is increased beyond 7-inches, the augmentation pressure would decrease proportionately at the die. Thus, for an 11-inch diameter billet, the extra force supplied by the 7-inch ram would result in an extra billet pressure at the die of 33,000 psi, or roughly 13 percent augmentation. This feature, which can be used to advantage for certain applications, is a consequence of the fact that the inner hydraulic system is designed to supply 6400 tons force on a 6-inch ram to achieve the 450,000 psi fluid pressure for the 6-inch bore container. Thus, up to 2800 tons extra force is available for augmentation, if the center ram diameter is held at 6 inches. However, the amount of augmentation force decreases to zero as the center ram diameter is increased to about 8 inches. This is because when the total 6400 tons is applied on an 8-inch ram, the maximum pressure which can be exerted by the ram is only 250,000 psi; this is the same as the maximum fluid pressure that can be developed in the 12-inch bore container and, thus, no

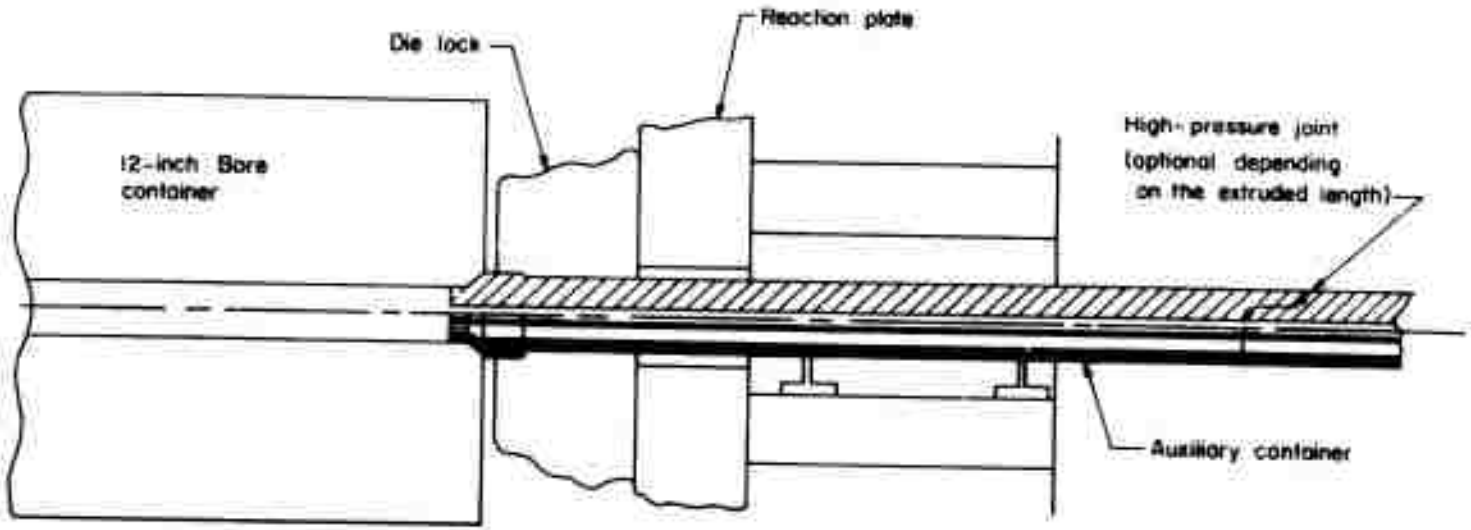

FIGURE 16. AN AUXILIARY CONTAINER EXTENSION TO PRODUCE LONG EXTRUSIONS USING FLUID-TO-FLUID TECHNIQUES

augmentation is achieved. As mentioned earlier, a 7-inch center ram would be stressed under the full 6400-ton load to about 330,000 psi. This stress level could be withstood by a conventional tool steel. Theoretically, an augmentation pressure of 200,000 psi would be possible with a 6-inch diameter center ram on a 6-inch diameter billet, and if the center ram were made of tungsten carbide.

For extrusion of tubing from the 12-inch bore container, one possible arrangement is to use dual concentric rams and attach the mandrel to the center ram for manipulation. In this way, the mandrel can be held fixed relative to the die while the outer ram pressurizes the fluid. Calculations indicate that tubes up to 10-1/2-inches ID can be extruded. This merely requires a 10-1/2-inch diameter mandrel attached to the center ram, which can be of the same diameter. The hollow outer ram, 12-inches OD x 10-1/2inches ID, would have adequate buckling resistance because the load imposed on it, even at 250,000 psi fluid pressure, is relatively low (about 3300 tons) over the small annular space. Smaller diameter mandrels could be attached to the 10-1/2-inch center ram, provided that the volume of the tube blank plus the volume displaced due to fluid compression is smaller than the volume displaced by the outer ram. Alternately, it is possible to use smaller diameter center rams for smaller mandrels should it be more advantageous to do so.

The stem arrangement for the 450,000 psi system is shown in Figure 52 and 53 in a later section. A material such as tungsten carbide is required for the center stem since no other commercial materials available can withstand stresses up to 500,000 psi (allowing for stem seal friction). The outer ram is only long enough to pressurize the support fluid so as to minimize the carbide stem length. Although the length of the 6-inch diameter portion of the stem is 60 inches (and thus the L/D = 10), the unsupported length is only 35 inches with an L/D = 5.8. Thus, buckling is not anticipated to be a problem, provided that the outer ram offers adequate external support and the assumptions made on material behavior are valid.

Although not a stem in the usual sense, the 6-inch diameter x 73-inch long inner support tube used to support the die during extrusion from 450,000 psi is stressed higher than the extrusion stem. This higher stress occurs because the tube is hollow and has a lower cross sectional area than the stem. When this support tube has a 3-inch ID hole, the tube length of 73 inches is less than the critical unsupported buckling length for 500,000 psi.

Dies

Dies of two general external forms would be used on this press. One typical geometry which would be used in the 12-inch liner at pressure up to 250,000 psi is shown on Figure 13. The second die geometry, which is for the 450,000 psi system, differs slightly to simplify materials handling in the 6-inch liner. This die configuration is shown in Figure 14.

Stress analysis has shown that the maximum diameter billet which can be extruded from either the 6- or 12-inch bore containers depends on the potential

problem of die failure due to high hoop tensile stresses developed in the thin leading edge of the die during extrusion. These stresses can be reduced to a tolerable level by increasing the die angle in order to thicken the leading edge. For the 250,000 psi, 12-inch container, an 11-inch diameter billet can be extruded without die failure, provided that the die angle is somewhat greater than 60 degrees. This analysis was based on using M-50 tool steel as the die material. For the 450,000 psi operation, tungsten carbide dies are required. Calculation of tensile hoop stresses indicate that billets up to 5 inches in diameter can be extruded through 60-degree entry dies without die failure.

Analysis of the die stresses also indicated that the fluid seals should be positioned at a point opposite the die land, to balance the stresses on the die wall exerted by the billet and the fluid support pressure. This design would help to prevent die failures.

Fluids and Seals

Castor oil would be used as the hydrostatic fluid in this press. This fluid has good stability, tends to assist lubrication for a wide range of materials, and has amply demonstrated consistent behavior in many experimental programs. With additives or thinners, castor oil has been successfully used at pressures up to about 350,000 psi. It was assumed at pressures of 450,000 psi that the castor oil with additives would be able to transmit pressure hydrostatically reasonably well, but this requires experimental verification. Pentane, i-alcohol, n-alcohol and the like have been used by Bridgman and others for pressures up to 450,000 psi. These fluids may boil at temperatures near 150 F and could cause a serious fire and health hazard on a production press in the volumes required in this study. If the proposed press were to be used exclusively at pressures of 250,000 psi or less, water with additives should be considered because of its relatively low cost.

Castor oil would be fed into a prefill tank to a predetermined level and injected into the working chamber through the fluid-injection device illustrated in Figure 17. A slightly negative pressure is applied to the chamber through the top orifice before the fluid is injected. The castor oil is then injected into the chamber at speeds up to 20 gps and at a pressure of 80 psi. The orifices are designed to minimize turbulent fluid flow. The slight negative pressure at the top of the feed device bleeds the chamber and minimizes entrapped air. Entrapped air in itself is not particularly harmful to the extrusion operation, but because of the high compressibility of the air compared to castor oil, an additional amount of ram stroke would be needed to compress the air before the castor oil is compressed and the maximum billet length would be shortened.

After extrusion, some castor oil could be withdrawn from the container through the bottom of the fluid-injection device. To minimize the time cycles, not all of the castor oil would be withdrawn and provisions would be made to catch and recycle the remaining fluid at the die end of the press.

The seals to be used in this design are basically an O-ring plus a miter ring, which are commonly used in high-pressure fluid systems. The seals are either fixed in the container wall or are attached to the stem. Figures 13 and 14 illustrate the seal locations and details of typical designs.

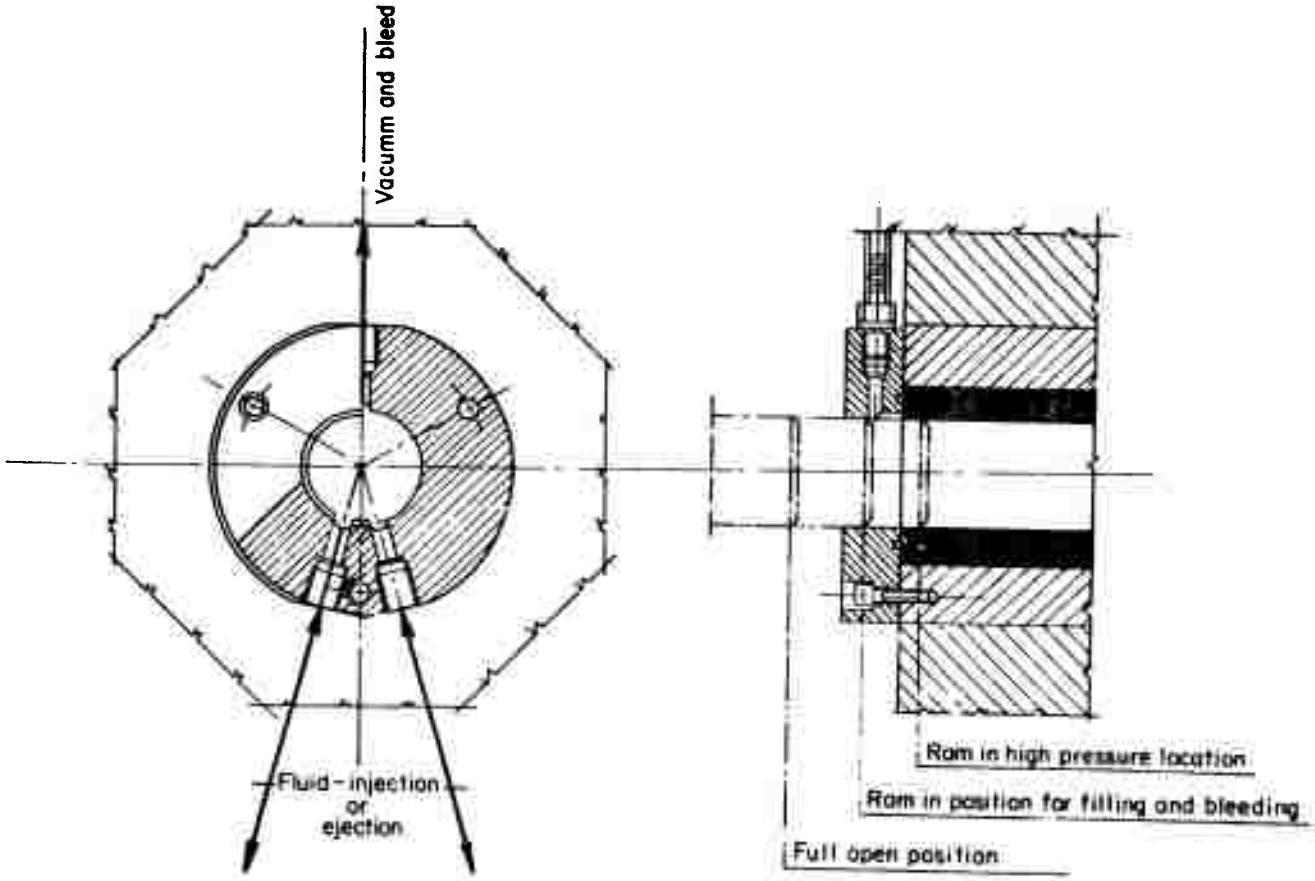

FIGURE 10. FLUID-INJECTION DEVICE AND RAM POSITION DURING FLUID-INJECTION SEQUENCE

ASEA [25] has reported that, after the first one or two extrusions have been made with the seal located in the container wall, the O-ring is no longer required. The O-ring can be eliminated because the miter-ring becomes very close fitting to the ram and container. It should be noted that there is no available information on high-pressure seal life beyond perhaps 100 to 200 cycles. For this reason, the seals have been located for easy maintenance and replacement.

Placing the seal in the container wall favors longer container life because for every extrusion cycle the liner undergoes only one cycle of stress. When the seal is placed on the ram, however, a stress gradient from zero to full pressure moves along the liner for the distance of the ram stroke. Near the end of the ram stroke, certain areas are exposed to an additional cycle of stress as the ram retracts. A further advantage of this seal location is that it simplifies die construction, since the die can have a uniform outside diameter and the seals do not have to be removed with the die each time. Analysis of this seal design, described in a subsequent section, indicates that a seal located in the liner does not significantly weaken the container. This seal location was used whenever possible. The seals could not be located in the container wall to seal the 12-inch outer ram of the dual-ram system, since in this case the high pressure fluid would collapse the outside ram onto the 6-inch center ram. This point is discussed further in the section on stem analysis, under the subsection on concentric stems.

Press Description

In general, the press design is of the longitudinal, die-slide, gate-lock type similar to the traditional conventional hot extrusion press. The die arrangement and extruded product are run out through the reaction platen at the conclusion of each stroke. The specific movements of the press for each type of extrusion operation are described in the section on Materials Handling System and Press Operating Sequences.

Structure of the Press

The main frame, main platen, and tie bar assembly are composed of a Barogenics-patented link-pin and rectangular plate element construction which is believed to be a substantial advance in heavy press frames. The use of this design provides for considerable economy in achieving accurate alignment of the structure in the shop as well as maintenance of this alignment during assembly. This design has been estimated to be about 20 percent cheaper than standard press frame construction.

The main frame consists of two rings of double tie-bar construction. The 100-percent fill factor design provides for maximum economy of the frame plate structure. A 100-percent fill factor, in effect, means that the space between interlocking plates is full utilized.

The pins are of a Barogenics-patented thin-wall, split sleeve, tapered ID design, and provide full bearing load transmittal through the accurately bored pin holes in the tie bars and the frame plates. The use of rolled steel plates, rather than castings with their inherent defects or round tie bars with highly stressed threads and nuts, provides a substantial safety factor for the life of the main frame.

Platens

The platens are fabricated of heavy welded plate to transfer the end loading of the cylinders and/or dies into the frame plates of the main-ring frame.

Cylinders and Rams

The main cylinders, 98-inch bore for the 17,000-ton cylinder and 58-inch bore for the 6400-ton cylinder, are constructed of hollow ring forgings. The 98-inch ID cylinder is of an open end design and sealed at the reaction end by means of a Barogenics-patented non-preloaded seal assembly. Long-length bearing bushings are used together with automatic chevron-type packings to provide accurate ram guidance and sealing at the open end of the cylinder. The main ram is a hollow forging with a plug welded on to close the rear end.

Fastened to the internal ram is the 6400-ton, center-ram cylinder, which is constructed in the same manner as the main ram. A mandrel forging is welded with a heavy plug to form the closed end of the cylinder. Since the cylinder must react through the front flange, a heavy flange is provided to prevent bellmouthing of the cylinder end and minimize the bending stress by means of the properly designed tapered transition area.

The lower tonnage pullback cylinders for the main ram, inner ram, container, gate lock, etc., are of forged construction.

Slip Cylinders

The conventional arrangements of supplying high pressure fluid to moving cylinders is through the cumbersome method known as "walking pipes". The "slip cylinders" method to provide high pressure connections to moving platens is a proven design and does not have construction and operating hazards posed by the older design.

Press Supports

The conventionally-accepted old design of a single massive heavy welded frame securely bolted to the concrete foundation is not only a substantial waste of money, but usually interferes with keeping the press in proper alignment. A heavy steel frame, even though accurately aligned at the onset of operation of a press, will follow the deflection of the foundation since the rigidity of the steel frame is much less than that of the entire foundation to which it is bolted.

A solution as proposed by Barogenics is to provide individual supports under the major elements of the press. Each support is easily adjustable and enables the press to be in proper alignment, notwithstanding local deflections of the foundation.

Alignment of the Press Elements

The moving crossheads of the press slide on ways which are radially arranged with respect to the centerline of the press. A bottom-guide assembly, which is set parallel to the axis of the press, is on a circle together with guides so that alignment of this bottom center guide rotates the particular crosshead. The bottom guide and the slide ways are equidistant from the center of the press so that these three points form a circumscribing circle around the press centerline, thus making for easy alignment. This construction is self-explanatory on cross section drawings shown in Figure 12, Sections C-C and D-D.

The adjustment at the moving-ways proper are again designed to maintain the integrity of alignment since the faces of the adjusting blocks are

radial to the center of the press. The alignment of the heavy fixed platen is also shown in Figure 12, Sections B-B and F-F. Heavy screws move and lock tapered wedges to shift the heavy platen up, down, sideways and axially as required.

Container and Container Housing

The container housing is a half circle arrangement with simple tie down straps to enable the container to be replaced by a straight lift between the two-ring tie bar frame. The shorter container for conventional hot extrusion would be arranged in an adaptor on the front end of the container housing.

Gate Lock Arrangement

The design of the gate lock movement and guide is clearly shown in Figure 12, Section F-F. A heavy frame is bolted onto the front face of the main reaction platen. The horseshoe-shaped, die-lock pieces are moved in heavily-gibbed slides by the gate-lock cylinders. The entire window frame of the slide arrangement can be easily adjusted by the captive jack screws arranged in the horizontal and vertical plane.

Runout Table

The runout table is chain driven and carries a 150 hp saw as well as a pulling arrangement. It also contains a lift-out mechanism to transfer the extrusion to the finishing table. The hydraulic pusher would be rated at 15 tons for materials handling purposes. For the HYDRAW operation, the capacity of this cylinder would be increased to about 300 tons.

Billet, Dummy Block, and Die Handling Arrangements

The entire process of billet handling, die handling, and extrusion handling is completely automated by guides and conveyor. Suitable interlocks are provided in the control panel so that the selection of a particular extrusion cycle provides for proper cycling of the transfer mechanism handling, the billet, die, extrusion, and butt.

Saw

The saw is driven by a 150 hp dc motor with an abrasive cut-off disc suitable for use with a refractory metal stock. The stroking and cut-off cycle

are integrated through the automatic sequencing of the entire press. An automatic guard arrangement envelops the saw blade during operation so that the chips of the cut-off do not contaminate the hydrostatic fluid system.

Hydraulic Systems Design

Both types of power stations proposed in this study are used conventionally to power large hydraulic presses. The accuracy of control of each installation is comparable, both in the directly-driven, oil-hydraulic installation and in the water-hydraulic, accumulator station. A cost analysis showed that, for the hydrostatic-extrusion applications and for the slower-speed conventional hot-extrusion press, the 9000 hp direct-drive oil-hydraulic installation is more economical than the 6000 or 8000 hp water-hydraulic accumulator station. In general, this lower cost is due to the higher rotational speed of oil pumps and simpler pump construction which eliminates the need of separately packed plungers. In addition, the investment cost of energy storage as typified by the large accumulator bottles in a water-hydraulic system is quite substantial.

If the press must operate at rapid speeds, say 720 ipm for the conventional hot extrusion of refractory alloys, then the instant demand of the system is well over three times the horsepower previously proposed. In this case, a water-hydraulic accumulator station is required from the standpoint of both the installed horse-power and the valving and pipe systems for a less viscous fluid. Pipe and valve speeds used with water as the operating fluid are three or four times the allowable speed for oil valves and piping.

The use of the terms water and oil should be qualified as follows: water used as the operating fluid contains approximately 1 to 2 percent of hydraulic additive to improve the lubricity of the fluid and help reduce oxidation and consequently rusting of internal parts. In addition, careful control must be maintained of the Ph level to preclude electrolytic corrosion. These items, of course, are a proper function of the engineering to be performed if and when the entire installation is constructed.

Because of the large volume of fluid contained in this system, it would be well to specify synthetic, fire-resistant fluids to reduce the danger of fire which is always present when a conventional mineral hydraulic oil is specified for a high-pressure system. There are many different grades of synthetic and so-called fire-resistant fluids. A proper evaluation will provide a considerable savings in cost when considering the entire problem of fluid properties, stability of fluid, fire insurance, and fire-control devices.

Oil Hydraulic System

The direct-drive, oil-hydraulic system proposed is a 5000 psi installation, with the pumps and controls being furnished by Towler. An operating pressure of 5000 psi is considered an optimum figure for this size of machine since there is an economic balance between smaller ID piping size and increased wall thickness requirements which results from increased fluid pressure.

Pumps. The main pumps are of the series "D" type, which are axial swash-plate-driven pumps developing 400 hp each at 1200 rpm. This is a conservative rating since the pump is rated for continuous duty at 500 hp at 1500 rpm. This design of pump requires approximately 7 percent total of supercharging pressure for proper performance. This is supplied by four 200 hp high-speed centrifugal pumps.

The main pumping system also includes a 150 hp double series "E" pump to provide additional staging for the incremental speed control. The series "E" pump is an inline pump which has been used for 15,000 psi continuous duty and obviously, is quite conservatively applied in this instance.

A 15 hp type "J" vane pump provides 600 psi pilot pressure for the pump controls and for the main controls.

Controls. Standard oil-hydraulic Towler valving, which is rated at 7000 psi, will be used in forged manifold blocks. These valves are successfully used to control some of the largest and most advanced hydraulic installations in the world. The pumps specified are of fixed delivery. However, the design of the control system is arranged to obtain speed steps of approximately 1 ipm at full tonnage from the pump controls alone. A metering valve is automatically introduced into the circuit to vary the delivery steplessly between pump delivery increments. The operator controls the speed of the press steplessly between zero and maximum.

The controls are designed to vary the speed plus or minus 1/2 of 1 percent at any set speed. This is basically a servo feedback from the ram speed. Conventional variable-delivery pumps maintain approximately 5 percent accuracy of set speed with conventional pressure-compensating systems.

The electrical controls for presses of this size are usually of the relay type and are easily serviced by the plant personnel. An improvement which has been applied to a few presses in the last few years has been the substitution of solid-state circuit elements for the relay control system. This has usually led to improvement of press performance because of the increased reliability of prepackaged solid-state circuit modules.

Another improvement, which would be of substantial interest in this application, would be the application of fluidic logic control modules in lieu of the electrical control usually specified. Fluidic controls have been installed on a developmental press at Bliss Research Center, Swarthmore, Pennsylvania. Preliminary findings indicated that a fluidic control system may be as much as 20 percent cheaper then current electrical systems. However, these controls must be fully evaluated before a definitive evaluation can be made. The decision as to control type could be made at the time the press controls system would be completely designed.

Water Hydraulic System

The water hydraulic accumulator system proposed as a possible alternative has been used in most present large presses and has a well-deserved reputation for dependability and control for large presses. The components are of proven construction and require only conventional maintenance. The installed cost, however, is far greater than a direct-drive power plant if relatively low speeds are planned. If high-speed extrusion (ram speeds in the order of 720 ipm) is required, however, then the water hydraulic system is less expensive.

Pumps. The pumps proposed for this system are of the vertical multiplunger design with a crankshaft speed of approximately 300 rpm. These pumps are the successors of the horizontal pumps which ran either at 78 rpm or at 120 rpm. Although the maintenance cost of the slower speed pumps are slightly lower because of slower plunger speeds and lower bearing loads, the higher speed pumps are approximately 30 percent lower in installed cost.

The pumps can be driven through gear boxes either by high speed or slow-speed, direct-driving, engine-type motors. In both cases, either induction motors or the somewhat more expensive, power-factor-correcting, synchronous motors can be used.

Pumps can be unloaded either in the circuit by means of a bypass valving arrangement or by means of a suction valve unloader. The former solution is usually preferred since this allows the water to circulate through the system and through the heat exchanger of the gravity tank rather than being trapped in the suction line during an extended period of press downtime.

Accumulator Bottles. The accumulator bottles are usually constructed of laminated plate. The use of newer alloys, latest design techniques and analyses in accordance with Section 3 of the Unfired Pressure Vessel Code (Nuclear Vessels) has led to a substantial reduction of the wall thicknesses in these vessels. As a result, very large bottles can be built to meet safety code requirements. The use of a single bottle as recommended in this design instead of a multiplicity of bottles reduces the number of pipe connections and reduces the velocity of liquid level during power stroke.

Controls. The valving and controls used in the accumulator station and for press control proper are of the poppet design with lapped seats. The valves proper, constructed of stainless steel and bronze for corrosion resistance, are mounted in forged steel blocks and driven by servo-operated, rocker-arm arrangements.

The conventional control of the press is through a relay system. However, the use of solid-state electrical control elements or fluidic logic modules can be specified subject to the decision and detailed investigation discussed earlier under Oil Hydraulic Systems--Controls.

Electrical Equipment

Motors. Standard drip-proof ball bearing motors are used for the pump drive. In the case of the oil hydraulic installation, the motor is double-ended and is mounted on a common base plate with two pumps. For the large water-hydraulic pumps, the motors are mounted separately on their own foundation pad next to the gear box.

The motors have been specified at 2300 volts since this is the minimum cost motor for large motors above 200 hp. In addition, the most economic balance of copper wiring versus cost of switch gear is obtained at this voltage.

The usual installation of the pumps is in a separate room or basement adjacent to the press. If the pumping equipment must be in the plant area dust protected motors should be utilized. Again, depending upon the final installation, forced ventilated motors may be utilized, if required. This, of course, requires ducting and external blowers and filters for the cooling air. Smaller motors are operated at 440 volts and, if located in the vicinity of the press, are of TEFC (totally-enclosed, fan cooled) construction.

Starters. Starting equipment has been preliminarily arranged and costed for a conventional modern installation. Full voltage starters are of the non-reversing circuit breaker type, arranged in a modern control center with integral buss and incoming-line switch arrangements for each group of starters. Transformers and other substation switchgear have not been examined in this study since they depend upon local site conditions.

Low voltage starters are arranged in a 440 volt control center; they are of the non-reversing type with suitable circuit breakers and incoming line switches.

Both motor control centers have been developed with NEMA 12, industrial dust-tight construction, on the assumption that they will be located in a separate protected room. If the final plant layout dictates another location, the cost of these items should be re-examined.

Instrumentation. Both the press and power station are provided with suitable instrumentation for observation, control, and recording. Ram and container pressures, ram velocity, container temperatures, and other important items will be available from suitable signals.

The operator's control desk will include a cycle selector (for hand, single-cycle, and fully-automatic operation), controls for all individual functions of the press, as well as indication of the status of the power station.

Piping

The piping for either the oil-hydraulic system or the water-hydraulic system, as well as the piping mounted on the press proper would be of heavy-walled, seamless steel tubing manufactured to ASTM A-106 and meeting the requirements of the Pressure Piping Code ASA B-31.1. The flange connections would be of a proven Barogenics design using captive copper joint rings or vulcanized fiber rings precompressed prior to pressurization.

Materials Handling System and Press Operating Sequences

The materials handling system is designed to load dies, unload the extrusion butt and die, cut the extrusion, and separate the extrusion butt from the die. Most operations take place at the die end of the press. Optionally, the system can apply a drawing stress to an extrusion as it leaves the die. The materials handling system will first be described in terms of function and then described in detail, as it applies to various operations, later in this section.

The major components of the materials handling system are shown on Figures 18, A, B, and C. In reference to Figure 18A, the "billet and die loading" sequence is shown as follows:

(1) Roll the 11-inch diameter billet (or the support tube for 450,000 psi system) into position in front of the hydraulic pusher ram.

(2) Advance the pusher ram and move the billet into the container.

(3) Retract the pusher ram past the die.

(4) Move the die in front of the pusher ram.

(5) Push the die into the container, close the main gate lock, retract the pusher ram and move it up out of the way of the extrusion.

In Figure 18B, the "extrusion, die and butt unloading" sequence is shown as follows:

(1) Extrude the billet.

(2) Grip the extruded product by the chain-driven puller.

(3) Open the gate locks and pull the extrusion, die, and butt into the sawing position.

In Figure 18C, the "sawing and butt-die separation" sequence is shown:

(1) Move the saw down and cut the extrusion which then rolls away.

(2) Lower the butt carrier as the pusher arm moves forward.

(3) Push the butt out of the die into the butt carrier, which raises the butt up and then ejects it into a separate bin.

(4) Move die holder and pusher ram to their original position and repeat cycle.

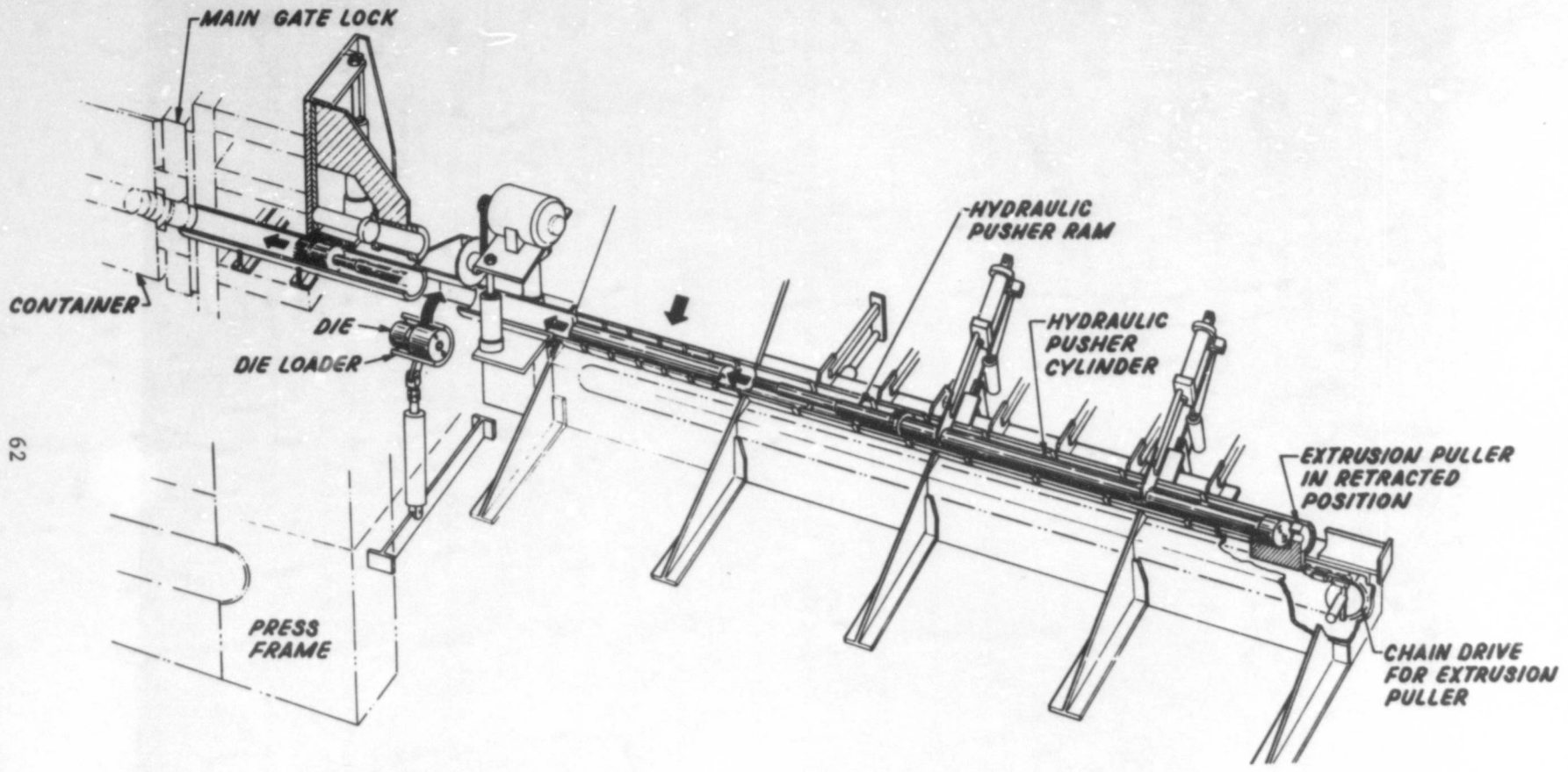

FIGURE 18A. MATERIAL-HANDLING SYSTEM - BILLET AND DIE-LOADING SEQUENCE

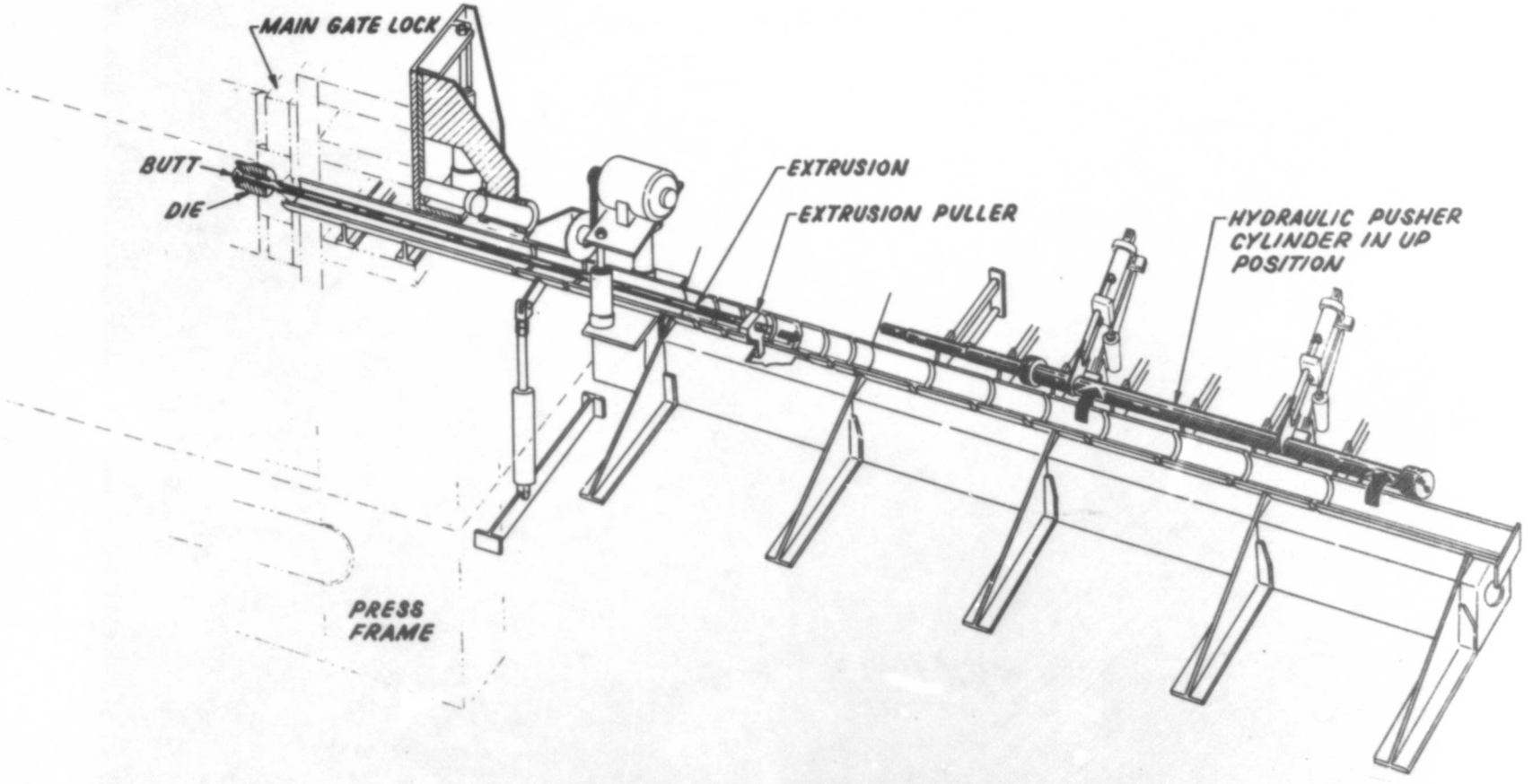

FIGURE 18B. MATERIAL-HANDLING SYSTEM - EXTRUSION, DIE, AND BUTT-UNLOADING SEQUENCE

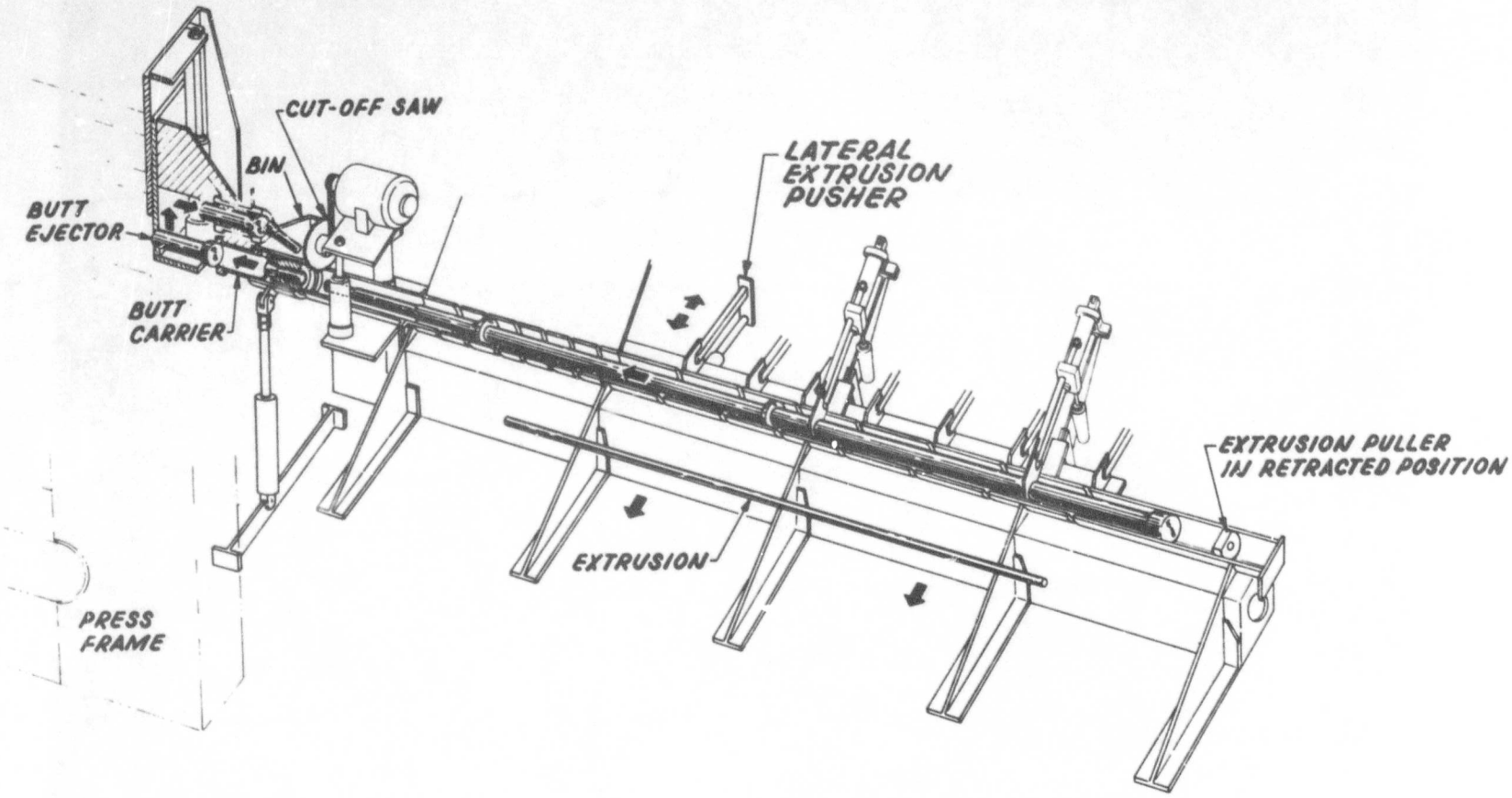

FIGURE 18C. MATERIAL-HANDLING SYSTEM - SAWING AND BUTT-DIE SEPARATION SEQUENCE

The cycle for the 6-inch liner is much the same, except that the billet and die are loaded in the support tube assembly, Figure 19. Then the support tube is treated much like a solid 11-inch diameter billet. The support tube is inserted into the 12-inch container and pushed against the 6-inch liner which, in turn, pushes the liner against the prepositioned outer ram. In this position, the inner support of the support tube can push the 6-inch diameter billet and die into the 6-inch liner. After extrusion, the extrusion butt and die are pushed into the support tube and removed from the press. The extrusion is extracted from the die in an separate operation away from and, therefore, independent of the press cycle. This and other possible sequences are illustrated in the following subsections.

The press and materials handling system were designed to produce solids, tubes, or shapes from either the 250,000 psi container or the 450,000 psi container into air (fluid-to-air), or from the 450,000 psi container into the 250,000 psi container (fluid-to-fluid). Further consideration was given to operating an additional auxiliary container so that very long extrusions could be produced by fluid-to-fluid techniques. Each of the operations will be described and schematically illustrated.

Solid Extrusions from the 250,000 psi Container

The sequence of operations is described to make a fluid-to-air solid extrusion, from the 250,000 psi, 12-inch ID container. The maximum billet size would be 11-inch diameter x 96 inches long. The billet could have any cross-section that could be circumscribed by a 11-inch diameter circle. See Figure 13 for typical billet and Figure 20 for a schematic drawing of the following operations sequence:

1) Billet with end cap moves into position in front of hydraulic pusher.

2) Pusher ram moves downward to operating position.

3) Pusher ram moves billet into container.

4) Pusher ram moves back for die.

5) Die moves into loading position.

6) Pusher ram moves die into container.

7) Main gate lock secures die; pusher ram moves back; center ram moves forward applying slight pressure on billet to insure seal; container is filled and bled.

8) Pusher ram moves upward to clear the way for extrusion; main ram moves forward to complete the bleeding operation, then proceeds to move forward at the extrusion speed and completes extrusion.

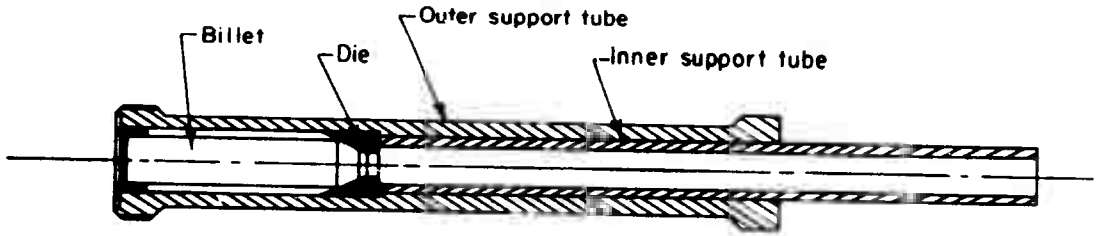

FIGURE 19. SUPPORT TUBE ASSEMBLY FOR LOADING BILLET INTO A 6-INCH CONTAINER

9) Main ram retracts to decompress chamber; main gate locks open and chain-puller grabs extrusion and pulls both extrusion and die into sawing position.

10) Extrusion is sawed.

11) Extrusion rolls off table.

12) Pusher ram and butt carrier move into position.

13) Pusher ram pushes butt out of die into butt carrier.

14) Pusher ram returns, butt carrier moves upward and butt is discarded; die moves out of way and is dropped into bin.

15) Pusher ram moves down and another cycle can start.

Since on unloading, castor oil will drip over a distance from the container to the die in the cut-off position, a catcher pan will be installed in the runout table to collect this oil, filter it and return it to the reservoir. This catcher pan will only extend to the die in the cut-off position.

The cut-off saw will be shielded on both sides, continuously flushed, and the chips will be collected in a separate catcher pan.

Tube Extrusion From the 250,000 psi Container

The sequence of operations is described for making a large-diameter tube from the 12-inch ID, 250,000 psi container. The maximum billet size is 11-inch OD x 10-1/2-inch ID x 96 inches long. The sequence assumes the center ram to be 10-1/2-inch diameter. The schematic drawing of the operations sequence in Figure 20 also applies in this case:

1) Hollow billet with hollow end cap moves into position in front of hydraulic pusher ram.

2) Pusher ram moves downward to operating position.

3) Pusher ram moves billet into container.

4) Pusher ram moves back for die.

5) Die is moved into loading position.

6) Pusher ram moves die into container.

7) Main gate locks secures die; pusher ram moves back; the center ram/mandrel moves slightly forward to extrusion position; the outer ram moves forward exerting sealing pressure through a spring between billet and die; container is filled and bled.

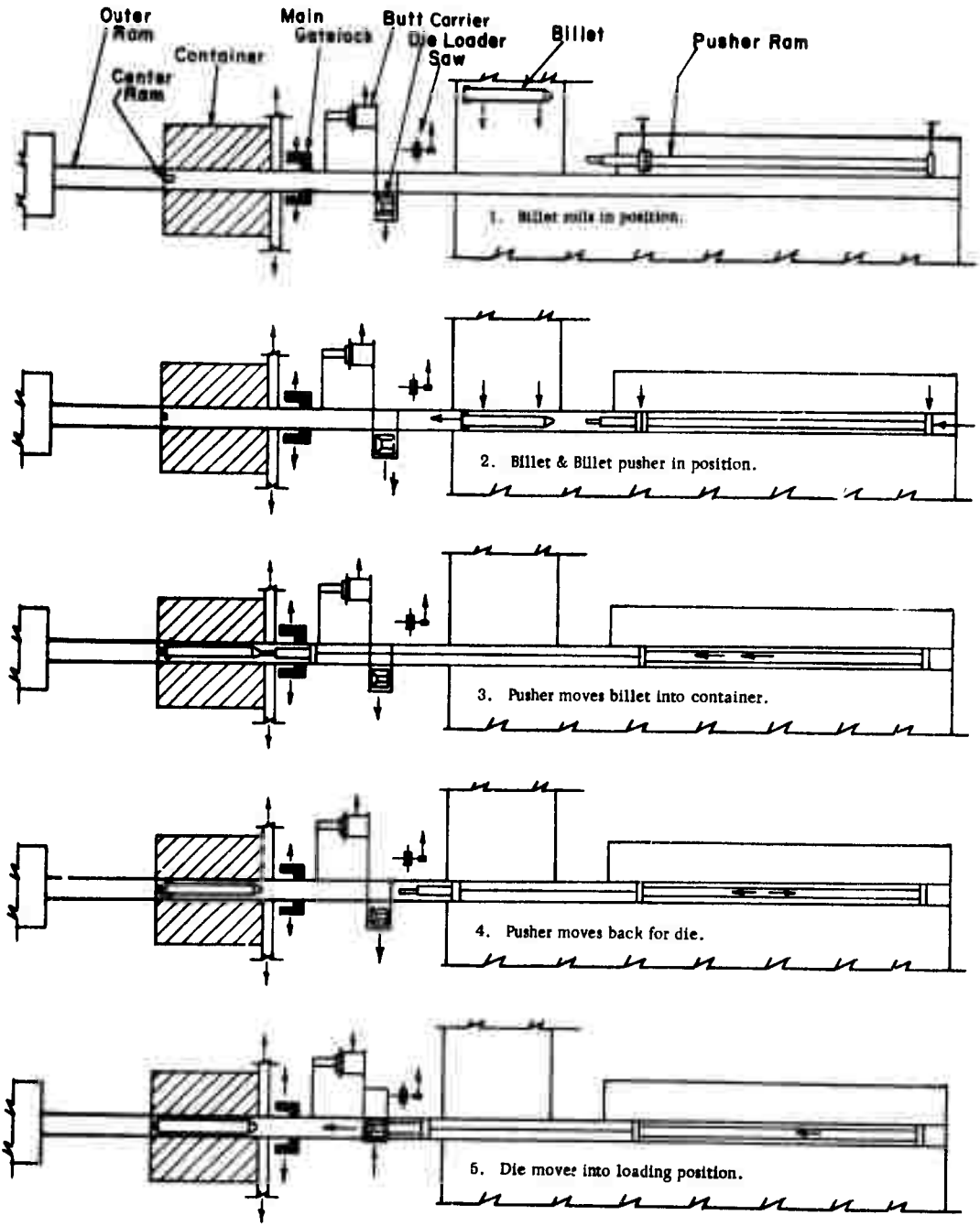

FIGURE 20. OPERATIONAL SEQUENCE FOR FLUID-TO-AIR EXTRUSION OF A 12-INCH BILLET AT 250,000 PSI

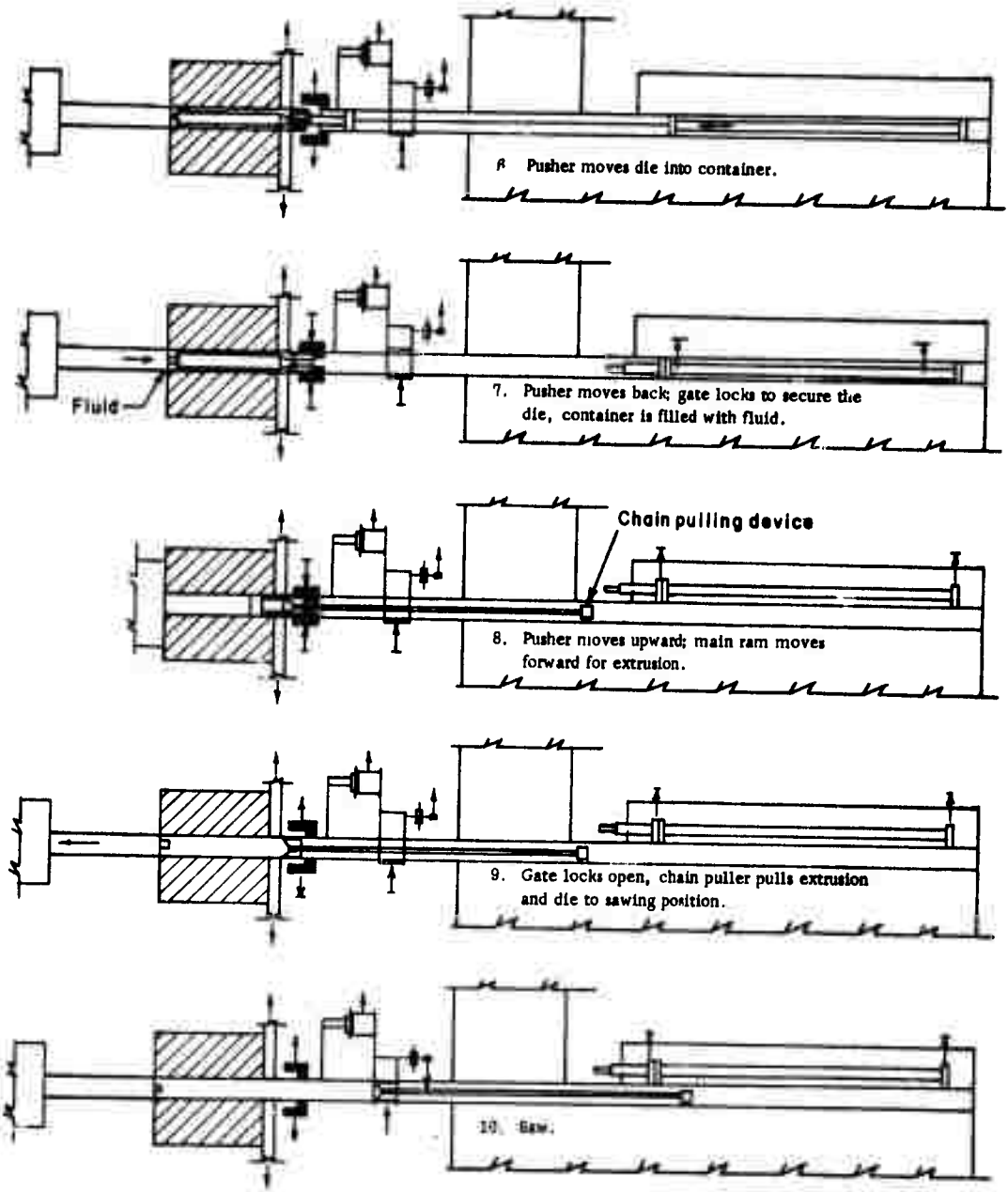

FIGURE 20. (CONTINUED)

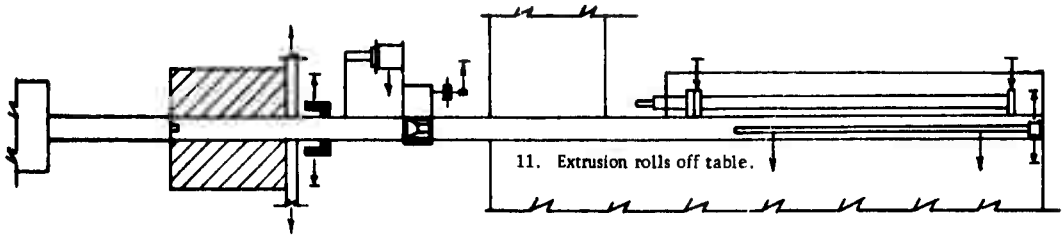

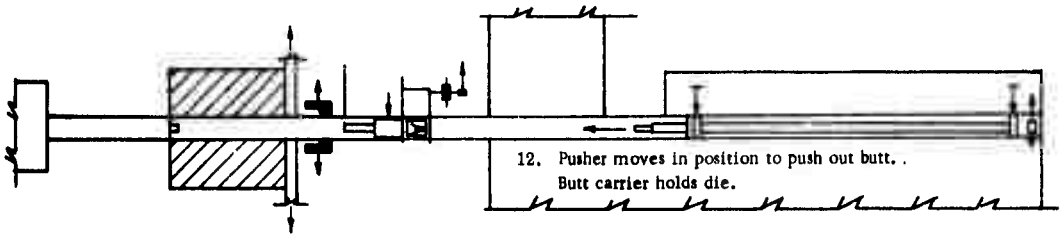

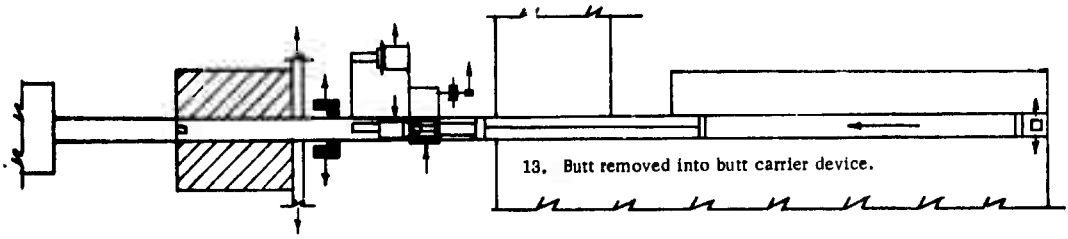

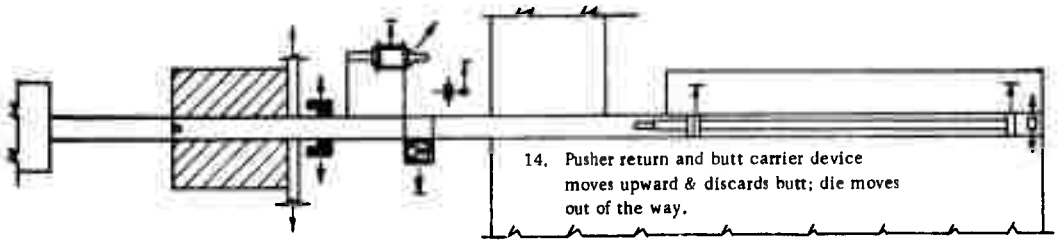

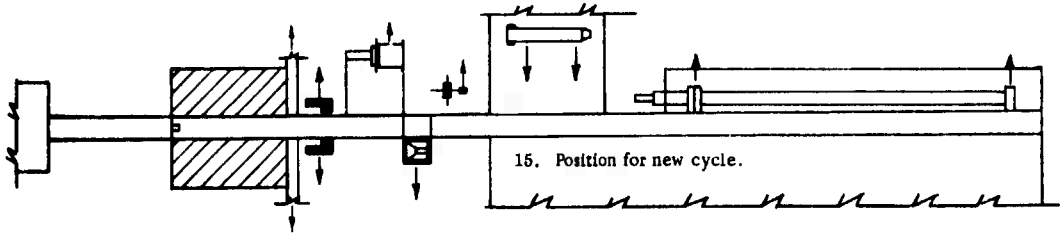

FIGURE 20. (CONTINUED)

8) Pusher ram moves upward to clear the way for extrusion; main ram moves slowly at first to complete the bleeding operation, then proceeds to move forward at the extrusion speed and completes extrusion. The center ram/mandrel is held fixed relative to the die.

9) Main ram retracts to decompress chamber; main gate locks open and the chain-puller grabs the extrusion and pulls the extrusion, die, and butt into sawing position.

10) Extrusion is sawed.

11) Extrusion rolls off table.

12) Pusher ram and butt carrier move into position.

13) Pusher ram pushes butt out of die into butt carrier.

14) Pusher ram returns butt carrier moves upward and butt is discarded; die moves out of way and is dropped into bin.

15) Pusher ram moves down and another cycle can start.

Extrusion Drawing from the 250,000 psi Container

This describes a sequence of operations to make extrusions with the addition of an applied draw force (HYDRAW). The billet may be a round, a hollow, or a shape but in any case the nose of the billet must be reduced to extend beyond the die about 4 feet. This extension could be obtained by joining an extension to the billet nose. A maximum force of 300 tons could be exerted over 40 feet of travel by a double acting hydraulic pusher ram which grips the end of the billet and pulls during the extrusion operation. The sequence is as follows:

(1) through (7) Same as that for solid extrusion from 12-inch container (Figure 20).

(8) Drawing grip on the end of the pusher ram is attached to the billet extension and the desired load applied; main ram ram moves slowly at first to complete the bleeding operation, then proceeds to move forward at the extrusion speed and completes extrusion. The actual draw force applied is based on the particular tube size and materials involved.

(9) Main ram retracts to decompress chamber; main gate locks open; draw cylinder pulls out die and butt into sawing position.

(10) through (15) Same as that for tubing.

Solid Extrusion from the 450,000 psi Container

This describes the operational sequence to make fluid-to-air solid extrusions from the 450,000 psi, 6-inch ID container. The maximum billet size is 5-inch diameter x 24 inches long. See Figure 14 for the typical billet size, Figure 19 for an illustration of the support tube with the billet and die in load position, and Figure 21 for a schematic of the following sequence:

(1) Support tube, loaded with billet and die, moves into loading position.

(2) Pusher ram moves into operating position.

(3) Pusher ram moves support tube into 12-inch container, pushing 6-inch container to rear position located by the outer ram; pusher ram moves back.

(4) Hollow end plug moves into loading position. (Same mechanism used for moving dies into loading position).

(5) Pusher ram moves end plug into sealing position at the same time, pushing billet into 6-inch container; main gate locks close.

(6) Outer ram and center ram move back to let fluid into the chambers; container is filled and bled; outer ram and center ram move forward and make the extrusion; pusher ram moves back.

(7) Outer and center rams retract to decompress chamber; main gate locks open; small gate locks close to keep 6-inch container from exiting 12-inch container; center ram moves forward, pushing the die out of the 6-inch container into the support tube; chain-puller grabs the extrusion.

(8) Support tube, die, butt, and extrusion are released at unload position and roll away.

Tube Extrusion from the 450,000 psi Container

The operational sequence to make tube extrusions is essentially the same as that required to make solid extrusions. Figure 22 illustrates a typical tube billet arrangement.

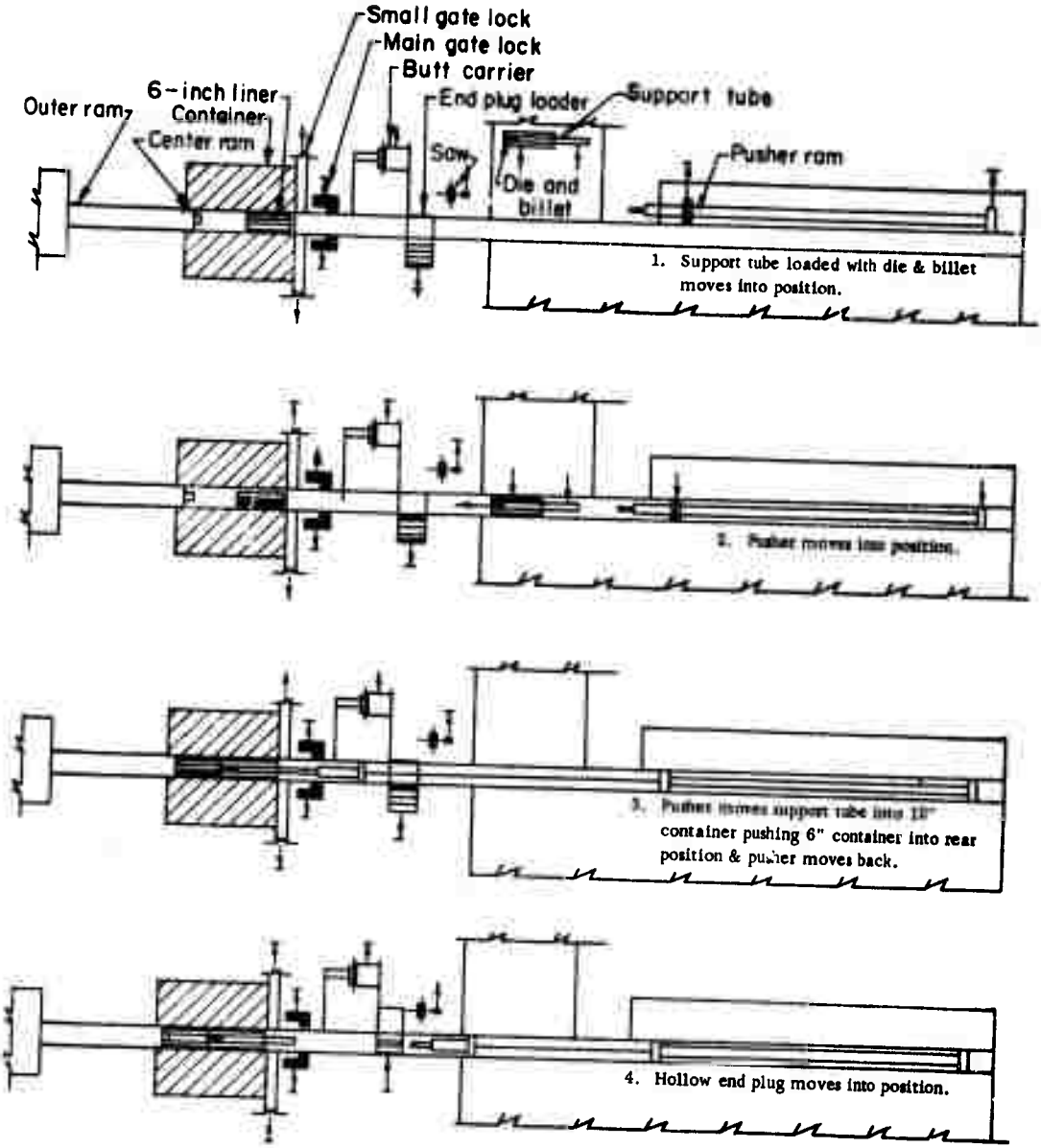

FIGURE 21. OPERATIONAL SEQUENCE FOR FLUID-TO-AIR EXTRUSION OF A 6-INCH BILLET AT 450,000 PSI

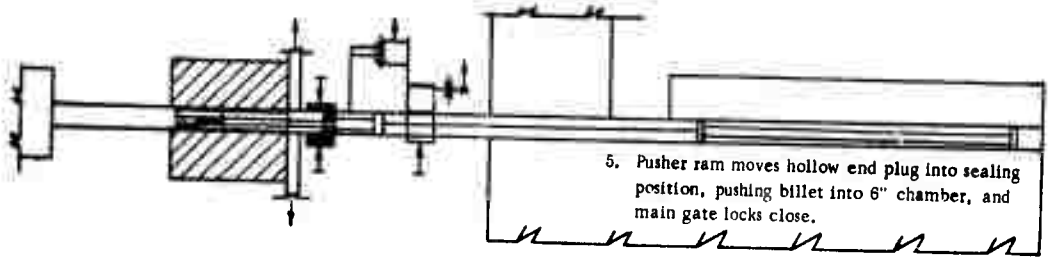

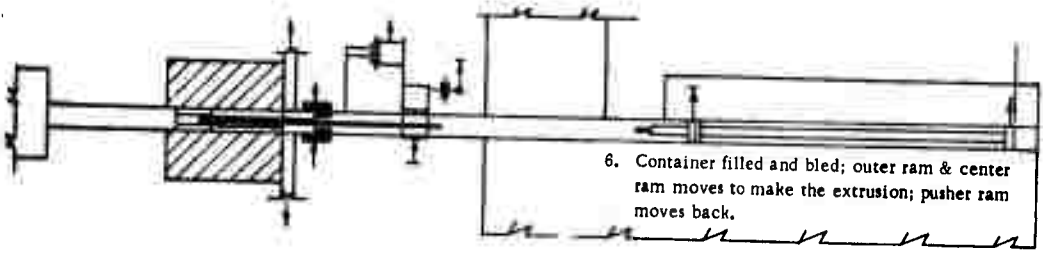

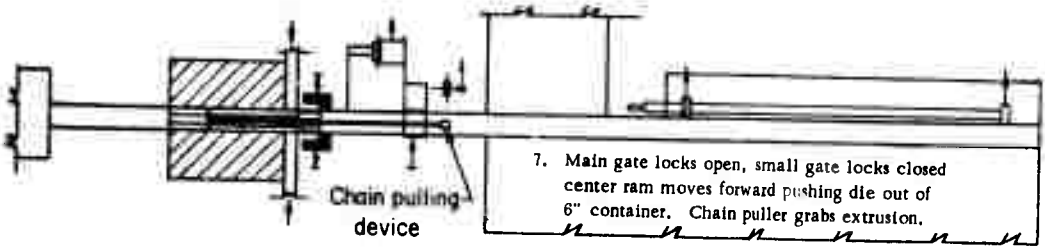

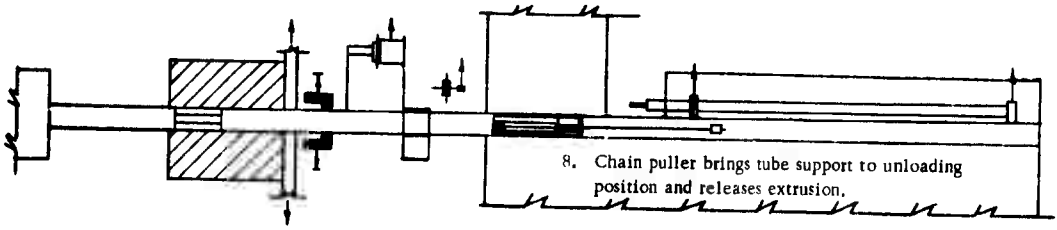

FIGURE 21. (CONTINUED)

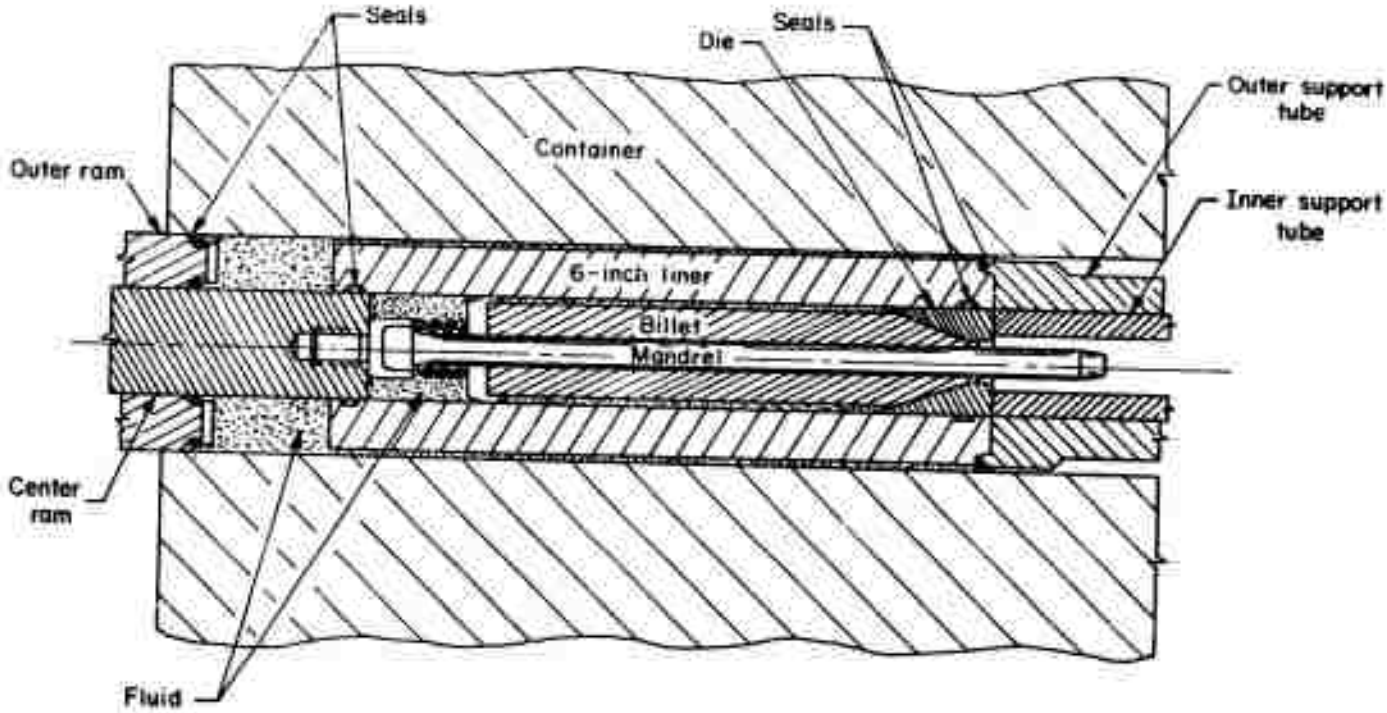

FIGURE 22. TYPICAL ARRANGEMENT FOR FLUID-TO-AIR OR FLUID-TO-FLUID EXTRUSION OF TUBES FROM 450,000 PSI CONTAINER

Fluid-to-Fluid Extrusion

This describes the operations sequence to make solid extrusions from 6-inch diameter, 450,000 psi container to the support tube at 250,000 psi. The maximum billet size is 5-inch diameter x 24 inches long. Figure 14 illustrates the tooling configuration for this operation except that the end plug would be solid and there would be no seal on the support tube. Figure 23 shows the schematic of the following sequences:

(1) Support tube loaded with billet and die moves into loading position.

(2) Pusher ram moves into operating position.

(3) Pusher ram moves support tube into 12-inch container, pushing 6-inch container to rear position located by the outer ram; pusher ram moves back.

(4) End plug moves into loading position. (Same mechanism used for moving dies into loading position).

(5) Pusher ram moves end plug into sealing position at the same time, pushing billet into 6-inch container; main gate locks close.

(6) Outer ram and center ram move back to let fluid into the chambers; container is filled and bled; outer ram and center ram move forward and make the extrusion; pusher ram moves back.

(7) Outer and center rams retract to decompress chamber; main gate locks open; pusher ram advances to remove end plug to unloading position.

(8) End plug moves out of the way; small gate lock closes to keep the support tube from exiting the 12-inch container; the center ram pushes the die with butt into the support tube.

(9) Small gate lock opens; outer ram pushes the 6-inch liner forward so that the support tube can be gripped by the chain puller, the chain puller extracts the support tube, die, and butt; small gate lock closes to prevent the 6-inch liner from leaving the 12-inch container.

(10) Support tube, die and extrusion are released and move to unloading area.

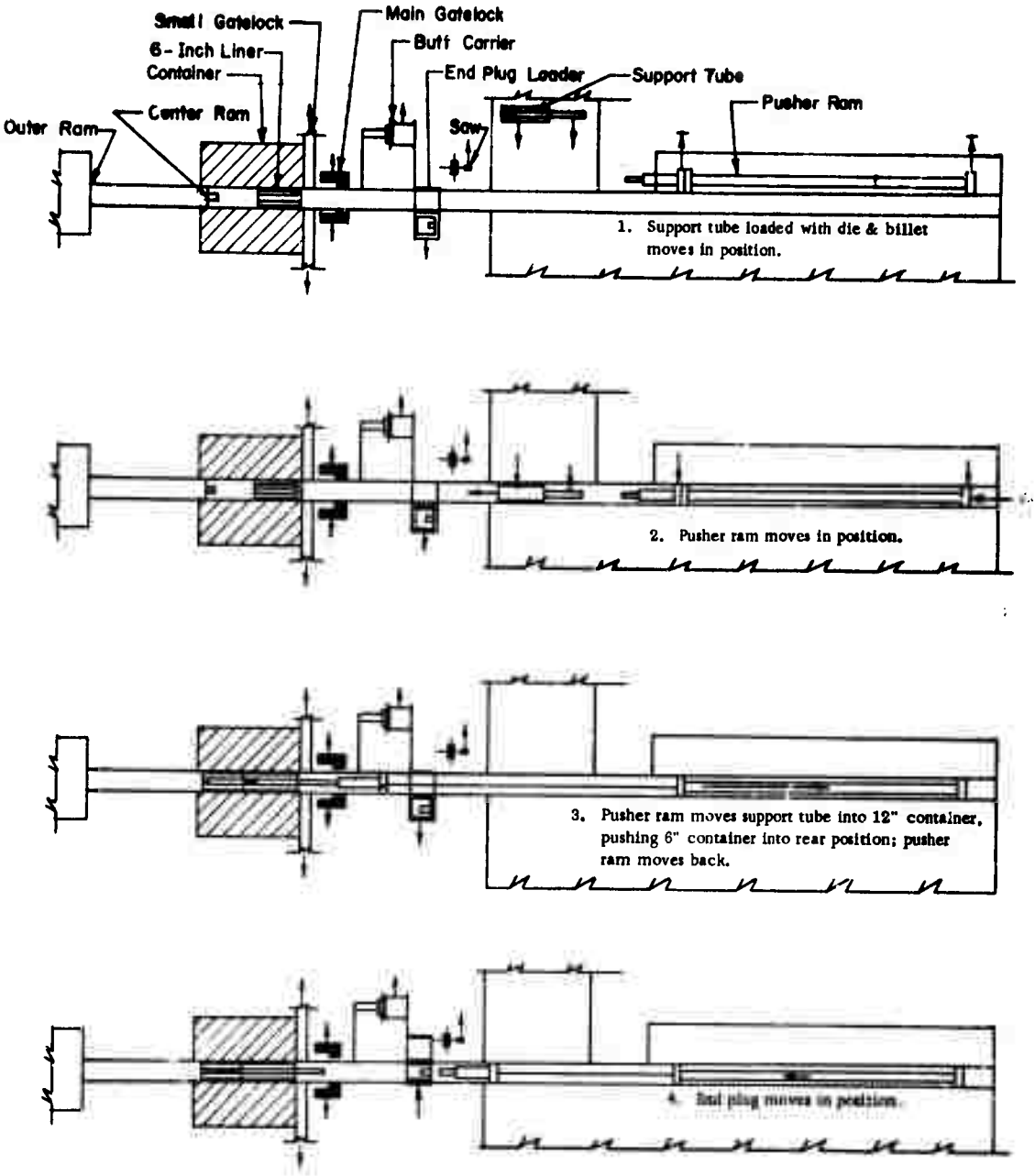

FIGURE 23. OPERATIONAL SEQUENCE FOR FLUID-TO-FLUID EXTRUSION OF A 6-INCH BILLET FROM 450,000 TO 250,000 PSI

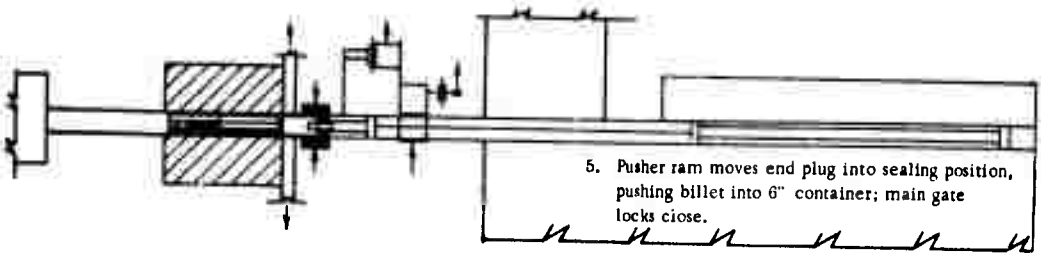

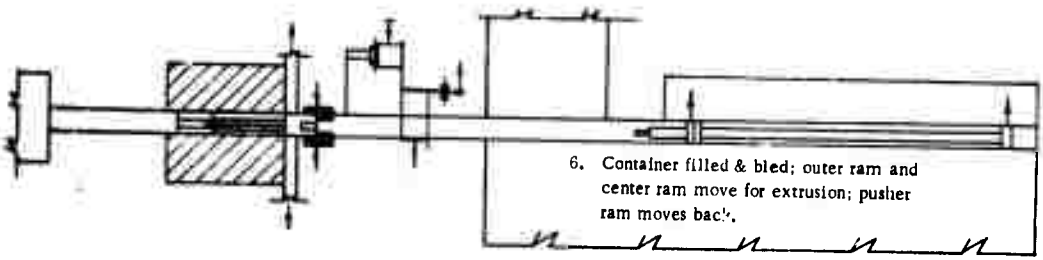

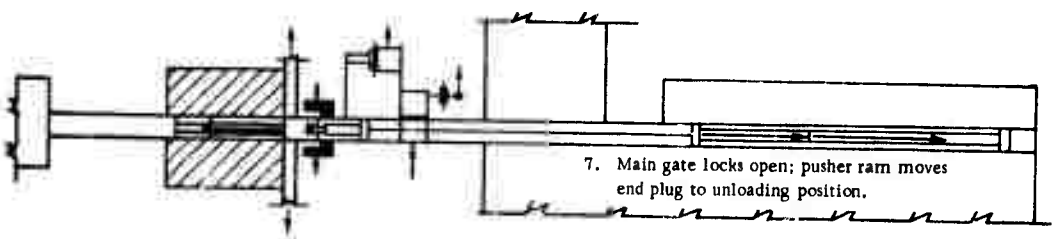

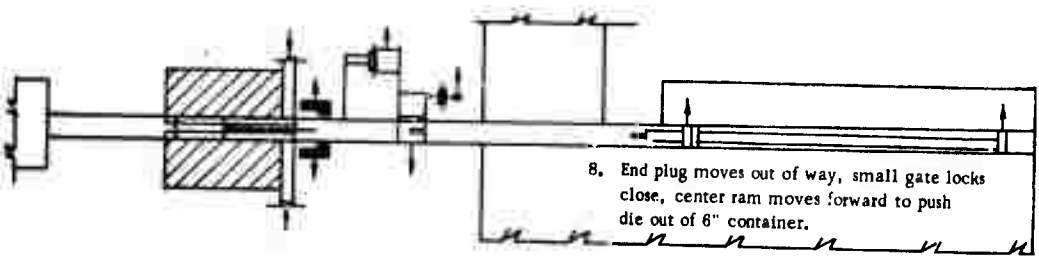

FIGURE 23. (CONTINUED)

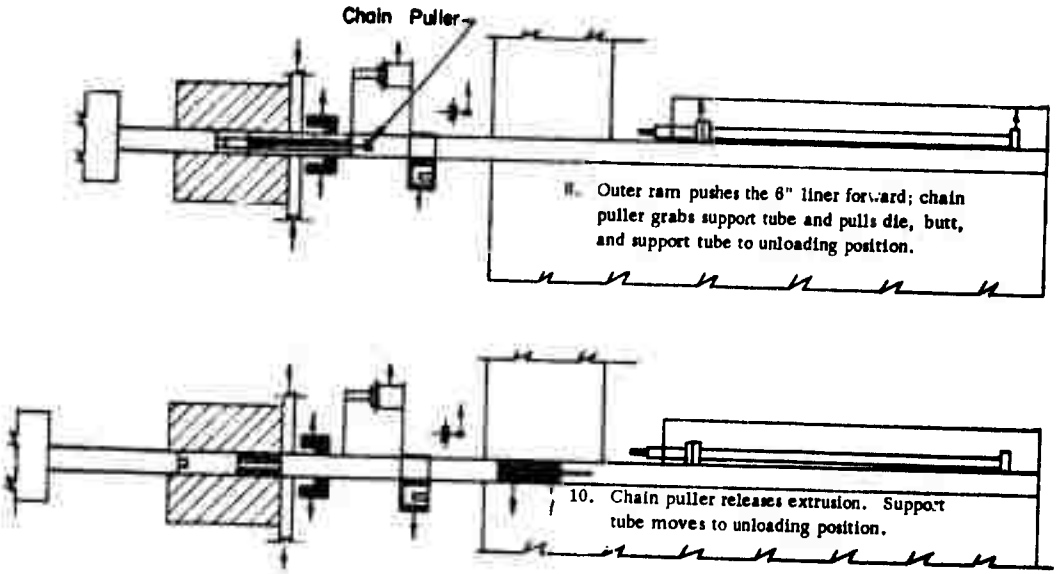

FIGURE 23. (CONTINUED)

This describes operations sequence to make solid extrusions from the 450,000 psi, 6-inch container (fluid-to-fluid) into an auxiliary container of 100,000 psi capacity. Figure 16 illustrated one possible arrangement of the auxiliary container. Figure 24 shows a schematic of the following sequence of operations.

(1) Support tube loaded with billet and die moves into loading position.

(2) Pusher ram moves into operating position.

(3) Pusher ram moves support tube into 12-inch container, pushing 6-inch container to rear position.

(4) Pusher ram moves back; auxiliary container moves into position.

(5) Pusher ram moves auxiliary container against the support tube and main gate locks close; main container is filled and bled; independently, the support tube and auxiliary container are filled and pressurized.

(6) Outer ram and center ram move forward for extrusion.

(7) Outer ram and center ram retract for decompression; main gate locks open; chain puller grabs auxiliary container; small gate locks open.

(8) Chain puller brings auxiliary container to unloading position; small gate locks close; center ram pushes the die with butt into the support tube.

(9) Small gate lock opens; outer ram moves forward, pushing 6-inch liner forward so that support tube can be gripped by chain puller; chain puller extracts support tube, die, and butt; small gate lock closes to prevent 6-inch liner from leaving 12-inch container.

(10) Chain puller brings support tube and extrusion into unloading position.

(11) Support tube and extrusion moved to reloading position.

Time Cycles for General Press Operations

Time cycles for various common operations were estimated and are shown below.

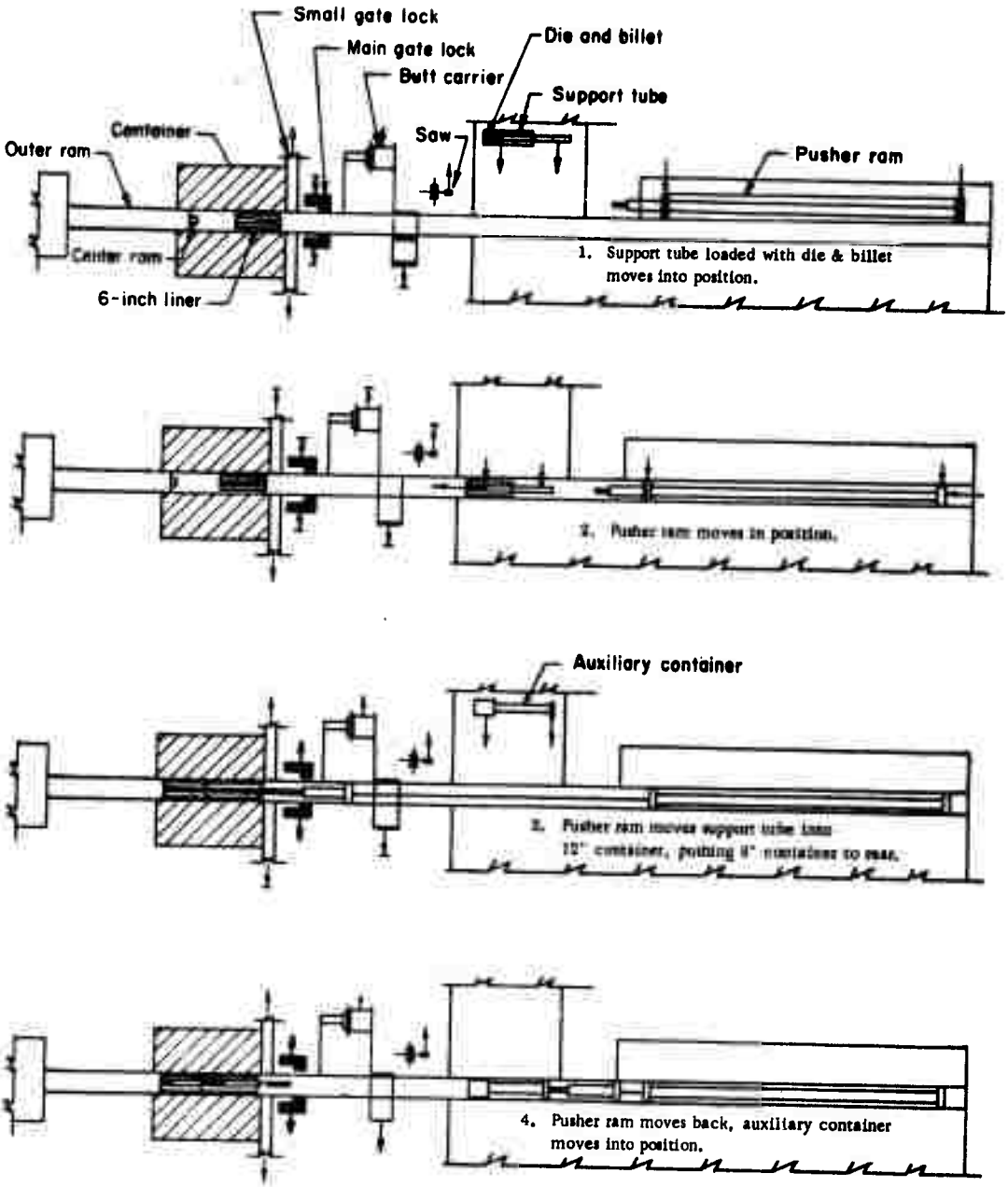

FIGURE 24. OPERATIONAL SEQUENCE FOR FLUID-TO-FLUID EXTRUSION OF A 6-INCH BILLET FROM 450,000 TO 100,000 PSI

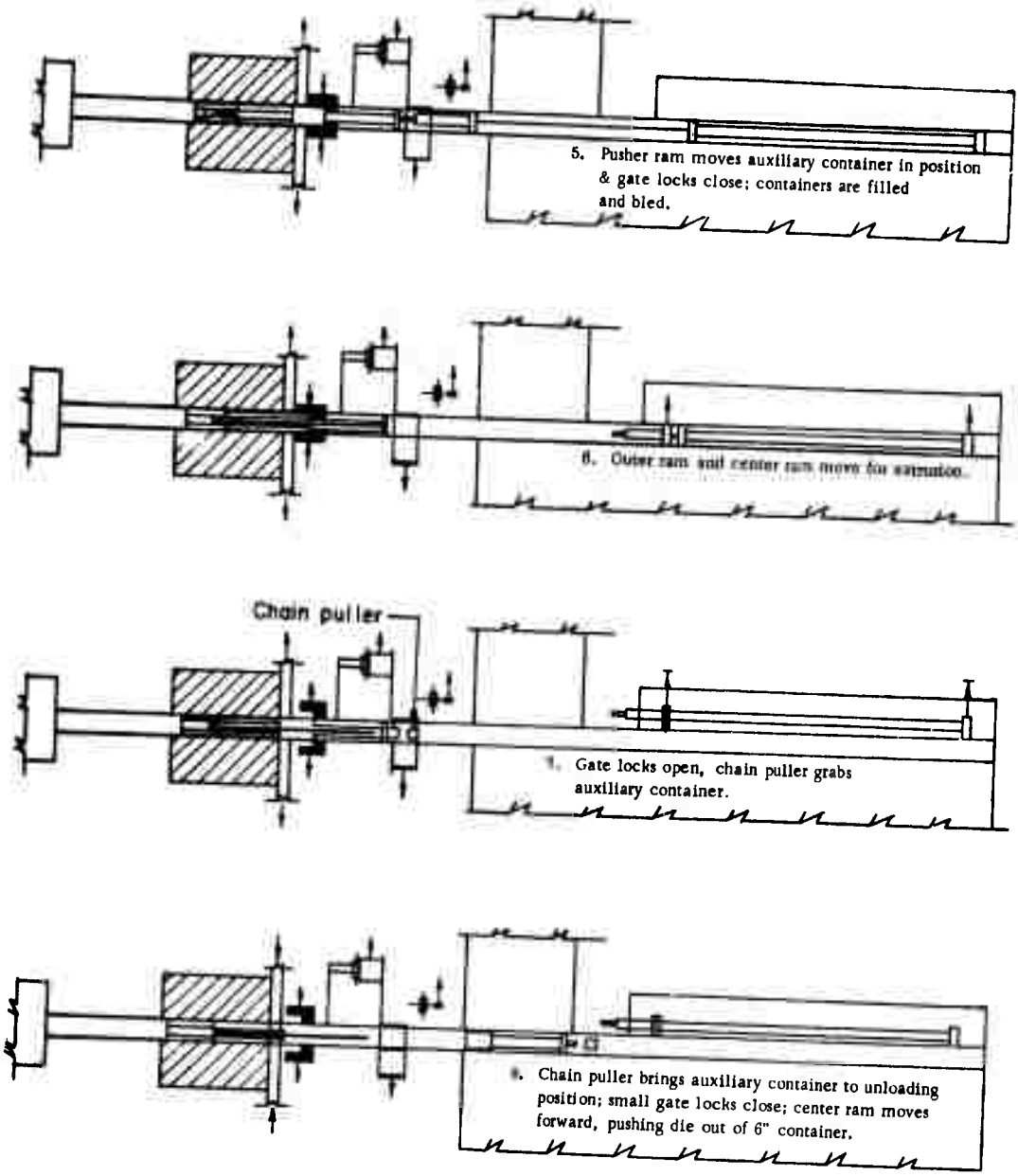

FIGURE 24. (CONTINUED)

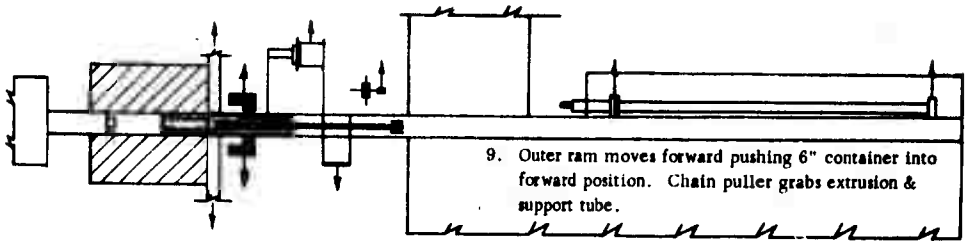

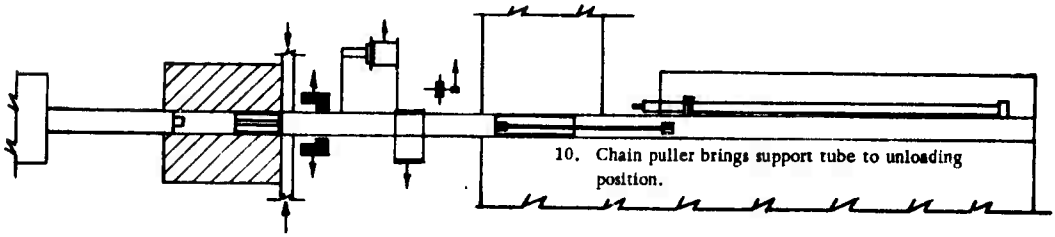

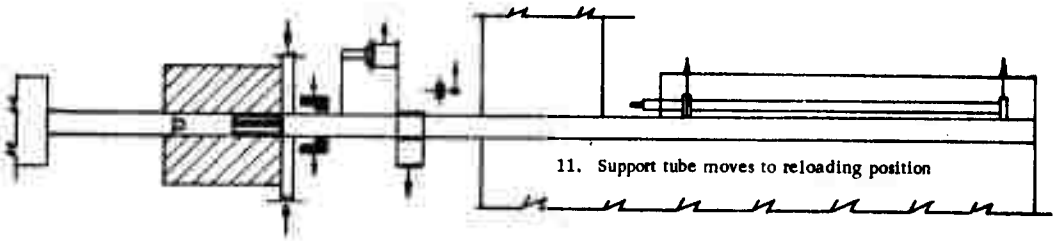

FIGURE 24. (CONTINUED)

Fluid-to-Air Extrusion - 12-inch, 250,000 psi Container. Maximum billet size: 11-inches diameter x 96 inches long. The following estimated times are approximately the same as those for production of tubes.

Step	Operation	Time, seconds
1	Outer stem stroke (compression and extrusion) 91" at 100"/min.	55
2	Decompression and liquid exhaust (continues during Step 3 as well)	3
3	Die lock release	2
4	Retraction of extrusion, die and butt: a) 200" at 20"/sec. = 10 sec. b) slowdown at the end = 1 sec.	11
5	Saw, down and up	9
6	Die and butt removed	2
7	Extrusion removal: simultaneously with Step 6	-
8	Billet loader action (billet and new die)	2
9	Pushing billet and die into chamber a) 200" at 20" per sec. = 10 sec. b) slowdown at the end = 1 sec.	11
10	Die locked	2
11	Inner stem advances (0.1 sec.) and seats billet in die (0.25 sec.)	0.35
12	Fluid handling a) Chamber evacuated: 2 sec. b) Chamber filled: 20 gallons 5 sec. at 4 gps	7
13	Chamber sealed by outer stem advance ((8 inches at 12 inches/sec.)	0.65
14	Total cycle time	105
15	Cycles per hour $\frac{3600 \text{ (sec/hr)}}{105 \text{ (sec/cycle)}}$ =	34.3/hr.
16	For the purpose of calculating the power requirements, the number of cycles assumed was:	35/hr.

Fluid-to-Air Extrusion - 6-inch 450,000 psi Container. Maximum billet size: 5-inch-diameter x 24 inches long. Extrusion of solids, shapes, and tubes (using floating mandrel techniques).

Step	Operation	Time, seconds
1	Inner ram stroke (compression and extrusion) 24.8" at 100"/min.	15
2	Pressurizing outer chamber: simultaneously with Step 1	-
3	Decompression of both chambers and exhaust of liquid from 6" chamber (continues during Step 4)	6
4	Push die and butt into support tube	2
5	Main die lock release	4
6	Small die lock closes (takes place during Step 7)	-
7	Retraction of extrusion die, butt and support tube	11
8	Die, butt and support tube removed	2
9	Extrusion removal (away from the press)	-
10	Billet loader action (billet new die and support tube)	2
11	Pushing billet, die, and support tube into main chamber: a) 200" at 20"/sec. = 10 sec. b) slowdown at the end = 1 sec.	11
12	End plug moves into position	3
13	Die locked	2
14	Outer and center ram retract to permit, fluid filling	5
15	Fluid handling a) inner chamber evacuated: 2 sec. b) inner chamber filled: 5 sec.	7

Step	Operation	Time, seconds
16	Chamber sealed by inner stem advancing a) 8" at 10"/sec. = 0.8 sec. b) slowdown = 0.2 sec.	1
17	Total cycle time	76
18	Cycles per hour:	47.4

Fluid-to-Fluid Extrusion. Maximum billet size: 5-inch diameter x 24 inches long. Six-inch liner located within the 12-inch chamber. Extrusion of shapes (or tubes with a floating mandrel) 450,000 psi against 250,000 psi back pressure to produce relatively short extrusions (72 inches long). The operational sequence will be similar to fluid-to-air extrusion from the 6-inch iner except that:

(1)	The stroke for the extraction of extrusion will be shorter	-2 sec.
(2)	Added time will be required to fill the support-tube volume	+1 sec.
(3)	Manipulation of the end plug	3 sec.
		+2 sec.

(4) Total cycle time = 76 sec. + 2 sec. = 78 sec.

(5) Cycles per hour: 46

Fluid-to-Fluid Extrusion Using an Auxiliary Container. The operational sequence will be similar to fluid-to-air extrusions except that:

(1)	The auxiliary container must be moved into and out of position. This time would be a function of its length, but may be in the order of	+20 sec.
(2)	An independent pumping system would be necessary to pressurize this chamber for flexibility; this would require about	+60 sec.
		+85 sec.

(3) Total cycle time: 76 sec. + 85 sec. = 161 sec.

(4) Cycles per hour: 22.4

ANALYSIS OF TOOLING

Container, stems, and dies are subjected to very high and complex stresses in the hydrostatic extrusion process. These key components were analyzed in detail to: (1) determine the practicability of various design concepts, (2) obtain general relationships that could be applied to a variety of designs, and (3) determine technical areas in which additional experimental data is needed.

Various design concepts for high-pressure containers were analyzed in detail in a prior research program.(14) Assuming a fatigue strength criterion and a high-strength liner, it was found that a multi-ring shrink-fit construction offered the most efficient design. In order to achieve a pressure capability of 450,000 psi, it was found necessary to use fluid-pressure support principles. The pressure capabilities of container designs were predicted based upon postulated fatigue behavior of high-strength steels under cyclic pressure conditions. Unfortunately, actual fatigue behavior under these conditions was found to be an unknown and this certainly warrants further study in a separate program. Also, the design predictions were based on a uniform pressure loading on the bore of the containers. Additional loadings should be analyzed for their effect upon fatigue lif- of the containers. It was also found that containers with large bores necessarily have large outside diameters which could, in some instances, make manufacture unfeasible.

In this report, design calculations are presented for a multi-ring container for 250,000 psi and a ring-fluid-ring container for 450,000 psi. The computer code MULTIR, developed in the preceding program(14), was used for these calculations. Analysis of additional loading effects is also presented, beyond that in the previous study. In addition, the knowledge to date on the general fatigue behavior of high-strength steels and the specific fatigue data available on thick-walled cylinders is reviewed. The employment of the autofrettage process as a means of reducing the size of the containers is also discussed. The previous study(14) was limited to five design concepts. In this report, an additional container concept was considered. This was a sectored container with no liner.

Choice of Materials for Container Design

One of the important aspects of the container design is the choice of material. In a previous study(14), the importance of a fatigue-strength criterion was emphasized for production containers. Therefore, container materials with high fatigue strengths would certainly be preferred for the design of an ultrahigh-pressure hydrostatic extrusion press for production purposes. However, there is a lack of triaxial and biaxial fatigue data under the combined stress states experienced at the bore of the liners of containers.

What are more generally known are the more common uniaxial fatigue data from rotating-beam or push-pull tests. A study of these data as related to the heat-treated condition of the material has been made to enable a choice of condition for the liner material that can also be expected to give similar fatigue-strength capability under cyclic internal pressure.

Material Fatigue Strength Considerations

Most of the available fatigue data on a variety of materials have been obtained on relatively small and simple laboratory specimens. The fatigue strength of actual parts under service conditions is affected by many factors, and it is often rather difficult to relate quantitatively the fatigue behavior of actual parts to that of laboratory specimens. However, many trends observed on laboratory specimens under various testing conditions do also apply to actual parts, at least in a qualitative sense.

In the selection of the material and its heat treatment for a part subjected to fatigue loading, the fatigue properties of the material are of primary importance. Depending on the application, some other material properties may also be important and it is often necessary to find a proper balance between the fatigue strength of the material and its other desired properties. In parts subjected to high loads, for example, high-strength materials must be often used to provide the necessary static strength. However, the fatigue strength of high-strength materials does not always increase in constant proportion to their static strength, and it may even decrease at very high static-strength levels.

Figure 25 (from Reference 30) illustrates results obtained from a large number of R. R. Moore--type rotating-beam fatigue tests on several alloy steels heat treated to various hardness levels. All these tests were conducted on unnotched speicmens at room temperature under similar test conditions. Because the static strength properties, ultimate and yield strengths, of steels do generally increase with the hardness, it can be stated from Figure 25 that there is an optimum strength (hardness) level for each steel at which the fatigue (endurance) limit reaches a maximum value. Using a steel at a strength level higher than this optimum level in a part subjected to fatigue loading would cause a decrease in the fatigue strength (life) of the part. It can be also deduced from the figure that the optimum strength level might be different for different steels and that the scatter in fatigue data increases with the static strength levels, even for the same steel. To assure a safe design against fatigue failure, the lower values of the scatter band must be used as the design criteria, which reduces somewhat the "useful" fatigue strength of high strength steels as compared to their average fatigue strength.

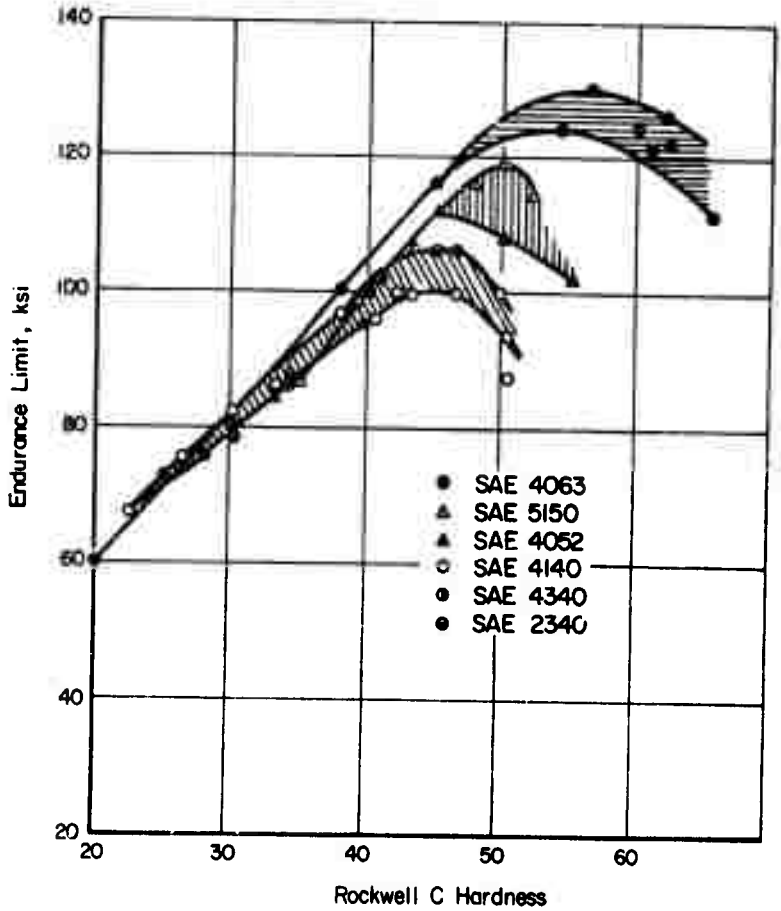

FIGURE 25. - OPTIMUM HARDNESS FOR MAXIMUM FATIGUE STRENGTH OF SEVERAL STEELS

Literature sources[30] provide several explanations for the decrease in fatigue strength of high-strength steels after reaching a certain maximum value. For example, it has often been mentioned that the notch and surface sensitivity, the susceptibility to flaws and defects, the detrimental residual stresses (from quenching), and the effects of some metallurgical factors all increase with the static strength level of steels. These factors are said to be responsible for the decrease in fatigue strengths beyond a certain ultimate strength level of steels. Two regions of different types of fatigue failure have been identified in reference to Figure 25. Failures to the left of the maximum fatigue strength values in Figure 25 are ductile failures, and those to the right are brittle failures.

Figure 26 illustrates further the general trends in the relationship between the static and fatigue strengths of steels at relatively high-strength levels. These data were taken from several sources[30-35]. They represent the results of rotating-beam fatigue tests conducted at room temperature on unnotched specimens made of various heat-treated steels at various strength levels. The fatigue limit was taken as the fatigue strength at 10^7 cycles. For specific applications, it would be better to have such separate plots for each steel grade obtained on specimens subjected to a fatigue loading that corresponds to the loading conditions in the particular application. However, there are not sufficient data of that kind available and not all of the available data can be considered as compatible. The unnotched rotating-beam fatigue data were selected for illustrative purposes in Figure 25 because these data are more readily available than other types of fatigue data.

Two general trends are apparent from Figure 26: (1) the scatter in fatigue data increases with the strength level of steels, and (2) the average fatigue strength of high-strength steels increases considerably less than their ultimate tensile strength. As was explained above, the fatigue strength of a certain steel grade may even decrease with an increase in its ultimate strength after reaching an optimum value. The fatigue data represented in Figures 25 and 26 were obtained on smooth, polished specimens. Because actual parts may not have such smooth, polished surfaces and the parts may contain geometric stress concentrations, fatigue tests conducted on specimens with surface finishes corresponding to the actual applications and on so-called "notched specimens" give results that are more representative of actual conditions. Although there have been many such tests conducted, it is difficult to correlate the results because of the large variety of notches and surface conditions used in these tests and because not enough data were obtained under each specific condition. However, some general trends have been observed and these are represented schematically in Figure 27. Although the shapes and relative values of the curves shown in Figure 27 may change for different materials, specimen configurations, and testing conditions, the general trends appear to prevail in all cases whenever there are sufficient fatigue data available. These trends are

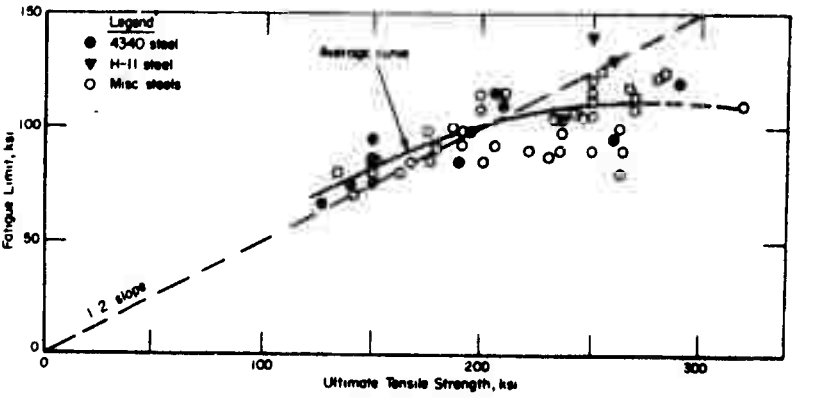

FIGURE 26. UNNOTCHED ROTATING-BEAM FATIGUE LIMIT FOR MISCELLANEOUS HEAT-TREATED STEELS AT VARIOUS ULTIMATE TENSILE STRENGTH LEVELS

Data taken from several sources.

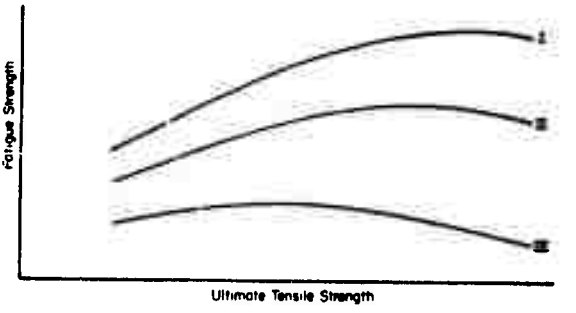

FIGURE 27. GENERAL TRENDS IN FATIGUE STRENGTH OF HEAT-TREATED STEELS AS A FUNCTION OF ULTIMATE TENSILE STRENGTH

I - Smooth, polished specimens.
II - Specimens with mild notches and/or medium smooth surfaces.
III - Specimens with severe notches and/or rough surfaces.

characterized by a decrease of fatigue strength and by a shift of the optimum ultimate tensile strength toward a lower value with increasing notch severity and/or surface roughness. The decrease of fatigue strength with the notch severity (and surface roughness) can be readily explained because notches cause stress concentrations, and the higher the stress concentration the lower is the expected fatigue strength. The main reason for the shift (lowering) of the optimum ultimate tensile strength is probably the higher notch sensitivity of high-strength steels.

From the foregoing discussion it should be apparent that materials with the highest possible ultimate tensile strength are not necessarily the best for application in parts subjected to fatigue loading. This is particularly true for parts that contain stress concentrations and that have less than perfectly smooth surfaces at critical locations. Material selection from among the many high-strength steels with their various available heat treatments (static-strength levels), therefore, should be based in large part on the available fatigue data. There are some indications, that high-strength steels exhibiting good ductility and toughness have also relatively good fatigue strength. These should receive the first consideration.

It should be noted that the fatigue strength values obtained on small laboratory specimens are seldom fully realized in actual parts because of the so-called "size effect", even if all the other conditions are similar. In addition, there are many other factors that may affect the fatigue behavior of an actual part in service and these must be evaluated for each individual application. Such additional effects in the hydrostatic container applications are discussed in the next section.

Fatigue Behavior of Thick-Walled Cylinders

The most extensive studies of the fatigue behavior of thick-walled cylinders have been conducted by Morrison, Crossland, Parry, Burns, and their co-workers in England. These studies were recently summarized at the High Pressure Engineering Conference in London, September 1967 by Burns and Parry[36]. They have limited the study primarily to one English steel, En 25 (Vibrac V-30). All fatigue specimens had approximately the same chemical composition* and heat treatment. The strength values were:

yield strength, σ_y = 103 to 112 ksi

ultimate strength, σ_u = 121 to 129 ksi.

---

* Chemical composition: 0.29 to 0.3 C, 0.14 to 0.17 Si, 0.64 to 0.69 Mn, 0.015 S, 0.013 P, 2.53 to 2.58 Ni, 0.57 to 0.60 Cr, 0.57 to 0.60 Mo.

This is a relatively low strength level. This material is comparable to AISI 4340 steel and therefore, at this strength level, it can be expected to exhibit ductile fatigue failure corresponding to points to the left of the peak of the endurance limit-hardness curve, Figure 25. The conclusion of the studies on En 25 steel was that the fatigue data correlates best with shear stress[34]. (This was the assumption made in Reference (14) and confirmed here.) Figure 28 shows a fatigue diagram for the semirange in shear stress S_r plotted versus the mean shear stress S_m. This figure is essentially the same as Figure 28.6 in Reference (36), except that here the semirange in shear stress is used instead of the total range, and the stress units, ksi, are used instead of tons/in^2. The data points in Figure 26 were taken from the original publications, References (36-42). Data for compressive mean stress for push-pull tests from Reference 40 are also plotted which were not included in Figure 28.6.

Figure 28 also shows data for torsion of tubes, push-pull of solid round specimens, and internal pressure cycling of monoblock cylinders, shrink-fitted cylinders, and autofrettaged cylinders. The shear stress in the torsion tests is the applied stress. The shear stress in the push-pull tests is:

$$S = \frac{\sigma_z}{2} \tag{1}$$

where σ_z = the applied axial stress. The largest shear stress in the cylinder test occurs at the bore and is

$$S = \frac{\sigma_\theta - \sigma_r}{2} \tag{2}$$

where σ_θ = the circumferential (hoop) stress and σ_r = the radial stress equal to the applied pressure at the bore. The semirange in shear stress is

$$S_r = \frac{S_{max} - S_{min}}{2} , \tag{3}$$

and the mean shear stress is

$$S_m = \frac{S_{max} + S_{min}}{2} . \tag{4}$$

(Reference: Equations (6a, b) Reference (14).

Figure 28 also shows the line for R = 0. The stress ratio R is a common fatigue parameter used in the U.S. It is defined as:

$$R = S_{min}/S_{max} .$$

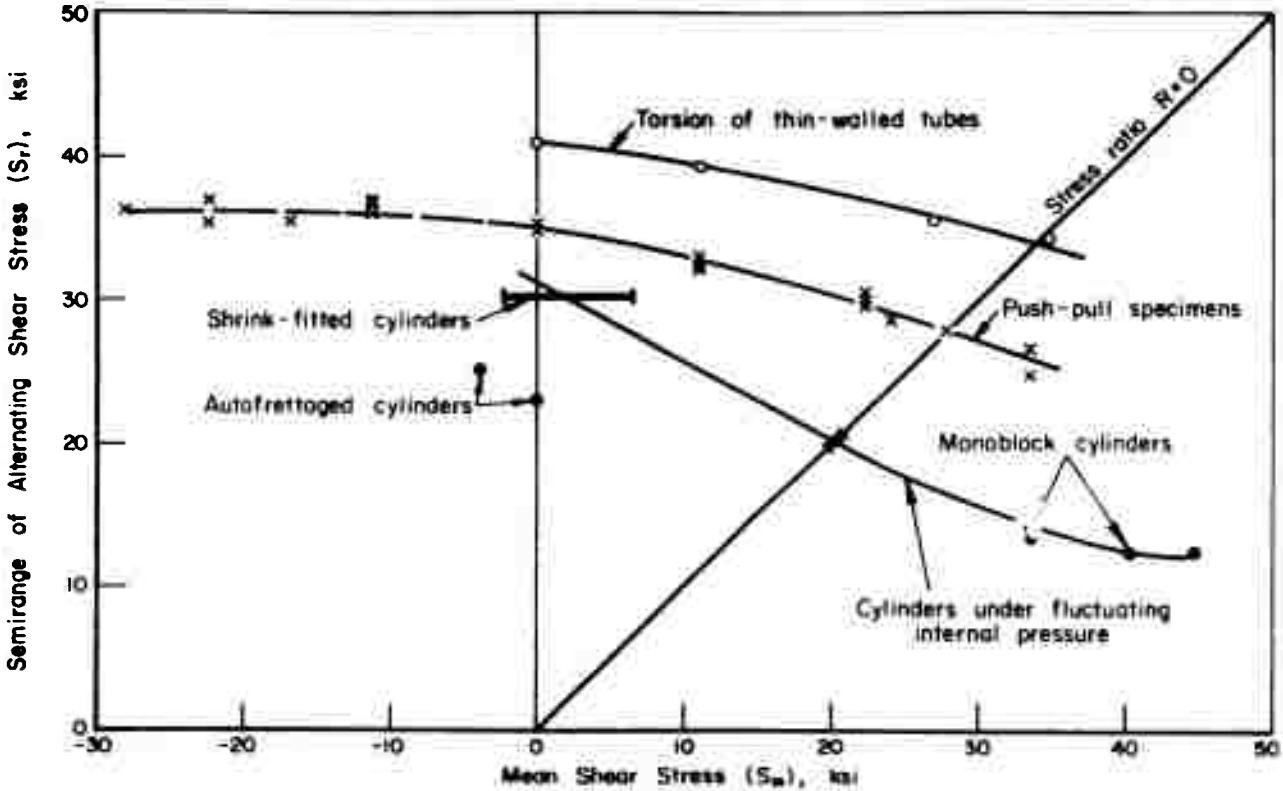

FIGURE 28. PORTIONS OF SHEAR STRESS RANGE DIAGRAMS FOR En 25 STEEL AT 10^7 CYCLES

Data in Figure 28 shows that hollow cylinders have a lower fatigue stress for 10^7 cycles than obtained by torsion and push-pull tests. This difference was also pointed out in Reference (14), in connection with discussion of the fatigue data reported by Watervliet Arsenal, Reference (43). Attempts have been made to correlate the data, but overall correlation cannot be obtained and is not apparent at this time. Apparently there are some other effects involved. It may be that fluid under pressure has a detrimental effect such as helping to propagate cracks by a wedge type of loading.

Autofrettaged cylinders also show the lowest fatigue strength, lower than shrink-fitted cylinders. This is believed to be due to an effect of cycling upon the residual stresses. The residual stresses result from plastic deformation during the autofrettage process. This residual stress state may not reach a lower and elastic repeatable value until after several pressure cycles. The steel may exhibit a Bauschinger effect and hysteresis. These effects would contribute to the lower fatigue strength for the autofrettaged specimens. The autofrettage data point on the compressive side of Figure 28 is a corrected value. It apparently was mistakenly reproduced on the tensile side of Figure 28.6, Reference (34).

The data all show an increasing trend for the semirange shear stress, S_r, when the mean shear stress, S_m, is decreased. The stress S_r, is proportional to the range of the applied pressure, p. Therefore, increasing S_r increases the pressure capability. But this does not mean $S_m < 0$ is necessarily desirable, for as pointed out in Reference (14), $S_m = 0$ corresponds to:

$$(\sigma_\theta)_m = -\frac{P_o}{2} \tag{5}$$

where $(\sigma_\theta)_m$ is the mean hoop stress. This means that the minimum hoop stress,

$$(\sigma_\theta)_{min} = -p \tag{6}$$

and the maximum hoop stress is

$$(\sigma_\theta)_{max} = 0 \tag{7}$$

when there is no residual bore pressure, i.e., the hoop stresses are entirely in the compressive range and $(\sigma_\theta)_{min} = -p$ is really the limitation imposed by $S_m = 0$.

Additional information and conclusions regarding Figure 28 and References (36-42) are now summarized as specific points:

(1) The torsional and push-pull data in Figure 28 are for specimens with unprotected surfaces at atmospheric pressures.
(2) The cylinder data are for virgin specimens with surfaces unprotected from the pressurized hydraulic oil, but with good, honed internal surfaces.
(3) Runout cylinder specimens (tested below the endurance limit), when retested, show a higher fatigue strength[38]. (This is probably due to what is known as a "coaxing" effect).
(4) Cylinder specimens that are honed (re-honed) after heat-treatment show a higher fatigue strength[38].
(5) Cylinder specimens with a rubber protective film show higher fatigue strengths, at least at 10^6 cycles and less[38]. (There are no data for longer life tests).
(6) The effect of anisotropy on the fatigue strength has been observed in torsional tests[38].
(7) Compressive push-pull fatigue strength seems to decrease after reaching a certain value of mean stress[40]. However, additional data does not show a marked decrease, Figure 28.
(8) Push-pull tests in oil under pressure (44.8 ksi) result in shorter fatigue life than tests conducted in air, but if the specimen surfaces are protected by a rubber film, then the fatigue life is longer than in air with no pressure[41]. (For reversed loading, the numbers for endurance limits are: (a) $\sim \pm 35$ ksi in air (b) $\sim \pm 32$ ksi under pressure, and (c) $\sim \pm 37$ ksi under pressure, protected).
(9) Under fluid pressure of 44.8 ksi, there are no fatigue failures at mean compressive stresses, but only yielding[41].
(10) In torsional tests on solid specimens, the effect of liquid and pressures is similar to those of push-pull tests: (a) for reversed tests in air ±44 ksi, (b) in oil bath (no pressure) ±39 ksi, (c) in oil under pressure (44.8 ksi) ±38 ksi, and (d) in oil pressure, protected ±56 ksi[40]. The same trends have been also observed for repeated loading.
(11) Nitrided surfaces increase the fatigue strength[42].
(12) For austenitic stainless steel the shear-stress correlation is poor. This has been explained by the effects of "natural" autofrettage, etc.[42].

Thus, although the fatigue strength of ductile steel cylinders has been extensively studied there are still some unresolved differences between cylinder tests and other conventional tests, and many influential factors have been uncovered. It must be emphasized that what is yet needed is a fatigue study of high-strength-steel cylinders under cyclic internal pressure. Until such a study is conducted, the best that can be done is to postulate the fatigue behavior of high-strength-steel cylinders based upon the available uniaxial fatigue data.

Manufacturing Considerations

The material tensile strengths and fatigue strengths determined on laboratory specimens may not be realized in actual containers because of manufacturing limitations. It appears that yield strength levels much above σ_y = 225,000 psi are difficult to achieve in H-11 cylindrical forgings in the large diameters considered in this study(44). To obtain higher strength liners of large diameter, an alternative is to use a maraging steel. A 250,000 psi yield strength, 18 percent nickel maraging steel cylinder, can be manufactured in relatively small sizes. Non-uniform properties are produced in rings manufactured from large ingots, the sizes of which are required to make a 12-inch ID container. The maraging steels, moreover, have exhibited appreciable notch sensitivity in fatigue tests(45).

Cylindrical forgings can also be expected to have appreciably different longitudinal and transverse properties. For example, the transverse ductility is normally expected to be only one-half that in the longitudinal direction. These manufacturing limitations can be expected to reduce somewhat the expected fatigue life of container designs.

The Autofrettage Process

The autofrettage process has found extensive use as a means of producing compressive residual stresses at the bore of a cylinder. In particular, it has been used on gun barrels(46). A cylinder is autofrettaged by an initial over pressure beyond the yield pressure but below the plastic collapse pressure. The autofrettage pressure produces yielding in an inner annulus of the cylinder due to expansion of the bore. Upon release of the pressure, the inner annulus tends to take a tensile permanent set (elongation) but is restrained from doing so by the outer annulus of material which has remained elastic or in the extreme case also yielded but to a lesser extent. Thus, the outer annulus compresses the inner annulus of material upon release of pressure. The compressive hoop stresses near the bore are balanced by tensile hoop stresses near the outside to satisfy the equilibrium condition under zero bore pressure. Thus, residual stresses can be achieved at the bore similar to shrinking the cylinder with a hoop. This is the origin of the French word "autofrettage" meaning "self-hooping".

It is not intended here to review the theory of autofrettage. This has already been very well done in a report by Watervliet Arsenal(46). However, some of the more important results are summarized here for a perfectly plastic material (no strain hardening). The application of the process to high strength steels, the effect of strain hardening and limitations of autofrettage are also discussed.

The term "percent overstrain" is often used in connection with autofrettage to indicate the percentage of the wall thickness that yielded. One hundred percent overstrain corresponds to plastic flow all the way to the outside diameter. The term "percent autofrettage" is also used. It is defined as the ratio of the residual hoop stress at the bore, for a given percent overstrain, to the maximum theoretically possible for a given wall ratio. It can be shown that 100 percent autofrettage is achieved for 100 percent overstrain for a wall ratio $K = 2.2$. For $K < 2.2$, 100 percent overstrain produces less than 100 percent, autofrettage, i.e., the residual hoop stress at the bore is lower in magnitude than the compressive yield strength.

It can also be shown for 100 percent overstrain and for 100 percent autofrettage, the maximum autofrettage pressure is $P_{max} = 0.91\ \sigma_y$ where σ_y is the yield stress for a perfectly plastic material. Thus, P_{max} is always less than σ_y.

In order to predict the successful application of the autofrettage process to high strength steels it is important to consider the ductility. The ductility (100 ϵ, where ϵ is the tensile strain in inch/inch) of some steels is given in Table IV. These data are for simple tensile tests on specimens from small rods or bars. In large forgings, it can be expected that the longitudinal ductility may reach these values but the transverse ductility (in the hoop direction) at the bore may be only 1/2 the values in Table IV, Reference (44). For example, consider the D-6A steel in Table IV with an expected transverse ductility of $\frac{7.5}{2} = 3.75$ percent. Compared with the maximum hoop strains calculated for 100 percent autofrettage for $\sigma_y = 250{,}000$ psi, 0.0375 is found to be larger than $(\epsilon_\theta)_{max}$. This comparison shows that, theoretically, autofrettage of these steels in Table IV should be possible because the percent elongation is greater than $(\epsilon_\theta)_{max}$.

TABLE IV. DUCTILITY OF STEELS

Steel	Tensile Yield Strength σ_y, ksi	Elongation (100 ϵ), percent
AISI 4340	228	11.0
	130	21.0
	270	11.0
AISI H-11 (modified)	244	10.0
D-6A	250	7.5
18% Ni maraging	268	11.0

However, caution is urged here; the ductility values are given for a necked down specimen. A better value may be the strain from a (conventional) stress-strain diagram at the peak of the curve where the stress begins to fall off. For example, for H-11 steel at the peak,

$$\sigma_u = 300{,}000 \text{ psi at } \epsilon_{peak} = 0.060$$

In the transverse direction, $(\epsilon_\theta)_{peak}$ might be 0.030. However, $(\epsilon_\theta)_{max}$ = 0.0275 at σ_y = 250,000 psi and K = 2.0. Thus, the difference between $(\epsilon_\theta)_{max}$ during autofrettage and the fracture strain of the material may be smaller than indicated by the ductility figures in Table IV.

This discussion indicated that autofrettaging of high strength steels is a possibility. However, it should be ascertained whether the ductility in the transverse direction is great enough to avoid fracture during autofrettage. Further discussion of strain-hardening effects in autofrettage is given in a later section.

Analysis of Multi-ring Containers

Multi-ring Container Designs for 250,000 psi

A multi-ring container of shrink-fit assembly was first considered. It was to have a 12.0-inch diameter bore and a pressure capability of 250,000 psi based upon a fatigue strength criterion. Both H-11 and Maraging 300 high-strength steels were considered for the liner material. An compressive yield strength of at least 250,000 psi was preferred because the liners were to be designed with a prestress of this value. However, these steels were found to be impossible to obtain in forgings of the size required, with guaranteed properties at these high strength levels (corresponding to ultimate tensile strengths, 280,000 to 300,000 psi). Higher-strength steels with σ_u > 300,000 psi such as a bearing steel, were not considered because they were expected to be beyond the optimum point of the fatigue strength versus ultimate strength curve, Figures 24, 25, and 26. Also, more brittle failures and greater notch sensitivity (Figure 26) under fatigue loading can be expected in steels at too high a strength level. It appears that 250,000 psi is the maximum ultimate tensile strength achievable in forgings with the large sizes of interest. This corresponds to a tensile yield strength of about 225,000 psi and an expected compressive yield strength perhaps, 10 percent greater.

It was decided that the maximum ultimate strength level to be considered should be σ_u = 250,000 psi. From Reference (14), Equation (44) gives:

$$p_{max} = 2\alpha_r \sigma_u \qquad (8)$$

for large overall wall ratio, K. For p_{max} = 250,000 psi and σ_u = 250,000 psi, the semi-range fatigue parameter α_r has to be 0.5. From the average fatigue data for both H-11 and maraging steels in Figure 42, Reference (14), page 165, $\alpha_r \approx 0.50$ can be expected to give about 10^4-10^5 cycles life (under ideal conditions). However, lifetimes of 10^5 cycles and greater are indicated by the fatigue data for H-11 in Table XLII, page 166 of Reference (14).

For the outer rings of the container, it was considered best to reduce the strength levels required. High strengths are more difficult to achieve in larger sizes and lower strength requirements correspond to more ductile conditions and a safer design. Accordingly, with the selected strength levels shown in Table V, it was found necessary to use 5 rings*. Table V also gives the dimensions of the rings. The material of the liner and the second ring are expected to be H-11 steel and the outer rings an AISI 4340 or comparable steel. The tensile strength of the liner is given because this is the typically available data and fatigue predictions have been made on this basis. However, the liner must also have a compressive yield strength of 250,000 psi because the liner bore is compressed (shrunk) to this value.

The dimensions of the design (Table V) have been calculated so that the design is optimum for the material strength levels chosen. For an optimum design, it can be shown that the wall ratios must be related as follows:

$$\frac{k_{n+1}^2}{k_n^2} = \frac{\sigma_{n+1}}{\sigma_n} \tag{9}$$

where k_n = OD/ID for ring number n, and σ_n = strength of ring number n.

Calculations were performed using computer code MULTIR. The mean hoop stress for the liner was preset to $(\sigma_\theta)_m$ = 125,000 psi. Thus, for p_{max} = 250,000 psi and $(\sigma_\theta)_r$ = 1/2 p_{max} at the limit, the maximum hoop stress is $(\sigma_\theta)_{max}$ = 0. (This corresponds to a maximum shear stress of $p_{max}/2$ = 125,000 psi. Allowing $(\sigma_\theta)_{max}$ > 0 would increase the maximum shear stress and may cause premature fatigue failure). For the outer rings the shear fatigue criteria has been used. (The outer ring can be considered as a safety ring. A factor of safety of about 1.6 on the fatigue strength was used on the outer ring.) The pressure capability calculated is

$$p = 255{,}479 \text{ psi for the 5-ring container.} \tag{10}$$

---

* This is based upon available uniaxial fatigue data. Biaxial and triaxial fatigue data for the cylinders under pressure are not available for high strength steels. If higher strength levels than those of Table V could be used, then it would be possible to design a 4-ring container.

TABLE V. DIMENSIONS AND REQUIRED STRENGTHS OF RINGS FOR THE 5-RING CONTAINER

Ring Number	ID, inches	OD, inches	Ultimate Tensile Strength, ksi	Yield Tensile Strength, ksi
1	12.0	21.0	300,000	260,000
2	21.0	33.5	250,000	215,000
3	33.5	47.8	200,000	170,000
4	47.8	68.2	200,000	170,000
5	68.2	91.6	175,000	150,000

The required manufactured interference-to-radius ratios (Δ_n/r_n) are given in Table VI. Also included are the assembly interferences (δ_n/r_n) for assembly of rings from the inside out and from the outside in. Formulas for the assembly interferences were derived. The assembly interferences in Table VI are found to be too high for differential temperature assembly.

TABLE VI. REQUIRED INTERFERENCES FOR THE 5-RING DESIGN

Between Rings Number	Manufactured Interference Ratio, $\frac{\Delta_n}{r_n}$	Assembly Interference Ratio, δ_n/r_n	
		Inside-Out	Outside-In
1 and 2	0.00406	0.00406	0.00891
2 and 3	0.00265	0.00388	0.00529
3 and 4	0.00288	0.00465	0.00315
4 and 5	0.000434	0.00257	0.000434

Press forces were also calculated for assembly. It is assumed that the rings will be manufactured with a slight taper. On this basis and with lubrication, a coefficient of friction $\mu = 0.1$ was assumed. The press force P is

$$P = \frac{2\pi r_n L\mu}{2000} q_n, \text{ tons} \qquad (11)$$

where L = length of rings, inches, $2\pi r_n L\mu$ = the lateral surface area, in^2, and where q_n is the interface pressure during assembly, corresponding to δ_m. For the calculations L = 120 inches. Results are given in Table VII. Press forces above 30,000 tons are required to assemble the 5-ring container.

TABLE VII. REQUIRED PRESS FORCES FOR ASSEMBLY OF THE 5-RING CONTAINER

Assembly Inside-Out	
Assembly of Rings	Required Force P, tons
2 onto 1	11,300
3 onto 1 and 2	17,400
4 onto 1, 2, and 3	31,000
5 onto 1, 2, 3, and 4	22,400
Assembly Outside-In	
Assembly of Rings	Required Force P, tons
4 into 5	2,600
3 into 4 and 5	18,200
2 into 3, 4, and 5	27,800
1 into 2, 3, 4, and 5	34,300

Because the interferences are high and the required press forces estimated for the 5-ring design are so high (based on $\mu = 0.1$), it was decided to investigate a 7-ring design to determine how much less press force per ring may be required if more rings were used. Tables VIII, IX, and X give the dimensions, interferences and required press forces for the 7-ring design. The press forces required are lower than the 34,000 tons for the 5-ring design, but are still relatively high. Thus, the advantage from the assembly forces standpoint is small for the 7-ring design. However, it is important to note that the OD is smaller for the 7-ring design. The pressure capability for the 7-ring design of Table VIII was calculated to be

$$p = 263,105 \text{ psi} \qquad (12)$$

Results of the computer print out from MULTIR for these container calculations are on file for future reference.

It should be kept in mind that the assembly forces are based on $\mu = 0.1$. It is likely that the friction coefficient could be reduced by almost one-half with good lubrication, and thus the assembly forces would be reduced proportionately.

TABLE VIII. DIMENSIONS AND REQUIRED STRENGTHS OF RINGS FOR THE 7-RING CONTAINER

Ring Number	ID, inches	OD, inches	Ultimate Tensile Strength, ksi	Yield Tensile Strength, ksi
1	12.00	18.62	300,000	260,000
2	18.62	26.38	250,000	215,000
3	26.38	33.38	200,000	170,000
4	33.38	42.20	200,000	170,000
5	42.20	53.40	200,000	170,000
6	53.40	67.60	200,000	170,000
7	67.60	80.60	175,000	150,000

TABLE IX. REQUIRED INTERFERENCES FOR THE 7-RING DESIGN

Between Rings Number	Manufactured Interference Ratio, $\frac{\Delta_n}{r_n}$	Assembly Interference Ratio, δ_n/r_n	
		Inside-Out	Outside-In
1 and 2	0.00265	0.00265	0.00905
2 and 3	0.00194	0.00292	0.00679
3 and 4	0.00213	0.00379	0.00522
4 and 5	0.00212	0.00436	0.00353
5 and 6	0.00213	0.00477	0.00213
6 and 7	-0.00060	0.00232	-0.00060

TABLE X. REQUIRED PRESS FORCES FOR ASSEMBLY OF THE 7-RING CONTAINER

Assembly Inside-Out	
Assembly of Rings	Required Force P, tons
2 onto 1	5,150
3 onto 1 and 2	7,420
4 onto 1, 2, and 3	12,500
5 onto 1, 2, 3, and 4	18,900
6 onto 1, 2, 3, 4, and 5	26,500
7 onto 1, 2, 3, 4, 5, and 6	15,000
Assembly Outside-In	
Assembly of Rings	Required Force P, tons
6 into 7	0
5 into 6 and 7	7,9[illegible]
4 into 5, 6, and 7	13,80[illegible]
3 into 4, 5, 6, and 7	17,200
2 into 3, 4, 5, 6, and 7	23,900
1 into 2, 3, 4, 5, 6, and 7	26,900

Pressure Capability of Multiring Containers at Temperature

This discussion refers to the two multiring container designs described in the previous sections. That analysis was based on room temperature strengths. The reduction of pressure capability for higher temperature operation is now considered for two conditions:

(1) Uniform change in temperature
(2) Change in temperature accompanied by thermal gradient through the wall of the container.

Effect of Uniform Temperature Change. It is first assumed that the container is preheated to temperature uniformly and slowly so that there is negligible temperature gradient across the wall of the container. There are two significant effects of the temperature change:

(1) The elastic moduli E_n decrease with temperature. This in turn decreases the shrink fit residual pressures q_n in proportion to the change in the E_n.

(2) The strengths of the rings decrease with temperature. Both of these effects reduce the pressure capability. For high-strength steels, the latter effect (2) is greater. Figures 29, 30, and 31 from Reference (47) show the decrease in strength versus temperature for the three steels considered. At 500 F, the strengths are reduced as follows:

(a) AISI 4340 - $\frac{\sigma_T}{\sigma_{RT}} = \frac{183,000}{200,000} = 0.915$

(b) AISI H-11 - $\frac{\sigma_T}{\sigma_{RT}} = \frac{256,000}{280,000} = 0.915$

(c) 18% Ni maraging - $\frac{\sigma_T}{\sigma_{RT}} = \frac{242,000}{275,000} = 0.880$

Consequently, the internal pressure p must be reduced by the minimum ratio for the steels used, i.e., if maraging steel is used, p must be reduced to:

$$p = 0.880\ (250,000) = 220,000 \text{ psi*} \tag{13}$$

for 500 F operation. At 800 F, the strengths are further reduced as follows:

(a) AISI 4340 - $\frac{\sigma_T}{\sigma_{RT}} = \frac{136,000}{200,000} = 0.68$

(b) AISI H-11 - $\frac{\sigma_T}{\sigma_{RT}} = \frac{233,000}{280,000} = 0.833$

(c) 18% Ni maraging - $\frac{\sigma_T}{\sigma_{RT}} = \frac{223,000}{275,000} = 0.813$

Using the smallest ratio, the pressure p must be reduced to

$$p = 0.68\ (250,000) = 170,000 \text{ psi} \tag{14}$$

for 800 F operation.

Exposure of AISI 4340 steel to temperature above 800 F is not recommended, of course, because a reduction in room temperature properties will result. Maraging steels are aged at 900 F and would not generally be used above 800 F for long times. Therefore, operation above 800 F is not possible unless the container could be made entirely of H-11 steel. In this case, the reduction in pressure capability from Figure 30 is:

$$p = \frac{194,000}{280,000}\ (250,000) = 173,000 \text{ psi} \quad , \tag{15}$$

* It is assumed in this calculation that the fatigue strength-to-ultimate strength ratio is the same at elevated temperature as it is at room temperature.

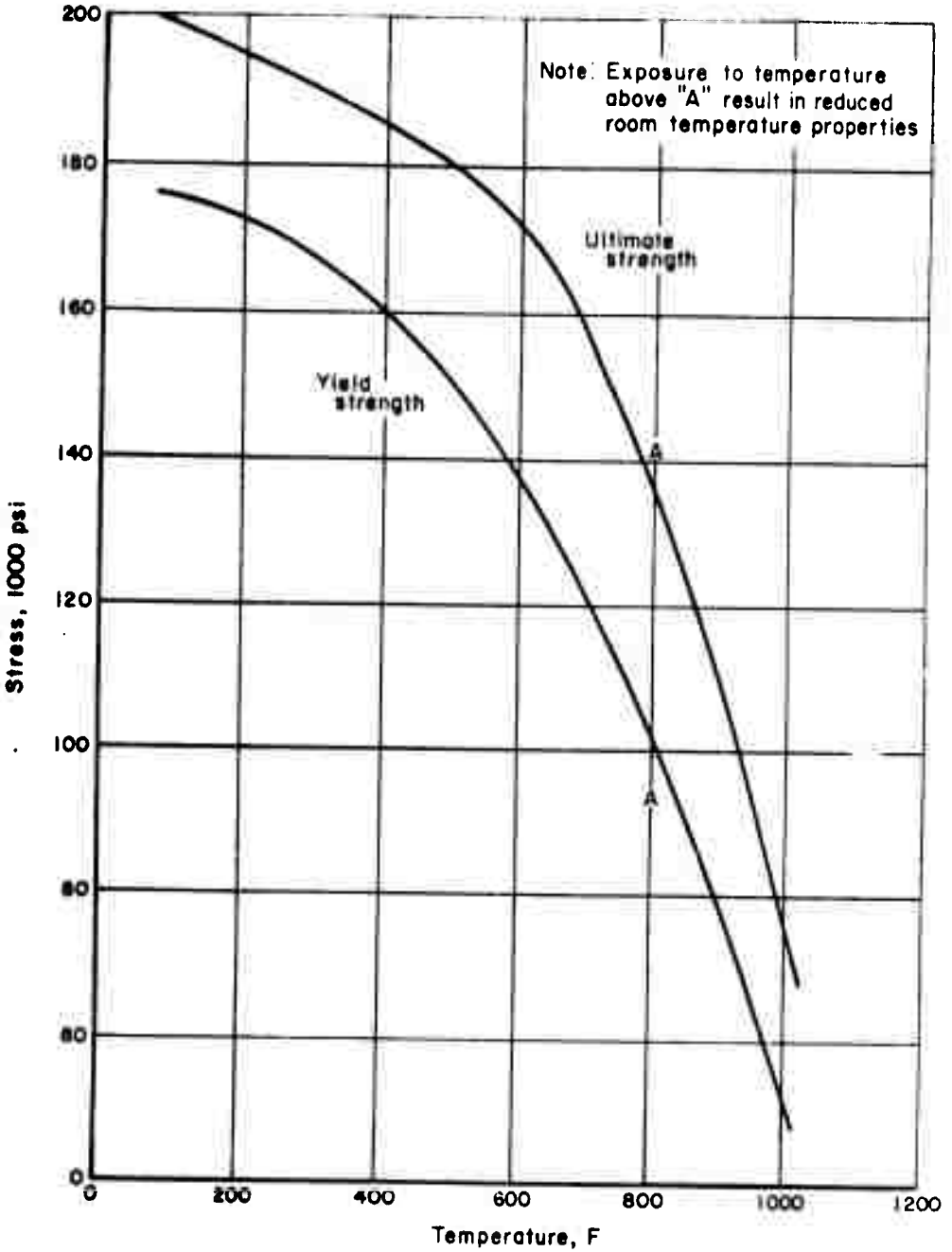

FIGURE 29. TENSILE ULTIMATE AND YIELD STRENGTH VERSUS TEMPERATURE FOR AISI-4340 STEEL HEATED TO 200,000 PSI

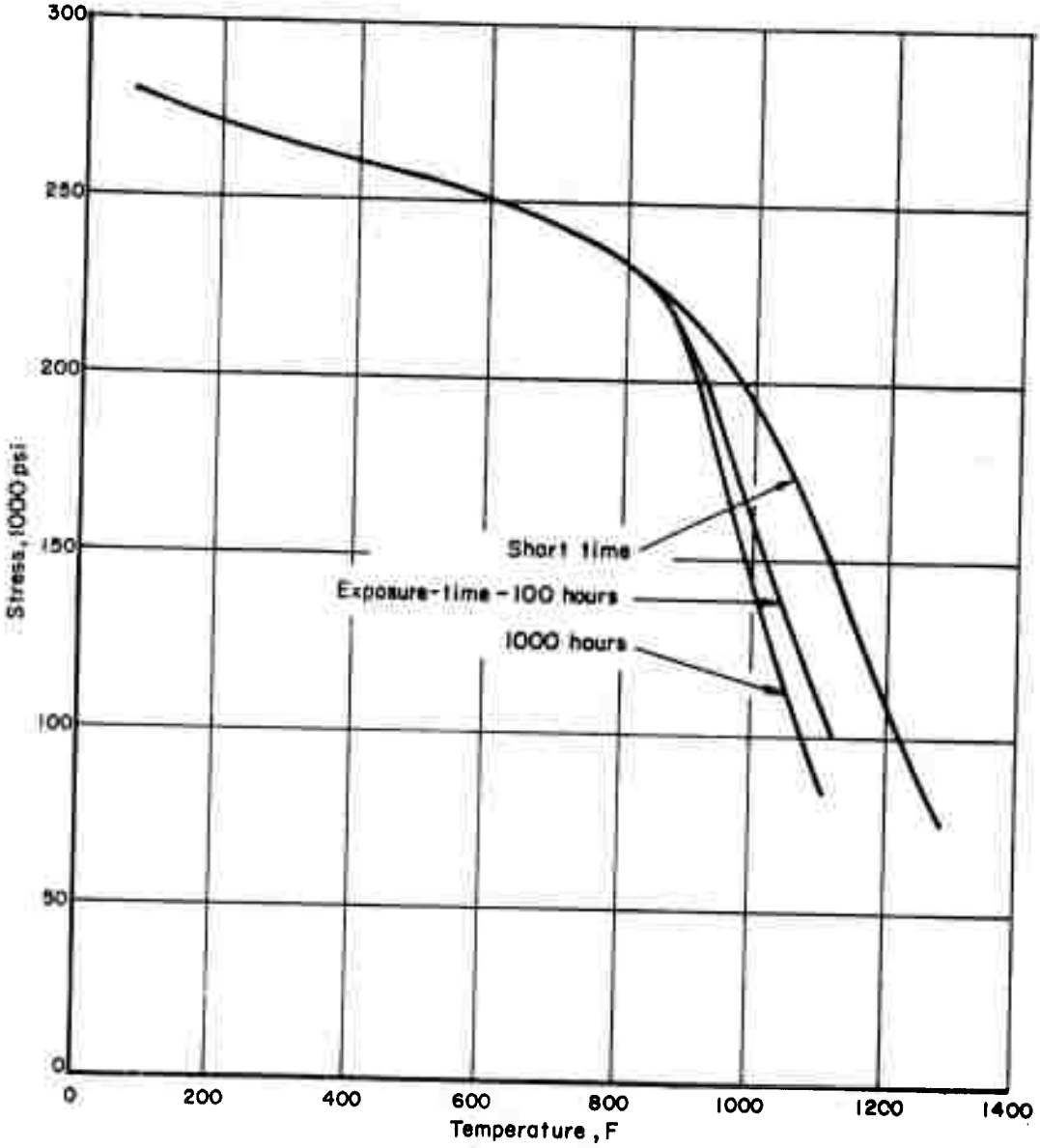

FIGURE 30. TENSILE ULTIMATE STRENGTH OF AISI-H11 ALLOY STEEL VERSUS TEMPERATURE AFTER VARIOUS EXPOSURE TIMES

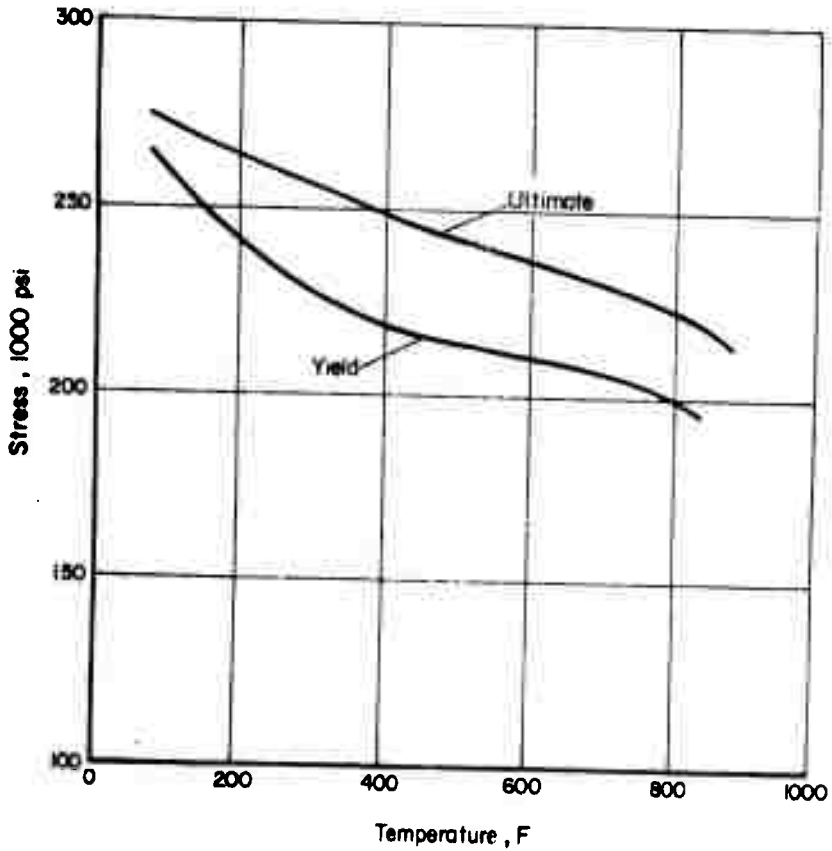

FIGURE 31. TENSILE ULTIMATE AND YIELD STRENGTH OF 18Ni-9Co-5Mo MARAGING 300 STEEL VERSUS TEMPERATURE

for 1000 F for short time exposure. It is noted from Figure 30 that long time at temperature may result in creep rupture unless the pressure is reduced still further, i.e.,

$$p = \frac{160,000}{280,000} (250,000) = 143,000 \text{ psi} \quad , \tag{16}$$

for 100 hours at 1000 F for a container made entirely of H-11 steel.

Effect of Temperature Gradient. If a temperature gradient is produced through the wall of the container, the pressure capability is reduced still further, because of the resulting thermal stresses. For steady-state heat transfer from the inside to the outside, compressive stresses develop on the inside and tensile on the outside* according to the formulas in Reference (46). It is found that a 100 F temperature differential, from the ID to OD, produces stresses of about -19,500 psi and +6,500 psi at the ID and OD respectively for wall ratios $6 \leq K \leq 7$ (in the range of the container designs, Tables V and VIII). A 100 F temperature differential is the maximum that can be allowed. Anything greater will substantially change the residual stress distribution and may cause compressive yield at the bore and tensile yield of the OD.

A container designed to operate with a temperature differential $\Delta T >$ 100 F should have less shrink-fit residual stresses than the room-temperature designs. A design incorporating a temperature differential would be successful, however, only if the temperature differential and thus the compressive residual stress at the bore could be accurately controlled and maintained. For example, consider a 500 F design with also a 500 F temperature differential. From Equation (13), p = 220,000 psi at 500 F. A thermal hoop stress of $\sigma_\theta = -195\ (500) = -97,500$ psi is calculated at the ID from $\Delta T = 500$ F. The manufactured interferences required now are smaller, i.e.,

$$\Delta_n^* = \left(\frac{220,000}{250,000}\right) \left[\frac{-220,000 - (-97,500)}{-220,000}\right] \Delta_n = 0.49\ \Delta_n \quad , \tag{17}$$

where Δ_n = the interference in Tables VI and IX. (A total compressive prestress (σ_θ) min = -p is desired for (σ_θ) max. $\approx$ o). Thus, the interference and also the press forces, are approximately 1/2 those for the RT design. Of course this design could not be used at RT.

The above calculation assumes that all rings of a multiring container are the same material, i.e., α, ϵ and ν are the same for each ring. For rings of different materials, a more detailed analysis would have to be made. However, the above calculations give a good indication of what can be expected with most steel materials.

---

* For the opposite condition--heating from the outside in, the stresses are reversed. ΔT becomes negative in the appropriate formulas in Reference (48).

Autofrettaged Multiring Container for 250,000 psi

In Tables V through X, the design requirements for 5-ring and 7-ring shrink-fit designs were given. These requirements were severe; large outside diameters were required, and consequently, large assembly forces (25,000 to 35,000 tons), were predicted.

Compressive prestress at the bore of a container can also be provided by using the autofrettage process. This process could reduce the size of containers because fewer shrink rings would be needed to provide the required prestress. Less shrink-fit also means lower assembly forces would be needed.

The autofrettage process has been used extensively on low-strength ductile steels. It has also been used on higher strength strain-hardening steels at relatively low pressures where a factor of safety could be used. However, the successful use of the autofrettage process for high-strength cylinders for high-pressure applications, at low factors of safety, has been impossible to predict heretofore because of lack of confidence in theoretical predictions.

Battelle now has a computer program (FEELAP, finite element elastic-plastic analysis) that has the capability of analyzing the elastic-plastic behavior of bodies of revolution made of strain-hardening materials. This program has been applied to the autofrettage problem on the present design study.

As a check of the program, a strain-hardening calculation of an AISI 4340 cylinder was performed. Stress-strain data from Reference (47) were used. The stress-strain curve at 80 F was represented by:

$$\sigma = 354{,}000\ \epsilon^{0.16} \quad \text{for } \sigma > \sigma_e, \qquad (18)$$

where σ_e = 152,000 psi at the elastic limit, and ϵ = total strain.

The computer results for the strain-hardening solution are shown in Figure 32 along with the experimental data from Reference (49). There is very good agreement as indicated. Therefore, it was believed that the computer program FEELAP could be used for accurate calculation for autofrettage of higher strength AISI H-11 steel cylinders as well.

A container design using an autofrettaged H-11 steel liner of wall ratio k_1 = 2.0 was analyzed.* A sufficiently large wall ratio for the liner is needed in order for the autofrettage process to be successful. It is assumed that the

---

* Since this calculation was made, it was learned that large H-11 forgings of this strength level cannot be obtained(44). However, this analysis indicates also the benefits that may be possible for autofrettaged 18% Ni maraging steel liners.

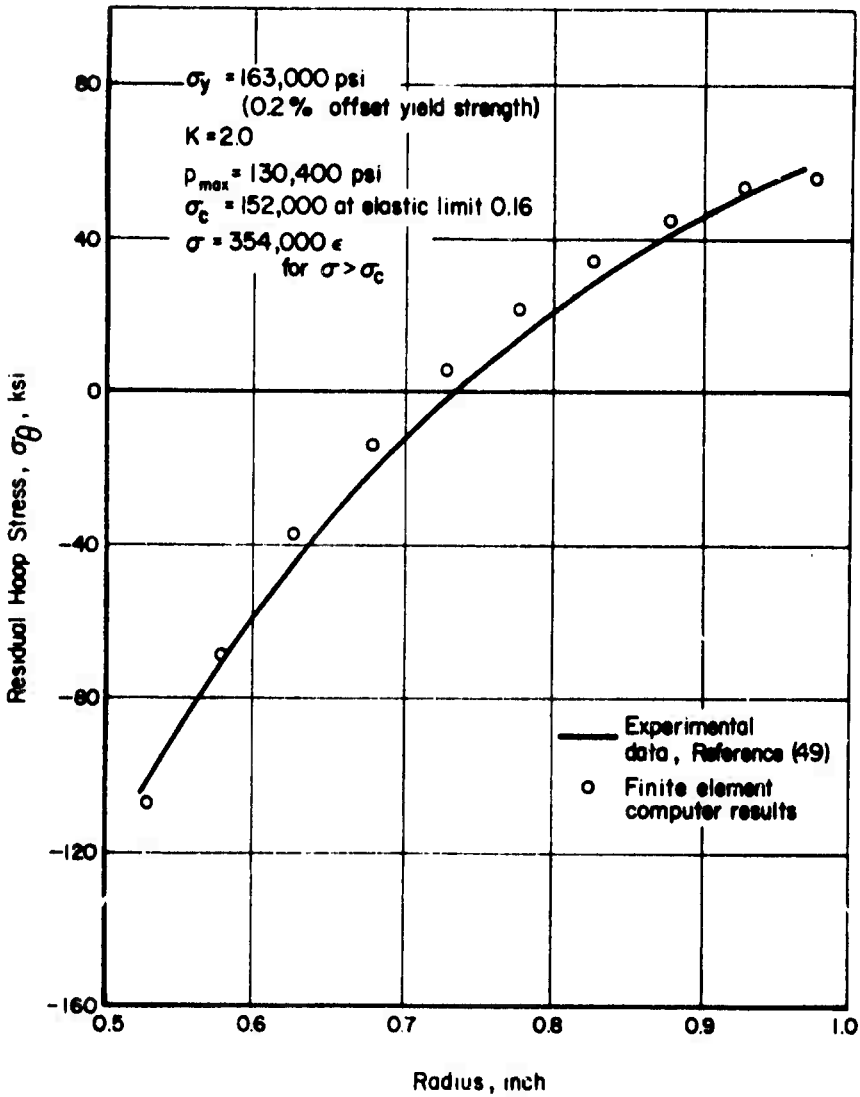

FIGURE 32. RESIDUAL HOOP STRESS IN AN AUTOFRETTAGED AISI 4340 CYLINDER WITH STRAIN HARDENING EFFECTS

liner could be autofrettaged by overpressure, finish machined by grinding to final dimensions, and then shrink-fit assembled into two outer rings. A single ring unit of large OD and a 12-inch-diameter bore is not considered practicable because of heat treatment difficulty of large sections. A large overall wall ratio, K, is necessary to keep the total range in hoop stress small, i.e.,

$$\sigma_\theta = p \frac{K^2 + 1}{K^2 - 1} \tag{19}$$

where, $K = OD/ID$.

Thus,

$$\sigma_\theta = 250{,}000 \left(\frac{5}{3}\right) = 416{,}000 \text{ psi, for } K = 2.0,$$

$$\sigma_\theta = 250{,}000 \left(\frac{10}{8}\right) = 313{,}000 \text{ psi, for } K = 3.0,$$

$$\sigma_\theta = 250{,}000 \left(\frac{17}{15}\right) = 283{,}000 \text{ psi, for } K = 4.0,$$

and $p = 250{,}000$ psi. An overall wall ratio, $K = 4.0$, is sufficiently large; $\sigma_\theta = 283{,}000 < 300{,}000$ psi, the maximum ultimate tensile strength of H-11 steel*.

Reference (50) gives a stress-strain diagram for H-11 steel of 300,000 psi ultimate tensile strength. The strain-hardening characteristics of this steel were represented by

$$\sigma = 406{,}000\ \epsilon^{0.10} \text{ for } \sigma > \sigma_e, \tag{20}$$

where $\sigma = 251{,}000$ psi at the elastic limit.

Results for autofrettaging a liner of this steel are shown in Figure 33. The autofrettage pressure is $p_{max} = 202{,}000$ psi. The residual stress at the bore from autofrettage is -200,000 psi. The cylinder was not autofrettaged 100 percent, but only about 80 percent (as noted in Figure 33 at the peak in the σ_θ curve at $r/r_o \simeq 1.8$). Autofrettaging to 100 percent (making the cylinder entirely plastic at the autofrettage pressure), is not recommended because of control problems; i.e., at this limit the OD begins to expand rapidly and has to be restrained to avoid failure by bursting.

A total hoop prestress of -250,000 psi is desired at the bore. The additional -50,000 psi can be provided by shrink-fit assembly of two outer rings. The dimensions and required strengths for this 3-ring container are given in Table XI. The strength required in the outer ring is only 175,000 psi. Use of a higher strength level, e.g., 200,000 psi, will provide a factor of safety on the outer ring.

---

* The total range in hoop stress $\sigma_\theta = \sigma_u = 300{,}000$ psi is equivalent to $\alpha_r =$ (where $\alpha_r = (\sigma_\theta)\ r/\sigma_u$) for 10^5 cycles life.

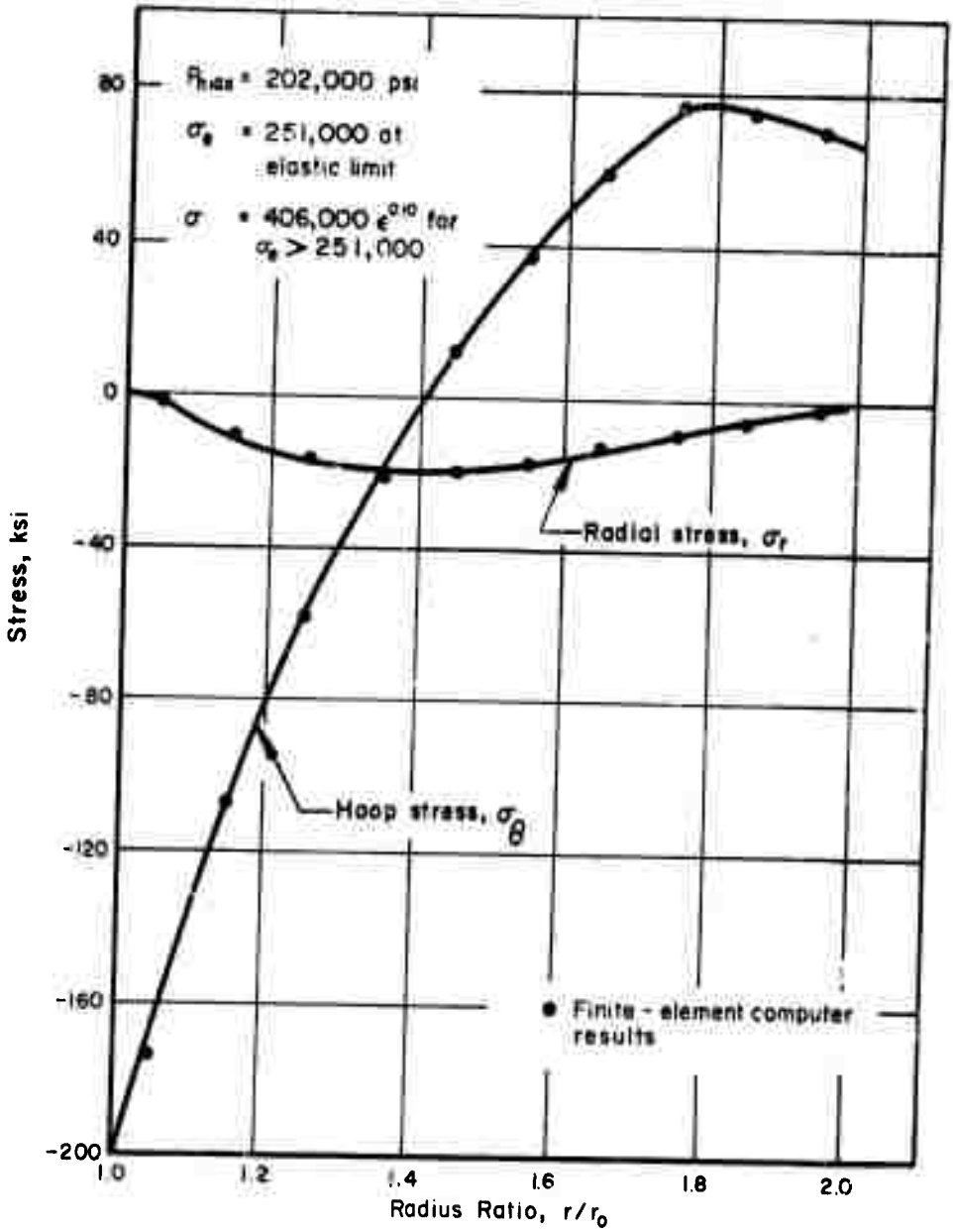

FIGURE 33. RESIDUAL STRESSES IN AUTOFRETTAGED AISI-H11 STEEL LINERS

TABLE XI. DIMENSIONS AND REQUIRED STRENGTHS OF RINGS FOR THE 3-RING CONTAINER WITH AN AUTOFRETTAGED LINER

Ring Number	ID, inches	OD, inches	Ultimate Tensile Strength, ksi	Yield Tensile Strength, ksi
1	12.0	24.0	300,000	260,000
2	24.0	36.0	210,000	180,000
3	36.0	48.0	175,000	150,000

Calculations for the shrink-fit of the 3-ring container were performed using the computer code MULTIR. The required interferences calculated are given in Table XII and the required assembly forces are given in Table XIII. Much smaller assembly forces are now required--8500 tons maximum for the 3-ring container. Also, the OD is much smaller, 48.0 inches. This means the press frame can also be smaller to accommodate a smaller container.

TABLE XII. REQUIRED INTERFERENCES FOR THE 3-RING DESIGN

Between Rings Number	Manufactured Interference Ratio, $\frac{\Delta_n}{r_n}$	Assembly Interference Ratio, δ_n/r_n	
		Inside-Out	Outside-In
1 and 2	0.00190	0.00190	0.00208
2 and 3	0.00031	0.00094	0.00031

TABLE XIII. REQUIRED PRESS FORCES FOR ASSEMBLY OF THE 3-RING CONTAINER

Assembly Inside-Out	
Assembly of Rings	Required Force P, tons
2 onto 1	6,000
3 onto 1 and 2	3,970
Assembly Outside-In	
Assembly of Rings	Required Force P, tons
2 into 3	1,025
1 into 2 and 3	8,500

The growth of the liner from autofrettage has also been calculated with use of the computer code FEELAP. The residual hoop strains after autofrettage are

$$(\epsilon_\theta)_{res.} = 0.0075 \text{ at the bore,}$$

$$(\epsilon_\theta)_{res.} = 0.0023 \text{ at the OD.}$$

Thus, the change in diameter is predicted to be

$$\Delta D = 0.0075\ (12) = 0.090 \text{ in. at the ID,}$$

$$\Delta D = 0.0023\ (24) = 0.055 \text{ in. at the OD.}$$

The autofrettage container design presents many advantages as already pointed out. There are some possible disadvantages, however. Burns and Parry(36) show that the fatigue strength of autofrettaged cylinders is 20 to 25 percent lower than that of shrink-fitted cylinders; i.e., less fatigue life can be expected for autofrettaged cylinders than for completely shrink-fitted ones. It is believed that the residual stresses in autofrettaged cylinders tend to shake down to lower values with continuous cycling. This warrants further investigation. For example, the change in residual strain during the first few cycles may be easily determined by use of strain gages on an experimental cylinder. Also, the possibility of a Bauschinger effect and, consequently, hysteresis effects should also be investigated because these could also contribute to earlier fatigue failure.

The total operating (maximum) stresses and residual (minimum) stresses (autofrettage residual stress + shrink-fit stresses) are given in Tables XIV and XV. The stresses for Rings 2 and 3 were based on shrink fitting only. The stresses for Ring 1 include the computer results for shrink-fit plus the autofrettage residual stresses.

A fatigue life of 10^5 cycles is expected for the liner and a life of 10^6-10^7 cycles is expected for the outer two rings for these residual stresses. However, reduction of the autofrettage residual stresses during cycling may result in a lower fatigue life than 10^5 cycles for the liner.

TABLE XIV. MAXIMUM OPERATING STRESSES IN AUTOFRETTAGED MULTI-RING CONTAINER

Radius, inches	Radial Stress, psi	Hoop Stress, psi	Shear Stress, psi
	Maximum Stresses in Ring No. 1		
6.0	-250,000	31,210	140,600
12.0	- 68,380	119,460	93,920
	Maximum Stresses in Ring No. 2		
12.000	- 68,375	108,542	88,458
18.000	- 19,231	59,399	39,315
	Maximum Stresses in Ring No. 3		
18.000	- 19,231	68,682	43,957
24.000	0	49,451	24,726

TABLE XV. MINIMUM RESIDUAL STRESSES IN AUTOFRETTAGED MULTI-RING CONTAINER

Radius, inches	Radial Stress, psi	Hoop Stress, psi	Shear Stress, psi
	Minimum Stresses in Ring No. 1		
6.0	0	-250,000	-125,000
12.00	-18,750	36,750	27,750

TABLE XV. (CONTINUED)

Radius, inches	Radial Stress, psi	Hoop Stress, psi	Shear Stress, psi
	Minimum Stresses in Ring No. 2		
12.000	-18,750	25,835	22,292
18.000	- 6,365	13,450	9,908
	Minimum Stresses in Ring No. 3		
18.000	- 6,365	22,733	14,549
24.000	0	16,368	8,184

Fluid-Support Container Design for 450,000 psi

A ring-fluid-ring container design with only one ring in the inner unit was considered. (See Figure 6). A fluid-supported liner with a bore pressure p_o and a support pressure p_1 is assumed. The pressure cycles are assumed to be proportionate and to vary from 0 to the maximum values of p_o and p_1 respectively. It is presupposed that if the maximum hoop stress at the bore is kept at zero, then a long fatigue life will be achieved. Two conditions of axial stress are considered: zero axial stress, $\sigma_z = o$; and $\sigma_z = -p_1$ for the case when the pressure p_1 also acts over the ends of the liner.

If the hoop stress at the bore of the liner is to be kept at zero, then the external pressure p_1 on the liner must be

$$p_1 = \frac{p_o}{2} \frac{(K^2 + 1)}{K^2} \geq \frac{1}{2} \qquad (21)$$

where p_o = bore pressure, and the maximum hoop stress is

$$(\sigma_\theta)_{max} = p_o \frac{K^2 + 1}{K^2 - 1} - 2p_1 \frac{K^2}{K^2 - 1} = 0 \quad ,$$

for an elastic stress state. The maximum shear stress at the bore is

$$S_{max} = \frac{\sigma_\theta - \sigma_r}{2} = \frac{0 - (-p_o)}{2} = \frac{p}{2} \qquad (22)$$

For p_o = 450,000 psi, S_{max} = 225,000 psi. Therefore, a high-strength material capable of withstanding this high shear stress is required. If it is assumed that a hydrostatic pressure p_1 does not increase the yield strength*, then a material like H-11 for example will yield at pressures below p_o = 450,000 psi. Therefore, it is necessary that an elastic-plastic analysis be conducted. It is expected that the liner will be autofrettaged (shake down to elastic stress cycling) after initial plastic yielding on the first application of pressure.

It is desired that the fluid support pressure be p_1 = 250,000 psi. Equation (21) shows that a wall ratio of K = 3 is then required for σ_θ = o if the stress state was entirely elastic. An alternative is chosen. A wall ratio K =2 is tried corresponding approximately to the proposed design with a 6-inch ID and a 11.75-inch OD liner. This means that the liner will have a shorter fatigue life (because of higher stresses for smaller K), but a fluid-supported liner can easily be replaced when it fails. However, whenever possible in design, it is recommended that p_1 and K be chosen to satisfy Equation (21).

The elastic-plastic autofrettage analysis was performed using the computer code FEELAP, previously described. Two problems were solved:

<u>Problem I</u>

p_o = 0 to 450,000 psi,
p_1 = 0 to 250,000 psi,
σ_z = 0,
K = 2.0,

<u>Problem II</u>

p_o = 0 to 450,000 psi,
p_1 = 0 to 250,000 psi,
$\sigma_z = -p_1$,
K = 2.0.

The pressure cycle is illustrated in Figure 34. The strain-hardening properties of H-11, Reference (50) were used. (Any effect of hydrostatic pressure on the stress strain curve was neglected).

The important results of the analysis are given in Table XVI. It is evident that fluid end pressure, $\sigma_z = -p_1$ for Problem II, is beneficial, i.e., for σ_z = 0 the percent overstrain is 96 percent, whereas for $\sigma_z = -p_1$, the percent overstrain is 82 percent. The corresponding residual strains are 0.04068 and 0.00823 respectively at the bore. These amount to a growth in a 6-inch ID of

* It is known that a hydrostatic pressure does increase the ductility. References (43), (44), and (45) of Reference (14).

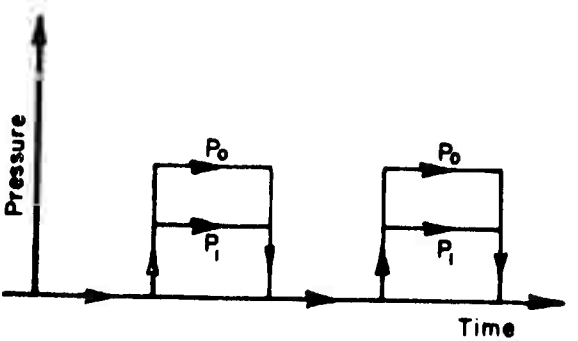

P_o = 0 to 450 ksi

P_i = 0 to 250 ksi

FIGURE 34. ASSUMED PRESSURE CYCLES ON A FLUID SUPPORTED LINER

$$\Delta D = 0.04068(6) = 0.24408 \text{ inch, and}$$

$$\Delta D = 0.00823(6) = 0.04938 \text{ inch, respectively.}$$

The diameter changes at the OD are

$$\Delta D = 0.00354(12) = 0.04248 \text{ inch, and}$$

$$\Delta D = 0.00186(12) = 0.02196 \text{ inch, respectively.}$$

From these results, it is evident that the all-around hydrostatic condition (p_1 = 250,000 psi) of Problem II is to be preferred. For the first case I, any slight reduction in material strength could result in gross plastic deformation beyond the 96 percent predicted, whereas for II a margin of safety above 82 percent is available.

TABLE XVI. RESULTS OF COMPUTER CALCULATION FOR FIRST PRESSURE CYCLE OF FLUID-SUPPORTED LINERS[a]

Condition	Problem I (zero axial stress, $\sigma_z = o$)	Problem II (axial stress, $\sigma_z = -p_1$)
First yield pressure, $(p_o)_y$, psi,	231,862	250,989
$(p_1)_y$, psi	128,800	139,400
Maximum hoop strain ϵ_θ, in/in, at ID,	0.04813	0.01721
at OD	0.00215	0.00286
Residual hoop strain ϵ_θ, in/in, at ID,	0.04068	0.00823
at OD	0.00354	0.00186
Overstrain, percent	96	82
Maximum hoop stress σ_θ, psi, at ID,	-125,000	-120,000
at OD	- 5,000	- 60,000
Residual hoop stress σ_θ, psi, at ID,	-205,000	-200,000
at OD	120,000	55,000

(a) p_o = 0 to 450,000 psi, p_1 = 0 to 250,000 psi, K = 2.0.

It is difficult to predict the fatigue life of the fluid-supported autofrettaged liner. It is well to be reminded here that autofrettaged cylinders are weaker in fatigue than are shrink-fitted cylinders, but the fluid-supported autofrettaged liner will be easier to remove and replace than a liner of a shrink-fitted container. Thomas, Turner, and Wall[51] report that pressures, p, up to 290,000 psi have been applied many times to a monoblock autofrettaged cylinder of 285,000 psi ultimate tensile strength. Assuming that the effective cyclic pressure in the present case (II) is 450,000-250,000 = 200,000 psi, it may be expected that appreciable fatigue life can be achieved. However, experiments are needed to determine the fatigue strengths of liners under these conditions.

Analysis of Additional Loading Effects in Liner

Pressure Discontinuity on Bore

If a seal is located at the end of the stem, the container bore will have a discontinuous pressure applied to it. A portion of the bore length will see the full fluid pressure, while the remaining length will be unpressurized. The stem seal will mark the point of pressure discontinuity, and during the extrusion stroke this point will move down the length of the container bore. It was felt that axial tensile stresses could be present in the liner in the region of the seal.* Such stresses are not accounted for by the Lame' equations used for container design. Therefore, these additional stresses have been calculated so that their effect on the fatigue life of the container liner could be considered.

The configuration studied is shown in Figure 35. This represents a long cylinder of wall ratio 2.0. Thus, container end effects were not included. The results, however, indicate that such effects will be significant only when the pressure discontinuity (or stem seal) is less than about one bore diameter from the end of the container. The bore pressure is shown in Figure 35 to decline rapidly over a small distance (0.05) to zero. This is believed to closely approximate the pressure distribution at a stem seal.

The stress distributions, calculated with Battelle's computer program for axisymmetric bodies, are shown in Figure 36. Axial stresses, σ_z, are present near the point of the pressure drop, and on the bore surface these approach 0.5 times the fluid pressure at the pressure discontinuity. The significance of these stresses on fatigue life was evaluated by considering the maximum shear stresses in this region. These shear stresses are relatively moderate and the analysis indicates that these local stresses in the seal region should not limit the fatigue life of a liner, since they are less severe than those predicted by the nominal container stress calculations.

---

* A liner without axial fluid end-pressure is assumed here.

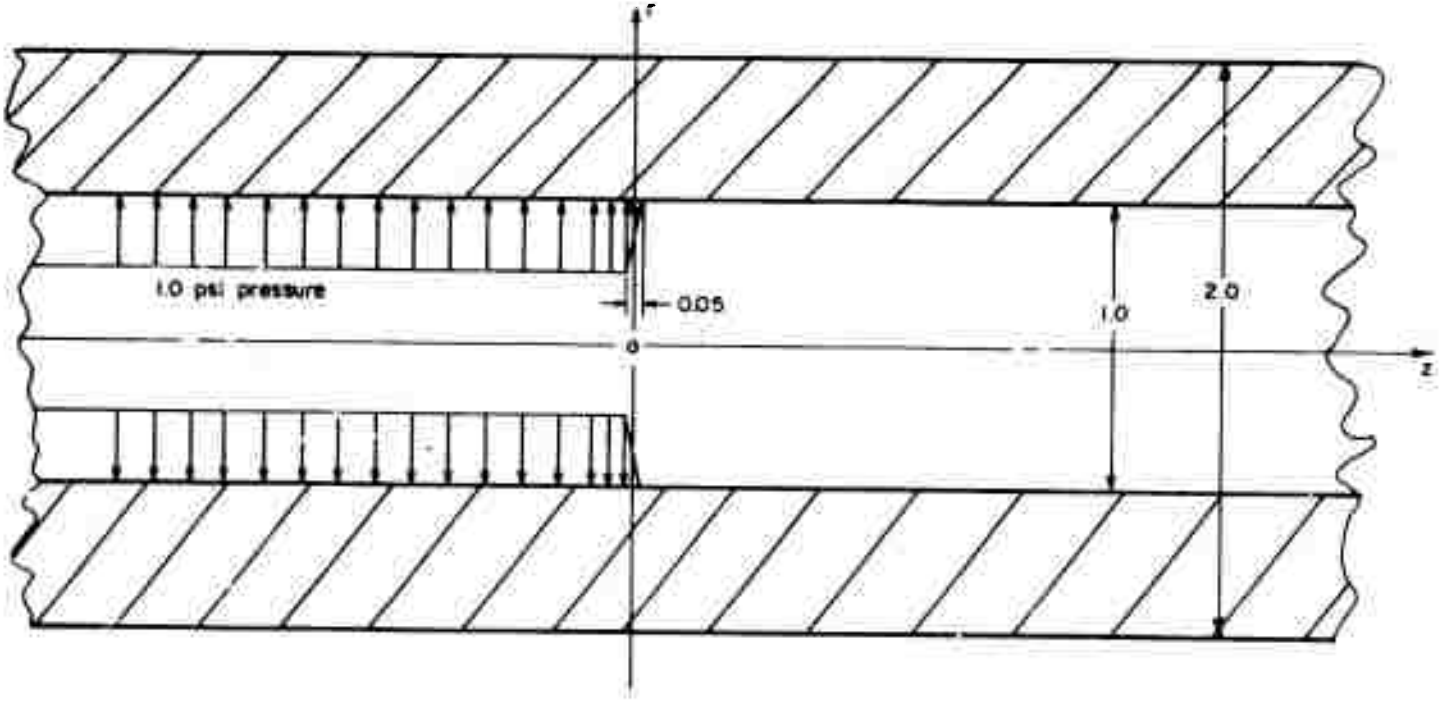

FIGURE 35. LINER AND ASSUMED DISCONTINUOUS PRESSURE LOADING ON THE BORE

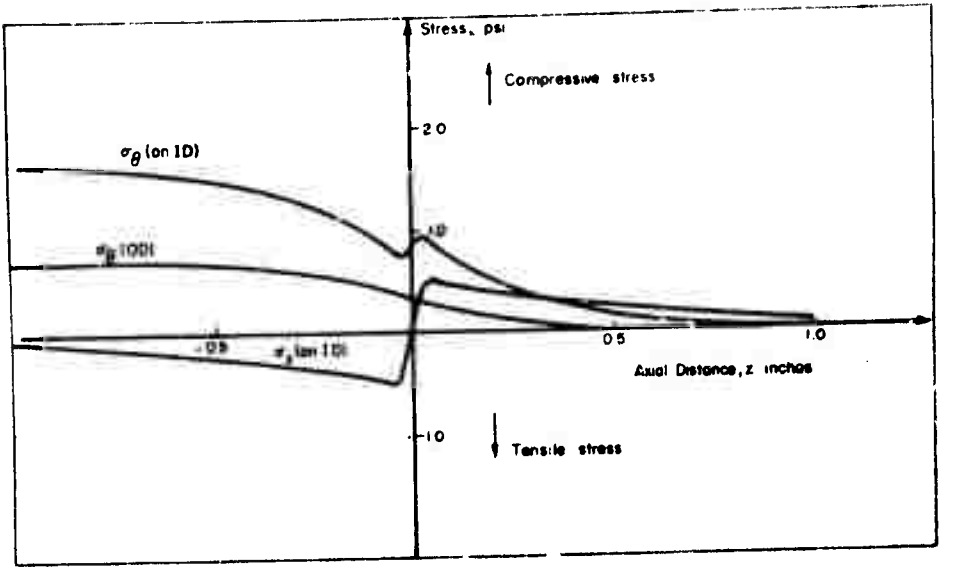

FIGURE 36. CALCULATED STRESSES FOR A LINER WITH A DISCONTINUOUS PRESSURE APPLIED TO THE BORE

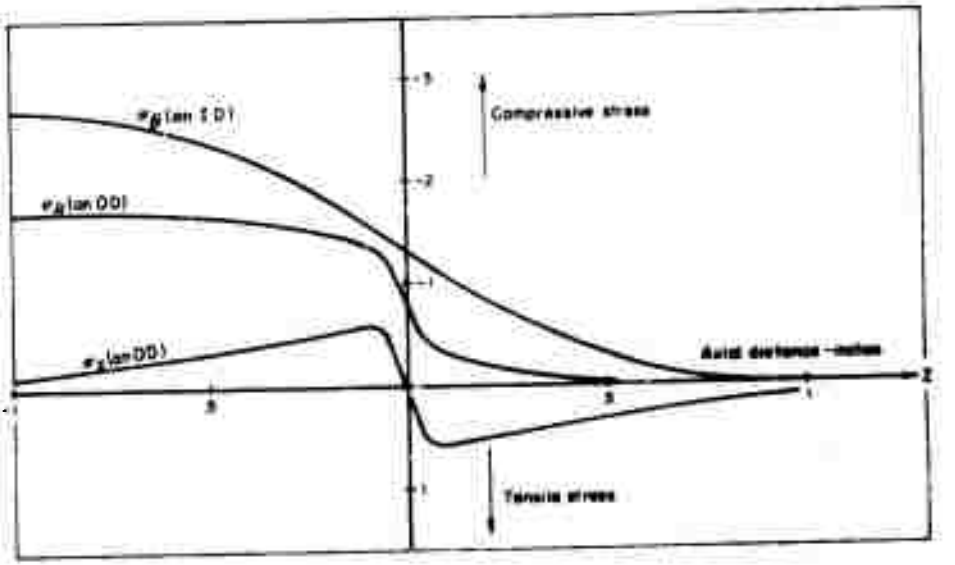

FIGURE 37. HOOP AND AXIAL STRESSES IN A LINER WITH DISCONTINUOUS PRESSURE APPLIED TO THE OUTSIDE SURFACE

Pressure Discontinuity on OD of Liner

During the assembly of a multi-ring container (as one ring is pressed onto another), axial stresses will appear in an inner ring, where the end of an outer ring bears on its outer surface.

Such stresses may result in a tensile failure of a brittle liner during assembly. Also in the design of side-bore containers, a set of outer shrink rings may be separated in the axial direction. If the rings, are not closely spaced, axially critical local stresses could appear where the ends of the outer rings bear on the liner. There is also the question of how close the rings must be spaced to maintain the compressive hoop stresses at the liner bore.

The configuration considered is that shown in Figure 35, but with the constant pressure of 1.0 psi* acting on its outer surface. The band of pressure represents the shrink-fit pressure of an outer ring.

The calculated stresses are shown in Figure 37 with the axial stress σ_z approaching a value of about 0.5 times the applied pressure. Thus, the liner material in this case must be capable of withstanding a tensile stress $\sigma_z = 0.5\ p_1$. This may limit the press fit assembly of liner materials such as tungsten carbide if the required shrink-fit pressure p_1 is too large.

Consideration of the shear stresses showed that the maximum values were not at the point of the pressure discontinuity but at the bore of the pressurized portion of the cylinder. This maximum shear stress is the same as in a uniform shrink fit of two rings of equal length.

Stresses in Region of Notch (Seal) in Liner

If the stem seal is set into the liner, a notch must be cut in the liner bore. The question arises whether a large stress concentration will occur at this notch which will reduce the liner fatigue life.

To answer this question, stresses were calculated for the notch configuration shown in Figures 38 and 39. This geometry was suggested by a design used by ASEA in Sweden; where possible, sharp corners in the notch were rounded to reduce stress concentration. A liner of wall ratio 2.0 was assumed and the effect of outer rings was not considered in the analysis. The loading was a hydrostatic pressure of 1.0 psi which was taken to act on the container bore and on the surface of the notch.

The contours of maximum shear stress are shown in Figure 40 and it can be seen that the maximum stress is not at the notch, but within the pressurized portion of the container, and corresponds to the stress predicted by the nominal container design calculations. This indicates that a notch of the design shown in Figures 38 and 39 will not reduce the liner fatigue life.

---

* The pressure is normalized to 1.0 psi. Stresses at any other pressure are proportional to the pressure.

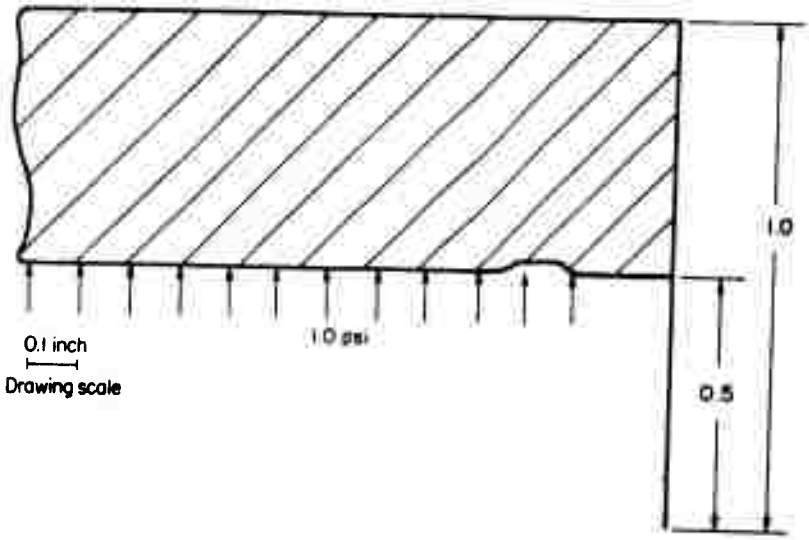

FIGURE 38. LOADING AND GEOMETRY OF THE NOTCHED LINER

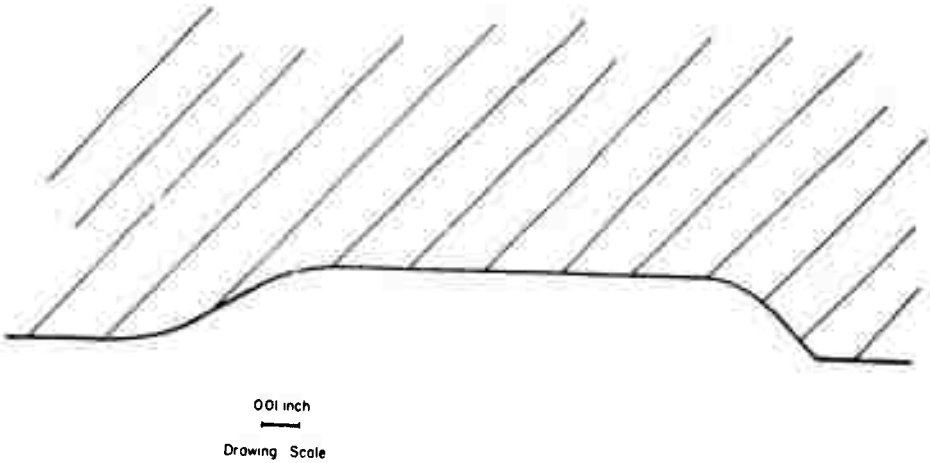

FIGURE 39. DETAIL OF ASSUMED NOTCH GEOMETRY

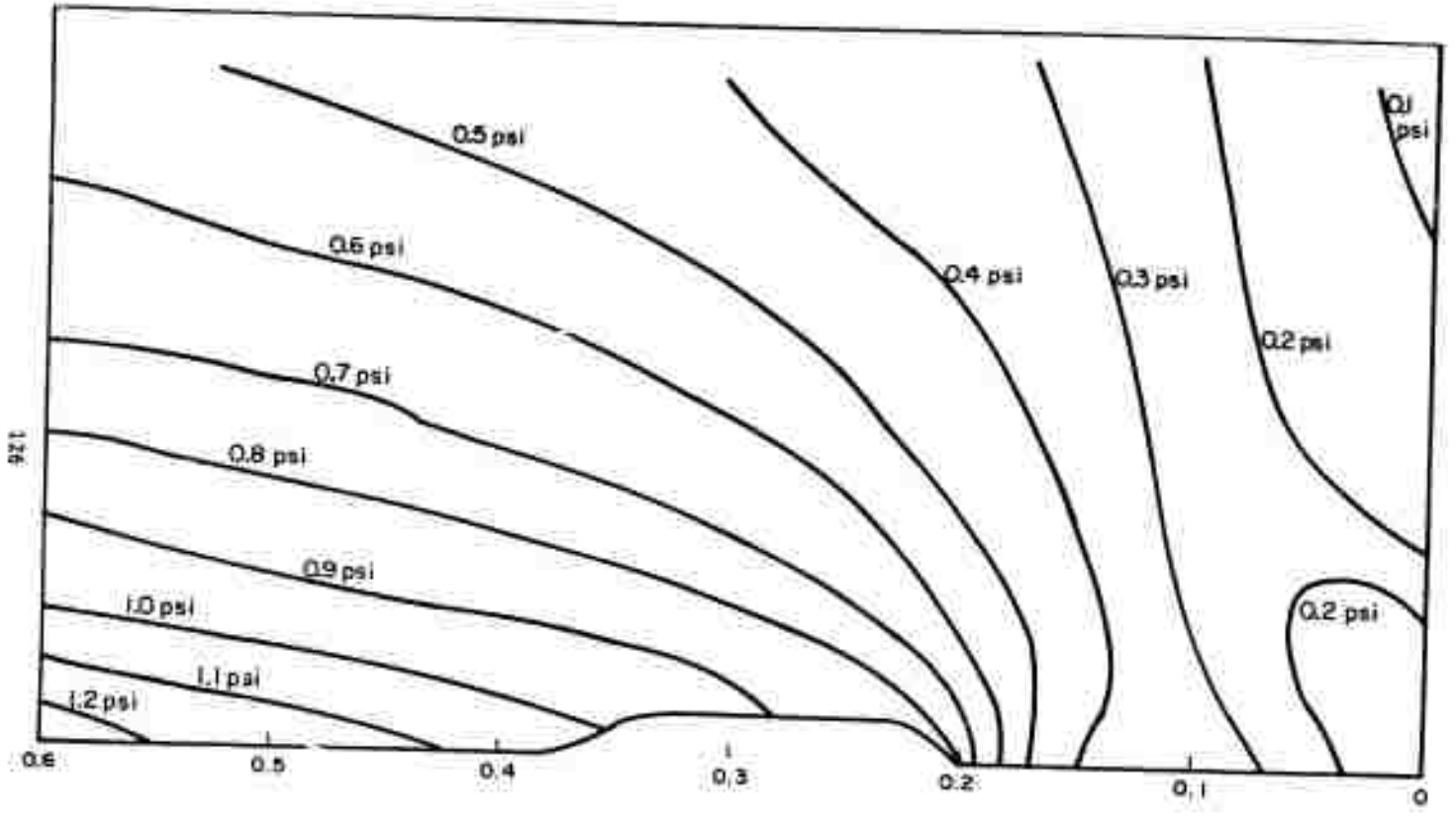

FIGURE 40. CALCULATED CONTOURS OF MAXIMUM SHEAR STRESS IN NOTCHED LINER

Analysis of Other Container Designs

Sectored Container with no Liner

In Reference (14), it was shown that a ring-segment container, was inferior to a multi-ring container. This comparison was based upon the fatigue strength of the liner.

Recently, in a paper at the High Pressure Engineering Conference[52], Wilson and Skelton show that a sectored vessel is superior to the multi-ring container, if the sectored vessel has no liner, or if it has a liner of zero stiffness that can withstand large strain. Their evaluation is based upon comparing the strength of the liner, Component 1 in the multi-ring container, with the strength of the first backup ring, Component 2 of the sectored container. (They ignore the strength of the liner.)

If a liner is used to seal the pressure at the bore from entering between the segments, the analysis in Reference (14) shows that the liner will fail first--thus, it is necessary to consider a high strength liner. However, if it is assumed that some other means of sealing between the segments is employed, the use of a sectored vessel then may be worth considering. This possibility is now considered on the following basis; it is assumed that sectors replace the liner of a multi-ring container as shown in Figure 41. Therefore, the sectored vessel may be thought of as a multi-ring container with N-1 rings but with a bore pressure on Component 2 (the first ring) of

$$p_1 = p_o/k_1$$

In Reference (52), the maximum burst and maximum autofrettage pressures were calculated. Here, however, the fatigue pressures of shrink-fitted containers are calculated. Using Equation (40) of Reference (14) for the shear fatigue strength of a multi-ring container with all rings of the same material ($\sigma_u \leq$ 200,000 psi), the following ratio is obtained:

$$\frac{p_m}{p_s} = \frac{N}{N-1} \left(\frac{K^{2/N}-1}{K^{2/N}}\right) \left(\frac{K^{2/(N-1)}}{K^{2/(N-1)}-k_1^{2/(N-1)}}\right) \frac{1}{k_1} \qquad (23)$$

where p_m is the maximum pressure for the multi-ring container, p_s is the maximum pressure for the sectored container, N is the total number of components in each container, K is the overall diameter ratio of each container, and K_1 is the liner wall ratio of the multi-ring container and the segment wall ratio of the sectored container.

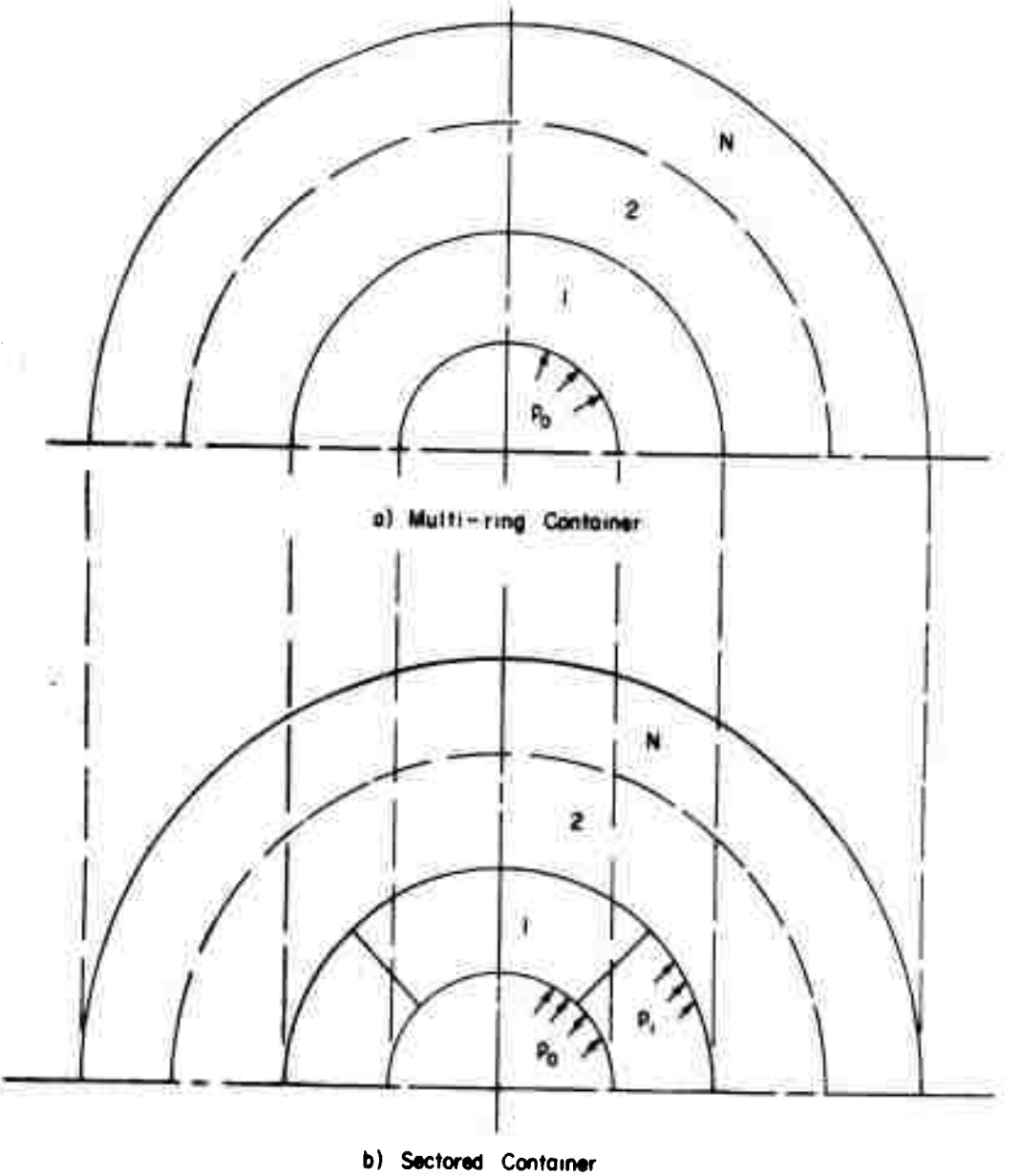

FIGURE 41. MULTI-RING AND SECTORED CONTAINER DESIGN CONCEPTS ANALYZED

The following calculations are made for the optimum geometry $K = k_1^N$:

$$N = 2,\ K = 3.0,\ k_1 = 1.732,\ \frac{p_m}{p_s} = 1.15$$

$$N = 2,\ K = 5.0,\ k_1 = 2.236,\ \frac{p_m}{p_s} = 0.895$$

$$N = 3,\ K = 4.0,\ k_1 = 1.590,\ \frac{p_m}{p_s} = 0.945$$

$$N = 3,\ K = 5.0,\ k_1 = 1.710,\ \frac{p_m}{p_s} = 0.878.$$

Thus, it is found that for large overall wall ratios, and consequently larger wall ratios for the sectors, that the pressure capability of the sectored vessel exceeds that of the multi-ring--if the sectored container has no liner or has a liner of zero stiffness (e.g., a rubber liner). However, the multi-ring container is yet superior for the case when the liner (or sector) wall ratio, k_1 is relatively small compared to the overall wall ratio K, for example above when $N = 2$. Furthermore, for a multi-ring container with a high strength liner, the fatigue pressure capability p_m will be even greater.

It was believed that the sealing problems for a sectored vessel with no liner, and its less rigidity did not warrant further consideration in the present study.

Stem Analysis

Since the stem in hydrostatic extrusion press must withstand high compressive stresses, a material with a compressive strength at least equal to the extrusion fluid pressure is required for this application. For 250,000 psi fluid pressure this requirement can be met by various tool steels; however, for 450,000 psi pressure one must consider tungsten carbide or a similar material. However, the design of a stem for hydrostatic extrusion cannot be based solely on the compressive strength of the material. In this study, several other potentially critical factors have been evaluated to determine possible limitations on stem load-bearing capacity. Foremost among these is buckling. In hydrostatic extrusion there is no limitation on billet length since there is essentially no billet/container friction, the billet is uniformly supported by the fluid, and buckling of the billet cannot occur. The maximum billet length is thus determined primarily by the length-to-diameter ratio (ℓ/d) of the stem at which buckling of the stem occurs. This critical length-to-diameter ratio is quite dependent on the compressive stress-strain behavior of the stem material. This includes not only the nominal value of Young's modulus of the material but also the tangent modulus at high compressive stresses. Other factors considered in this study have been the sensitivity of the stem stresses and buckling loads to press misalignment, and the required rigidity of lateral support for the stem if such support is needed to increase the stem-buckling resistance.

In addition to the above factors which have rather general application to hydrostatic extrusion stems, several additional questions have been considered which relate more specifically to the press design evolved during this study. These factors include the possible stress concentration at the notch at the end of the stem, axial surfaces stress produced by a pressure discontinuity on the lateral surface of the stem, and limitation on concentric stem designs.

Stem Buckling

As the stem length-to-diameter ratio increases, the possibility of column-type buckling becomes greater. The elastic buckling load of compression members as given by the classical Euler buckling formula[53] is

$$P_{cr} = \frac{\pi^2 EI}{\ell_e^2}$$

where

P_{cr} = buckling load

E = Young's modulus

I = moment of inertia of cross section

ℓ_e = effective length.

The stem-buckling loads predicted by this relation are shown by the solid curves in Figure 42 as a function of the length-to-diameter ratio ℓ/d. It is assumed that the upper end of the stem is prevented from rotating (i.e., is fixed). At the lower end, two limiting end conditions (hinged and fixed) are considered for which the effective lengths are 0.7ℓ and 0.5ℓ, respectively. A value of 30×10^6 psi for Young's modulus is assumed for steel.

The proposed 12-inch-diameter stem design for 250,000 psi fluid pressure is indicated on Figure 42. It is about 108 inches long and has an ℓ/d ratio of 9. The 6.0-inch-diameter stem design will be discussed in greater detail in a following section, and is not indicated on Figure 42. Experience at Battelle shows that, due to frictional drag at the stem seal, the stem pressure can be as much as 15 percent higher than the fluid pressure. The design stem pressures for the two stems, therefore, have been taken as 300,000 psi and 500,000 psi, rather than 250,000 psi and 450,000 psi. Figure 42 indicates that the 12.0-inch design does not exceed the theoretical elastic Euler buckling load for steel with $E = 30 \times 10^6$ psi. The design pressure of 500,000 psi for the 6.0-inch stem means that a material such as tungsten carbide with a very high compressive strength must be used for this application.

At high stress levels, stress-strain curves commonly become nonlinear. Consequently, the effective elastic modulus which governs buckling behavior decreases. The so-called tangent-modulus theory(53) accounts for this effect by using the Euler buckling formula with Young's modulus replaced by the compressive tangent modulus at the appropriate stress level. On the linear portion of the stress-strain curve, the two moduli are equal and, thus, the predicted buckling load is unchanged. However, at higher stress levels, the modified value of the buckling load can be much lower. The dashed curves in Figure 42 are the buckling load curves based on stress-strain data for a steel with an ultimate compressive strength of 504,000 psi. The curves indicate that the buckling resistance decreases rapidly as the stress-strain curve becomes nonlinear for the small ℓ/d ratios.

Compressive stress-strain data are limited for the very high-strength materials that are required for the high stem pressures, and the tangent moduli of these materials are not known with any certainty. However, for high-strength steels the linear portion of the compressive stress-strain curve typically extends to about 50 to 80 percent of the ultimate strength. The results shown by Figure 42 are based on high temperature bearing steel whose ultimate compressive strength of 504,000 psi seems to be as high as for any available steel, and is sufficient for the 250,000-psi fluid-pressure design. Data from Allegheny Ludlum(54) gave detailed stress-strain information to about 350,000 psi; above this level, the shape of the curve was assumed. For higher stress levels a tangent modulus which varied linearly with stress and decreased to zero at the ultimate strength was assumed. The buckling pressures from the tangent-modulus theory and this stress-strain curve are shown in Figure 42. The buckling pressures of cylindrical compression members as reported by Allegheny Ludlum are also indicated in Figure 42. Although the end conditions for these tests were not reported, the buckling pressures appear to be consistent with the tangent-modulus curves. These results indicate that the 250,000 psi stem design should not buckle, assuming a steel such as HTB-3 at R_c 60 is used.

---

* Allegheny Ludlum Steel Corporation designation.

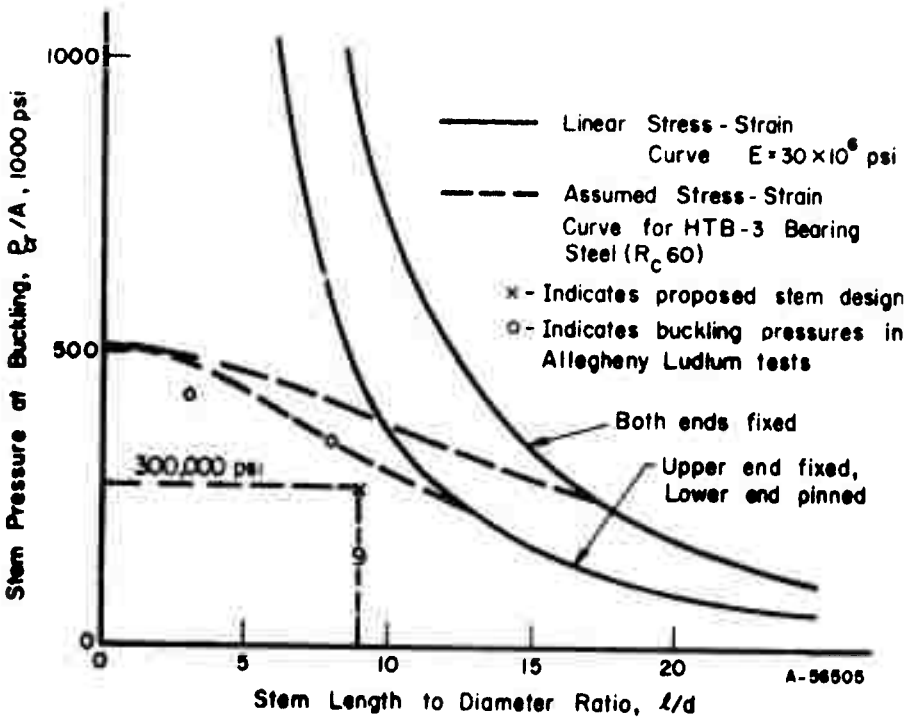

FIGURE 42. STEM BUCKLING PRESSURES BASED ON EULER AND TANGENT-MODULUS THEORIES

Small eccentricities in the axial load or superimposed lateral loads could possibly lead to premature buckling. In hydrostatic extrusion, the load is applied as a uniform pressure to the end of the stem and, thus, there appears to be little chance of the axial load being applied off-center. However, due to press or stem misalignment, lateral loads could result from contact of the stem with the container bore. This problem is analyzed in a following section to determine the magnitude of the problem and to determine the alignment tolerances which will have to be built into the production extrusion press.

Lateral Support of Stems

By providing lateral support at the midpoint of the stem length, the theoretical buckling load can be increased from

$$P_{cr} = \frac{4\,\pi^2\,EI}{\ell^2}$$

to

$$P_{cr} = \frac{8.18\,\pi^2\,EI}{\ell^2}$$

assuming that both ends of the stem are fixed. The lateral support serves to decrease the effective length of the stem. To achieve this increase in buckling load, however, the support must have sufficient stiffness. The critical support stiffness, α_{cr}, in this case is

$$\alpha_{cr} = 208\,\frac{EI}{\ell^3} \quad \text{(lb per inch)} \; .$$

No benefit is gained with a greater stiffness, while a less stiff support will not be as effective. This critical support stiffness can be compared with stiffness of the stem to lateral deflections due to a load applied at its midpoint, which is

$$\alpha = 192\,\frac{EI}{\ell^3} \quad \text{(lb per inch)} \; .$$

Thus, the support should have about the same stiffness as the stem.

Besides being sufficiently stiff, any lateral support must be able to retract so the stem can fully enter the container. The supports must also be maintained in precise alignment with the stem and the container bore.

Lateral support will not be required for the 12.0-inch-diameter stem since its length-to-diameter ratio should not be critical. However, for the 6.0-inch-diameter stem in the concentric stem arrangement, buckling is predicted if no lateral support is present. With this arrangement the lateral support is provided by an outer concentric stem which clearly is considerably more stiff (because of its larger diameter) than the inner stem which it supports.

Analysis of Composite Stems

As the stem is constructed of a high-strength but brittle material, its fracture is likely to be explosive in nature. The surrounding of a hard, stiff, high-strength inner core with a more ductile lower-strength sleeve could safely contain brittle failure of the core. Analysis, however, indicates that the stem load-bearing capacity would be largely limited by the strength of the sleeve material and that the additional strength of the core material would not be fully utilized.

Under axial loading, a composite stem will deform so that the axial strain in both materials is the same. Thus, the stresses in the two materials will be unequal, but proportional to their elastic moduli. Ideally, the materials should have their moduli proportional to their respective strengths, so that both materials would reach their failure stress at the same axial strain.

The amount of reduction in stem load-bearing capacity versus a solid stem of the core material is shown in Figure 43 as a function of the core and sleeve diameters and elastic moduli ratio. These curves are for the ideal situation with the moduli-to-strength ratios being the same for both materials, and it is assumed that buckling does not occur. The corresponding reduction in the Euler buckling load is indicated in Figure 44. The reduction in the buckling load is quite severe, since the bending stiffness, EI, of the stem is more sensitive to the outer material. Figures 45 and 46 present the relative strength of a composite stem in a somewhat different light; the comparison is made between a composite stem and a solid stem made of the weaker sleeve material. Again, the results assume the moduli and strength are proportional. One possibility would have a tungsten-carbide core and a high-strength steel sleeve, for which the moduli ratio is about 3.0. Assuming an ultimate compressive strength of 650,000 psi for the tungsten carbide, the corresponding strength of the steel should be at least 216,000 psi. Taking a core-to-sleeve, outer radii ratio of 0.75, compressive failure would occur (Figure 45) at an average stem pressure of 465,000 psi (i.e., 2.15 x 216,000 psi). This would be accompanied by an increase in the buckling load by a factor of 1.65 (Figure 46). In this case, both the core and stem would fail at the same time. If a steel of strength greater than 216,000 psi is used, the compressive failure will occur first in the core material, and thus the added strength of the sleeve will not be utilized.

Plastic deformation of the relatively ductile sleeve material could occur during extrusion if it is exposed to the fluid pressure. A critical situation will exist at the seal where stress concentrations arise from geometric and loading discontinuities. Another critical situation would result if the fluid pressure were to penetrate the interface between the sleeve and core materials, and separate the materials. These considerations seem to exclude the use of a ductile outer sleeve if the seal is set into the wall of the container, since contact with the fluid is unavoidable. However, if the seal is positioned at the end of the stem, contact with the fluid pressure could be avoided with a design that terminated the sleeve just short of the seal, as shown in Figure 47.

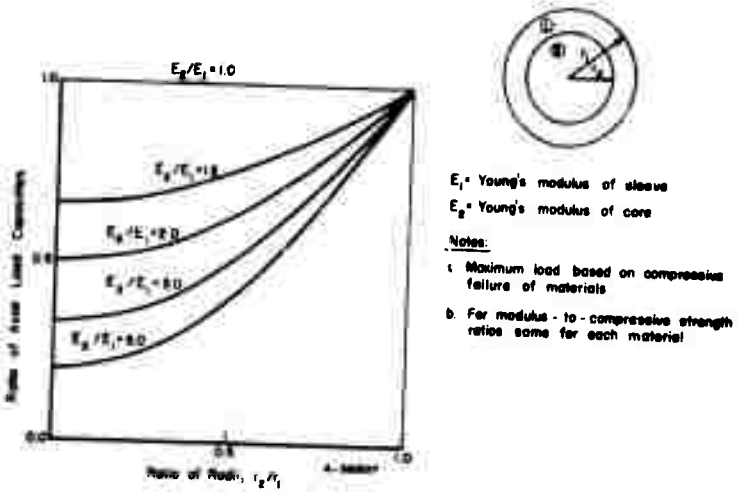

FIGURE 43. REDUCTION IN LOAD CAPACITY OF COMPOSITE STEM VERSUS SOLID STEM OF CORE MATERIAL

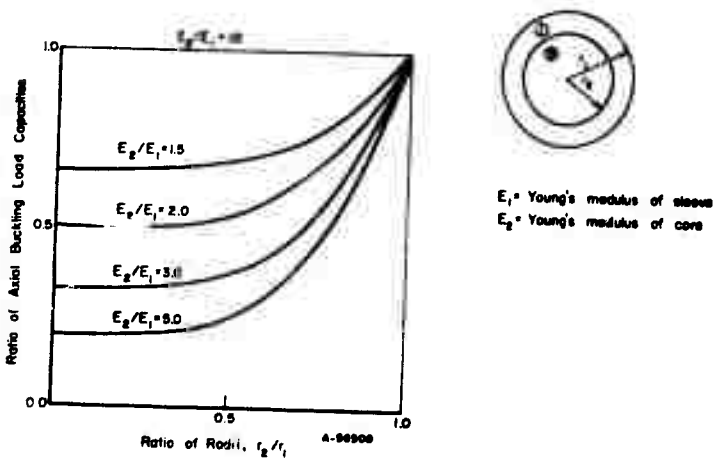

FIGURE 44. REDUCTION IN BUCKLING LOAD OF COMPOSITE STEM VERSUS SOLID STEM OF CORE MATERIAL

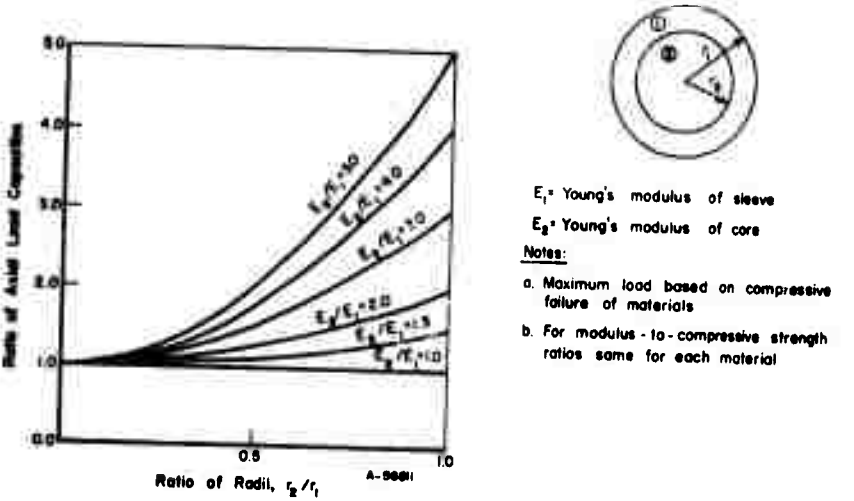

FIGURE 45. INCREASE IN LOAD CAPACITY OF COMPOSITE STEM VERSUS SOLID STEM OF SLEEVE MATERIAL

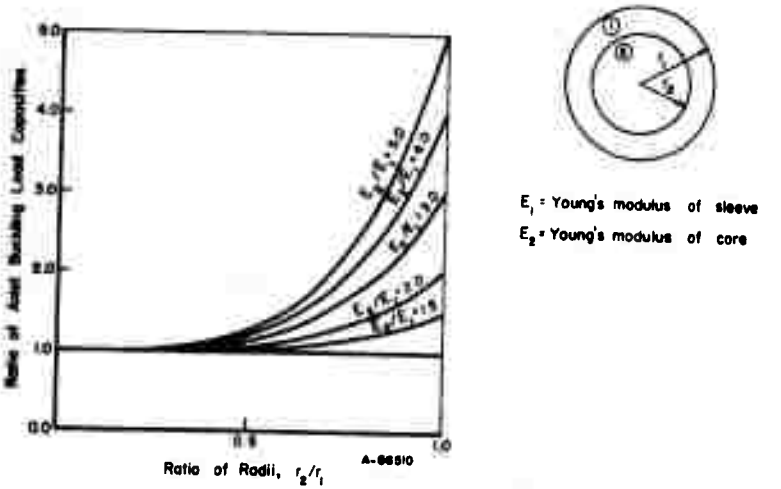

FIGURE 46. INCREASE IN BUCKLING LOAD OF COMPOSITE STEM VERSUS SOLID STEM OF SLEEVE MATERIAL

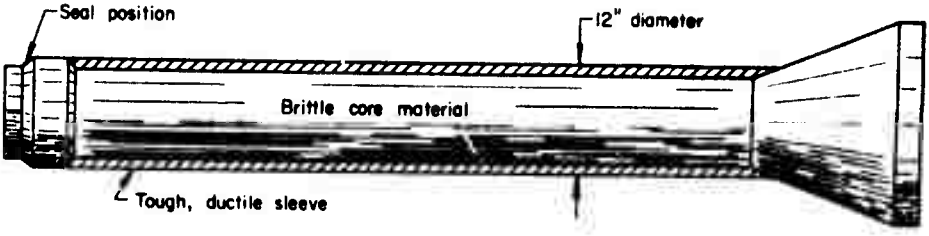

FIGURE 47. COMPOSITE DESIGN FOR THE 12-INCH-DIAMETER STEM

In summary, except possibly for safety considerations, application of composite stems does not appear promising. Use of solid stems offers advantages of both greater strength and less chance for undesirable plastic deformation.

Localized Stresses at Seal Location

One possible seal arrangement has the seal set into a recess in the container bore. This means that only the portion of the stem below the seal is exposed to lateral fluid pressure. At the seal, this pressure rapidly drops to zero, and a complex, elastic stress state results. The surface variation in the axial stress in the stem in the region of the pressure discontinuity is indicated in Figure 48 which has been replotted from Reference (48). At the surface, the axial compressive stress increases to 1.5 times its nominal value (i.e., 1.5 times the stem pressure). Below the surface, the stress rise is less severe. Similar behavior is exhibited by the radial, tangential, and shear components of the stress. The solid and dashed curves in Figure 48 indicate the effect of both an ideally sharp pressure drop and a more gradual drop in fluid pressure across the seal.

Study of the local stress state in the seal region indicates that the maximum shear stress does not significantly exceed one-half the stem pressure. Thus, there is no increase in the maximum shear stress over that in the upper part of the stem which also equals one-half the stem pressure. The variation of the

stress components in the seal region from their nominal values is largely hydrostatic in character and, consequently, little increase in shear stress occurs.

The results shown in Figure 48 are valid when the pressure discontinuity is a distance of one stem diameter or more from the end. End effects are influential if the discontinuity is closer to the end. However, in this case, they are helpful because they make for a less severe increase in the axial surface compression.

If the seal is located at the end of the stem rather than in the container bore stress concentrations may appear due to the notch in the stem needed to accommodate the seal. These stresses are considered in a following section.

Stem Misalignment

If the stem and container bore are not in precise axial alignment, side loads can be imposed on the end of the stem. These side loads besides producing bending stresses in the stem may also decrease its buckling resistance. The sensitivity to misalignment has been evaluated by considering the idealized case shown in Figure 49. Here, the stem is represented as a cantilever beam supporting an axial load, P. The free end of the beam is deflected an amount, δ, through contact with a smooth rigid wall (e.g., the container bore). It is assumed that this contact results in a side load, Q, at the end of the beam, but no restraining bending movement.

For the above conditions, the resulting bending stresses in the beam have been determined through a beam-column type of analysis.(53) Such an analysis accounts for the effect of the axial load, P, on the bending of the beam, and yields relations which give the bending stress in the beam for a given axial load, P, and lateral deflection, δ. These relations have been programmed for evaluation on Battelle's CDC 6400 digital computer. Numerical results were generated for the solid 12.0-inch-diameter stem of this design study, and are shown in Figure 50. These indicate, for example, that, at an extrusion pressure of 250,000 psi and for a relatively large misalignment of 0.25 inch, the bending stress is about 12,000 psi. A stress of 12,000 psi is relatively small compared to 250,000 psi, and thus it does not seem that the misalignment significantly reduces the stem load-bearing capacity in this case.

The effect of a decreasing tangent modulus at higher stresses is not accounted for in the curves of Figure 50. A decreasing tangent modulus would shift the point at which the curves of Figure 50 begin their rapid rise to a lower stress level. The bending stresses due to axial misalignment again will be significant only if the stem is loaded nearly to its buckling load (i.e., 80 to 90 percent) and then only if the misalignment is fairly large (i.e., 0.25 inch for the 12.0-inch stem).

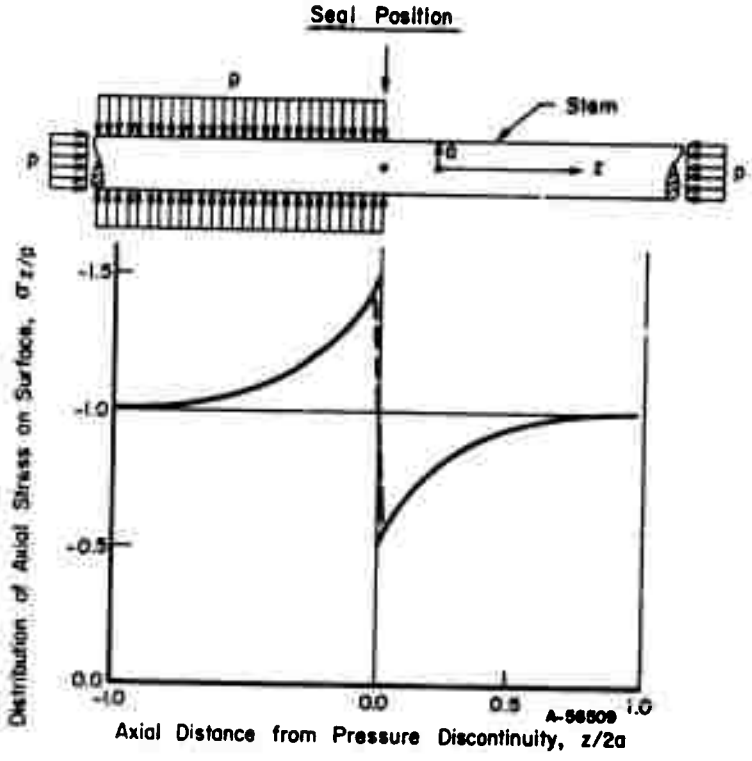

Note:

(a) Solid curve corresponds to sharp pressure discontinuity on surface.

(b) Dashed curve corresponds to gradual pressure drop over distance of about 0.1 along the surface

a = stem radius

z = distance along stem axis

p = fluid pressure

σ_z = surface axial stress.

FIGURE 48. AXIAL STRESS RISE ON STEM SURFACE DUE TO PRESSURE DROP AT SEAL POSITION

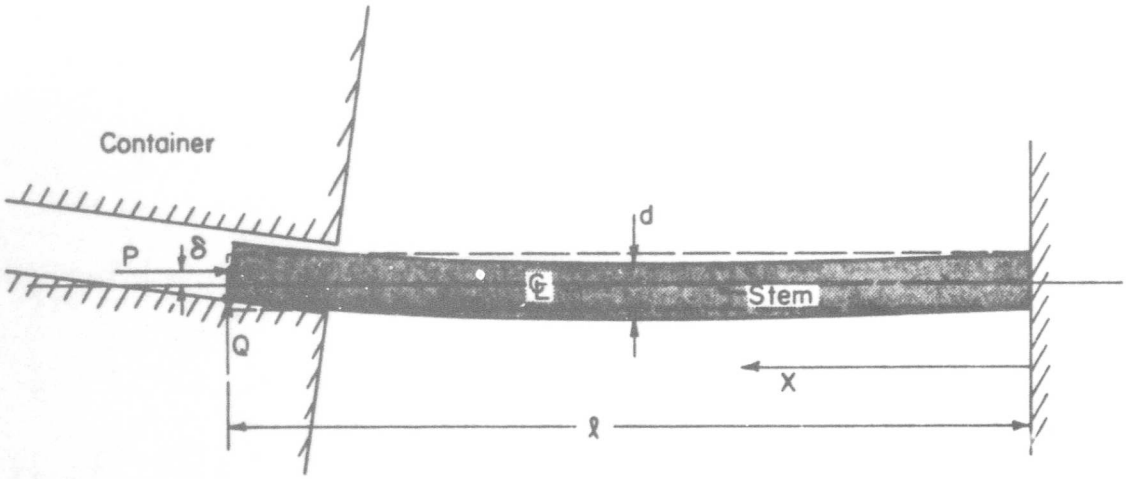

FIGURE 49. ASSUMED CONDITIONS OF STEM AND CONTAINER MISALIGNMENT

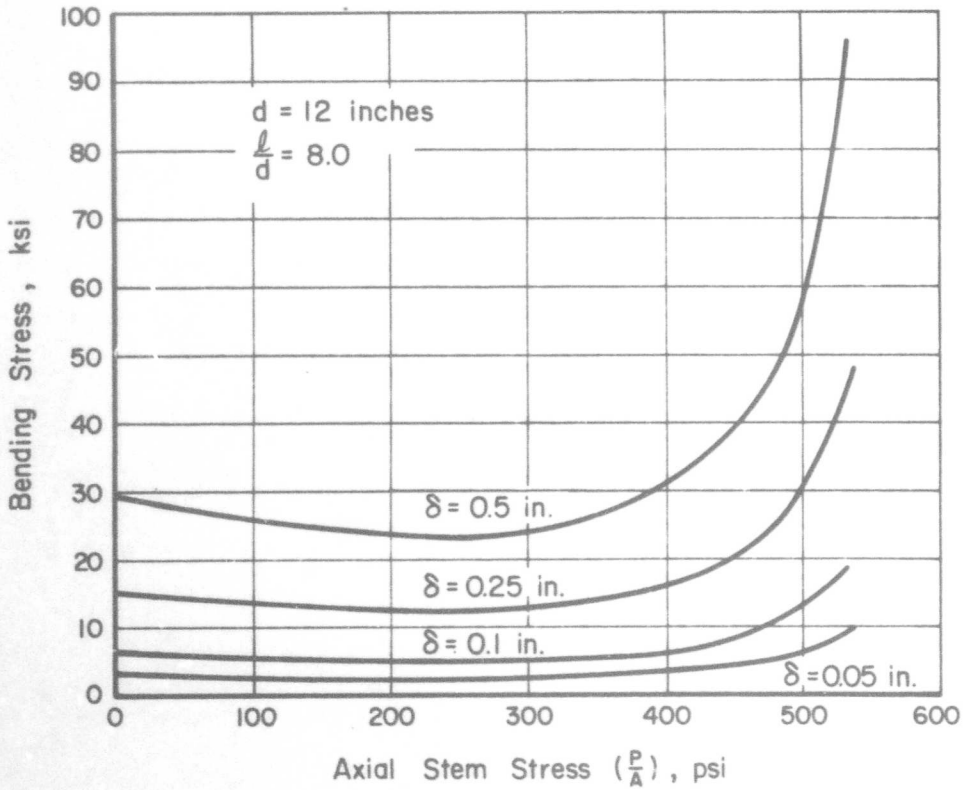

FIGURE 50. BENDING STRESS IN 12-INCH STEM DUE TO MISALIGNMENT AS A FUNCTION OF AXIAL STEM STRESS

Analysis of Notch at End of Stem

With the seal at the end of the stem rather than in the container bore, there is a notch in the stem. This notch is a possible source of stress concentration, which could cause cracking or plastic deformation (mushrooming). To investigate this question, the elastic stress state at the end of a notched stem was analyzed. The configuration considered is shown in Figure 51.

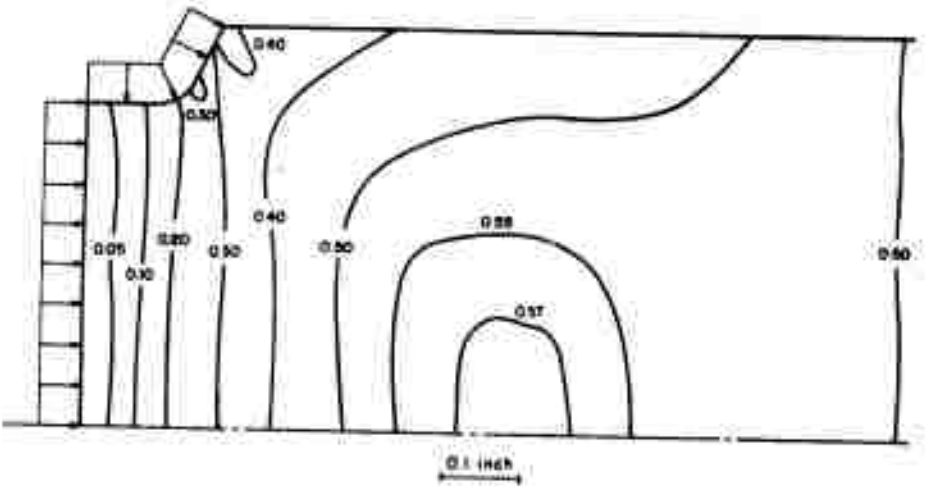

FIGURE 51. ASSUMED LOADING AND CALCULATED MAXIMUM-SHEAR-STRESS CONTOURS FOR ANALYSIS OF A STEM SEAL

The stem diameter is normalized to 1.0 inch and the notch is normalized to a depth of 0.1 inch. A small fillet (0.05-inch radius) was placed at the base of the notch to reduce the stress concentration there. The loading corresponds to a extrusion fluid pressure of 1.0 psi. This pressure was assumed to be transmitted hydrostatically through the seal to give a uniform pressure on the entire surface of the notch. In practice, friction between the seal and container bore would, no doubt, result in some variation from this constant distribution.

The calculated contours of maximum shear stress are shown in Figure 51. The nominal value is 0.50 times the axial compressive stress and at notch the maximum shear is less than this. The greatest value of shear stress occurs away from the notch and in the interior of the stem, and is about 0.57 times the fluid pressure. The results of the stress calculations thus indicate that the notch does not produce a significant stress concentration.

Design of Concentric Stems

The stem arrangement evolved in this design study for extrusion at 450,000 psi uses a 12.0-inch-diameter hollow outer stem to pressurize the 250,000 psi fluid, and a 6.0-inch-diameter inner stem to pressurize the 450,000 psi fluid. Also, it has been proposed to use concentric stems for extrusion at 250,000 psi. Here, the inner stem will apply a positive load to the end of the billet and aid in the handling of the billet during loading. This section discusses this concept from the stress analysis viewpoint and presents some analysis which apply to this design. The following discussion will concentrate primarily on the 450,000 psi design.

Required Length of Inner Stem

Since the inner stem is only 6.0 inches in diameter and is required to support 450,000 psi of fluid pressure, it is important to determine its length for buckling considerations. The concentric stem arrangement is shown conceptually in Figures 52 and 53. The outer hollow stem is quite short so that the highly stressed inner stem can be as short as possible. The required lengths of the stems have been determined, and these lengths are based primarily on the estimated travel of the outer stem in compressing the supporting fluid to 250,000 psi, and that of the inner stem needed to compress the 450,000 psi fluid and displace the billet.

A total length of about 96 inches is needed for the inner stem. Of this, 60 inches must be of 6-inch diameter, while the remaining 36 inches can be of larger diameter (10 inches to 12 inches). Figures 52 and 53 indicate the configuration considered. The outer stem must travel 12 to 15 inches to compress the fluid, depending on whether fluid-to-air or fluid-to-fluid techniques are employed. These lengths plus an allowance for seals and a tapered section on the outer ram determined that the outer stem must have a uniform bore 25 inches long, as shown in Figure 52. The determination of the length of the 6.0-inch inner stem is based on the configuration of Figure 53. The length of 60.0 inches is accounted for as follows:

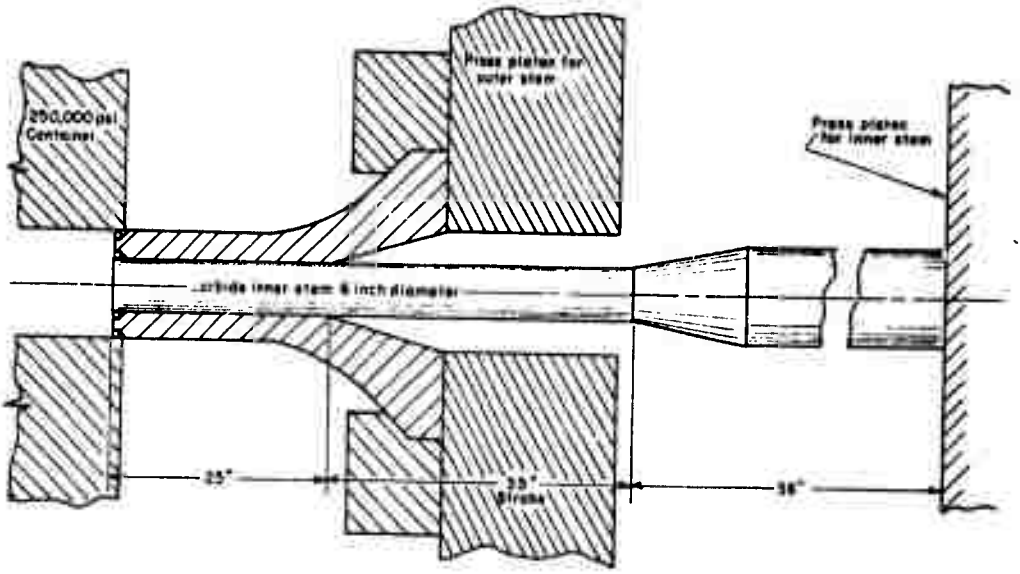

FIGURE 52. CONCENTRIC STEM CONFIGURATION SHOWN WITH OUTER STEM FULLY EXTENDED AND INNER STEM FULLY RETRACTED

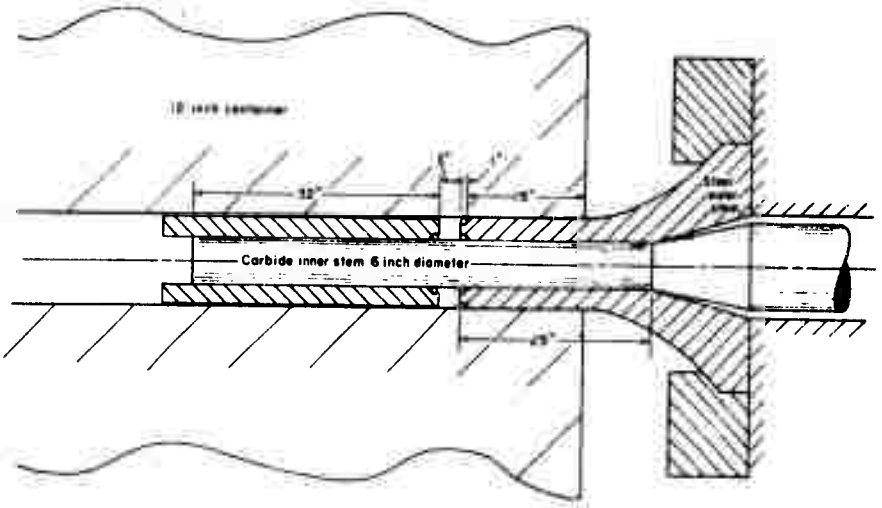

FIGURE 53. CONCENTRIC STEM CONFIGURATION, SHOWN WITH INNER STEM IN FULLY EXTENDED POSITION

(a)	Distance that the 6.0 inch stem must enter the 6.0 inch container to extrude the billet and to eject the die and butt	=	32.0 inches
(b)	Length of 6.0 inch stem that is needed to pass through bore of outer stem	=	25.0 inches
(c)	Allowance for separation of end of outer stem and end of 6.0-inch container	=	3.0 inches
	Total length		60.0 inches

In addition, the larger-diameter portion of the ram must extend back about 36 inches to reach the press head. In all, this accounts for a total length of 96 inches.

By expanding the diameter of the inner stem from 6 inches to 12 inches, the axial compressive stress can be reduced from 450,000 psi to only 112,000 psi. This means that steel could be used for this 12-inch-diameter length.

Buckling of Inner Stem

With the above estimate of the length of the 6.0-inch-diameter inner stem, buckling of this stem can be considered. A design pressure for the stem design is taken as 500,000 psi to account for friction at the seals. To support this stress, tungsten carbide or a similar material with high compressive strength will be required. In addition to its high compressive strength, tungsten carbide has a high value of Young's modulus which increases buckling resistance. To estimate the critical length for a 6.0-inch-diameter stem, the Euler buckling formula for a cylindrical column with one end fixed and one end hinged can be applied:

$$\frac{P_{cr}}{A} = \left(\frac{4.493}{\ell}\right)^2 E\left(\frac{\ell}{d}\right)^{-2} .$$

For P_{cr}/A = 500,000 psi, d = 6.0 inches, and E = 80 x 10^6 psi (i.e., tungsten carbide), the critical length is 85.3 inches. Although the total length of the inner stem is 96.0 inches, the effective length for buckling considerations should be much less. The fact that part of the length is of 12-inch diameter will increase the buckling resistance. In addition, the outer stem can provide lateral support to the inner stem to further increase its buckling resistance. The maximum unsupported length (Figure 52) is 35.0 + 36.0 = 71.0 inches, and since about half of this is of 12.0-inch diameter, the effective length based on a 6.0-inch-diameter stem should be significantly less than 71.0 inches. Thus, with the critical length being 85.3 inch, the inner stem should have sufficient buckling resistance. A more precise but more lengthy buckling analysis to account for the variable diameter could be used to check this conclusion.

Hoop Stress in Outer Stem

Stress calculations show that ti is not advisable, with the concentric stem arrangement, to locate the seal for the outer hollow stem in the container bore. This is because the outer surface of the hollow stem is then exposed to 250,000 psi of fluid pressure and this results in a large compressive hoop stress, which could lead to inward collapse of the outer stem. For a solid stem such as the 6.0 inch inner stem, this large hoop stress does not occur, and the seal may be placed the container bore. The large hoop stress in the outer stem does not occur if e seal is placed at the end of the stem.

The standard Lame relations, when applied to the concentric stem arrangement of the present design study, give for the inward displacement and hoop stress at the bore of the outer stem

$$u = -0.067 \text{ inch}$$

$$\sigma_\theta = -667{,}000 \text{ psi} \quad ,$$

where the fluid pressure p_o = 250,000 psi, OD = 12 inches, ID = 6 inches, and $E = 30 \times 10^6$ psi. This means that if the ID of the outer stem is initially 6.000 inches, then 250,000 psi of external fluid pressure reduces it to 6.000 - 2 x 0.067 = 5.8666 inches.

If the allowable compressive stress of the stem material is 300,000 psi (about the compressive yield strength of HTB-3), the allowable external pressure is 113,000 psi, for which the radial displacement at the bore is 0.030 inch. By manufacturing a clearance of exactly 0.030 inch between the inner and outer stems, the two can be made to contact at this pressure. As the pressure on the outer surface is increased beyond 113,000 psi to 250,000 psi, yield at the bore of the outer stem could be prevented by supporting it with the inner stem. This, however, will result in large contact stresses, which, in turn, will result in friction to oppose relative movement of the concentric stems. At 250,000 psi fluid pressure, a radial contact stress of 250,000 - 113,000 = 137,000 psi will exist at the interface of the inner and outer stems. The axial force required to overcome this friction is

$$F = \mu \times (\text{contact stress}) \times (\text{area in contact}).$$

Taking the coefficient of friction μ = .1, the length of contact as 6 feet = 72 inches, and diameter of contact as 6 inches, the friction force is F = 9,300 tons. This force is quite large. Thus, the stems would be effectively "locked" together and relative movement would not be possible.

Differential Poisson Expansion of Stems

With the inner and outer stem made of different materials, and loaded axially by different fluid pressures, differential lateral Poisson expansion of the two members will occur. Considering the concentric stem arrangement of the

present design study with steel for the outer stem and tungsten carbide for the inner stem, so that $E_2 = 30 \times 10^6$ psi, $\nu_2 = .25$, $E_1 = 80 \times 10^6$ psi, and $\nu_1 = .25$. Then, for $P_2 = 250{,}000$ psi, $P_1 = 450{,}000$ psi, the change in clearance is calculated from standard elasticity relations as

$$\Delta d_2 - \Delta d_1 = .0041 \text{ inch.}$$

Thus, a gap appears between the stems, and this is a result of the relatively high modulus of the carbide inner stem. In contrast, if both stems are steel, an interference will develop and binding will occur if proper clearance is not provided.

Tungsten Carbide as a Stem Material

The stem for extrusion at 450,000 psi will require a material with a high compressive strength to resist crushing and a high elastic modulus to resist binding. On both these counts, tungsten carbide appears to be suitable material. However, tungsten carbide cannot be recommended at this time without qualification, mainly because much material property data of potential importance to the design of stems are not available.

The above calculations for the critical length for buckling of a 6.0 inch diameter tungsten carbide stem were based on an assumed strictly linear stress strain curve. If the actual stress strain curve deviated significantly at high stress levels from linearity giving a decreasing tangent modulus, the calculations could be in serious error. It is felt that for tungsten carbide the curve is quite linear, but this is not documented as no stress-strain curves could be obtained. Tests were reported to be in progress(55) to measure the buckling loads of tungsten carbide column specimens of various slenderness ratios. When these results become available, they should reflect any tangent modulus effect and indicate whether buckling calculations based on a nominal value of Young's modulus are valid.

Two other factors that could be of importance in design of stems are size effect and scatter in compressive strength data. Both these factors are important in design and are known for tensile applications, but data are lacking for compressive applications. However, the indications are that these factors are relatively minor for compressive loadings. The above mentioned tests hould provide some data on these factors.

Another behavior of tungsten carbide which needs further study is its reported spontaneous cracking after removal of high compressive stresses. The indication is that this cracking occurs only if the compressive stress is nearly equal to the ultimate compressive strength. Since the design stem loadings are up to 450,000--500,000 psi while the ultimate compressive strength of tungsten carbide is about 650,000 psi, the stresses at which such spontaneous cracking can occur should be known rather precisely.

Die Design

The dies used in hydrostatic extrusion are locally subjected to billet pressures in excess of those exerted solely by the fluid. At 250,000 psi fluid pressure, dies made of AISI M-50 tool steel have been generally satisfactory in experimental work done at Battelle[11]. When pressures of the order of 450,000 psi are considered, however, the die stresses are expected to be very near to the limit of material strength, even if the die were constructed from tungsten carbide. In view of these considerations, a theoretical analysis was made of the stress state which may exist in a die during hydrostatic extrusion.

The results of the following analysis indicate the required strength of die materials for extrusion at the design fluid pressures of 250,000 psi and 450,000 psi. In addition, the results show limitations on maximum feasible die openings and clearly show the benefit of fluid pressure support in reducing hoop stress in the die.

The analysis centered on the die design is shown in Figure 54. This particular design has been used successfully at Battelle to extrude various materials at fluid pressures up to 260,000 psi in a 2-3/8-inch diameter bore container. To make the analysis general, the OD of the die was normalized to one inch as indicated in Figure 54 (geometrically similar dies of larger OD all have the same stress state). The die stress analysis was performed using Battelle's computer program for elastic stresses in bodies of revolution. This program is designed to calculate stresses for arbitrary cross sections subjected to arbitrary axisymmetric loadings and is ideally suited for the analysis of extrusion dies.

Assumed Die Loadings

The pressures and other loadings that act on a die during extrusion are not precisely known. Figure 55 shows the pressures that were assumed. For generality, a hydrostatic extrusion pressure of 1.0 psi was considered. To obtain the results for any other pressure, one must only increase the stresses proportionally. The assumed die loading is described as follows:

(1) a fluid pressure of 1.0 psi acting on the top and exterior of the die above the seal.

(2) a constant normal pressure of 1.0 psi acting on the seal land to support the seal ring forced against it by the fluid pressure.

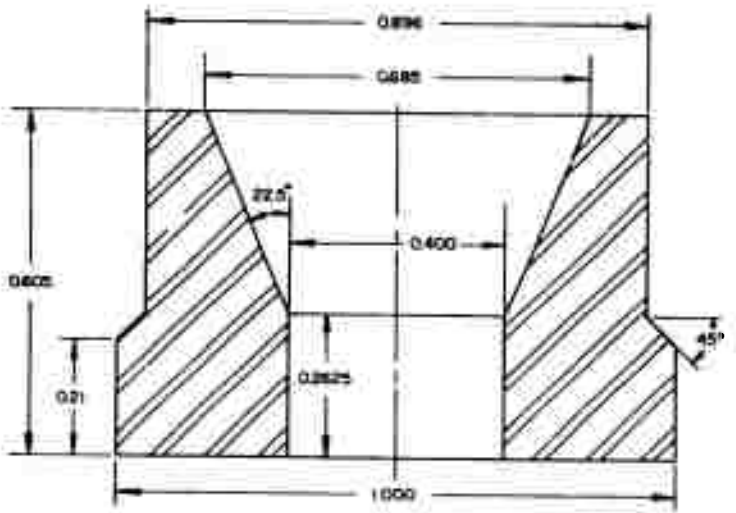

FIGURE 54. DIE DESIGN 1 - BASIC DESIGN CONSIDERED IN STRESS ANALYSIS

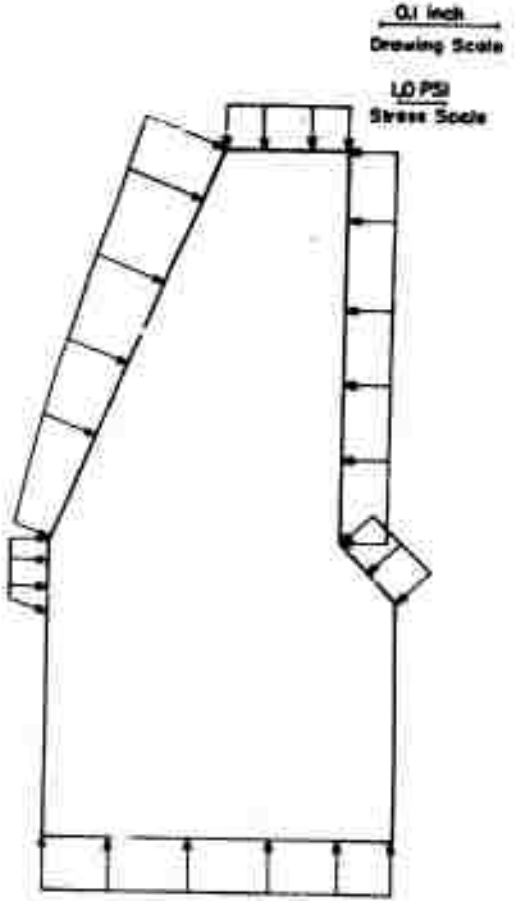

FIGURE 55. ASSUMED LOADING OF DIE DESIGN 1 - DURING HYDROSTATIC EXTRUSION

(3) the outer die surface below the seal is unloaded, which assumes that there is no contact between the die and container bore.

(4) a uniform contact stress on the base of the die of magnitude sufficient to support the die. A simplification is involved in this assumption since the actual contact stress would be non-uniform and related to the elastic deformation of the backup tooling. However, this non-uniform behavior would have an important influence on the die stresses only at relatively small distances from the base.

(5) on the die face the pressure of billet was taken to decrease from the entrance towards the exit of the die. This variation is discussed in detail below.

(6) a uniform pressure was assumed to act on the die land of magnitude equal to the billet pressure at the exit of the die. The analysis below estimates this pressure to be equal to the billet yield strength.

The distribution of the billet pressure on the die face should be considered in calculating the die stresses. The stresses that exist in a billet during extrusion through a conical die have been investigated by Shabaik, Lee, and Kobayashi (56) and Shabaik and Kobayashi (57) using the visio-plasticity method. This method unfortunately does not give highly accurate results for the stresses at the billet/die interface. The results do, however, clearly indicate that the billet pressure is highest at the die entrance and lowest at the exit.

Pugh and Ashcroft (58) have applied a theoretical solution formulated by Sachs and Eisbein (59) to the deformation of the billet in hydrostatic extrusion. It is assumed that proper lubrication would reduce the friction on the die face, so that the shear stresses on the die face will be small and can be neglected. Data compiled by Pugh (60) supports this assumption. The following relation between the billet/die pressure distribution and the fluid pressure was obtained.

$$\sigma(r)\ p_f \left\{ 1 + 1/\ln\left(\frac{a^2}{b^2}\right) \left[1 - \ln\left(\frac{a^2}{r^2}\right) \right] \right\} \qquad (24)$$

where p_f is the fluid pressure, a is the billet radius at the entrance of the die, b is the billet radius at the exit of the die, and r is the radial distance from the centerline of the die to a point on the die face. The above relations give $\sigma = p_f + Y$ for the pressure at the entrance of the die ($r = a$) and $\sigma = Y$ at the exit of the die ($r = b$). The assumed pressure distribution of Figure 55 used for the die stress analysis was calculated using Equation 24.

Calculated Results for Particular Die Designs

Die Design 1

The deformation as computed for the loadings previously described is presented in Figure 55. This particular die is designated Design 1 to distinguish it from variations from it to be designated Designs 2, 3, 4, and 5. Assuming the fore-mentioned loading, Figure 56a shows the computed deformation of the die (greatly exaggerated in scale) superimposed on the undeformed shape. As indicated, the die is actually deformed inward, due to the fluid support acting on the outside. In contrast, Figure 56B shows the resulting computed outward deformation of the same die, if the fluid support were absent (as in conventional extrusion without shrink rings on the die). The distribution of hoop stress corresponding to the deformation of Figure 56a almost entirely compressive, and this clearly indicates the benefit of fluid support. In contrast, the hoop stress distribution of the unsupported die (Figure 56b), shows tensile hoop stresses, which are as high as 2 - 3 times the extrusion pressure.

When the stresses in the die are entirely compressive, the failure of the die can result from stresses other than tensile hoop stresses. One criterion for failure of brittle materials in compression with some experimental basis, is that of maximum shear stress. That is, the material fails when the maximum shear stress exceeds the maximum shear stress at failure in a simple axial compression test. This shear stress in the simple compressive test is one-half the compressive strength of the material. For the deformation of the fluid supported die shown in Figure 56a, the overall maximum shear stress was calculated to be about 0.8 times the extrusion pressure, p_f. Basing the design stress on a maximum shear stress criterion, a material with an ultimate compressive strength of about 1.6 times p_f would be required. It is significant to note that the maximum shear stress occurs at the base of the die. The base of the die must always support a compressive stress greater than the fluid pressure, since the total force over the annular area of the base must equal the total force developed by the fluid pressure acting over the entire area of the extrusion chamber. In effect, Die 1 will be limited by compressive failure at the base.

Die Design 2

Die Design 2 is the same as Design 1, but with a larger die opening. The loadings were equivalent and the included die angle of 45 degrees was preserved. Figure 57a shows the deformation of Die Design 2 and indicates that during extrusion considerable outward expansion of the die occurs. This can be related to the increase in the ratio between billet/die interface pressure and fluid pressure, and the thinner wall section of Design 2. Tensile

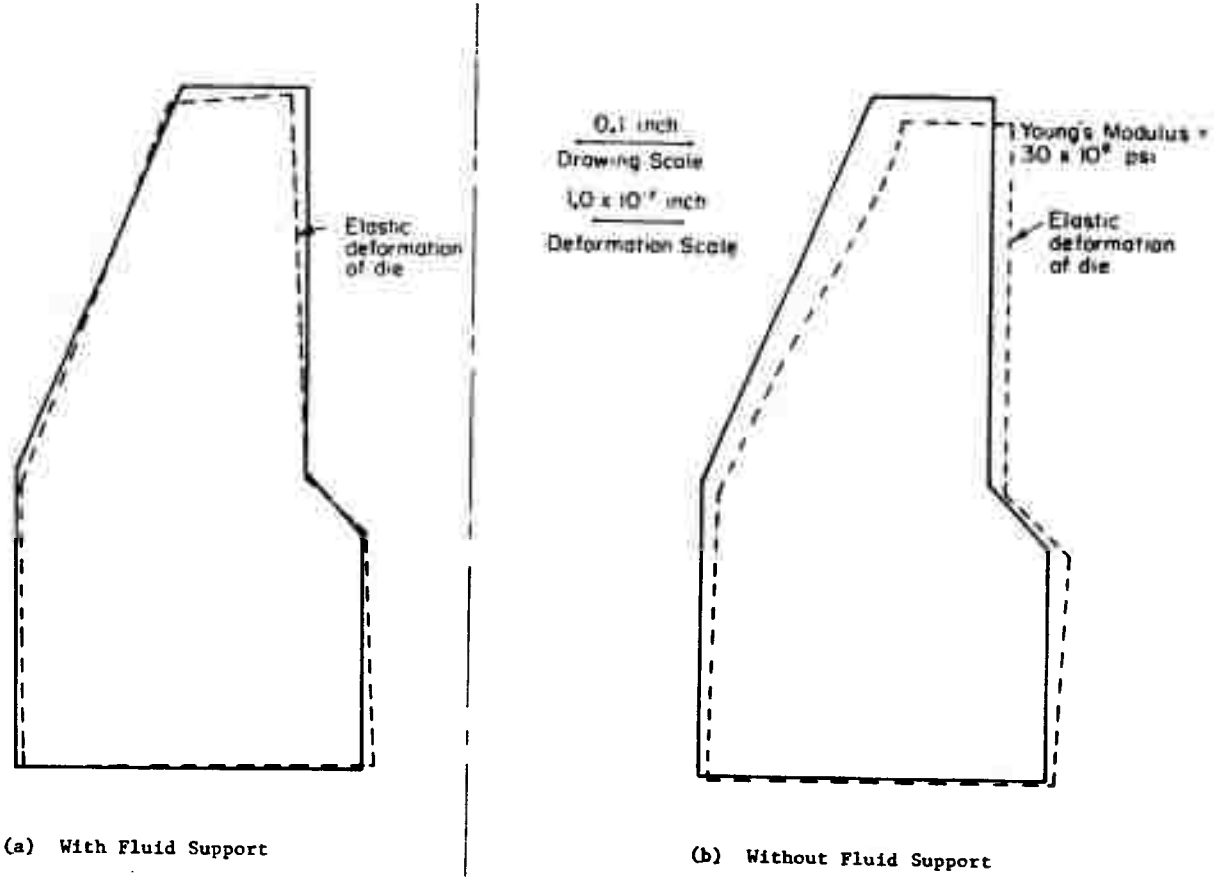

(a) With Fluid Support

(b) Without Fluid Support

FIGURE 56. ELASTIC DEFORMATION OF DIE DESIGN 1 DURING HYDROSTATIC EXTRUSION WITH AND WITHOUT FLUID SUPPORT

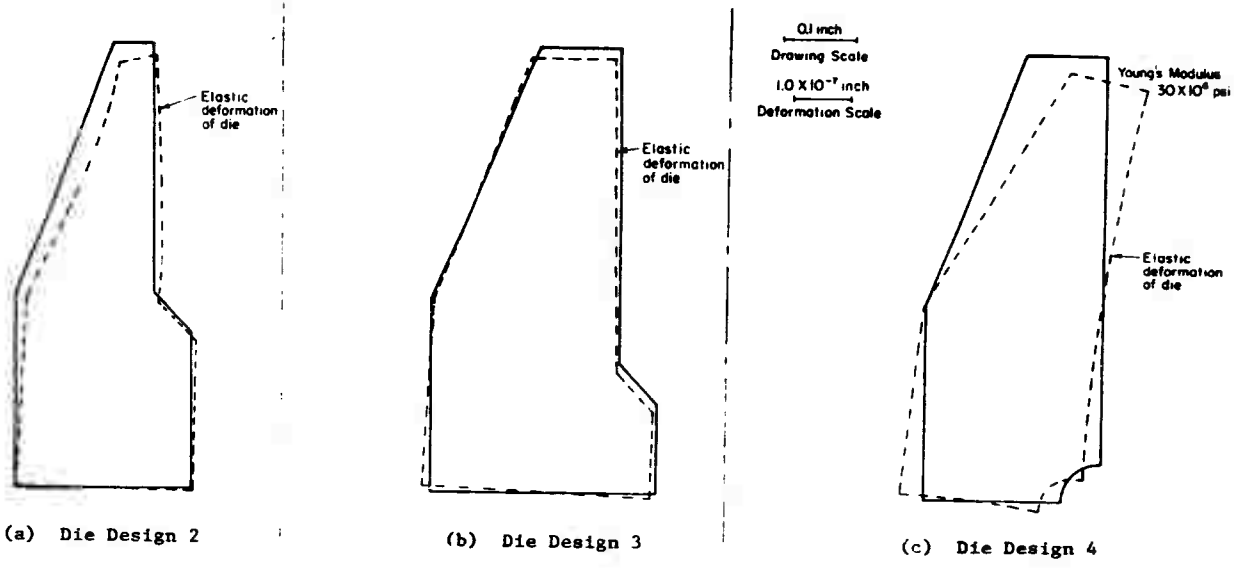

(a) Die Design 2

(b) Die Design 3

(c) Die Design 4

FIGURE 57. ELASTIC DEFORMATION OF VARIOUS DIE CONFIGURATIONS DURING HYDROSTATIC EXTRUSION WITH FLUID SUPPORT

hoop stresses appear in this design with the maximum value about 1.1 times the fluid pressure. The maximum shear stress was calculated to be about 1.5 times the fluid pressure. For a material such as steel where the tensile and compressive yield strengths are roughly equal, the pressure capability of Design 2 would be about 50 percent that of Design 1. For a material such as tungsten carbide with a compressive strength roughly 4 times its tensile strength, the pressure capability of Design 2 would be only about 35 percent that of Design 1.

Die Design 3

Die Design 3 is the same as Design 1, except that the die seal is placed closer to the base of the die, which gives fluid support over a greater length of the die. The assumed loadings were again as described for Design 1. The die is forced inwards as shown in Figure 57b, and the compressive hoop stress at the die base is quite large (up to 2 to 3 times the fluid pressure). The corresponding shear stresses are about 1.2 times p_f and this indicates that a die of this design would require a material with a compressive strength of about 2.5 times the fluid pressure. It is, thus, seen that too much fluid support can be detrimental in certain cases. The additional fluid support as compared to Design 1 has effectively resulted in a die with only about 65 percent the fluid pressure capacity.

Die Design 4

Die Design 4 is a modification of Design 2. This arrangement has a single rubber O-ring at the base of the die as a seal. A greater die-wall thickness is possible and fluid support extends to the very base of the die. The deformation of this is shown in Figure 57c. Large compressive hoop stresses are produced at the base or the die by the fluid pressure on the outside of the die, and the rotation or twisting of the cross section gives tensile hoop stresses of about 4.0 p_f at the top of the die. This is in contrast to a tensile hoop stress of 1.1 p_f for Die Design 2, which had an identical internal geometry (i.e. die opening). Additional fluid support has in this case resulted in a drastic reduction in pressure capacity.

This problem can be alleviated by locating the die orifice bearing in line with the O-ring at the die base. This arrangement, which should reduce the twisting of the cross section and consequently the hoop tensile stresses, has worked satisfactorily in actual practice.

Die Design 5

The dimensions and assumed loadings for Die Deisgn 5 are shown in Figure 58. This die represents a tentative design based on consideration of

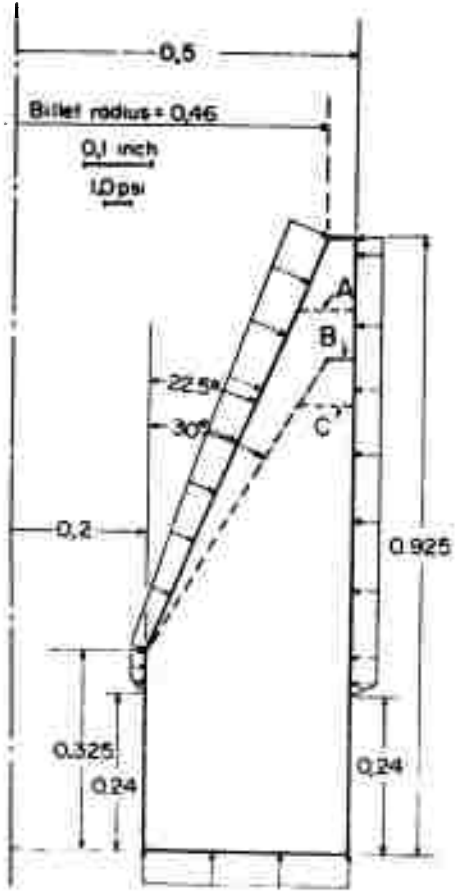

FIGURE 58. DIE DESIGN 5, WITH MODIFICATIONS A, B, AND C

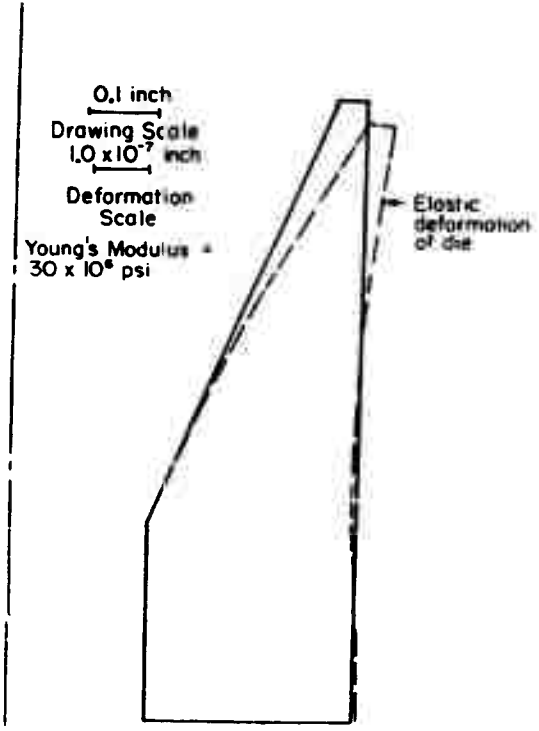

FIGURE 59. ELASTIC DEFORMATION OF DIE DESIGN 5 DURING HYDROSTATIC EXTRUSION WITH FLUID SUPPORT

previous die configurations, billet handling, and seal arrangements. This concept places the die seal in a groove in the container bore, with the position of the seal being apparent in Figure 58 by the extent of fluid pressure on the outside of the die. In the analysis, the dimensions were normalized to a one-inch container bore diameter, with the billet dimension corresponding to a 11-inch diameter billet in 12-inch bore container.

The calculated deformation is shown in Figure 59. The results indicate that the fluid support maintains compressive hoop stress in the exit region of the die, but that tensile stresses appear in the thin leading edge, where the hoop stress is calculated to be about 2.2 times the fluid pressure, while the corresponding maximum shear stress is about 1.8 times the fluid pressure.

Since the high stress levels at the leading edge of the die would limit the pressure capability of the die severely, die design modifications were investigated to reduce these stresses. These die modifications are designated as A, B, and C in Figure 58, and Table XVII. Three approaches were used. The first approach was to reduce the billet diameter (Modification A), in order to increase the die wall thickness. The second approach was to increase the die angle from 22.5 degrees to 30.0 degrees (Modification B). Modification C combines both of these modifications. The computed values of the critical stresses at the leading edge are listed in Table XVII for each of the modifications, and it is seen that significant stress reductions are achieved.

TABLE XVII. SUMMARY OF CALCULATED STRESSES IN LEADING EDGE OF DIE DESIGN 5 AND MODIFICATIONS A, B, AND C FOR LARGE BILLET/BORE DIAMETER RATIOS

	Billet Bore Diameter Ratio	Half Die Angle	Billet Reduction in Area, percent	Critical Stresses: Maximum Tensile Stress[a]	Critical Stresses: Maximum Shear Stress[a]	Pressure Limitations Imposed by Die Material	Fluid Pressure Capability[b]: M-50 Steel	Fluid Pressure Capability[b]: Tungsten Carbide
Design No. 5	11/12	22.5°	87.2	2.2	1.8	0.45 x tensile strength 0.555 x shear strength	112,000 psi[c]	67,500 psi[d]
Modification A	5/6	22.5°	77.0	0.8	1.0	1.25 x tensile strength 1.0 x shear strength	200,000 psi[c]	187,000 psi[d]
Modification B	11/12	30.0°	87.2	1.1	1.0	0.91 x tensile strength 1.00 x shear strength	200,000 psi[c]	137,000 psi[d]
Modification C	5/6	30.0°	77.0	0.1	0.7	10.0 x tensile strength 1.43 x shear strength	285,000 psi[c]	460,000 psi[c]

(a) Based on a fluid pressure normalized to 1.0 psi.

(b) Limits imposed only at the relatively high billet/bore diameter ratios indicated.

(c) Pressure limitation due to shear stress most severe.

(d) Pressure limitation due to tensile stress most severe.

From the foregoing analysis, the pressure capability of the Die Design 5 was estimated for two materials; M-50 tool steel and tungsten carbide. The strength values assumed for M-50 tool steel were:

tensile yield strength	= 350,000 psi
ultimate tensile strength	= 410,000 psi
ultimate compressive strength	= 540,000 psi

The maximum allowable die tensile stress was taken as 350,000 psi, the tensile yield strength. The maximum allowable shear stress was taken as 0.5 times the compressive yield strength which was estimated to be 400,000 psi. The strength values for tungsten carbide were taken as:

ultimate tensile strength	= 150,000 psi
ultimate compressive strength	= 650,000 psi

A maximum allowable shear stress was taken as 0.5 times the compressive strength.

The estimated pressure capabilities of the four dies are listed in the final column of Table XVII. The relatively low tensile strength of tungsten carbide limits its use for the first three designs. However, for Modification C, with the maximum hoop tensile stress reduced to 0.1, the high compressive strength can be utilized.

The calculations show that there is a limitation on the maximum billet diameter for a given container bore diameter. In particular, for a 11.0-inch billet in a 12.0-inch chamber (and for a billet reduction of 87 percent), the fluid pressure is limited to about 200,000 psi. Pressures up to 250,000 psi may be possible for this billet diameter if the billet reduction is somewhat greater, or if the die half angle is increased beyond 30 degrees. Based on the data of Table XVII, an estimate of the maximum billet diameter for extrusion at 250,000 psi has been made. With an included angle of 30 degrees, the maximum billet diameter for a carbide die is 10.5 inches, and for a M-50 tool steel die 10.25 inches. It should be emphasized that these estimates of die-pressure capabilities are based on such factors as assumed die/billet pressure distributions and allowable die stresses. Thus, the stated pressure capabilities could be either conservative or optimistic, and precise die limitations can only be determined through experience.

In the die calculations, one further aspect considered was the effect of allowing the die to have a sharp leading edge rather than the small flat as shown in Figure 58. It was found that this addition of material was not detrimental and, in fact, a slight reduction in stress at the leading edge was observed.

Approximate Die Analysis

The results of the computer stress calculations for the various die designs illustrate the sensitivity of the die stress-distribution to variations

in design parameters. However, to show the factors which lie behind the die response, and to determine limitations on extrusion, an approximate analysis has been formulated. The die was represented as a thick-walled ring as shown in Figure 60. It was assumed that the ring thickness, t, approximates the mean die wall thickness. If a fluid pressure, p_f, acts on the outer radius r_o and a billet pressure p_b acts on the inner radius r_i, and A_1 and A_2 are the original and extruded cross sectional areas of the billet respectively. The hoop stress, σ_θ, can then be expressed as a ratio to the fluid pressure as follows:

$$\frac{\sigma_\theta}{p_f} = \frac{2\frac{A_2}{A_1} - \frac{t}{r_o}(2 - t/r_o)}{t/r_o(2 - t/r_o)\ (1 - \frac{A_2}{A_1})} \quad , \tag{25}$$

where $t = r_o - r_i$ is the wall thickness of the ring. The hoop stress as predicted by this relation is plotted in Figure 60 as a function of percent reduction in area, $(1 - A_2/A_1) \times 100$ for a range of wall thickness. While these curves cannot be expected to give accurate quantitative results, they do show qualitative behavior which is consistent with the results of the computer stress calculations. For large reductions in area, the hoop stress is compressive even when the wall thickness is small and this results from the fact that the billet pressure on the die face very nearly balances the fluid pressure. For smaller reductions, the hoop stress is many times the fluid pressure even for a very thick-walled die.

The fact that high hoop stresses result from small reductions, is balanced by the fact that pressures for small reductions are relatively low. The pressure required for extrusion can be estimated as

$$P_f = Y_m \ln \frac{A_1}{A_2} \quad , \tag{26}$$

where Y_m is the mean yield strength of the metal. Equation (26) can then be rewritten as a ratio of σ_θ to the yield strength as follows:

$$\frac{\sigma_\theta}{Y_m} = \ln \frac{A_1}{A_2} \frac{2\frac{A_2}{A_1} - \frac{t}{r_o}(2 - t/r_o)}{t/r_o\ (2 - t/r_o)\ (1 - \frac{A_2}{A_1})} \quad . \tag{27}$$

This relation is plotted in Figure 61. It is seen that for small reductions in area, the die hoop stress approaches the metal yield strength for a very thick walled die. On the other hand, for a very large reduction the hoop stress can have compressive values much higher than the metal yield strength.

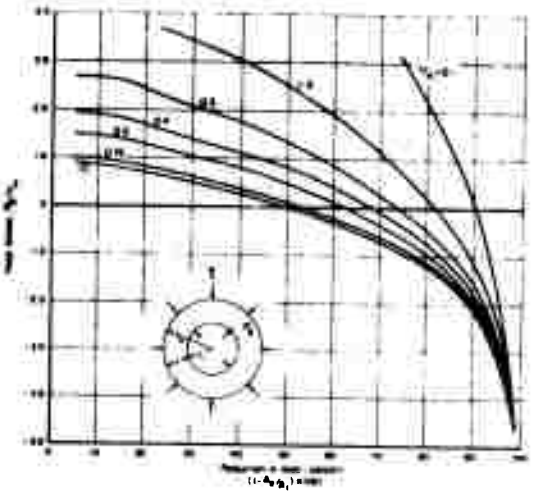

FIGURE 60. MAXIMUM CALCULATED HOOP STRESS IN RING DIE COMPARED TO BILLET YIELD STRENGTH AS A FUNCTION OF PERCENT REDUCTION IN AREA AND WALL THICKNESS

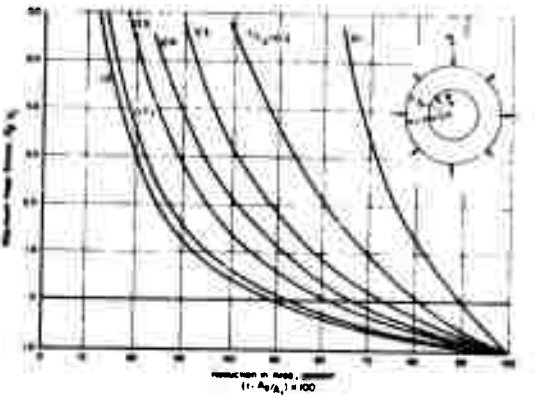

FIGURE 61. MAXIMUM CALCULATED HOOP STRESS IN RING DUE COMPARED TO FLUID PRESSURE AS A FUNCTION OF PERCENT REDUCTION IN AREA AND WALL THICKNESS

Summary

The purpose of this analysis was to calculate the stresses that exist in dies during hydrostatic extrusion and to relate them to die pressure capabilities and material strength requirements. The results show that die stresses are highly dependent on other factors in addition to the fluid extrusion pressure, such as, percent reduction in area, the extent of fluid support on the outside of the die, die wall thickness, and other complex geometric factors. Some of the important conclusions of this study are:

(1) Fluid pressure support can in many cases completely eliminate tensile hoop stresses during extrusion. It appears that this always will occur when the percent billet reduction in area is relatively large (say, greater than 70%).

(2) Excessive fluid support can in some cases result in very large compressive stresses, so that failure of the die material in shear can occur. In other cases, fluid pressure acting at the base of the die causes twisting of the cross section, and this produces large tensile stresses in the top portion of the die. The amount of fluid support should thus be controlled by positioning the die seal so that it is in line with the die orifice bearing surface.

(3) In cases of relatively large area reductions with the proper amount of fluid support, the limiting factor in die design will be the compressive stress which can be supported at the base of the die. This stress is always greater than the fluid pressure.

(4) For small area reductions (say, less than 50%) there will be a limitation on the maximum fluid pressure capability which is determined by the tensile hoop stresses in the die. This limitation can be made less severe by increasing the die wall thickness.

(5) While the analysis performed herein applies strictly only to dies with circular orifices, similar conclusions concerning the proper amount of fluid support would also be generally valid for other die orifices (such as tee sections).

ECONOMIC ANALYSIS OF HYDROSTATIC EXTRUSION

The purpose of this section is to evaluate the economics of the hydrostatic extrusion process and to relate the findings to more conventional processes. The hydrostatic extrusion process can manufacture certain products in competition with conventional extrusion, drawing, and shear forming. While combining many features of these conventional metalworking processes, hydrostatic extrusion does not completely displace any one process. Therefore, economic comparisons must be considered on the basis of making a particular product. The features of the hydrostatic extrusion process will be described and the basic assumptions of the economic analysis given. An economic analysis will then be made and applied to processing of conventional materials, refractory materials, difficult-to-extrude materials, and to the production of tubes and shapes.

Hydrostatic extrusion offers the following advantageous features:

(1) There is no contact between container and billet

(2) Long billets with high L/D ratios may be extruded

(3) Billets may be of any cross-sectional shape

(4) Long liner and die life

(5) Small die angles can be used because the hydrostatic fluid supports the dies

(6) Tungsten-carbide dies may be used for exceptionally long life

(7) Because of the low die wear, excellent dimensional control can be maintained over the length of the extruded product

(8) Hard-to-work or brittle materials may be hydrostatically extruded without cladding.

(9) Heavier reductions are possible relative to a conventional drawing operation

(10) Increased strength due to cold working.

The limiting features of the hydrostatic extrusion process are:

(1) Dimensions of the stem, liner, and die must be maintained within close tolerances to effect sealing

(2) The billets must be nosed to conform to the die angle so that a high-pressure seal can be established. This may be costly in the case of re-extrusion of shapes.

(3) Manipulation of seals and fluid could raise the processing costs.

(4) Hydrostatic extrusions have a cold-worked structure which may require annealing for some materials and applications.

(5) Smaller extrusion ratios are possible compared to the hot extrusion process.

As with most new processes, hydrostatic extrusion is subject to some unknowns, such as the life of seals and tooling (container, stem, and die), which have not been completely evaluated at this point. Thus, the analysis of hydrostatic extrusion is necessarily more uncertain than would be a similar economic analysis of conventional extrusion.

Using empirical equations[11] relating pressure and extrusion ratios for the hydrostatic extrusion of several materials, the following maximum extrusion ratios were calculated for fluid pressures of 250,000 psi and 450,000 psi:

Material	Estimated Extrusion Ratios for a Given Pressure	
	250,000 psi	450,000 psi
Beryllium (hot pressed)	7:1	40:1
TZM Molybdenum (recrystallized)	7:1	40:1
A-286 Iron Base Superalloy (hot worked and solution treated)	6:1	32:1
Inco 718 Nickel Base Superalloy (hot worked and solution annealed)	4:1	12:1
Ti-6Al-4V Titanium Alloy (mill annealed)	5:1	16:1
AISI 4340 Steel (mill annealed)	7:1	32:1
7075-0 Aluminum Alloy (annealed)	2100:1	--

These values are rounded-off to the nearest whole number and are meant only as guides. The extrusion ratios indicated for 450,000 psi were extrapolated from data obtained up to about 250,000 and therefore are very approximate. No limiting value is shown for aluminum at pressures of 450,000 psi, since the large reductions predicted may be neither very accurate nor practical.

In this economic study, it is assumed that both hydrostatic extrusion and conventional extrusion would be done on the same 17,000 ton press with appropriate changes in tooling. Most of the economic analyses were based on using a 250,000 psi container because many of the appropriate parameters have been established in experimental programs at this pressure level. Some general analysis of hydrostatic extrusion was performed to establish approximate conversion costs on the same press using fluid pressures of 450,000 psi.

Press and Average Conversion Costs

The cost of the basic hydrostatic extrusion press and a variation of the original design were determined using standard industrial techniques. The basic press will meet the design goals of this program and has been described in a previous section. The press variation referred to as a dual purpose press would have a ram stroke of 150 inches so as to be adaptable to conventional extrusion and could have either a ram speed of 100 ipm or 720 ipm, depending on the hydraulic pumping system selected.

Estimated press costs were obtained by determining the cost of: (1) engineering, (2) manufacturing press components and tools, and (3) commercial items which would be required to build the basic hydrostatic extrusion press. These figures were then modified to determine the cost of the design variations. The estimated costs of the basic hydrostatic extrusion press and the dual purpose press capable of extruding at 720 ipm are shown on Table XVIII.

These estimated costs for a press of 17,000 ton capacity can be used to obtain approximate costs for similar presses of different tonnages, by using the following factor:

$$\left(\frac{\text{Tonnage of Press A}}{\text{Tonnage of Press B}}\right)^{0.7}$$

The factor is applied to the known cost of one press to estimate the cost of another press. For example, a 14,000 ton basic hydrostatic extrusion press would cost approximately:

$$\left(\frac{14,000}{17,000}\right)^{0.7} = 0.8729$$

$$\$5,989,152 \times 0.8729 = \$5,228,000$$

This factor should only be used to compare presses with tonnage ratings within about 50 percent of the press for which the cost is known.

TABLE XVIII. SUMMARY OF THE COSTS TO CONSTRUCT A HYDROSTATIC EXTRUSION PRESS AND A DUAL PURPOSE PRESS OF 17,000-TON CAPACITY

Items[a]	Basic Hydrostatic Extrusion Press	Dual Purpose Press
Hydraulic Pumping System[b]	$1,090,600	$1,878,850
Press and Materials Handling System	3,672,602	3,965,102
Tooling (containers, stems, mandrel, etc.)	385,950	1,218,425
Cost at the Construction Site	$5,149,152	$7,062,377
Installation Costs	840,000	840,000
TOTAL COST	$5,989,152	$7,902,377

(a) These costs are a summary of a detailed cost breakdown made of all major press components. Standard commercial estimating techniques were employed to determine these values.

(b) The hydraulic pumping systems are designed to permit extrusion in the basic hydrostatic extrusion press at 100 ipm and in the dual purpose press at 720 ipm.

A 17,000 ton extrusion press cannot function efficiently without proper support equipment. The amount and size of the support equipment required by a 17,000 ton press makes it unlikely that this equipment would be available in an existing industrial plant. Therefore, in order to obtain a realistic estimate of conversion costs for both hydrostatic and conventional extrusion an entirely new extrusion plant was postulated as necessary and used in calculating conversion costs. The estimated extrusion plant costs for a hydrostatic extrusion press and a dual-purpose extrusion press are shown in Table XIX. The major differences between the two proposed plants are in the construction costs, press costs, and billet heating facilities.

Estimated conversion costs for both hydrostatic and conventional extrusion on a dual-purpose press are given in Table XX. For this dual-purpose plant, the cost per hydrostatic extrusion was calculated to be $46.29 and a corresponding value for conventional extrusion was found to be $77.50. Assuming the typical billet sizes shown in Table XX, it is seen that the volume of a conventional extrusion can be more than twice the volume of a hydrostatic extrusion. On this volume basis then, the conversion cost per cubic inch for hydrostatic extrusion ($0.00528) is 25 percent more than the comparable cost for conventional hot extrusion ($0.00417). Hydrostatic extrusions made in a plant designed exclusively for this operation would have a slightly lower conversion cost per cubic inch of extrusion ($0.00490). This lower cost would be due to the reduced capital outlay required to build a single purpose hydrostatic extrusion facility. Conversion costs for conventional extrusion would not appreciably change if the plant was designed soley for conventional extrusion. This is because, in this case, the only major reduction in capital expense would be in the cost of hydrostatic extrusion tooling and this cost amounts to less than 2 percent of the total plant cost.

There are many deviations from average cost values which can change the relative costs between the two processes. Further there are many commercial processes in which costs are related to the product dimensions or shape rather than the theoretical weight output of the process. Several of these cases will be illustrated and discussed in the following sections.

TABLE XIX. TOTAL ESTIMATED COST FOR AN EXTRUSION PLANT WITH A HYDROSTATIC EXTRUSION PRESS OR A DUAL-PURPOSE EXTRUSION PRESS OF 17,000-TONS CAPACITY

Items	Hydrostatic Extrusion Plant	Dual Purpose Plant
Land (40 acres)	$ 30,000	$ 40,000
Construction (land improvements, buildings, and cranes)	3,743,000	4,715,000
Equipment:		
Extrusion Press	5,989,000	7,902,000
Stretch-straightener (2500-ton capacity)	2,000,000	2,000,000
Billet heating furnaces	-	1,500,000
Heat treating furnaces	1,500,000	1,500,000
Materials handling (not related to the press)	758,000	880,000
Miscellaneous (accessory tooling, etc.)	350,000	350,000
Service equipment (maintenance, shipping, laboratories, etc.)	1,215,000	1,215,000
TOTAL PLANT COST	$15,585,000	$20,102,000

TABLE XX. ESTIMATED ANNUAL OPERATING COSTS FOR BOTH HYDROSTATIC EXTRUSION AND CONVENTIONAL EXTRUSION ON THE 17,000-TON DUAL PURPOSE PRESS[a]

	Hydrostatic Extrusion	Conventional Extrusion	Total Annual Costs for Both Operations
Personnel (85 salaried and 122 hourly employees)	$ 874,800	$ 901,800	$1,776,600
Maintenance (4% equipment + 2% buildings)	320,000	388,140	780,140
Depreciation (5% equipment + 2.5% buildings)	397,000	488,170	885,170
Miscellaneous supplies (20% direct labor)	82,000	82,000	164,000
Major tooling (containers and stems)	134,000	151,000	285,000
Liquid make-up and seals	62,500	-	62,000
Water	5,000	5,000	10,000
Electric power ($0.015/kwhr)	114,000	114,000	228,000
Building heat (141,000 sq ft)	24,750	24,750	49,500
Industrial heat (billet heating and heat treating)	300,000	1,720,000	2,020,000
TOTAL ANNUAL OPERATING COST	$2,314,050	$3,874,860	$6,188,910
Operating cost/hr	$1,157	$1,937	
Number of extrusions per year (71% efficiency)	50,000	50,000	
Cost per extrusion (without die and mandrel costs)	$46.20	$77.50	
Cost per extrusion (including a prorated die and mandrel cost)	$48.20	$85.27	
Typical billet size	11 in. OD x 96 in. long	20 in. OD x 65 in. long	
Typical billet volume	9123 $in.^3$	20,420 $in.^3$	
Conversion cost/$in.^3$ of extrusion	$0.00528	$0.00417	

(a) It was assumed that each process is used 2000 hr/yr.

Economic Analysis Applied to Various Materials

An analysis was made of the relative merits of the hydrostatic and conventional extrusion processes as applied to the extrusion of rounds and simple shapes from steel, aluminum, titanium, refractory metals, nickel alloys, and beryllium. This analysis was based upon the operating costs estimated for the dual-purpose extrusion press designed during this program. Only direct conversion costs were calculated. These conversion costs indicate how much it costs to process a particular metal through an extrusion operation. The cost figures shown in these sections should not be confused with selling prices which would also include material costs, profit, selling expenses, packing and shipping charges, corporate overhead, etc. Each of the conversion costs estimated here is subject to modifications reflecting expected process yields. The yield figures vary greatly depending on the alloys extruded, the shape of the extruded product, and tolerances. As a general guide, the process yield would be in the range of 70 to 90 percent and the calculated conversion costs should be adjusted proportionally.

AISI 4340 Steel

An analysis was made of the extrusion of AISI 4340 steel into relatively simple shapes by hydrostatic and conventional techniques. Steels are normally hot extruded in the temperature range from 2000 to 2300 F. In this temperature range, high extrusion ratios are possible, but both glass lubricants and high extrusion speeds must be employed to obtain reasonable tool life. Hydrostatic extrusion and conventional hot extrusion processing parameters for AISI 4340 steel can be compared from the data in Table XXI. These parameters assume that the 17,000-ton dual press developed in this study would be used for both types of extrusion. Using these parameters, the conventional hot-extrusion process can outproduce the hydrostatic extrusion process more than 2 to 1 on a weight basis. Further, the hot extrusion process can produce a product with a smaller cross-section than can the hydrostatic extrusion process except when a drawing force is applied to the product (HYDRAW).

One of the important factors which significantly influence conversion cost per pound, however, is die cost. Die life is relatively short in hot extrusion, especially in the production of shapes where the die can only be reworked a few times before it must be scrapped. Because die life can only be roughly estimated for each method, the conversion cost per pound was calculated over a probable die life range for each process to indicate the general trends.

TABLE XXI. CONDITIONS USED IN ECONOMIC COMPARISON OF CONVENTIONAL AND HYDROSTATIC EXTRUSION OF AISI-4340 STEELS

Item	Conventional Extrusion	Hydrostatic Extrusion
Billet:		
Diameter, in.	20[a]	11[c]
Length, in.	65[b]	96[c]
Weight, lb	5779	2580
Production rate, billet/hr	35	35
Potential output, lb/hr	202,260	90,300
Maximum practical extrusion ratio	50:1	7:1
Extrusion size:		
Minimum cross section, in.^{2}	6.24	17.35
Minimum diameter, in.	2.82	4.7
Maximum extrusion ratio practical with HYDRAW (100,000 psi draw stress)	-	17.9:1
Extrusion size with HYDRAW:		
Minimum cross section, in.^{2}	-	5.307
Minimum diameter, in.	-	2.59

(a) This billet diameter was based on an assumed pressure requirement of 110,000 psi developed by 17,000 tons of press force.

(b) This billet dimension represents the longest length that could be conventionally extruded on the dual-purpose press.

(c) It was assumed that these are the maximum billet dimensions for the 12-inch bore x 120 inches long hydrostatic extrusion container.

Hydrostatic Extrusion Die Costs. The die costs to produce a simple shape using the hydrostatic extrusion process were calculated in the following manner:

Starting Blank Size:	12-inch diameter x 9.8 inches long
Weight:	315 pounds
Die Material:	M-50

Material Cost:	$ 945
Machining Cost (relatively simple shape):	350
Scrap Value (15 percent original cost):	141
Net Die Cost:	$1154

The life of hydrostatic extrusion dies is expected to approximate the life of conventional cold extrusion dies, since the stress levels, reductions, and lubrication systems are similar for both processes. Cold extrusion dies may be used to make 50,000 to 100,000 pieces that may be 2 to 4 inches long. (A die life up to 1,000,000 pieces have been reported for carbide dies but these dies will not be considered in this study although there is no technical reason not to use carbide dies in a production operation.) On this basis and assuming each hydrostatic extrusion is 56 feet long (billet length, 8 ft x extrusion ratio, 7), a die life from 150 (50,000 pieces each, 2-inches long) to 600 (100,000 pieces each, 4 inches long) extrusions is predicted. As with conventional extrusion dies, however, these hydrostatic extrusion dies can be reworked, perhaps four times, to obtain a die life in the order of 2400 extrusions. To keep the economic comparison on a conservative basis, however, no die reworking was assumed and a die life range of 150 to 600 extrusions was used in this study.

Conventional Extrusion Die Costs. The die costs for the conventional hot extrusion process were calculated in a similar manner to those for hydrostatic extrusion:

Starting Blank Size:	20-inch diameter x 12-8/8 inches long
Weight:	1070 pounds
Die Material:	H-11

Material Cost:	$1070
Machining Cost (relatively simple shape):	500
Scrap Value (15 percent original cost)	160
Die Cost:	$1410
Rework 4 times at $150/rework:	600
Net Die Cost:	$2010

Hot extrusion dies have been reported to have a die life which may vary from 1 to 75 extrusions before the die must be reworked. The life depends on the die material, billet material, amount of reduction, and the shapes required. Despite the reported long die life, a die life of 25 extrusions per die before reworking is generally considered very good. Conversion costs were estimated for a total die life range of 40 to 100 extrusions, based on a die life range of 10 to 25 extrusions before reworking and upon reworking four times. Conversion costs were also calculated for a total die life of 25 and 150 extrusions to illustrate the cost trends in these ranges.

With these estimated net die costs, the billet weights shown in Table XXI, and the conversion cost data given in Table XX, Table XXII was constructed. This table shows the influence of die life on the conversion cost per extrusion and on the conversion cost per pound of extrusion, based on the assumptions used in this analysis. It is seen that if the die life of 40 extrusions is assumed for conventional extrusion, the cross-over point for roughly equal conversion costs per pound is a die life of 100 extrusions for hydrostatic extrusion. As pointed out earlier, hydrostatic extrusion die life is estimated to be in the range of 150 to 600. If this range would be achieved, the conversion costs per pound for hydrostatic extrusion would be less. However, if a conventional extrusion die life of 100 is obtained, the conventional extrusion process would be cheaper, regardless of the die life achieved in hydrostatic extrusion. However, it should be kept in mind that the two processes produce different quality products. Hydrostatic extrusion will produce a product having mechanical properties and surface finish comparable to a cold-drawn shape and have tolerances of the order of ±0.002 inch. The hot-extruded product, on the other hand, would be relatively soft and would have tolerance of the order of ±1/16 inch. To get a comparable surface finish, the hot-extruded product would have to be machined or cold drawn, both of which would add appreciably to the conversion cost.

In order to produce a hydrostatic extrusion equivalent in size to one obtainable from hot extrusion, the HYDRAW technique would have to be used. In this case, however, the extrusion length would be limited to the draw stroke of the pulling apparatus.

A calculation of conversion costs from the 450,000 psi liner illustrates that this container would be used only for very special products. A billet for the 450,000 psi chamber may measure up to 5 inches diameter x 24 inches long and would weigh 133 pounds, if made from steel. Roughly, the conversion costs for this billet would be:

$$\$46.29/\text{extrusion} \div 133\ \text{lb/extrusion} = \$0.347/\text{lb} \quad .$$

To this value must be added a die charge. Since this conversion cost is at least an order of magnitude greater than most conventional primary metalworking processes, it is apparent that this container and pressure level, while capable of making large reductions, will find use only in very special applications which cannot at this time be considered commercial items.

TABLE XXII. HYDROSTATIC AND CONVENTIONAL EXTRUSION COSTS FOR 4340 STEEL AS A FUNCTION OF DIE LIFE

Item	Hydrostatic Extrusion		Conventional Extrusion	
Cost Parameters				
Cost per die	$1154.00		$2010.00	
All other conversion costs per extrusion[a]	$46.29		$77.50	
Weight per extrusion[b]	2580 lb		5780 lb	
	Conversion Cost Per Extrusion	Conversion Cost per lb of Extrusion	Conversion Cost Per Extrusion	Conversion Cost per lb of Extrusion
Die Life (Total Number of Extrusions)				
25	-	-	$157.90	$0.0273
40	-	-	$127.75	$0.0221
100	$57.83	$0.0224	$97.60	$0.0168
150	$53.99	$0.0209	$90.90	$0.0157
600	$48.21	$0.0186	-	-
2400	$46.77	$0.0181	-	-

(a) From Table XX.

(b) From Table XXI.

The economic analysis of hydrostatic extrusion compared to conventional hot extrusion as developed in the foregoing can be applied, with only slight modifications, to a wide variety of materials as will be shown in subsequent sections.

Aluminum and Aluminum Alloys

Aluminum and aluminum alloys are generally considered to be easy to extrude. In conventional processing, these metals flow at relatively low pressures when heated between 650 and 950 F and are generally extruded without lubricants through flat-face dies. Aluminum and its alloys are also easy to hydrostatically extrude. These metals can be reduced by large amounts at room temperature using only modest fluid pressures, (100,000 to 150,000 psi). Hydrostatic extrusion and conventional extrusion will be compared on the basis of the conditions shown in Table XXIII.

The production output for conventional extrusion of aluminum and aluminum alloys are restricted by metallurgical factors. Aluminum and aluminum alloys are sensitive to the extrusion exit speeds. At high exit speeds, these materials tend to develop surface cracks due to incipient melting. Commercial-purity aluminum is extruded at exit speeds up to 50 fpm. Relatively soft alloys such as Al-Mn, Al-Si, and Al-Mg_2Si require that the exit speeds be limited to 30 fpm which 7075 aluminum alloy and other high-strength structural alloys exit the die at only 3 to 4 fpm.[60] Experimentally, Fiorentino, et al,[11] have demonstrated that 7075 aluminum alloy can be hydrostatically extruded at exit speeds of 250 fpm. Such a large spread in exit speed is a major difference between hydrostatic and conventional extrusion of this metal and its influence on process economics was examined in detail.

Production output measured in lb/hr was determined as a function of exit speeds for each process using the following formula:

$$\frac{\text{(Billet Weight, lb)} \times \text{(Exit Speed, fpm)} \times \text{(60 min/hr)}}{\text{(Billet Length, ft)} \times \text{(Extrusion Ratio)}} = \text{Extrusion Output, lb/hr.}$$

The extrusion outputs are summarized in Table XXIV for a variety of exit speeds. The hydrostatic extrusion process using exit speeds of 250 fpm, can outproduce the conventional extrusion process when the conventional extrusion exit speed is less than 30 fpm. The cross-over point is approximately 30 fpm; at higher exit speeds, conventional extrusion results in the higher production rates. If the exit speed for hydrostatic extrusion is assumed to be as high as 300 fpm, the theoretical extrusion output would be 34,080 lb/hr. However, the actual output is limited by the capacity of the materials handling system, which is about 35 billets/hr or 31,850 lb/hr.

TABLE XXIII. CONDITIONS USED IN ECONOMIC COMPARISON OF CONVENTIONAL AND HYDROSTATIC EXTRUSION OF ALUMINUM ALLOYS

Item	Conventional Extrusion	Hydrostatic Extrusion
Billet:		
Diameter, in.	32[a]	11[c]
Length, in.	65[b]	96 [c]
Weight, lb	5228	910
Maximum practical extrusion ratio	60	60
Extrusion size:		
Minimum cross section, in.^{2}	13.40	1.58
Minimum diameter, in.	4.13	1.42

(a) This billet dimension was based on using a 32-inch diameter liner. This liner size is practical only for relatively soft materials such as aluminum which can be extruded at relatively low unit pressures.

(b) This billet dimension represents the longest that could be conventionally extruded on the dual-purpose press.

(c) It was assumed that these are the maximum billet dimensions for the 12-inch bore x 120-inch long hydrostatic extrusion container. This billet diameter could be much larger in a container designed exclusively for aluminum.

TABLE XXIV. HYDROSTATIC AND CONVENTIONAL EXTRUSION COSTS FOR ALUMINUM AND ALUMINUM ALLOYS AS A FUNCTION OF EXTRUSION EXIT SPEEDS

Item	Hydrostatic Extrusion		Conventional Extrusion	
Press operating cost/hr	$1157[a]		$1937[a]	
Weight per extrusion, lb	910		5228	
	Extrusion Output lb/hr	Conversion Cost per lb of Extrusion	Extrusion Output lb/hr	Conversion Cost per lb of Extrusion
Extrusion Exit Speed, ft/min				
4	-	-	3,840	$0.504
30	-	-	28,800	$0.067
40	-	-	38,400	$0.0504
50	5,680	$0.2036	48,200	$0.0407
150	17,040	$0.0679		
200	22,740	$0.0509		
250	28,440	$0.0406		
300	31,850[b]	$0.0363		

(a) These operating costs were obtained from Table XIX.

(b) This is limit of output as restricted by maximum extrusion rate of 30 billets/hr for the proposed press. The theoretical output would be 34,080 lb/hr.

The conversion costs shown in Table XXIV were determined by dividing the hourly press operating cost for each process by the hourly extrusion output at each exit speed. Hourly operating costs shown in Table XIX were determined on the basis of a two-shift operation (2000 hr/yr/shift) with the press time divided equally between the two extrusion processes. An hourly press cost was then determined by dividing the total annual costs by 2000 hr/hr. Values of $1157/hr and $1937/hr were obtained for hydrostatic and conventional extrusion, respectively.

For the extrusion of aluminum and aluminum alloys the cost of dies were found to contribute little to the conversion cost. The low die cost is due to the fact that the life of a die used for aluminum is long; a die life of 2000 extrusions is quite common for these alloys. A die that cost $2100 would add $1.05 to the cost of each conventional extrusion, but on the basis of weight this additional cost amounts to less than $0.0002/lb. The hydrostatic extrusion billet is relatively small compared to the conventional extrusion billet; therefore, a higher die cost was calculated for the hydrostatic extrusion process. This die cost, based on a die cost of $1154 (same as that for steel), would add $0.0006/lb of extrusion. These die costs are considered negligible and are not included in the conversion costs shown in Table XXIV. From the tabulated data, it may be concluded that a hydrostatic extrusion operation using an exit speed of 250 fpm is cheaper than a conventional operation employing an extrusion speed of 40 fpm or less. For an exit speed of 300 fpm in hydrostatic extrusion the exit speed for conventional extrusion must exceed 50 fpm to be competitive.

It is also noteworthy to compare the two extrusion processes <u>for the production of an identical product</u>. For example, conventional extrusion is limited to a minimum extrusion cross-sectional area of 13.40 square inches (See Table XXIII.) for an extrusion ratio of 60:1. If the same product were made in the proposed hydrostatic extrusion tooling, the extrusion ratio would be only 7:1. From the previous formula, it is seen that the extrusion output is inversely proportional to extrusion ratio; thus, for an extrusion ratio of only 7:1 the theoretical extrusion output for hydrostatic extrusion could be increased by a factor 60/7 or 8.5. (This assumes an increase in ram speed to maintain a given exit speed at the lower extrusion ratio.) With this in mind, consider the case for hydrostatic extrusion at 50 fpm in Table XXIV. The extrusion output for this case is 5680 lb/hr. Theoretically, the output could be increased by 8.5 times to 48,300 lb/hr. However, as mentioned before, the maximum output for the proposed press is only 31,850 lb/hr. Even at this lower output, however, the production rate at 50 fpm (5680 lb/hr) would be increased almost 6 times and the corresponding conversion cost would be reduced by a similar factor to $0.0363/lb. Under these conditions, hydrostatic extrusion is the cheaper process even when limited to only 50 fpm, the maximum exit speeds attainable in conventional extrusion. Thus, for aluminum alloys it would appear that reducing the extrusion ratio is a very effective means of increasing output and reducing conversion cost.

In summary, it has been shown that aluminum and aluminum alloys can be processed at lower conversion costs by hydrostatic extrusion over a wide range of exit speeds.

Titanium and Titanium Alloys

Titanium and titanium alloys are conventionally hot extruded between 1850 and 1950 F using glass lubricants. Lubrication of titanium is a very critical parameter, since titanium will gall dies severely whenever the lubrication film fails. Care also must be taken not to embrittle the titanium with pickup of oxygen and hydrogen during heating to the extrusion temperature. Titanium can be hydrostatically extruded at room temperature. Room temperature processing minimizes embrittlement from gas pickup and facilitates good lubrication. Hydrostatic extrusion was compared to conventional hot extrusion using the parameters shown on Table XXV. The high yield strengths at room temperature of titanium metal and alloys restrict the practical extrusion ratio obtainable in hydrostatic extrusion to values 1/5 of those obtained in conventional hot extrusion. Both processes can make extrusions comparable in size only if the conventional process is limited to reductions of less than 16:1 and a draw-force is assumed to be applied to the hydrostatic extrusion.

Titanium metal and alloys are notorious for galling dies whenever the lubrication systems fail and the titanium contacts the die. This galling results in a very short die life. The lubrication systems developed for the hydrostatic extrusion of titanium generally prevent galling and thus the die life and costs can be assumed equivalent to those derived previously for the hydrostatic extrusion of steel. Hydrostatic extrusion conversion costs will be estimated using those die costs ($1154 per die).

In conventional extrusion the lubrication of hot titanium is a problem. Several commercial extrusion companies in the titanium industry have determined that using precision-cast dies for one to five extrusions, and then remelting the dies, results in the lowest die cost per extrusion. The dies are coated with a ceramic prior to each extrusion. This coating usually must be repaired or replaced after each run. Costs based on cast dies will be estimated for conventional titanium extrusion and the resultant conversion costs calculated.

Conventional Extrusion Cast-Die Costs. The cost of a cast die was determined by calculating the volume of a typical die and applying factors for the casting cost, machining cost and ceramic coating. These calculations are shown below:

Die Size: 20-inch OD x 12-7/8 inches long. The inside configuration of the die was assumed to be a 10-inch high cone having a 20-inch diameter base.

Die Weight: 774 pounds

Die Material: H-11

Material Cost: $387.00 (based on a finished casting cost of $0.50/lb)

TABLE XXV. CONDITIONS USED IN ECONOMIC COMPARISON OF CONVENTIONAL AND HYDROSTATIC EXTRUSION OF TITANIUM ALLOYS

	Conventional Extrusion	Hydrostatic Extrusion
Billet:		
Diameter, in.	20[a]	11[c]
Length, in.	65[b]	96[c]
Weight, lb	3267	1458
Production rate, billet/hr	35	35
Potential output, lb/hr	114,340	51,090
Maximum practical extrusion ratio	50:1	5:1
Extrusion Size:		
Minimum cross section, in.^{2}	6.24	19.
Minimum diameter, in.	2.82	4.92
Maximum extrusion ratio with HYDRAW (100,000 psi draw force)	-	10.
Extrusion size with HYDRAW		
Minimum cross section, in.^{2}	-	9.50
Minimum diameter, in.	-	3.47

(a) This billet diameter was based on an assumed pressure requirement of 110,000 psi developed by 17,000 tons of press force.

(b) This billet dimension represents the longest length that could be conventionally extruded on the dual-purpose press.

(c) It was assumed that these are the maximum billet dimensions for the 12-inch bore x 120 inches long hydrostatic extrusion container.

Machining Cost:	$100.00
Scrap Value (20 percent of the original cost)	$ 77.40
Ceramic Coating Cost per extrusion	$ 15.00
Net Die Cost	$424.60

The value of $0.50/lb for material cost represents the average selling cost of alloy castings. The machining costs represent the cost of finishing the cast dies and thus are much lower than the machining costs for wrought die. The scrap value for a casting is generally a higher percentage of the original cost than a similar value for wrought products. For this reason, the scrap value in this example was estimated at 20 percent rather than 15 percent of the initial cost. Coating and recoating the dies with a ceramic was estimated to cost $15.00 per application and it was assumed that this would have to be done prior to each extrusion.

The conversion costs which resulted from this analysis are shown on Table XXVI. Hydrostatic extrusion can produce titanium extrusions at a lower cost than conventional extrusion when relative die life is considered. As mentioned previously, cast dies are used only a few times before they are remelted. A die life of five extrusions for conventional titanium extrusion is exceptional and it is unlikely that a longer die life would be achieved. Longer die life was listed only for comparison with hydrostatic extrusion costs.

Titanium becomes embrittled when exposed to hydrogen and oxygen at elevated temperatures. Despite precautions to prevent contamination during heating, a layer of embrittled metal commonly forms on the surface of titanium extrusions. This layer must be removed either by pickling or machining. Either operation will add to the conventional processing costs shown in Table XXVI. No additional surface conditioning is required on titanium produced by hydrostatic extrusion.

Refractory Metals

Refractory metals are broken down at temperatures from 2000 F to 3000 F. These materials are hot extruded only on a limited basis, because of very short tool life. In the case of refractory materials, not only do dies wear out rapidly, but the extrusion liners also have a very short life.

TABLE XXVI. HYDROSTATIC AND CONVENTIONAL EXTRUSION COSTS FOR TITANIUM AS A FUNCTION OF DIE LIFE

Item	Hydrostatic Extrusion		Conventional Extrusion	
Cost Parameters				
Cost per die	$1154.00[a]		$424.60[b,c]	
All other conversion costs per extrusion[d]	$ 46.29		$ 77.50	
Weight per extrusion[e]	1458 lb		3267 lb	
Die Life (Total number of extrusions)	Conversion Cost per Extrusion	Conversion Cost per lb of Extrusion	Conversion Cost per Extrusion	Conversion Cost per lb of Extrusion
1	-	-	$502.10	$0.1537
2	-	-	$297.30	$0.0910
3	-	-	$229.03	$0.0701
4	-	-	$194.90	$0.0596
5	-	-	$172.42	$0.0528
10	-	-	$133.46	$0.0408
25	$92.45	$0.0634	$108.88	$0.0333
50	$69.37	$0.0476	-	-
100	$57.83	$0.0397	-	-
150	$53.98	$0.0370	-	-
200	$52.06	$0.0357	-	-
600	$48.21	$0.0331	-	-

(a) As previously described in section on AISI 4340 steel.

(b) Cost for a cast die derived in this section.

(c) $15.00 for a ceramic coating was added to the die cost for each extrusion after the first one.

(d) From Table XX.

(e) From Table XXV.

Since refractory metals can be hydrostatically extruded at room temperature, the life of hydrostatic tooling is not greatly influenced by the materials being extruded. TZM molybdenum alloys have been successfully hydrostatically extruded at room temperature. Special dies are required to produce a crack-free product at room temperature, but in all other aspects of behavior, this alloy is hydrostatically extruded much like steel. Consequently, the economic analysis of the hydrostatic extrusion of refractory metals was based on the die costs derived for steel.

The conventional extrusion processing costs must be modified to reflect the expected reduction in extrusion liner life. The conventional extrusion cost of $77.50 per extrusion contains a factor of $1.00 per extrusion for the cost of a liner. This cost was based on a $50,000 liner which had a life of 50,000 extrusions. The temperatures used to extrude refractory metals could easily reduce the life of a liner to 5000 extrusions and a life as short as 500 extrusions would not be unexpected. Based on the life of 5000 extrusions a net charge of $9.00 would have to be added to the cost of each extrusion. The cost of a conventional extrusion would then be $86.50 rather than $77.50.

Because of the short die life expected extruding refractory materials, a cast die would likely be used. The cost of a cast die would be the same as derived for titanium, $424.60. The hydrostatic and conventional conversion costs for TZM molybdenum alloy as a function of die life as shown in Table XXVII.

The conversion costs for each process are comparable at a die life of 4 for conventional processing and a die life of 25 for hydrostatic extrusion. If a conventional liner life of only 500 extrusions had been assumed, the conversion costs would be comparable at die lives of 10 and 25 extrusions for conventional and hydrostatic extrusions, respectively. The conversion costs per pound can be adapted to any refractory metal by applying the relative density factor compared to the density of molybdenum.

Nickel-Base Superalloys

The nickel-base superalloys are extruded at high speeds using glass lubricants much in the same manner as steel. Nickel alloys must be worked over a very narrow temperature range to prevent cracking. Despite billet heating techniques designed to produce temperature gradients which will prevent the tail end of the billet from chilling below the desired extrusion temperature, only relatively small short billets can be hot-extruded successfully. In contrast, hydrostatic extrusion can cold work long billets of these materials significant amounts. Cold working these alloys entirely eliminates the problems associated with billet heating.

TABLE XXVII. HYDROSTATIC AND CONVENTIONAL EXTRUSION COSTS FOR MOLYBDENUM AS A FUNCTION OF DIE LIFE

Item	Hydrostatic Extrusion	Conventional Extrusion
Cost Parameters		
Cost per die	$1154.00[a]	$424.60[b]
All other conversion costs per extrusion	$46.29[c]	$ 86.50[d]
Weight per extrusion[e]	3366 lb	7535 lb

Die Life (Total Number of Extrusions)	Conversion Cost per Extrusion	Conversion Cost per lb of Extrusion	Conversion Cost per Extrusion	Conversion Cost per lb of Extrusion
1	-	-	$511.10	$0.0678
2	-	-	$306.30	$0.0406
3	-	-	$238.03	$0.0316
4	-	-	$203.90	$0.0271
5	-	-	$183.42	$0.0243
10	-	-	$142.46	$0.0189
25	$92.45	$0.0275	$117.88	$0.0156
50	$69.37	$0.0206	-	-
100	$57.83	$0.0172	-	-
150	$53.98	$0.0160	-	-
200	$52.06	$0.0155	-	-
600	$48.21	$0.0143	-	-

(a) As previously determined in the section on AISI 4340 steel

(b) As previously determined in the section on titanium alloys.

(c) From Table XX.

(d) From Table XX as modified in this section to reflect a short liner life.

(e) Based on the billet dimensions shown on Table XXV and the density of molybdenum, 0.369 lb/in.^{3}

A close estimate of conversion costs as a function of die life for nickel-base superalloys is shown in Table XXII. While the calculations summarized in the table were formulated for steels, there are no significant differences between the two metals with respect to the economic analysis. The calculated conversion costs per pound of extrusions, however, would be about 5 percent less for nickel alloys than those shown in Table XXII for steel. This factor is simply determined on the basis of the relative density between the two metals (density of steel/density of a nickel-iron-chrome alloy = 0.943).

The same assumptions and restrictions stated for the two extrusion processes for steels are applicable to nickel alloys. Thus, for nickel-base alloys as in the case of steel, it was concluded that the hydrostatic extrusion process can in many cases produce a high quality extrusion at a lower cost than the conventional extrusion process.

Beryllium

Beryllium is normally clad in steel jackets to prevent cracking during extrusion at temperatures from 1800 to 1950 F. The cladding required to conventionally extrude beryllium prevents attaining precise dimensions on rod or tubes, makes exceptionally difficult the production of shapes having uniform close-tolerance dimensions, and increases the processing costs. The steel cladding does eliminate lubrication problems since only steel, and not beryllium surfaces need be lubricated. In other aspects, the hot extrusion behavior of clad beryllium is quite similar to that of steel.

Hydrostatic extrusion techniques have been used to extrude crack-free beryllium rods at room temperature without cladding.[11] Reductions up to 7:1 are theoretically possible with hydrostatic fluid pressures of 250,000 psi. Special dies are required to produce crack-free beryllium using unclad billets but this is the major item in which the hydrostatic extrusion of beryllium differs from that of steel.

Clearly, the results of the economic analysis for steel is generally applicable to beryllium for both processes. The cost per extrusion remains the same for both materials but the conversion cost per pound of beryllium will be 4.2 times that for steel shown on Table XXII. This factor represents the relative densities between beryllium and steel. The effect of using cast dies on the conventional processing costs of beryllium can be shown by applying a titanium/beryllium density factor (2.40) to the conversion cost shown in Table XXVI.

The results of these analyses illustrate that the magnitude of conversion costs reflect changes caused by the processing of various materials, but the relative merits between hydrostatic extrusion and conventional extrusion are consistent over a wide range of extrusion conditions.

Economic Analysis Applied to the Production of Tubing and Thin-Section Shapes

Hydrostatic extrusion techniques may be used to produce long parts with very accurate dimensions. This ability could be applied to the production of items such as gear blanks. An extrusion would be made with the desired tooth form around the circumference and gears sliced off the extrusion. By proper die design, spiral gears could be produced. Helixes for twist drills could be produced in much the same manner. These applications, while feasible, tend to be quite specialized; therefore hydrostatic extrusion processing costs were determined only for the production of parts having broader applications. The capacity of the hydrostatic extrusion process was analyzed with respect to manufacturing large diameter tubes and moderately complex shapes and comparison made to conventional production techniques.

Production of Large-Diameter Thin-Walled Tubing

Hydrostatic extrusion techniques have been used successfully to produce thin-wall tubes. The analysis of hydrostatic extrusion of tubes as compared to the conventional process is generally similar to that made for 4340 steel, in that, hydrostatic techniques could produce a cheaper high-quality product when the longer tooling life possible with hydrostatic extrusion is considered. Conventional tube extrusions, however, are limited by available press capacity to a wall thickness-to-diameter ratio of approximately 0.03 for aluminum and 0.05 for steel or titanium and tubes of these sizes are often made by a combination of hot extrusion followed by either hot or cold drawing.

The costs of making thin-wall large-diameter tubes 10-inch OD x 1/2 wall and 10-inch OD x 0.1-inch wall will be determined for the hydrostatic extrusion process and compared to the cost of conventional processing. These tube dimensions were selected to represent in the first case, the limit of conventional extrusion capability and the second case, to represent a part that could not be made by conventional extrusion techniques, but would have to be made by shear forming.

The selling costs for aerospace parts made from 7075 Al, Ti-6Al-4V, and 4130 have been reported by Evans, Strohecker, Olofson, and Clark[62]. This reference is a source of cost information for both machining and forming operations and will be used several times in this report. The authors claim the cost information to be accurate within ±20 percent of the actual price.

In the following sections, the cost of producing 10-inch OD x 1/2-inch wall tubes from various materials was calculated and compared to the selling price of similar tubes produced by conventional processing. Next, a cost for shear forming tubes 10-inch OD x 0.1-inch wall was determined and compared to processing cost for identical parts made by a hydrostatic extrusion.

Hydrostatic Extrusion Costs for Producing 10-inch OD x 1/2-inch-Wall Tubes

The cost for producing hydrostatic extruded tubes, 10-inch OD x 1/2-inch wall tubes were determined using the following parameters and tooling costs:

Extrusion Conditions:

Billet dimensions:	11-inch OD x 1-inch wall x 8 feet long
Extrusion ratio:	2:11:1
Extrusion dimensions: (allows 5 percent loss)	10-inch OD x 1/2-inch wall x 16 feet long

Die Costs:

Die blank size	12-inch diameter x 4 inches long
Die blank weight	128 lb
Die material:	AISI-M-50
Material cost:	$384
Machining cost:	225
Scrap allowance (15 percent material cost):	57
Net die cost:	$552
Expected die life: 150 extrusions (minimum)	
Die cost per extrusion	$3.68

Mandrel Cost:

Mandrel blank size	9-inch OD x 120 inches long
Mandrel blank weight:	2160 lb
Mandrel material:	AISI-D7
Material cost:	$2160
Machining cost:	$2245
Scrap allowance (15 percent material cost)	$ 324
Net mandrel cost:	$4081
Expected mandrel life:	100 extrusions
Mandrel cost per extrusion:	$4.08

Total Conversion Costs:

Die cost per extrusion	$ 3.68
Mandrel cost per extrusion:	$ 4.08
All other costs per extrusion:	$46.29
TOTAL COST PER EXTRUSION:	$54.05

In order to determine the manufacturing costs for these tubes, the starting material costs must be considered. The material costs for tubes measuring 11-inch OD x 1-inch wall are:

7075 Al:	\$87.83/ft
4340 steel:	\$23.80/ft
Ti-6Al-4V:	\$296/ft

The manufacturing cost to produce tubes were determined as follows:

$$\frac{\text{Starting Materials Cost + Conversion Costs}}{\text{Length of Material Produced}} = \$/\text{ft} \quad .$$

For example, for 4340 steel:

$$\frac{(\$23.80/\text{ft})(8\ \text{ft}) + \$54.05}{16\ \text{feet}} = \$15.28/\text{ft} \quad .$$

These manufacturing costs of hydrostatically extruding the tubes are shown on Table XXVIII with selling price of the same tubes produced commercially.

The manufacturing cost for hydrostatic extrusion of these tubes allow price markups from 59 to 112 percent, based on the selling price of commercial tubes. These percentages for markups are generally considered ample in many industrial operations and especially in the metals processing industry. These data indicate that hydrostatic extrusion techniques may be able to produce close-tolerance, large-diameter tubes at costs perhaps significantly below those by conventional processing methods.

Hydrostatic extrusion techniques can produce large diameter seamless tubing which have very thin walls which cannot be produced by conventional tube making techniques. Ratios of wall thickness to diameter of 0.01 are considered practical using hydrostatic extrusion techniques. An example of this product would be a tube 10 inches OD x 0.100 inch wall x 60 inches long. The only other common technique that could make this size tube would be shear-forming. The conversion cost of shear forming a tube of these dimensions will be determined and then compared to making the same tube by hydrostatic extrusion.

TABLE XXVIII. SELLING PRICE OF COMMERCIALLY PRODUCED 10-INCH OD BY 1/2-INCH-WALL TUBES AND THE MANUFACTURING COST OF A SIMILAR TUBE PRODUCED BY HYDROSTATIC EXTRUSION TECHNIQUES

Material	Selling Price of Commerically Produced Tubes	Manufacturing Costs of Hydrostatically Extruded Tubes	Potential Markups Using Hydrostatic Extrusion Techniques
7075 Al	$ 75.00/ft	$ 47.29/ft	67%
4340 steel[a]	$ 26.47/ft	$ 15.28/ft	59%
Ti-6Al-4V titanium alloy	$321.00/ft	$151.38/ft	112%

(a) Price for this steel was assumed to be equivalent to that for 4130 steel which was evaluated by Evans.[62]

Shear-Forming Costs for Producing
10-Inch OD x 0.1-Inch Wall Tubes

Shear-forming costs were estimated from cost equations derived by Evans, et al.[62] Equations were derived for shear-forming which separate the material costs, tooling costs, material preparation costs and forming costs. The material costs per pound would be the same for both shear-forming and hydrostatic extrusion. The tooling costs for shear-forming are insignificant for quantities in excess of 1000 pieces. Thus, only the equations dealing with material preparation and forming costs were evaluated. Each of these equations will be described and evaluated for production of a tube 10-inch OD x 0.1-inch wall x 60 inches long.

Material Preparation Costs. Material preparation consists of machining the blank to obtain a good surface finish. These costs were evaluated from the following formula:

$$C_p = (0.00353\ D\ G\ T)\ L_2$$

where,

C_p = processing costs in collars

D = tube OD, in.

H = tube length, in.

Y = machinability factor

= 0.333 for 7075 aluminum alloy

= 4.54 for Ti-6Al-4V titanium alloy

= 2.22 for AISI 4340 steel

L_2 = labor rate, $15.00/hr.

Forming Cost. The actual cost to shear form a tube was determined from the following formula:

$$C_f = 0.093\ D\ H\ X\ L_2\ q + 0.00314\ D\ t\ e\ H\ L_1$$

where,

C_f = forming costs in dollars

X = forming factors

= 1 for mild steel

= 1.25 for aluminum and low alloy steel

= 4.0 for titanium

q = learning curve factor 0.3499

t = wall thickness, inch

e = material density

L_1 = labor rate, $12.00/hr

All other terms are as previously defined.

The preceding equations were evaluated for producing tubes 10-inch OD x 0.1-inch wall x 60 inches long from Ti-6Al-4V titanium alloy, AISI 4340 steel, and 7075 aluminum alloy. The results of the individual equations and the sum of the equations which equals the total conversion cost are shown in Table XXIX.

Hydrostatic Extrusion Costs for Producing 10-Inch OD by 0.1-Inch Wall Tubes

The hydrostatic extrusion processing costs of producing 10-inch OD x 0.1-inch wall tubes were estimated from the following parameters and tooling costs:

Extrusion Conditions

Billet dimensions:	10.75-inch OD x 9.80-inch ID x 8 feet long
Extrusion ratio:	5:1
Extrusion dimensions: (allows 5 percent loss)	10-inch OD x 0.1-inch wall x 38 feet long

Die Costs

Die blank size:	12-inch diameter x 4 inches long
Die blank weight:	128 lb
Die material:	AISI-M-50

Material cost:	$384
Machining cost:	225
Scrap allowance (15 percent material cost)	57
Net die cost	$552
Expected die life: 150 extrusions (minimum)	
Die cost per extrusion	$3.68

Mandrel Cost

Mandrel blank size:	9.8-inch OD x 120 inches long
Mandrel blank weight:	2560 lb
Mandrel material:	AISI-D7

Material cost:	$2560
Machining cost:	$2664
Scrap allowance (15 percent material cost)	$ 384
Net mandrel cost:	$4838
Expected mandrel life: 1000 extrusions	
Mandrel cost per extrusion	$4.84

TABLE XXIX. COSTS FOR CONVERTING VARIOUS MATERIALS TO 10-INCH OD X 0.1-INCH WALL X 60-INCH LONG TUBES BY SHEAR-FORMING AND BY HYDROSTATIC EXTRUSION[a]

Operation	Material		
	Ti-6Al-4V	4340 Steel	7075 Al
Shear-Forming Cost			
Materials preparation[a]	$ 144.00	$ 70.50	$ 10.50
Forming[b]	1172.00	367.00	366.00
Total conversion cost/pc	$1316.00	$437.50	$376.50
Hydrostatic Extrusion Cost			
Material preparation[b]	$1154.00	$564.00	$ 85.00
Extrusion	54.81	54.81	54.81
Total conversion cost[c]	$1208.81	$618.81	$139.81
Total conversion cost/pc	$ 172.68	$ 88.40	$ 19.97
Conversion Cost Reduction/pc by Hydrostatic Extrusion	87%	80%	95%

(a) The cross-section of the starting material for both processes measured 10.75 OD x 9.8 ID.

(b) These costs were calculated from equations developed by Evans.[62]

(c) In hydrostatic extrusion 7 lengths of tube each 60 inches long are produced in one operation.

Total Conversion Cost

Die cost per extrusion:	$ 3.68
Mandrel cost per extrusion:	4.84
All other costs per extrusion:	46.29
TOTAL COST PER EXTRUSION:	$54.81

Hydrostatic extrusion conversion costs per 60-inch long tube would be:

$$\$54.81 \div 7 \text{ pc} = \$7.63/\text{tube}.$$

One hydrostatic extrusion would make 38 feet or seven tubes each 5 feet long.

To obtain the desired extruded tolerances it may be necessary to machine the starting hydrostatic extrusion tube billet all over, much like the shear-forming billet. The starting length of a hydrostatic extrusion billet was assumed to be 8 times that of a shear-forming blank and therefore the machining cost was estimated at eight times that for shear-forming. Adding this material preparation factor to the hydrostatic extrusion conversion costs, the total conversion costs for various materials were calculated and are shown in Table XXIX.

Hydrostatic extrusion techniques are shown to be potentially capable of producing large-diameter, thin-wall tubing at 80 to 95 percent less than cost of similar parts produced by shear-forming.

Production of Large Thin Sections of a Moderately Complex Shape

There are requirements in the aerospace industry for thin-section extrusions of large circumscribed sizes. These sections are currently produced by hot extruding relatively thick sections and then machining all surfaces of the parts. The technical feasibility of drawing some shapes to size using draw benches has been demonstrated elsewhere on various developmental programs, but this operation apparently is not economically justifiable at the present time. The hydrostatic extrusion process could use hot-extruded sections as preformed billets and hydrostatically extrude the preform to produce a finished thin-section part. This technique will be evaluated and compared to a machining operation.

There are infinite combinations of shapes and sizes that could be compared; therefore, an arbitrary size, shape, and material was selected as a typical aerospace part. The part selected was a channel section of Ti-6Al-4V titanium alloy, circumscribed by a 9-inch circle and assumed to measure 8 inches across the flat, have legs each 4 inches long, a total length of 30 feet, and have a uniform section thickness of either 1/4-inch or 1/8-inch. Conventional extrusion techniques can produce such a shape which could have a section thickness from a minimum size of 3/8 inch up to 1-1/2-inches. The minimum section thickness of 3/8-inch is a function of the billet size needed to extrude a shape circumscribed by a 9-inch circle and is not an absolute minimum for titanium alloys.

The processes that will be compared are:

(a) Conventionally hot extrude to a thick cross section; straighten; machine lightly all over, and hydrostatically extrude 4:1 to size (either 1/4 or 1/8-inch thick).

(b) Conventionally hot extrude to the minimum section thickness (3/8 inch); straighten; and machine to finish cross section (1/4- or 1/8-inch thick).

Costs for Hydrostatic Extrusion of Ti-6Al-4V Channels

An extrusion ratio of 4:1 was used for hydrostatic extrusion of Ti-6Al-4V titanium alloy in this analysis although a 5:1 extrusion ratio is theoretically possible. The reduced extrusion ratio will allow for a shape factor which tends to increase the extrusion forces for given extrusion ratio. The manufacturing costs of this channel would be:

$$\frac{\left[\begin{array}{c}\text{Starting}\\\text{Material}\\\text{Costs}\end{array}\right] + \left[\begin{array}{c}\text{Straightening}\\\text{Costs}\end{array}\right] + \left[\begin{array}{c}\text{Machining}\\\text{Costs}\end{array}\right] + \left[\begin{array}{c}\text{Hydrostatic}\\\text{Extrusion}\\\text{Costs}\end{array}\right]}{\text{Extruded Length}} = \text{Cost/ft} \quad .$$

These costs were estimated as follows:

(a) Starting material cost

Base cost: \$6.60/lb in an extruded shape

	Finish Section 1/4 in.	Finish Section 1/8 in.
Starting material section thickness, in.	1-1/8	5/8
Starting material cost, \$/ft	34.56	19.20
Starting billet weight per 8 feet, lb	276.40	153.00
Starting billet cost	\$1824.77	\$1013.76

(b) Straightening costs

It was assumed that: (1) straightening is done immediately after extrusion on a 35-ft stretch-straightener, (2) it requires 5 minutes of machine time, and (3) the labor required would be two helpers each at \$12/hr and one operator at \$15/hr. Straightening cost per starting billet would then cost:

$$\frac{(2)\ (\$12.00) + (1)\ (\$15.00)}{4 \text{ billets per operation}} \times \frac{5 \text{ min/hr}}{60 \text{ min}} = \$0.81 \quad .$$

(c) Machining Costs

Machining costs were estimated from the following formula developed by Evans[62] for milling costs:

$$C = 0.0166 Z_m\, Y(w,l,t) + 0.5755\, n L_2 Q^{-0.152}$$

where:

0.0166 = a conversion factor between minutes and hours

w,l,t = width, length, and thickness of cut (equivalent to volume removed)

Z_m = reciprocal metal removal rate for B 1112 steel, 0.831 min/in.^{3}

Y = machinability factor for Ti-6Al-4V 4.54

0.5755 = allowance for nonproductive time and inspection

L_2 = labor rate assumed to be \$15/hour

Q = quantity

n = number of operations.

Application of the preceding formula to remove 1/16 inch all over the hydrostatic extrusion blank results in a machining cost of $88.63.

(d) Hydrostatic Extrusion Conversions Cost

The hydrostatic extrusion conversion costs were calculated as follows:

Die Cost

Die blank size:	12-inch diameter x 1-1/2 inches long
Die blank weight:	48 pounds
Die material:	AISI-M50

Material costs:	$143.90
Machining costs:	375.00
Scrap allowance (15 percent material cost):	21.58
Net die cost:	$497.31

Expected die life: 150 extrusions (minimum)

Die cost per extrusion:	$3.31

Total hydrostatic extrusion conversion costs:

Die cost per extrusion:	$ 3.31
All other costs per extrusion: (as shown in Table XX)	$46.29
Net cost:	$49.60

Costs for Conventional Processing of Ti-6Al-4V Channels

The conventional hot extrusion process can produce a section thickness as thin as 3/8-inch. This section would have to be straightened, and machined all over to the final size. The manufacturing costs would be:

$$\frac{\begin{bmatrix}\text{Starting}\\\text{Material}\\\text{Costs}\end{bmatrix} + \begin{bmatrix}\text{Straightening}\\\text{Costs}\end{bmatrix} + \begin{bmatrix}\text{Machining}\\\text{Costs}\end{bmatrix}}{\text{(Extruded Length)}} = \text{Cost/ft} \quad .$$

These costs were estimated as follows:

Starting material cost:

Base cost: $6.60/lb in an extruded shape:

Starting material section thickness, in.	3/8
Starting extruded weight, lb/ft	11.5
Starting extruded weight per 30 feet, lb	345.6
Starting extrusion cost:	$2277.00

Straightening costs:

It was assumed that: (1) the straightening is done on a 35-foot stretch-straightener, (2) it requires 5 minutes, and (3) the labor required would be two helpers each at $12/hr and one operator at $15/hr. Straightening cost per 30 foot section would then cost:

$$\frac{(2)\ (\$12.00) + (1)\ (\$15.00)}{1 \text{ extrusion}} \quad \frac{5 \text{ min/hr}}{60 \text{ min}} = \$3.25$$

Machining costs:

Costs were determined to machine section thickness of 1/4 and 1/8-inch from a 3/8-inch extrusion using the same equation applied to the hydrostatic extrusion billet. These costs were found to be:

	Finish Section Size	
	1/4	1/8
Machining costs:	$332.39	$670.15

Summarizing and adding the processing costs in Table XXX illustrate that hydrostatic extrusion techniques can produce this channel from 40 to 75 percent cheaper than the conventional processing. This analysis should be a typical comparison between the two processes, since neither process was unduly restricted.

Summary of the Economic Analysis

Based on the assumptions stated in the preceding analysis, it may be concluded that hydrostatic extrusion techniques can economically produce close-tolerances, high quality products from a variety of materials. Examples of these products and potential cost savings are as follows:

TABLE XXX. PROCESSING COSTS OF Ti-6Al-4V TITANIUM ALLOY CHANNELS PRODUCED BY HYDROSTATIC EXTRUSION TECHNIQUES AND CHANNELS MACHINED FROM HOT EXTRUSIONS

Operation	Finish Section Size 1/4-inch	1/8 inch
Hydrostatic Extrusion Costs		
Starting material (8 ft billets)	$1824.77	$1013.76
Straightening	0.81	0.81
Machining	88.63	88.63
Hydrostatic extrusion conversion	49.60	49.60
Total conversion cost	$1963.81	$1152.80
Cost per foot	$ 65.46	$ 38.43
Cost per pound	$ 8.52	$ 10.00
Conventional Processing Cost		
Starting material (30 ft extrusions)	$2277.00	$2277.00
Straightening	3.25	3.25
Machining	332.39	670.15
Total conversion cost	$2612.64	$2943.40
Cost per foot	$ 87.09	$ 98.11
Cost per pound	$ 11.34	$ 25.55
Cost Savings per pound by Hydrostatic Extrusion	25%	60%

(a) Thin-wall, large-diameter tubes (10-inch OD x 0.1 inch wall) could be made from aluminum, steel, and titanium at a respective potential savings of 95, 80, and 87 percent, compared to tubes produced by shear forming.

(b) Large-diameter tubes (10-inch OD x 0.5-inch wall) could be produced from aluminum, steel, and titanium at a cost that would allow potential markups of 67, 59, and 112 percent, respectively. These markups were based on the market selling price of tubes made by conventional hot extrusion followed by conventional tube drawing. These markups are believed to be appreciable for the metal-working industry and indicate that perhaps a potentially significant cost saving may be possible by hydrostatic extrusion.

(c) Titanium hot extruded channel shapes may be re-extruded into finished channel shapes by hydrostatic extrusion techniques 25 to 60 percent cheaper than hot-extrusion and machining techniques currently employed.

(d) Simple shapes of steel, titanium, molybdenum, nickel-based alloys, and beryllium may be produced at a lower cost by hydrostatic extrusion when the long die life achievable in hydrostatic extrusion is related to that obtained in the conventional extrusion operation. Die life in hydrostatic extrusion is predicted to be 10 to 30 times greater than that in the conventional process.

(e) Aluminum alloys can be hydrostatically extruded at a lower cost than conventional processing, independent of relative die life, because of the high extrusion exit speeds obtainable in the hydrostatic extrusion processing of these materials.

APPENDIX I

ESTIMATED TIMETABLE AND MILESTONE CHART FOR CONSTRUCTION OF A DUAL PURPOSE (HYDROSTATIC/CONVENTIONAL) EXTRUSION PRESS

BLANK PAGE

ESTIMATED TIMETABLE AND MILESTONE CHART FOR CONSTRUCTION
OF A DUAL PURPOSE (HYDROSTATIC/CONVENTIONAL) EXTRUSION PRESS

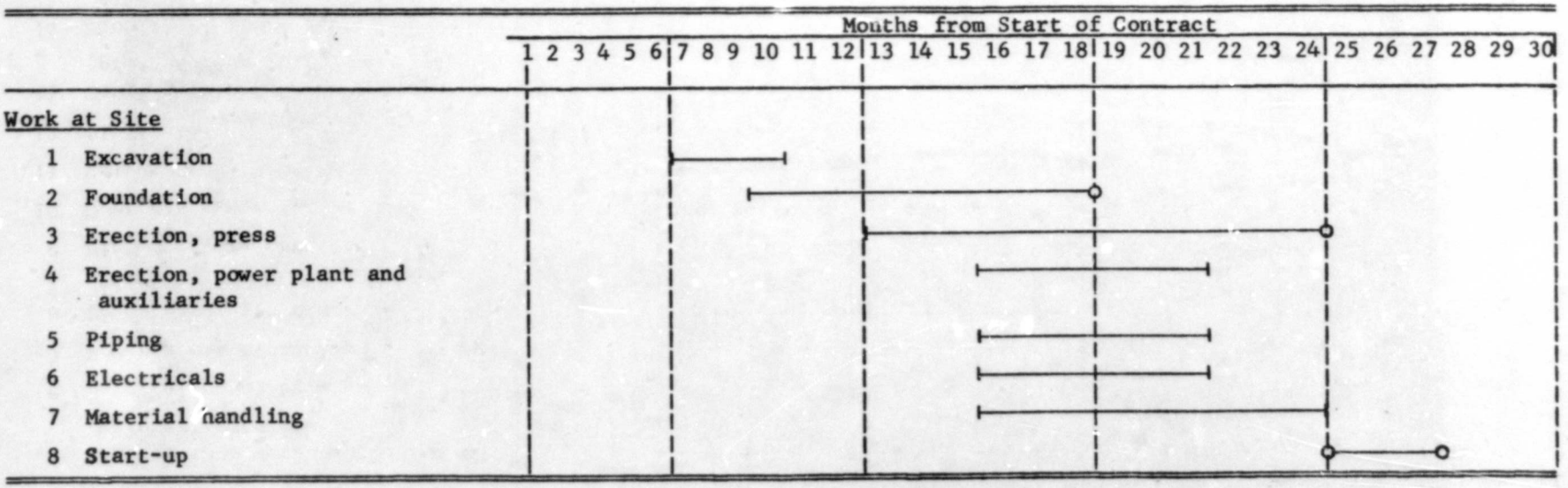

o Milestones

ESTIMATED TIMETABLE AND MILESTONE CHART FOR CONSTRUCTION OF A DUAL PURPOSE (HYDROSTATIC/CONVENTIONAL) EXTRUSION PRESS

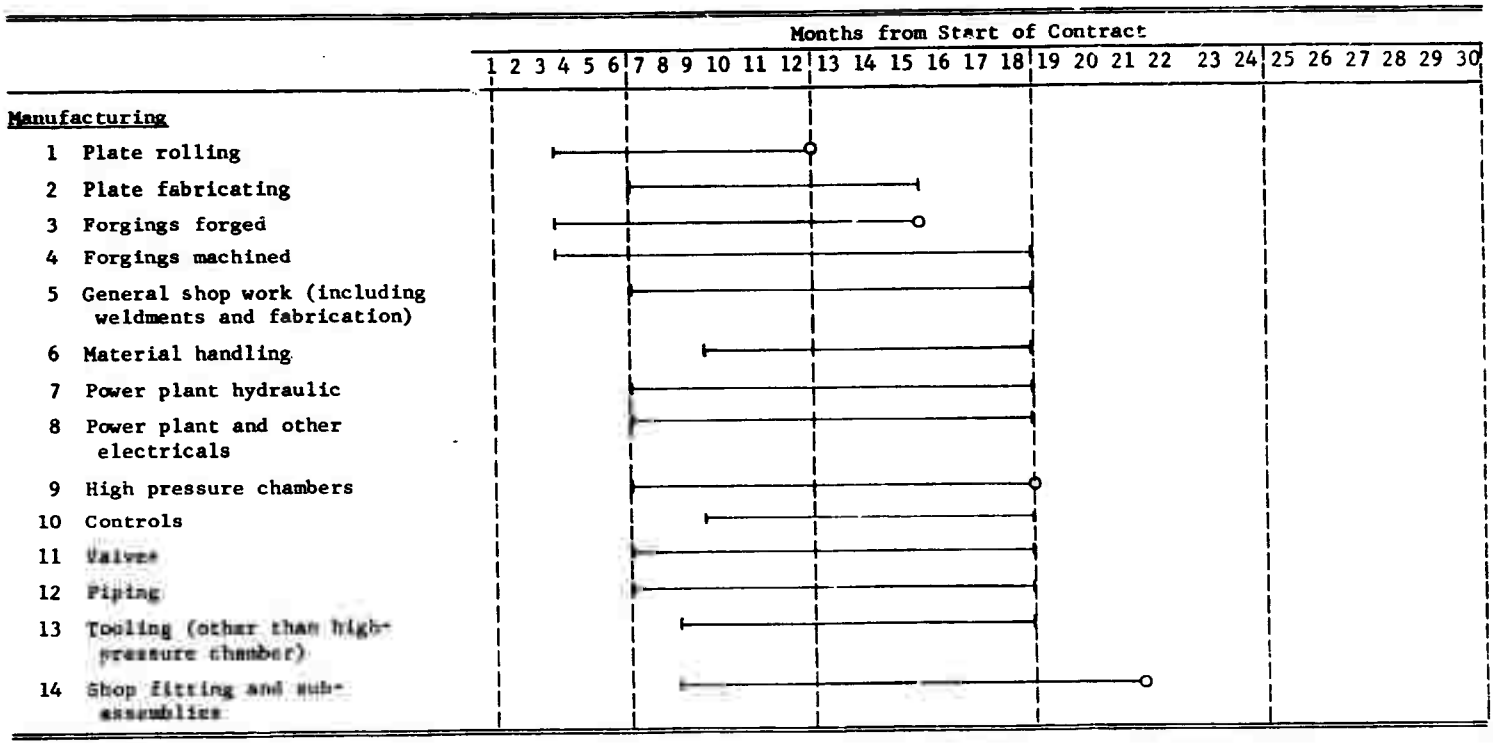

o Milestones

ESTIMATED TIMETABLE AND MILESTONE CHART FOR CONSTRUCTION
OF A DUAL PURPOSE (HYDROSTATIC/CONVENTIONAL) EXTRUSION PRESS

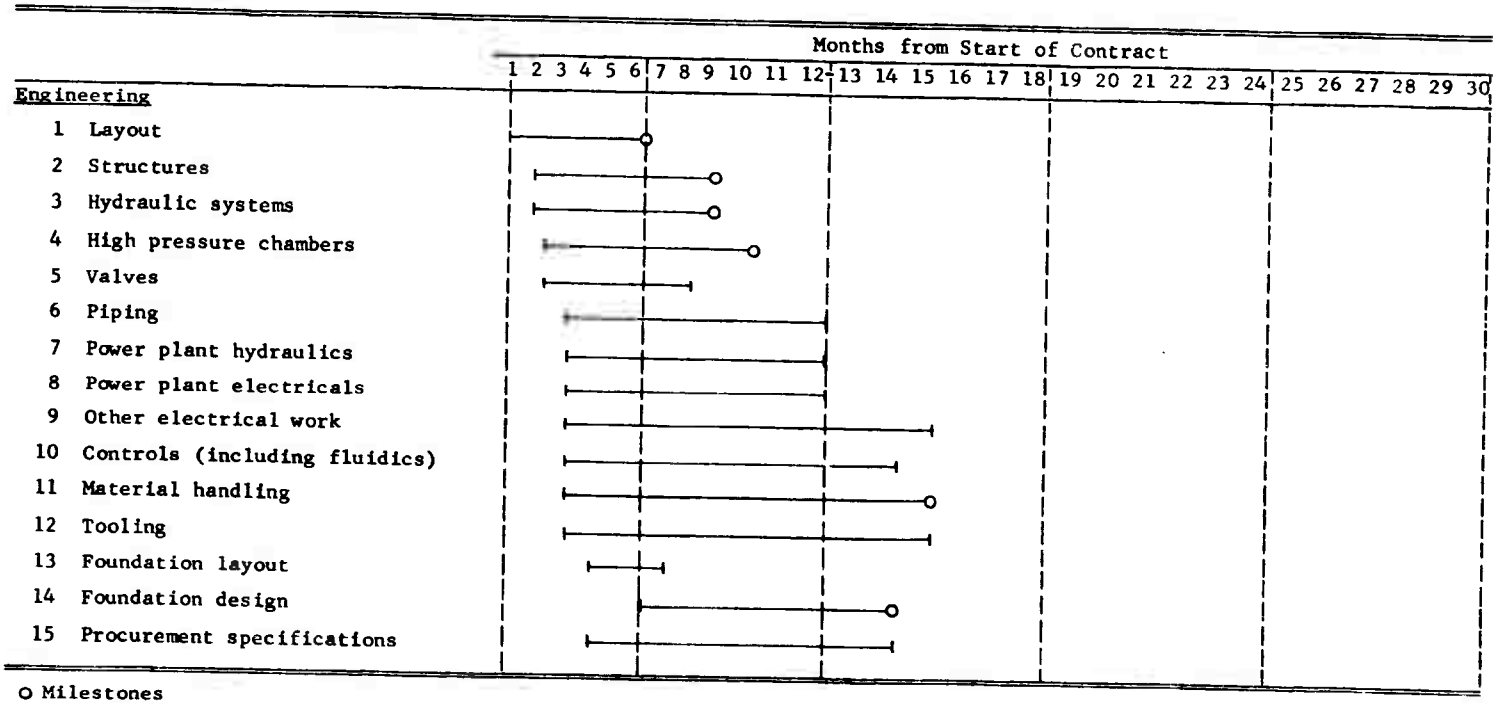

o Milestones

Milestone Points

Months	Engineering	Manufacturing	Work at Site
6	Layout completed	-	-
9	Structural portion	-	-
12	Plate rolled	-	-
15	Material handling completed Foundation design completed	Forgings forged	-
18	-	High pressure container finished	Foundation completed
21	-	All fittings completed	-
24	-	-	Press erection completed. All work completed Press start-up
27	-	-	Test runs completed

REFERENCES

(1) Bridgman, P. W., Studies in Large Plastic Flow and Fracture, McGraw Hill, London and New York (1952)

(2) Beresnev, B. I., Vereshchagin, L. R., and Ryabinin, Yu. N., "Characteristics of Rheological Behavior of Metals Extruded Under Hydrostatic Pressure", Izv. Akad. Nauk. SSSR; Otdel, Tech. Nauk., 5, 48 (1957).

(3) Beresnev, B. I., Vereschagin, L. F., and Ryabinin, Yu. N., "Extrusion of Metals by Means of a Liquid Under High Pressure", Izv. Akad. Nauk, SSSR; Mekh i. Mashin, 7, 128 (1959).

(4) Beresnev, B. I., Bulychev, D. K., and Rodionov, K. P., "Features of the Process of Extruding Metals With High Pressure Liquid at Elevated Temperatures", Fiz. Metal Metalloved, 11 (1), 115 (1961).

(5) Pugh, H. Ll. D., and Ashcroft, K., "Hydrostatic (Ramless) Extrusion of Metals by Liquid Pressure", Symposium on the Physics and Chemistry of High Pressure, London Society of Chemical Industries, 163-176 (1962).

(6) Pugh, H. Ll. D., "The Cold Extrusion of Metals by a High-Pressure Liquid", Int. Conf. on Prod. Eng. Res. Pittsburgh, Published by ASME, 394-405 (September, 1963).

(7) Pugh, H. Ll. D., and Low, A. H., "The Hydrostatic Extrusion of Difficult Metals", J. Institute Metals, 93, 201 (1964-1965).

(8) Fiorentino, R. J., Sabroff, A. M., and Boulger, F. W., "Hydrostatic Extrusion of Metals at Battelle", Machinery Lloyd (European Edit), 17, 18 (1963).

(9) Fiorentino, R. J., Sabroff, A. M., and Boulger, F. W., "Investigation of Hydrostatic Extrusion", Final Report, Battelle Memorial Institute, Columbus, Ohio, on Air Force Contract AF 33(600)-43328 (January, 1965).

(10) Bobrowsky, A., and Stack, E. A., "Deformation of Metals Under High Pressure", Symposium on Metallurgy at High Pressures and High Temperatures, Gordon and Breach Science Publishers (1964).

(11) Fiorentino, R. J., Richardson, B. D., Meyer, G. E., Sabroff, A. M., and Boulger, F. W., "Development of the Manufacturing Capabilities of the Hydrostatic Extrusion Process", Technical Report AFML-TR-67-327, Volume I, Battelle Memorial Institute, October, 1967.

(12) Alexander, J. M., and Lengyel, B., "Semi-Continuous Hydrostatic Extrusion of Wire", Paper 7 Appl. Mechanics Conf., Proc. Inst. Mech. Engrs., 180, 317 (1965-1966).

(13) Slater, H. K., and Green, D., "Augmented Hydrostatic Extrusion of Continuous Bar", Paper 14, High Pressure Engineering Conference, London, September, 1967. Published by Inst. of Mech. Eng., London.

(14) Fiorentino, R. J., Gerdeen, J. C., Richardson, B. D., Sabroff, A. M., and Boulger, F. W., "Development of the Manufacturing Capabilities of the Hydrostatic Extrusion Process", Technical Report AFML-TR-67-327, Volume II, Battelle Memorial Institute, October, 1967.

(15) Manning, W.R.D., "High Pressure Engineering", University of Nottingham, Bulleid Memorial Lectures, Vol II (1963).

(16) Manning, W.R.D., "The Design of Compound Cylinders for High Pressure Service", Engineering, pp 349-352 (May 2, 1947).

(17) Manning, W.R.D., "Residual Contact Stresses in Built-Up Cylinders", Engineering, 464 (December 8, 1950).

(18) Poulter, T. C., "High Pressure Apparatus", U.S. Patent No. 2,544,499 (May 9, 1951), Code No. P67.35., Annotated Bibliography on High Pressure Technology, ASME, Butterworths (May, 1964).

(19) Meissner, M., "Hydrostatic Pressure Device", Barogenics, Inc., U.S. Patent No. 3,224,042 (December 21, 1965).

(20) Ballhausen, C., German Patent No. 1,143,341 (January 17, 1963).

(21) Gerard, G., and Brayman, J., "Hydrostatic Press for an Elongated Object", Barogenics, Inc., U.S. Patent 3,091,804 (June 4, 1963).

(22) Fuchs, F. J., Jr., "Production Metal Forming With Hydrostatic Pressures", Western Electric Company, ASME Publication No. 65-PROD-17 (June 1, 1965).

(23) Zeitlin, A., Brayman, J., and Boggio, F. G., "Isostatic and Hydrostatic Equipment for Industrial Applications of Very High Pressure", ASME Paper No. 64-WA/PT -14.

(24) Berman, I., "Design and Analysis of Commercial Pressure Vessels to 500,000 psi", ASME Paper No. 65-WA/PT-1, to be published in Trans. ASME, J. Basic Engineering.

(25) Alexander, J. M., and Lengyel, B., "High Pressure Containers", Prov. Spec. No. 15294/66. Briefly described in The Chartered Mechanical Engineer (September, 1966).

(26) Crawley, J., Saunders, A., and Pennell, J., Vickers' Ltd., Newcastle, England. Private discussions.

(27) Johnson, Larssen, Zander, Sandin, ASEA, Sweden. Private discussions.

(28) Newhall, D. H., and Abbot, L. H., "A Contemporary Version of the Bridgman-Birch 30-kb Apparatus and Certain Ancillary Devices", Paper 32, High Pressure Engineering Conference, London, September, 1967. Published by Inst. of Mech. Eng. London.

(29) Crawley, J., Pennell, J. A., and Saunders, A., "Some Problems in Design and Development of Hydrostatic Extrusion Systems", Paper 23, High Pressure Engineering Conference, London, September, 1967. Published by Inst. of Mech. Eng. London.

(30) Garwood, M. F., Zurburg, H. H., and Erickson, M. A., "Correlation of Laboratory Tests and Service Performance", Interpretation of Tests and Correlation With Service, American Society for Metals, Cleveland, Ohio, pp 1-77 (1951).

(31) Grover, H. J., Gordon, S. A., and Jackson, L. R., Fatigue of Metals and Structures, U.S. Government Printing Office, Washington, D.C. (1954).

(32) Aerospace Structural Metals Handbook, Volume I, Ferrous Alloys, Aeronautical Systems Division (1967).

(33) Cummings, H. N., Stulen, F. B., and Schulte, W. C., "Investigation of Materials Fatigue Problems Applicable to Propeller Design", WADC TR 54-531 (May, 1955).

(34) Sachs, George, and Scheven, G., "Relation Between Direct Stress and Bending Fatigue of High-Strength Steels", ASTM Proceedings, Vol. 57 (1957), pp 667-681.

(35) Vascomax 250 and 300, 18% Nickel Ultrahigh Strength Maraging Steels, Vanadium-Alloys Steel Company, Latrobe, Pennsylvania (1962).

(36) Burns, D. J., and Parry, J.S.C., "Effect of Mean Shear Stress on the Fatigue Behavior of Thick-Walled Cylinders", Paper No. 28, I. Mech. Eng., High Pressure Engineering Conference, London, September 11-15, 1967.

(37) Morrison, J.L.M., Crossland, B., and Parry, J.S.C., "Fatigue Under Triaxial Stress: Development of a Testing Machine and Preliminary Results", Proc. Instn. Mech. Engrs., 1956, 170, 697.

(38) Parry, J.S.C., "Further Results of Fatigue Under Triaxial Stress", Proc. Int. Conf. Fatigue of Metals, 1956, 130, (Instn. Mech. Engrs., London).

(39) Parry, J.S.C., "Fatigue of Think Cylinders: Further Practical Information", Ibid, 1965-66, 180 (Pt. 1), 387.

(40) O'Connor, H. C., and Morrison, J.L.M., "The Effect of Mean Stress on the Push-Pull Fatigue Properties of An Alloy Steel", Proc. Int. Conf., Fatigue of Metals, 1956, 102 (Instn. Mech. Engrs., London).

(41) White, D. J., Crossland, B., and Morrison, J.L.M., "Effect of Hydrostatic Pressure on the Direct-Stress Fatigue Strength of An Alloy Steel", J. Mech. Engng. Sci., 1959, 1 (No. 1), 39.

(42) Morrison, J.L.M., Crossland, B., and Parry, J.S.C., "Strength of Thick Cylinders Subjected to Repeated Internal Pressure", Proc. Instn. Mech. Engrs., 1960, 174, 95.

(43) Davidson, T. E., Eisenstadt, R., and Reinir, A. N., "Fatigue Characteristics of Open-End Thick-Walled Cylinders Under Cyclic Internal Pressure", Watervliet Arsenal Technical Report WVT-TI-6216 (August, 1962).

(44) Private discussions with Mr. Acker, Chief Metallurgist, Midvale-Heppenstall Company.

(45) Lunn, J. A., Sampson, H. B., Federico, A. M., and Macaulay, J. R., "Nickel Maraging Steels, Preliminary Investigation of 250 and 300 Bar", North American Aviation Report No. NA 63H-202, (March 15, 1963).

(46) Davidson, T. E., Barton, C. S., Reiner, A. N., and Kendall, D. P., "The Autofrettage Principle As Applied to High Strength (180,000 psi) Light Weight Gun Tubes", IPM Project, Watervliet Arsenal, New York, October, 1959.

(47) North American Aviation Materials Properties Handbook, Volume II, Section 6, pages 6-5-3, 6-7-3, 6-11-3 and 6-4-7-3.

(48) Timoshenko, S., and Goodier, J. N., Theory of Elasticity, 2nd Edition, McGraw Hill, p 413 (1951).

(49) Davidson, T. E., Barton, C. S., Reiner, A. N., and Kendall, D. P., "The Autofrettage Principle as Applied to High Strength Light-Weight Gun Tubes", IPM Project Report, Watervliet Arsenal (October, 1959).

(50) Cryogenic Materials Data Handbook, p. E. 3. h.

(51) Thomas, B.L.S., Turner, H. S., and Wall, W. F., "Piston-Cylinder High Pressure Apparatus for Use up to 25 kb", Paper No. 11, I. Mech. E. High Pressure Engineering Conference, London, September 11-15, 1967.

(52) Wilson, W.R.D., and Skelton, W. F., "Design of High Pressure Cylinders", Paper No. 5, I. Mech. E. High Pressure Engineering Conference, London, September 11-15, 1967.

(53) Timoshenko, S. P., and Gere, J. M., Theory of Elastic Stability, McGraw-Hill, New York (1961).

(54) Private Communication with P. R. Borneman, Allegheny Ludlum Steel Corporation, Research Center, Brakenridge, Pennsylvania.

(55) Private Communication with Mr. Ali Aleu, Kennametal, Inc., Latrobe, Pennsylvania.

(56) Shabaik, A., Lee, C. H., and Kobayashi, "Application of the Visioplasticity Method to Extrusion Through a Conical Die", 7th International M.T.D.R. Conference, September 12-16, 1966.

(57) Shabaik, A., and Kobayashi, S., "Investigation of the Application of Visioplasticity Methods of Analysis to Metal Deformation Processing", (Prepared under Navy, Bureau of Naval Weapons Contract NOw 65-0374-d) February, 1966.

(58) Pugh, H. Ll. D., and Ashcroft, K., "The Hydrostatic or Ramless Extrusion of Metals by Fluid Pressure", National Engineering Laboratory, Department of Scientific and Industrial Research, NEL Report No. 32, May, 1962.

(59) Sachs, G., and Eisbein, W., "Power Requirement and Flow-Processes in Extrusion Presses", (In German) Mitt. dtach. Mat Pruf Anst. 16, pages 67-96, 1931.

(60) Pugh, H. Ll. D., "Application of Static High Pressure to the Forming of Metals-Hydrostatic Extrusion", Metal Deformation Processing, Volume II, page 125, Defense Metals Information Center, Battelle Memorial Institute, (DMIC Report 226). July, 1966.

(61) Pearson, C. E., and Parkins, R. N., The Extrusion of Metals, John Wiley and Sons, Inc., New York, 1960.

(62) Evans, R. M., Strohecker, D. E., Olofson, C. T., and Clark, R. W., "The Development of a Technique for Improving Rocket Motor Designs Through Production Cost Analysis", Battelle Memorial Institute, Columbus, Ohio, Final Report to U.S. Army Missile Command, Redstone Arsenal, Alabama, on Contract DA-01-021-AMC-15595(Z).

Unclassified

Security Classification

DOCUMENT CONTROL DATA - R&D

(Security classification of title, body of abstract and indexing annotation must be entered when the overall report is classified)

1. ORIGINATING ACTIVITY *(Corporate author)* Battelle Memorial Institute Columbus Laboratories Columbus, Ohio 43201	2a. REPORT SECURITY CLASSIFICATION Unclassified 2b. GROUP

3. REPORT TITLE

Design of a Production Hydrostatic Extrusion Press

4. DESCRIPTIVE NOTES *(Type of report and inclusive dates)*

Technical Report (Final) March, 1967 - June, 1968

5. AUTHOR(S) *(Last name, first name, initial)*

Meyer, George E., Simonen, Fredric A., Gerdeen, James C., Fiorentino, Robert J., Sabroff, Alvin M.

6. REPORT DATE June, 1968	7a. TOTAL NO. OF PAGES 205	7b. NO. OF REFS 62
8a. CONTRACT OR GRANT NO. F 33615-67-C-1434 b. PROJECT NO. 140-7 c. d.	9a. ORIGINATOR'S REPORT NUMBER(S) AFML-TR-68-52 9b. OTHER REPORT NO(S) *(Any other numbers that may be assigned this report)* --	

10. AVAILABILITY/LIMITATION NOTICES

This document is subject to special export controls and each transmittal to foreign governments or foreign nationals may be made only with prior approval of the Manufacturing Technology Division of the Air Force Materials Laboratory.

11. SUPPLEMENTARY NOTES	12. SPONSORING MILITARY ACTIVITY Air Force Materials Laboratory, Manufacturing Technology Division, Air Force Systems Command Wright-Patterson Air Force Base, Ohio 45433

13. ABSTRACT

A 17,000-ton hydrostatic extrusion press was designed to pressurize both a 12-inch bore, 250,000 psi, multi-ring container, 10 feet long and a 6-inch bore, 450,000 psi, fluid-supported container, 3 feet long. A stress analysis was made of hydrostatic extrusion containers, stems, and dies.

An economic analysis indicated that there were important areas, such as the production of tubes and shapes, in which hydrostatic extrusion techniques could produce close-tolerance products at a lower cost than conventional processing.

This document is subject to special export controls and each transmittal to foreign governments or foreign nationals may be made only with prior approval of the Manufacturing Technology Division of the Air Force Materials Laboratory, Wright-Patterson Air Force Base, Ohio 45433.

DD FORM 1 JAN 64 1473

Unclassified

Security Classification

Unclassified

Security Classification

14. KEY WORDS	LINK A ROLE	LINK A WT	LINK B ROLE	LINK B WT	LINK C ROLE	LINK C WT
Hydrostatic extrusion						
Hydrostatic extrusion-drawing						
Hydrostatic extrusion tooling						
Design						
Construction						
Analysis						
Hydrostatic extrusion press design						
Economic analysis - hydrostatic extrusion						
Steel - 4340						
Aluminum alloys						
Titanium alloys						
Nickel-base alloys						
Beryllium						
Shapes						
Tubes						

Security Classification